The Chemistry of Cyclopentadienyl Ruthenium Complexes Containing Thiolato or Catenated Polysulfano Ligands

by

Pierre-Yves Plouffe

A thesis submitted to the
Faculty of Graduate Studies and Research
in partial fulfillment of the requirements for
the degree of Doctor of Philosophy

Department of Chemistry
McGill University
Montréal, Québec
Canada

September 1990

The Chemistry of Cyclopentadienyl Ruthenium Complexes Containing Thiolato or Catenated Polysulfano Ligands

Ph.D. Pierre-Yves Plouffe Chemistry

ABSTRACT

The reactive complexes $CpRu(PPh_3)_2SR$ (Cp = η^5-cyclopentadienyl; R = H, 4-C_6H_4Me, 1-C_3H_7, $CHMe_2$) were prepared by briefly heating $CpRu(PPh_3)_2Cl$ with LiSR in refluxing THF. Treatment of the thiolates with CO gave $CpRu(PPh_3)(CO)SR$. The reaction of CS_2 with $CpRu(PPh_3)_2SR$ gave the thioxanthate complexes $CpRu(PPh_3)(S_2CSR)$ (R = 4-C_6H_4Me, 1-C_3H_7, $CHMe_2$), wherein the CS_2 inserted into the Ru-S bond. A study of the kinetics of this reaction and the crystal structure of $CpRu(PPh_3)(S_2CS(1\text{-}C_3H_7))$ is also reported. Refluxing a toluene solution of $CpRu(PPh_3)_2SR$ (R = 1-C_3H_7, $CHMe_2$) gave, via sequential loss of PPh_3 the dimeric complexes $[CpRu(PPh_3)SR]_2$ which converted into the complexes $[CpRuSR]_3$. The crystal structure of $[CpRuS(1\text{-}C_3H_7)]_3$ is reported. The reaction of SO_2 with $CpRu(PPh_3)_2SR$ (R = 4-C_6H_4Me, 1-C_3H_7, $CHMe_2$) gave the complexes $CpRu(SO_2)(PPh_3)S(SO_2)R$. A reaction mechanism is proposed and the x-ray structure of $CpRu(SO_2)(PPh_3)S(SO_2)(4\text{-}C_6H_4Me)$ was determined. The stable complex $CpRu(PPh_3)(CO)S(SO_2)(CHMe_2)$ was observed by ^1H and IR spectroscopy. The complex $CpRu(SO_2)(PPh_3)S(4\text{-}C_6H_4Me)$ was prepared by melting $CpRu(SO_2)(PPh_3)S(SO_2)(4\text{-}C_6H_4Me)$. The complexes $CpRu(PPh_3)(CO)SER$ (E = S, SS and S(O); R = 4-C_6H_4Me, 1-C_3H_7, $CHMe_2$) were prepared by the reaction of the thiol $CpRu(PPh_3)(CO)SH$ with the appropriate phthalimide sulfur transfer reagents REphth (phth = phthalimide). The x-ray structures of $CpRu(PPh_3)(CO)SS(CHMe_2)$, $CpRu(PPh_3)(CO)SSS(1\text{-}C_3H_7)$, $CpRu(PPh_3)(CO)SS(O)(CHMe_2)$ and $CpRu(PPh_3)(CO)SS(O)_2(4\text{-}C_6H_4Me)$ are discussed.

La Chimie des Complexes Cyclopentadiényl Ruthénium Contenant des Ligands Thiolato et des Chaînes Sulfurées

Ph.D. Pierre-Yves Plouffe Chemistry

RÉSUMÉ

Les complexes réactifs $CpRu(PPh_3)_2SR$ (Cp = η^5-cyclopentadiényl; R = H, 4-C_6H_4Me, 1-C_3H_7, CHMe) ont été préparés en chauffant brièvement le $CpRu(PPh_3)_2Cl$ en présence de LiSR dans du THF à reflux. Le traitement des complexes thioliques avec du CO donne les complexes $CpRu(PPh_3)(CO)SR$. La réaction du CS_2 avec les complexes $CpRu(PPh_3)_2SR$ forme les complexes thioxanthates $CpRu(PPh_3)(S_2CSR)$ (R = 4-C_6H_4Me, 1-C_3H_7, $CHMe_2$), où le CS_2 s'est inséré dans le lien Ru-S. Des études cinétiques effectuées sur cette réaction sont rapportées. La structure aux rayons-X de $CpRu(PPh_3)(S_2CS(1\text{-}C_3H_7))$ a été déterminée. Le reflux d'une solution de toluène et de $CpRu(PPh_3)SR$ (R = 1-C_3H_7, $CHMe_2$) provoque la perte séquencielle des ligands PPh_3 pour former des dimères $[CpRu(PPh_3)SR]_2$ et les trimères $[CpRuSR]_3$. La structure du complexe $[CpRuS(1\text{-}C_3H_7)]_3$ a été déterminée par cristallographie aux rayons-X. La réaction du SO_2 avec $CpRu(PPh_3)_2SR$ (R = 4-C_6H_4Me, 1-C_3H_7, $CHMe_2$) donne les complexes $CpRu(SO_2)(PPh_3)S(SO_2)R$. Un mécanisme réactionnel est proposé et la structure du complexe $CpRu(SO_2)(PPh_3)S(SO_2)(4\text{-}C_6H_4Me)$ a été obtenue. Le complexe stable $CpRu(PPh_3)(CO)S(SO_2)(CHMe_2)$ a été observé par spectroscopie RMN-^{1}H et par IR. Le complexe $CpRu(SO_2)(PPh_3)S(4\text{-}C_6H_4Me)$ a été obtenu par la décomposition thermique du complexe $CpRu(SO_2)(PPh_3)S(SO_2)(4\text{-}C_6H_4Me)$ en fusion. Les complexes $CpRu(PPh_3)(CO)ER$ (E = SS, SSS et S(O); R = 4-C_6H_4Me, 1-C_3H_7, $CHMe_2$) ont été obtenus par la réaction du thiol $CpRu(PPh_3)(CO)SH$ en utilisant les réactifs de transfert de soufre phthalimido appropriés. Les structures aux rayons-X des

complexes $CpRu(PPh_3)(CO)SS(CHMe_2)$, $CpRu(PPh_3)(CO)SSS(1\text{-}C_3H_7)$, $CpRu(PPh_3)(CO)S(O)(CHMe_2)$ et $CpRu(PPh_3)(CO)SS(O)_2(4\text{-}C_6H_4Me)$ ont été obtenues.

to Nicky

ACKNOWLEDGMENTS

It is with great gratitude that I wish to express my appreciation to Dr. Alan Shaver, for his undying enthusiasm and patience in guiding me though this project (and writing of this manuscript). His guidance has showed me that well directed perseverance can lead to great fulfilment.

A special thanks must be directed to Dr. Jim Britten for the creative number crunching involved in the numerous x-ray structure determinations in this thesis. His assistance was greatly appreciated.

I would like to acknowledge my colleagues from lab. 435 (i.e. François Gauvin, Bruno Côte, Jacques Demers, Steven Morris, Clair Aitken, Ricardo Turin, Huagin Liu, Ying Mu and Shixuan Xin) for creating a pleasant working atmosphere and stimulating discussions. A special thanks to Bernadette Soo Lum (Harkness) for the valuable discussions and proof reading of sections of this thesis.

I also acknowledge Drs. David Liles and Peter Bird for their x-ray structure studies.

My appreciations is carried to Renée Charron for unravelling the bureaucratic red tape involved in funding, Dr. Françoise Sauriol for her professionalism relating to all aspects of NMR spectroscopy, and George Kopp for his talented glass blowing without which this work would not have been possible.

For finantial support, I thank the Natural Sciences and Engineering Research Council of Canada and Les Fonds pour la Formation de Chercheurs et l'Aide à la Recherche du Québec.

In recognition of the effort required, I give my special thanks to Jenny Papadopoulos for the final proof reading of this manuscript.

I am very grateful to my lovely wife Nicky, for the numerous proof readings of

this thesis and especially for her moral support throughout this project. Finally, to my family, for their patience and understanding.

TABLE OF CONTENTS

	Page
ABSTRACT	*I*
RÉSUMÉ	*II*
ACKNOWLEDGMENTS	*IV*
TABLES OF CONTENTS	*VI*
LIST OF TABLES	*IX*
LIST OF FIGURES	*XII*
LIST OF SCHEMES	*XIV*
LIST OF ABBREVIATIONS	*XV*
LIST OF COMPOUNDS	*XVII*
GENERAL INTRODUCTION	1
SCOPE OF THESIS	6
CHAPTER 1: Preparation of $CpRu(PPh_3)(L)SR$ (L = PPh_3, CO and R = 4-C_6H_4Me, 1-C_3H_7, $CHMe_2$) and The Aggregation of $CpRu(PPh_3)_2SR$ (R = 1-C_3H_7, $CHMe_2$)	
Introduction	7
Results	10
Discussion	20
CHAPTER 2: The Reaction of $CpRu(PPh_3)_2SR$ (R= 4-C_6H_4Me, 1-C_3H_7, $CHMe_2$) with CS_2	
Introduction	28
Results	30
Discussion	[illegible]
CHAPTER 3: The Reaction of $CpRu(PPh_3)_2SR$ (R = 4-C_6H_4Me, 1-C_3H_7, $CHMe_2$) with SO_2	
Introduction	43
Results	46
Discussion	57

TABLE OF CONTENTS (cont'd)

Page

CHAPTER 4: The Preparation and Structures of Polysulfano Complexes Containing the $CpRu(PPh_3)(CO)$ Moiety

Introduction 67

I Preparation of $CpRu(PPh_3)(CO)SSR$ (R = $4\text{-}C_6H_4Me$, $1\text{-}C_3H_7$, $CHMe_2$)

Results 77

Discussion 82

II Preparation of $CpRu(PPh_3)(CO)SSSR$ (R = $4\text{-}C_6H_4Me$, $1\text{-}C_3H_7$, $CHMe_2$)

Results 85

Discussion 93

III Preparation of $CpRu(PPh_3)(CO)SS(O)R$ (R = $4\text{-}C_6H_4Me$, $1\text{-}C_3H_7$, $CHMe_2$)

Results 105

Discussion 114

IV Preparation of $CpRu(PPh_3)(CO)SS(O)_2R$ (R = $4\text{-}C_6H_4Me$)

Results 116

Discussion 119

V Final Address 121

EXPERIMENTALS 122

CONTRIBUTION TO ORIGINAL KNOWLEDGE 151

REFERENCES 153

APPENDIX I Structural Analysis of $[CpRuS(1\text{-}C_3H_7)]_3$, **3c** 162

APPENDIX II Structural Analysis of $CpRu(PPh_3)(S_2CS(1\text{-}C_3H_7))$, **6d** 172

APPENDIX III Structural Analysis of $CpRu(SO_2)(PPh_3)S(SO_2)(4\text{-}C_6H_4Me)$, **8b** .. 178

APPENDIX IV Structural Analysis of $CpRu(PPh_3)(CO)SS(CHMe_2)$, **10d** 184

TABLE OF CONTENTS (cont'd)

		Page
APPENDIX V	Structural Analysis of $CpRu(PPh_3)(CO)SSS(1\text{-}C_3H_7)$, **11c**	190
APPENDIX VI	Structural Analysis of $CpRu(PPh_3)(CO)SS(O)(CHMe_2)$, **12d**	195
APPENDIX VII	Structural Analysis of $CpRu(PPh_3)(CO)SS(O)_2(4\text{-}C_6H_4Me)$, **13b** ..	201

LIST OF TABLES

		Page
Table 1.1	Comparison of Ru-Ru and Ru-S bond lengths of complex **3c** with reported structures.	14
Table 1.2	Table of IR data for $CpRu(PPh_3)(CO)SR$, **4a-d**.	17
Table 3.1	NMR spectra after 15 minutes of rapid SO_2 flow through solutions of **1b-d**.	47
Table 3.2	NMR data for the reaction of **1b,d** with SO_2in the presence of free PPh_3.	49
Table 4.1	List of known inorganic acyclic polysulfides.	68
Table 4.2	^1H NMR for $CpRu(PPh_3)(CO)S_XR$, where X = 1,2,3 and $CpRu(PPh_3)(CO)SS(O)_YR$, where Y = 1,2.	78
Table 4.3	$\nu_{(CO)}$ stretching frequency for $CpRu(PPh_3)(CO)S_XR$, where X = 1,2,3 and $CpRu(PPh_3)(CO)SS(O)_YR$, where Y = 1,2. Recorded in toluene.	79
Table 4.4	Bond lengths and dihedral angles of known metal sulfides.	84
Table 4.5	$\nu_{(CO)}$ stretching frequency for $CpRu(PPh_3)(CO)SSSR$ and $CpRu(PPh_3)(CO)SS(O)R$. Recorded in CCl_4.	90
Table 4.6	Bond lengths and dihedral angles of ruthenium systems.	103
Table 4.7	Table indicating results of thermal treatment of **12b**.	109
Table 4.8	List of known organic thiosulfonate S-S bond lengths.	120
Table E.1	Melting points, yields and IR bands observed for each crops of **12b**.	146
Table E.2	Relative intensity of the Cp signals in the ^1H NMR of **12b**.	147
Table A1.1	Crystal data for $[CpRuS(1\text{-}C_3H_7)]_3$.	163
Table A1.2	Atomic coordinates, x, y, z and B_{iso} for $[CpRuS(1\text{-}C_3H_7)]_3$.	164
Table A1.3	Anisotropic thermal factors for $[CpRuS(1\text{-}C_3H_7)]_3$.	166
Table A1.4	Selected bond lengths and angles for $[CpRuS(1\text{-}C_3H_7)]_3$.	168
Table A2.1	Crystal data for $CpRu(PPh_3)(S_2CS(1\text{-}C_3H_7))$.	173
Table A2.2	Atomic coordinates, x, y, z and B_{iso} for $CpRu(PPh_3)(S_2CS(1\text{-}C_3H_7))$.	174

LIST OF TABLES (cont'd)

Page

Table A2.3 Anisotropic thermal factors for $CpRu(PPh_3)(S_2CS(1\text{-}C_3H_7))$ 175

Table A2.4 Selected bond lengths and angles for $CpRu(PPh_3)(S_2CS(1\text{-}C_3H_7))$ 176

Table A3.1 Crystal data for $CpRu(PPh_3)(SO_2)S(SO_2)(4\text{-}C_6H_4Me)$ 179

Table A3.2 Atomic coordinates, x, y, z and B_{iso} for $CpRu(PPh_3)(SO_2)S(SO_2)(4\text{-}C_6H_4Me)$ 180

Table A3.3 Anisotropic thermal factors for $CpRu(PPh_3)(SO_2)S(SO_2)(4\text{-}C_6H_4Me)$ 181

Table A3.4 Selected bond lengths and angles for $CpRu(PPh_3)(S_2CS(1\text{-}C_3H_7))$ 182

Table A4.1 Crystal data for $CpRu(PPh_3)(CO)SS(CHMe_2)$ 185

Table A4.2 Atomic coordinates, x,y,z, and B_{iso} for $CpRu(PPh_3)(CO)SS(CHMe_2)$ 186

Table A4.3 Anisotropic thermal factors for $CpRu(PPh_3)(CO)SS(CHMe_2)$ 187

Table A4.4 Selected bond lengths and angles for $CpRu(PPh_3)(CO)SS(CHMe_2)$ 188

Table A5.1 Crystal data for $CpRu(PPh_3)(CO)SSS(1\text{-}C_3H_7)$ 191

Table A5.2 Atomic coordinates, x, y, z and B_{iso} for $CpRu(PPh_3)(CO)SSS(1\text{-}C_3H_7)$ 192

Table A5.3 Anisotropic thermal factors for $CpRu(PPh_3)(CO)SSS(1\text{-}C_3H_7)$ 193

Table A5.4 Selected bond lengths and angles for $CpRu(PPh_3)(CO)SSS(1\text{-}C_3H_7)$ 194

Table A6.1 Crystal data for $CpRu(PPh_3)(CO)SS(O)(CHMe_2)$ 196

Table A6.2 Atomic coordinates, x, y, z and B_{iso} for $CpRu(PPh_3)(CO)SS(O)(CHMe_2)$ 197

Table A6.3 Anisotropic thermal factors for $CpRu(PPh_3)(CO)SS(O)(CHMe_2)$ 198

LIST OF TABLES (cont'd)

Page

Table A6.4 Selected bond lengths and angles for $CpRu(PPh_3)(CO)SS(O)(CHMe_2)$. 199

Table A7.1 Crystal data for $CpRu(PPh_3)(CO)SS(O)_2(4\text{-}C_6H_4Me)$. 202

Table A7.2 Atomic coordinates, x, y, z and B_{iso} for $CpRu(PPh_3)(CO)SSS(O)_2(4\text{-}C_6H_4Me)$. 203

Table A7.3 Anisotropic thermal factors for $CpRu(PPh_3)(CO)SS(O)_2(4\text{-}C_6H_4Me)$. 204

Table A7.4 Selected bond lengths and angles for $CpRu(PPh_3)(CO)SS(O)_2(4\text{-}C_6H_4Me)$. 205

LIST OF FIGURES

		Page
Figure 1	Fe-Mo-S cluster in the FeMo cofactor of nitrogenase.	3
Figure 1.1	Thermal decomposition of $CpRu(PPh_3)_2S(1\text{-}C_3H_7)$, **1c**, as a function of time. Relative concentrations of the various species present in a sealed NMR tube.	12
Figure 1.2	ORTEP of $[CpRuS(1\text{-}C_3H_7)]_3$, **3c**.	15
Figure 1.3	COSY spectra of $[CpRuS(1\text{-}C_3H_7)]_3$, **3c**.	16
Figure 1.4	Wire model generated from x-ray determination of $[CpRuS(1\text{-}C_3H_7)]_3$, **3c**, showing the ^1H NMR assignments and the proton sulfur interactions.	17
Figure 1.5	The $p\pi$-$d\pi$ interaction between the metal and the thiolato ligand.	21
Figure 1.6	The expected NMR spectra of all possible isomers of $[CpRu(PPh_3)SR]_2$.	24
Figure 1.7	Structure of the complex $[CpRu(PPh_3)SR]_2$ with both Cp rings cis and "down", showing the Cp ring interactions.	25
Figure 2.1	ORTEP of $CpRu(PPh_3)(S_2CS(1\text{-}C_3H_7))$, **6d**.	31
Figure 2.2	Calculated curves and experimental rates data for the reaction of **1d** with CS_2.	39
Figure 3.1	The frontier orbitals of SO_2.	44
Figure 3.2	Reaction of SO_2 with **1b** at high concentration of SO_2.	51
Figure 3.3	Reaction of SO_2 with **1b** at low concentration of SO_2.	52
Figure 3.4	ORTEP of $CpRu(PPh_3)(SO_2)S(SO_2)(4\text{-}C_6H_4Me)$, **8b**.	55
Figure 3.5	Th xy plane showing the interaction between the metal d_{xz}, the thiolate-bonded SO_2 LUMO, the metal-bonded SO_2 HOMO, and the 3p orbital on the thiolate.	64
Figure 3.6	General MO diagram of 4 electrons in 4 orbitals.	65
Figure 4.1	ORTEP of $CpRu(PPh_3)(CO)SS(1\text{-}C_3H_7)$, **10d**.	80
Figure 4.2	Interaction between adjacent sulfur lone pairs.	83
Figure 4.3	^1H NMR spectrum of $CpRu(PPh_3)(CO)SSS(4\text{-}C_6H_4Me)$, **11b**.	86
Figure 4.4	^1H NMR spectrum of $CpRu(PPh_3)(CO)SSS(1\text{-}C_3H_7)$, **11c**.	87

LIST OF FIGURES (cont'd)

Page

Figure 4.5 ^{1}H NMR spectrum of $CpRu(PPh_3)(CO)SSS(CHMe_2)$, **11d**. 88

Figure 4.6 ORTEP of $CpRu(PPh_3)(CO)SSS(1\text{-}C_3H_7)$, **11c**. 95

Figure 4.7 Selected bond lengths from organic and inorganic sulfur compounds. . . . 101

Figure 4.8 Interaction of lone pairs between first and third sulfurs in trisulfides. 102

Figure 4.9 ^{1}H NMR spectrum of $CpRu(PPh_3)(CO)SS(O)(4\text{-}C_6H_4Me)$, **12b**. 106

Figure 4.10 ^{1}H NMR spectrum of $CpRu(PPh_3)(CO)SS(O)(1\text{-}C_3H_7)$, **12c**. 107

Figure 4.11 ^{1}H NMR spectrum of $CpRu(PPh_3)(CO)SS(O)(CHMe_2)$, **12d**. 108

Figure 4.12 ORTEP of $CpRu(PPh_3)(CO)SS(O)(CHMe_2)$, **12d**. 111

Figure 4.13 ORTEP of the thiosulfinate ligand showing the disorder. 112

Figure 4.14 ORTEP of $CpRu(PPh_3)(CO)SS(O)_2(4\text{-}C_6H_4Me)$, **13d**. 117

Figure E.1 Apparatus used for the manipulation of H_2S. 123

LIST OF SCHEMES

		Page
Scheme 2.1	Oligomerization of $CpRu(PPh_3)_2SR$, **1c**, **1d**, to form the trimers **3c**, **3d**.	32
Scheme 2.2	Possible mechanism for the formation of **6b-d**.	35
Scheme 2.3	Mechanism of insertion of CS_2 into the Ru-S bonds of **1b-d**.	37
Scheme 2.4	Proposed reaction scheme for the reaction of **1a** with CS_2.	41
Scheme 3.1	Proposed mechanism of the reactions between **1b-d** and SO_2.	59
Scheme 4.1	Preparation of catenated derivatives of $CpW(CO)_3SH$, **III**.	72
Scheme 4.2	Preparation of $Cp_2Ti(SR)(SSSR)$, **VII**.	73
Scheme 4.3	Possible rotomers of $CpRu(PPh_3)(CO)SSSR$, **11b-d**.	95
Scheme 4.4	Proposed mechanism for the production of $CpRu(PPh_3)(CO)SSSR$, **11b-d**.	98
Scheme 4.5	Proposed mechanism for the production of $CpRu(PPh_3)(CO)SS(S)R$, **XIII**.	99

LIST OF ABBREVIATIONS

General Abbreviations

Cp	η^5-Cyclopentadienyl
1-C_3H_7	n-propyl
$CHMe_2$	i-propyl
4-C_6H_4Me	p-tolyl
dppe	1,2-bis(diphenylphosphino)ethane, $Ph_2PCH_2CH_2PPh_2$
dppm	1,2-bis(diphenylphosphino)methane, $Ph_2PCH_2PPh_2$
phth	phthalimido
Ph	phenyl
R	organic group
Me	methyl
Et	ethyl
M	transition metal
e^-	electron
THF	tetrahydrofuran
Å	Ångström (1 Ångström = 10^{-10} m)
NMR	nuclear magnetic resonance
IR	infrared
ORTEP	Oak Ridge Thermal Elipsoid Plot
Anal.	elemental analysis
Calcd.	calculated
FAB	fast atom bombardment

Abbreviations used in NMR

TMS	tetramethylsilane
s	singlet
d	doublet
t	triplet
sept	septet
m	multiplet
ABq	AB quartet
J	coupling constant
Hz	Hertz
ppm	part per million
COSY	correlated spectroscopy
a	axial
e	equatorial

Abbreviations used in IR

w	weak
m	moderate
s	strong
sh	shoulder
br	broad
v	frequency, cm^{-1}

LIST OF COMPOUNDS

Formula	R-group	Label
$CpRu(PPh_3)_2SR$	H	**1a**
	$4\text{-}C_6H_4Me$	**1b**
	$1\text{-}C_3H_7$	**1c**
	$CHMe_2$	**1d**
$[CpRu(PPh_3)S(R)]_2$	$1\text{-}C_3H_7$	**2c**
	$CHMe_2$	**2d**
$[CpRuSR]_3$	$1\text{-}C_3H_7$	**3c**
	$CHMe_2$	**3d**
$CpRu(PPh_3)(CO)SR$	H	**4a**
	$4\text{-}C_6H_4Me$	**4b**
	$1\text{-}C_3H_7$	**4c**
	$CHMe_2$	**4d**
$CpRu(dppe)SR$	$1\text{-}C_3H_7$	**5c**
$CpRu(PPh_3)S_2CSR$	$4\text{-}C_6H_4Me$	**6b**
	$1\text{-}C_3H_7$	**6c**
	$CHMe_2$	**6d**
$CpRu(PPh_3)(S_2CS)RuCp(PPh_3)_2$		**6e**
$CpRu(PPh_3)(S_2CS)RuCp(CS)(PPh_3)$		**6f**
$CpRu(PPh_3)_2S(SO_2)R$	$4\text{-}C_6H_4Me$	**7b**
	$1\text{-}C_3H_7$	**7c**
	$CHMe_2$	**7d**

LIST OF COMPOUNDS (cont'd)

$CpRu(PPh_3)(SO_2)S(SO_2)R$	$4\text{-}C_6H_4Me$	**8b**
	$1\text{-}C_3H_7$	**8c**
	$CHMe_2$	**8d**
$CpRu(PPh_3)(SO_2)SR$	$4\text{-}C_6H_4Me$	**9b**
$CpRu(PPh_3)(CO)SSR$	$4\text{-}C_6H_4Me$	**10b**
	$1\text{-}C_3H_7$	**10c**
	$CHMe_2$	**10d**
$CpRu(PPh_3)(CO)SSSR$	$4\text{-}C_6H_4Me$	**11b**
	$1\text{-}C_3H_7$	**11c**
	$CHMe_2$	**11d**
$CpRu(PPh_3)(CO)SS(O)R$	$4\text{-}C_6H_4Me$	**12b**
	$1\text{-}C_3H_7$	**12c**
	$CHMe_2$	**12d**
$CpRu(PPh_3)(CO)SS(O)_2R$	$4\text{-}C_6H_4Me$	**13b**

GENERAL INTRODUCTION

Sulfur was known by the ancients because it exists in nature in its elemental form.[1] It was used for pharmaceutical purposes, in gun powder and by alchemists for the "transmutation" of elements.[1] Sulfur has been known for over six thousand years and referred to as brimstone in Genesis 19:24.[2] In addition, it exists throughout the solar system in various forms. For example, deposits of elemental sulfur have been found near the crater Aristarchus on the moon.[1] Jupiter's moon Io has an atmosphere of sulfur dioxide, and has volcanos that continuously spew sulfur.[3]

A person's first exposure to sulfur in organic compounds is through one's delicate sense of smell. Examples of malodorous sulfur compounds include: various low molecular weight thiols, RSH; rotten eggs, H_2S; garlic, allyl propyl disulfide; and skunk, dibutyl disulfide.[4] This is not to say that all organic compounds containing sulfur are malodorous. Many higher molecular weight disulfides and thiols are odorless, as are highly polar disulfides and thiols, such as cystine and cystein.

Also of importance are the pharmaceutical applications of sulfur containing organic compounds. For example, Allicin, a thiosulfinate found in onion, garlic and chives, is a broad spectrum antibacterial agent and a potent inhibitor of platelet aggregation.[5] The same compound also reduces liver cholesterol and serum lipids. The compound E,Z-ajoene has recently been isolated from fresh garlic and was found to produce complete inhibition of collagen-induced platelet aggregation for 24 hours in rabbits.[6,7] Other applications of sulfur containing drugs include antirheumatics and anaesthetics.[5]

The cosmetics industry also benefits from our knowledge of sulfur chemistry. The coupling reaction between neighboring cystein fragments in human hair (cystein accounts for 18% of hair protein[4]) forms a new amino acid, cystine, and gives the hair a "permanent wave".[8]

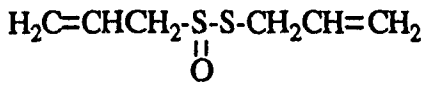

Allicin

E,Z-ajoene

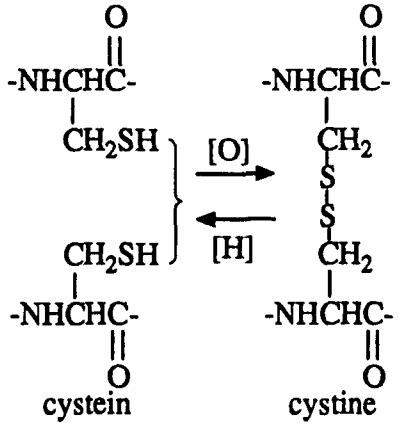

(in hair protein chain)

The chemistry of metallic thiols and thiolates is essential to biological systems. Many microorganisms can reduce inorganic sulfur (e.g. sulfate) and incorporate it in aminoacids such as cysteine and methionine.[9] These aminoacids often bind to metals through the sulfur to form biologically active molecules. Iron-sulfur proteins are responsible for many biological redox sites.[10] Examples include ferredoxins and rubredoxin which contain iron-sulfur sites which are involved in the reduction of sulfate to cysteine and methionine.[9] Furthermore, the protein responsible for reducing

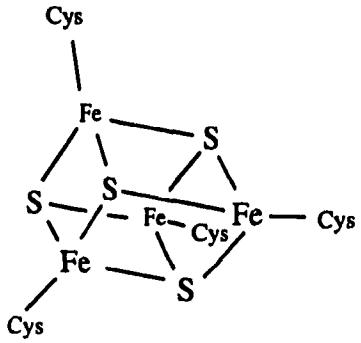

4 Fe-ferredoxin

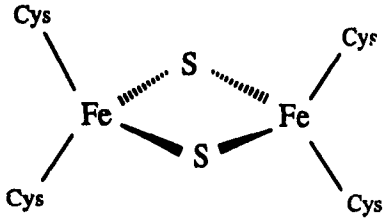

2 Fe-ferredoxin

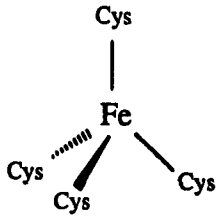

rubredoxin

Where Cys = cystein

atmospheric nitrogen to ammonia in microorganisms, nitrogenase, consists of two

proteins, both of which are essential for activity.[10] The smaller protein has an active site similar to 4Fe-ferredoxin while the large protein has a much larger active site composed of a cluster of $Mo_2Fe_{24}S_{24}$. A smaller fragment called the FeMo cofactor has been isolated from the large protein and was found to contain two iron-sulfur cubanes bridged by Mo_2S_3 fragment, Figure 1.[10] The importance and unique chemistry

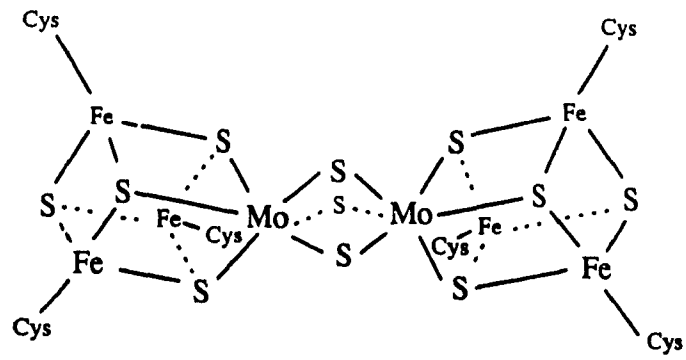

Figure 1 Fe-Mo-S cluster in the FeMo cofactor of nitrogenase.

of these systems have prompted much research in this field.

The presence of sulfur in combustible fuels is the largest source of atmospheric SO_2 emission. Due to recent concerns about air quality, the removal of sulfur in fuels has become very important. Hydrodesulfurization of fossil fuels is now a major area of research (equation 1).[10] As a consequence of the large volume of fossil fuel treated, 61

$$RSR' + H_2 \longrightarrow R\text{-}R' + H_2S \qquad (1)$$

million barrels of petroleum per day worldwide in the first quarter of 1990[11], hydrodesulfurization may presently be the most important industrial chemical process. Because of the hydrodesulfurization of fossil fuels and the removal of H_2S from natural gas, Canada has become the world's largest producer of elemental sulfur.[12] Presently, the catalytic industrial process employed to achieve hydrodesulfurization is a

heterogeneous process which uses sulfided Co or Mo oxides, supported on α-Al_2O_3, as a catalyst.[13,14] This process is efficient although the side reactions, hydrogenolysis of C-C and C-N bonds (equation 2 and 3, respectively) and the hydrogenation of unsaturated compounds (equation 4), lead to a significant waste of hydrogen and the generation of undesired byproducts. The H_2S produced in hydrodesulfurization can be

$$RCH_2CH_2R' + H_2 \longrightarrow RCH_3 + R'CH_3 \qquad (2)$$

$$RNH_2 + H_2 \longrightarrow RH + NH_3 \qquad (3)$$

(4)

reduced to elemental sulfur via the Claus process which uses activated Alumina as a catalyst.[15] This process is carried out in two stages: a) a fraction of the H_2S is burned in air to form SO_2 and b) the SO_2 and the remainder of the H_2S are reacted over the catalyst to form elemental sulfur and H_2O. The exact mechanism of hydrodesulfurization has not been determined, however, Angelici *et al.* and others have recently investigated soluble complexes as models in an attempt to resolve this problem.[13] The mechanism of the Claus process is also not known and thus, the study of catenated sulfur on metal complexes and the reaction of SO_2 with metal complexes could give some insight into this process.

The study of model metal sulfur compounds could eventually be useful in the development of less costly, more selective, and potentially more efficient catalysts for hydrodesulfurization of crude oils. Of particular interest are complexes of ruthenium which are already known to be excellent hydrodesulfurization catalysts[16], although not competitive against heterogeneous catalysts. Thus, a detailed understanding of ruthenium thiolates and polysulfides might be valuable in the development and

improvement of hydrodesulfurization catalysts or in the synthesis of catalysts with activities similar to nitrogenases or ferredoxins.

While organic sulfur complexes of the type RS_XR where x = 1,2 are well known, the metal analogs MS_XR are very rare. Similarly, oxidized organic disulfides such as $RSS(O)_XR$, where x = 1,2 are also known, whereas the metal analogs are virtually unknown. Thus, there is a fundamental interest in exploring the synthesis, structure and reactivities of these metal analogs.

SCOPE OF THESIS

This work introduces a series of systems involving Cp-ruthenium sulfur species of the type M-S*X*, where X = R, SR, SSR, S(O)R or $S(O)_2R$, and M = $CpRu(PPh_3)_2$, $CpRu(PPh_3)(CO)$ or $CpRu(PPh_3)(SO_2)$. In the first part of the thesis, the lability of PPh_3 in the complexes $CpRu(PPh_3)_2SR$ was exploited to generate: dinuclear and trinuclear oligomers; η^2-thioxanthates; SO_2 adducts; and carbonyls. The mechanism of insertion of CS_2 into metal thiolate bonds was studied. Furthermore, the interaction of metal thiolates with SO_2 was also examined. The second part of this thesis relates to the preparation and characterization of the catenated sulfur systems listed above. A series of novel catenated sulfur ligands was prepared and the x-ray crystal structure of some of them are reported.

CHAPTER 1

Preparation of $CpRu(PPh_3)(L)SR$ (L = PPh_3, CO and R = 4-C_6H_4Me, 1-C_3H_7, $CHMe_2$) and The Aggregation of $CpRu(PPh_3)_2SR$ (R = 1-C_3H_7, $CHMe_2$)

INTRODUCTION

The chemistry of metal thiolates has great biological importance and therefore, has been studied intensively.[17] Rubredoxin and nitrogenase are examples of important biologically active molecules containing iron-sulfur bonds.[10] Consequently, many iron sulfides and thiolates have been investigated as models for these proteins. On the other hand, the chemistry of ruthenium-sulfur complexes has been barely examined mainly because they are of no direct biological relevance.[18] However, ruthenium has become increasingly important in the study of hydrodesulfurization.[16] Particularly neglected is the chemistry of cyclopentadienylruthenium. Some complexes have been reported: $CpRuL_2S(C_6H_5)$[19], where L = PMe_3, $P(OMe)_3$, $P(OMe)_2Ph$, $P(OPr)_3$ or L_2 = $Ph_2PCH_2CH_2PPh_2$; $(C_5Me_5)Ru(CO)_2S(C_6H_5)$[18]; and $CpRu(CO)_2SR$ where R = C_6F_5, Me, $CH_2C_6H_5$, t-butyl and C_6H_5[20]. The cationic thiol $[CpRu(PPh_3)_2SH(1\text{-}C_3H_7)]^+$[21] and the thiols $CpRu(PPh_3)_2SH$[21,22] and $CpRu(PPh_3)(CO)SH$[21,22] have also been reported.

The most widely used method of preparation of metal thiolates is through the metathesis of a metal halide with a metal thiolate as in equation 1.1. Many metal thiolates are prepared in this way because, in most cases, the chloride analog is available and is usually easily substituted. The driving force for this reaction is the precipitation of the alkali halide. In cases where the chloride is not easily substituted,

$$M\text{-}Cl + M'\text{-}SR \longrightarrow M\text{-}SR + M'\text{-}Cl \qquad \text{where } M' = \text{alkali metal},\ M = \text{transition metal} \tag{1.1}$$

$$CpW(CO)_2(PPh_3)(H) \xrightarrow[2)\ +RSphth]{1)\ +MeLi} CpW(CO)_2(PPh_3)(SR) + Hphth \qquad \text{where phth = phthalimido} \tag{1.2}$$

$$ML_2 + RS\text{-}SR \longrightarrow M(SR)_2 + 2L \tag{1.3}$$

$$Ni(cod)_2 + Ph\text{-}S\text{-}Ph + 2PEt_3 \longrightarrow PhNi(SPh)(PEt_3)_2 + cod \tag{1.4}$$

$$CpW(NO)(R)_2 + \tfrac{1}{4} S_8 \longrightarrow CpW(NO)(SR)_2 \tag{1.5}$$

the starting chloride may be reacted with $AgNO_3$ to form the cation, followed by the addition of the thiolate. In this case, the driving force is the precipitation of AgCl.

The reaction of a metal anion with a sulfur transfer agent has also been used successfully in cases where the metathesis route was ineffective.[23] This novel route has proven to be very effective in the preparation of $CpW(CO)_2(PPh_3)SR$ (equation 1.2). The metal anion was prepared in situ by reaction of the hydride with methyl lithium.

Some bisthiolates and thiolates can be obtained through the oxidative addition of disulfides and sulfides to a low valent metal as in the case of $Cp_2Ti(CO)_2$[24] and $Ni(cod)_2$[25] respectively, (equations 1.3 and 1.4). Oxidative addition of disulfides onto dimeric species can also lead to thiolates, as is the case for addition of RSSR onto $[CpRu(CO)_2]_2$ to form $CpRu(CO)_2SR$.[20b]

Recently the insertion of elemental sulfur in a metal alkyl bond was achieved. This unique reaction gave $CpW(NO)(SR)_2$ (equation 1.5).[26]

Few thiolato clusters of ruthenium can be found in literature. Dinuclear

complexes of ruthenium(II) such as $[CpRu(CO)SR]_2$ and $[CpRuS(C_6F_5)]_2(\mu\text{-}CO)$ have been reported.[20] Recently, the dinuclear complexes of ruthenium(III), $[(C_5Me_4Et)RuS_2]_2$, $[MeCpRuS_3]_2$ and $[CpRuS_2]_2$ have also been reported.[18] Trimeric

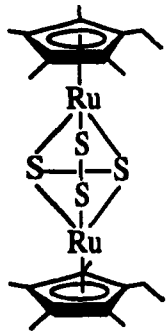

$[C_5Me_4EtRuS_2]_2$

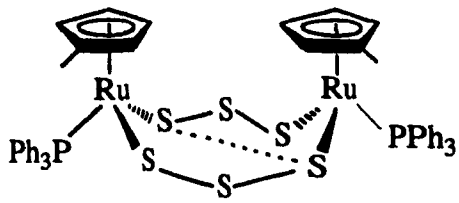

$[MeCpRu(PPh_3)S_3]_2$

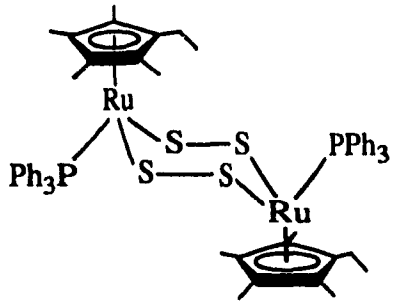

$[MeCpRu(PPh_3)S_2]_2$

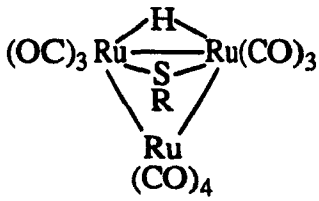

$Ru_3H(CO)_{10}(SR)$

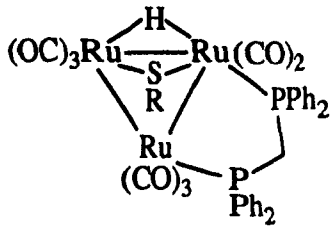

$Ru_3(\mu\text{-}SPh)(\mu\text{-}H)(CO)_8(\mu\text{-}dppm)$

clusters are rarer still. Only two trimeric hydrido complexes, $Ru_3H(CO)_{10}(SR)$[27], where R = CH_2COOH, C_7H_4NS, and $Ru_3(\mu\text{-}SPh)(\mu\text{-}H)(CO)_8(\mu\text{-}dppm)$[28] have been structurally determined to date.

In this work, the complexes $CpRu(PPh_3)(L)SR$, where L = PPh_3, CO and R = H, 4-C_6H_4Me, 1-C_3H_7, $CHMe_2$ have been prepared. The stability of these complexes was related to the lability of the ligand L. Thus, the complexes $[CpRu(SR)(PPh)_3]_2$ and $[CpRu(SR)]_3$ have also been prepared from $CpRu(PPh_3)_2SR$ for R = 1-C_3H_7 and $CHMe_2$, by sequential loss of PPh_3. The crystal structure of the trimeric complex $[CpRu(S\text{-}1\text{-}C_3H_7)]_3$ was determined.[29]

RESULTS

The preparations of $CpRu(PPh_3)_2SR$, where R = H, 4-C_6H_4Me, 1-C_3H_7 and $CHMe_2$, **1a-d**, required careful control of the reaction conditions. A stoichiometric

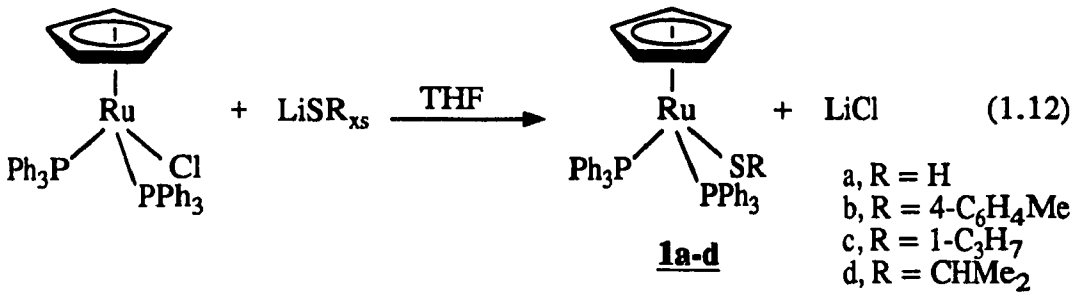

ratio of $CpRu(PPh_3)_2Cl$ with LiSR always gave mixtures of the chloro complex and **1a-d** regardless of the reaction time. Prolonged heating gave a mixture of Cp-containing complexes due to thermal decomposition of the expected product, as shown by the NMR spectrum of the crude product. The optimum condition for this preparation involved an excess (2 fold) of lithium thiolate and a brief reflux time (15 minutes), see equation 1.12. In this way, the thiolates **1a-d** were all obtained in good yield (68-71%).

The brown complexes **1a** and **1d** are moderately stable in air. Storage under nitrogen for prolonged periods (weeks) results in a darkening of the solids and in the case of **1a**, slow evolution of H_2S. The red complexes **1b** and **1c** are both indefinitely stable in air, as solids. Upon melting, **1a** decomposes with evolution of H_2S. All solutions of complexes **1a-d** are dark red and moderately sensitive to air where they form black solutions within minutes. The complexes **1a-d** are soluble in THF, chloroform, CCl_4 and benzene and insoluble in EtOH and hexanes. They react with chloroform, methylene chloride, carbon tetrachloride and 1-propylchloride to form $CpRu(PPh_3)_2Cl$ and the corresponding sulfide as shown by the NMR spectra, see

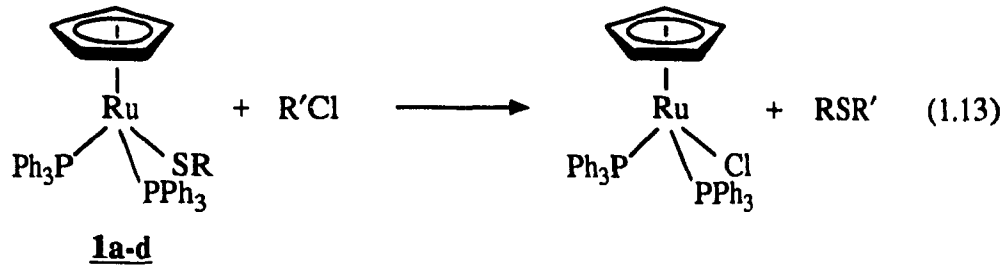

equation 1.13. Similar electrophilic attacks have been observed in some platinum thiolates and indicate a high nucleophilicity for the coordinated sulfur atom.[30] The NMR spectra of **1a-d** show peaks due to one Cp ring, two PPh_3 ligands and the expected R group, in the appropriate ratios.

Refluxing solutions of **1c** and **1d** in toluene led to the formation of dimers, **2c** and **2d**, and trimers, **3c** and **3d**, via the loss of triphenylphosphine, as shown in Scheme 1.1. On the other hand, refluxing **1b** in toluene gave no reaction regardless of the

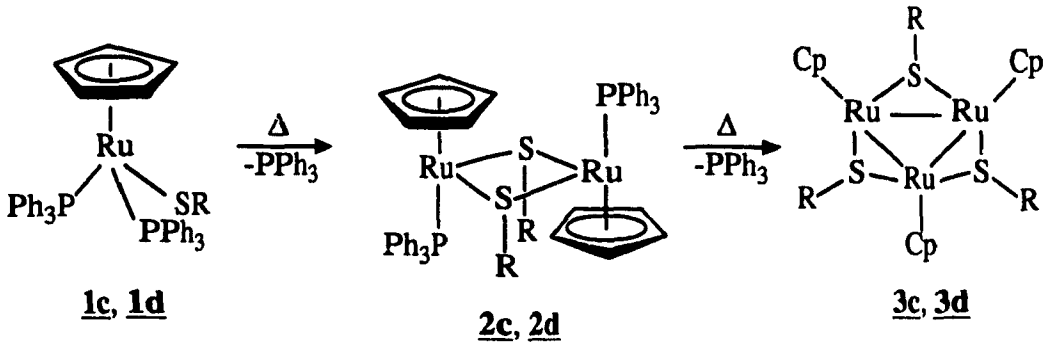

Scheme 1.1 Oligomerization of $CpRu(PPh_3)_2SR$, **1c**, **1d**, to form the trimers **3c**, **3d**.

reaction time. The red dinuclear complex **2c** was prepared by heating a toluene solution of **1c** for 5 minutes, and isolated by column chromatography as an impure product as shown by its NMR spectrum. Complex **2d** was observed by NMR spectroscopy but was not isolated. The NMR spectra of **2c** and **2d**, each showed 2 Cp signals in ratio of 1:1, and a single environment was observed for the 1-C_3H_7 group of **2c** in the appropriate intensity. The isopropyl group of complex **2d** was not clearly

observed due to overlap of signals with hexanes, present as the major contaminant.

The dark red trimeric complexes 3c and 3d were prepared in 50% yield from a 4 hour reflux of 1c and 1d in toluene, followed by column chromatography. Longer reflux time did not improve the yield because an equilibrium was reached, equation 1.14. This equilibrium was determined by heating 1c or 1d in a sealed NMR tube to

$$\underset{\mathbf{1c},\ \mathbf{1d}}{6\ CpRu(PPh_3)_2SR} \rightleftharpoons \underset{\mathbf{2c},\ \mathbf{2d}}{3\ [CpRu(PPh_3)SR]_2} + 3\ PPh_3 \rightleftharpoons \underset{\mathbf{3c},\ \mathbf{3d}}{2\ [CpRuSR]_3} + 6\ PPh_3 \quad (1.14)$$

105°C and measuring the relative integration of the Cp-containing species present in the solution (see Figure 1.1). Other unassigned species were observed in this reaction

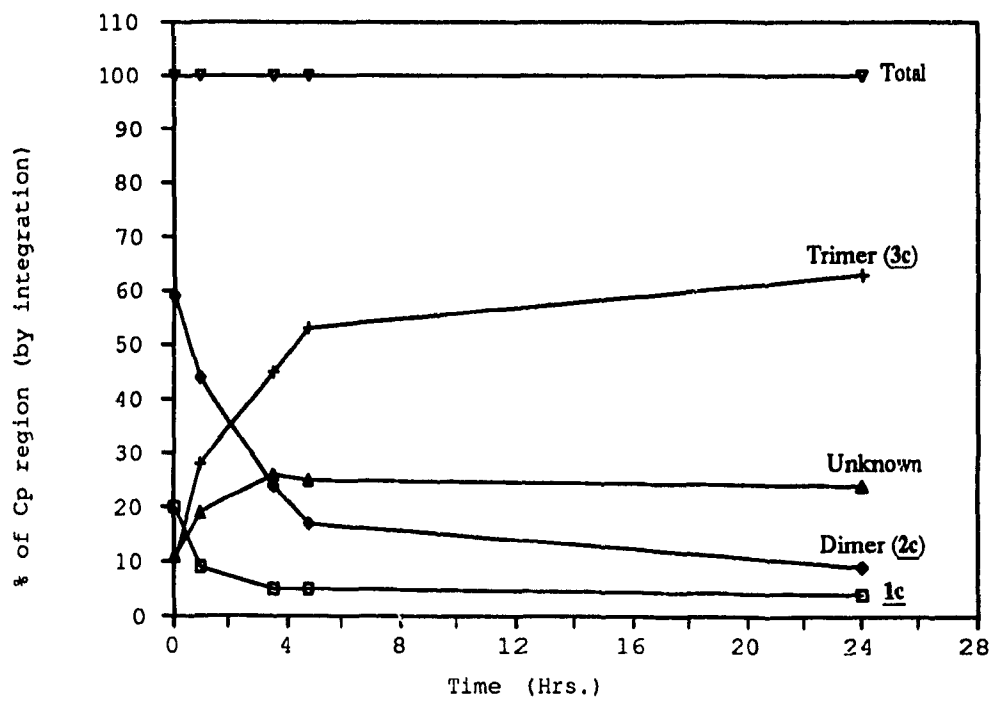

Figure 1.1 Thermal decomposition of $CpRu(PPh_3)_2S(1\text{-}C_3H_7)$, 1c, as a function of time. Relative concentrations of the various species present in a sealed NMR tube.

and were labeled collectively as unknown. Complexes 3c and 3d are soluble in THF, benzene, Et_2O, and hexanes. Both these complexes are stable in solution for hours upon exposure to air. The NMR spectrum of 3c showed two Cp signals at 4.55 and 4.59 ppm in the ratio of 2:1 respectively. The two n-propyl groups were observed in the ratio of 2:1. The methylene protons on the α carbon of the less intense R group resonate at 3.05 ppm, which is unusually downfield. The other protons of the propyl group are in the normal range for aliphatic protons. No signals were observed in the PPh_3 region. The NMR spectrum of the 3d is similar to 3c, in that it also has two Cp signals in the ratio of 2:1 at 4.50 and 4.58 ppm respectively. The isopropyl group shows two diastereotopic methyl groups and one non-diastereotopic methyl group at 1.06, 1.54 and 1.55 ppm in the ratio of 1:1:1 respectively. The methyne proton associated with the non-diastereotopic methyl groups has an unusual downfield displacement at 4.97 ppm, while the methyne proton associated with the diastereotopic methyl groups appeared at 0.80 ppm. The ratio of the methyne protons is 1:2. The NMR spectrum of 3c did not change when recorded at 20°C or 100°C. Elemental analyses of 3c and 3d are in agreement with their respective formulations. Based on elemental and NMR similarities between 3c and 3d, both are assumed to have a similar structure.

The crystal structure of 3c was determined and is presented in Figure 1.2.[31] The crystal data, atom coordinates, bond angles and bond lengths are given in Appendix I, Tables A1.1-A1.4 respectively. Two independent molecules were found in the unit cells. The structure consists of a triangular arrangement of ruthenium with three Cp below the plane defined by the three metal centers, and three bridging thiolato groups above the plane. Two of the three R groups occupy equatorial positions relative to the metal-sulfur "basket", while the third R group is axial. The averaged Ru-S bond length

is 2.296 Å, which is slightly shorter than similar ruthenium-sulfur bonds found in other

Table 1.1 Comparison of Ru-Ru and Ru-S bond lengths of complex 3c with reported structures.

	Ru-Ru (Å)	Ru-S (Å)
3c	2.716-2.712	2.302-2.289
I	2.839	2.388
II	2.867	2.387, 2.395

bridging thiolato complexes such as $Ru_3H(CO)_{10}(SCH_2COOH)$[27] (I) and $Ru_3(\mu\text{-SPh})(\mu\text{-H})(CO)_8(\mu\text{-dppm})$ (II)[28]. The averaged Ru-Ru bond length is 2.715 Å

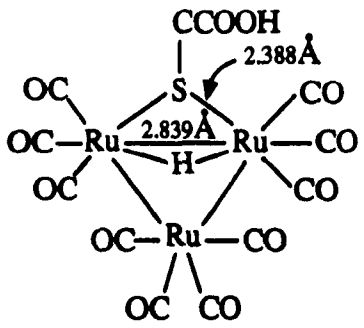

I

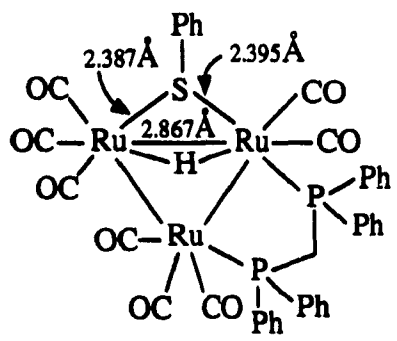

II

which is slightly short compared to similar complexes, I and II, in Table 1.1. To our knowledge, only one example of a trimeric ruthenium complex containing a bridging thiolato ligand unsupported by a hydride has been reported, $Cp_3Ru_3(SMe)_3(CO)_2$.[20] However, the crystal structure was not determined. In structure 3c, the calculated distances between proton $H\alpha_{a1}$, and S5 and S6, are 2.776 and 2.619 Å, respectively. This distance is less than the sum of the Van der Waal distances (3.05 Å) and is within hydrogen bonding distance as defined by Raston and White.[32]

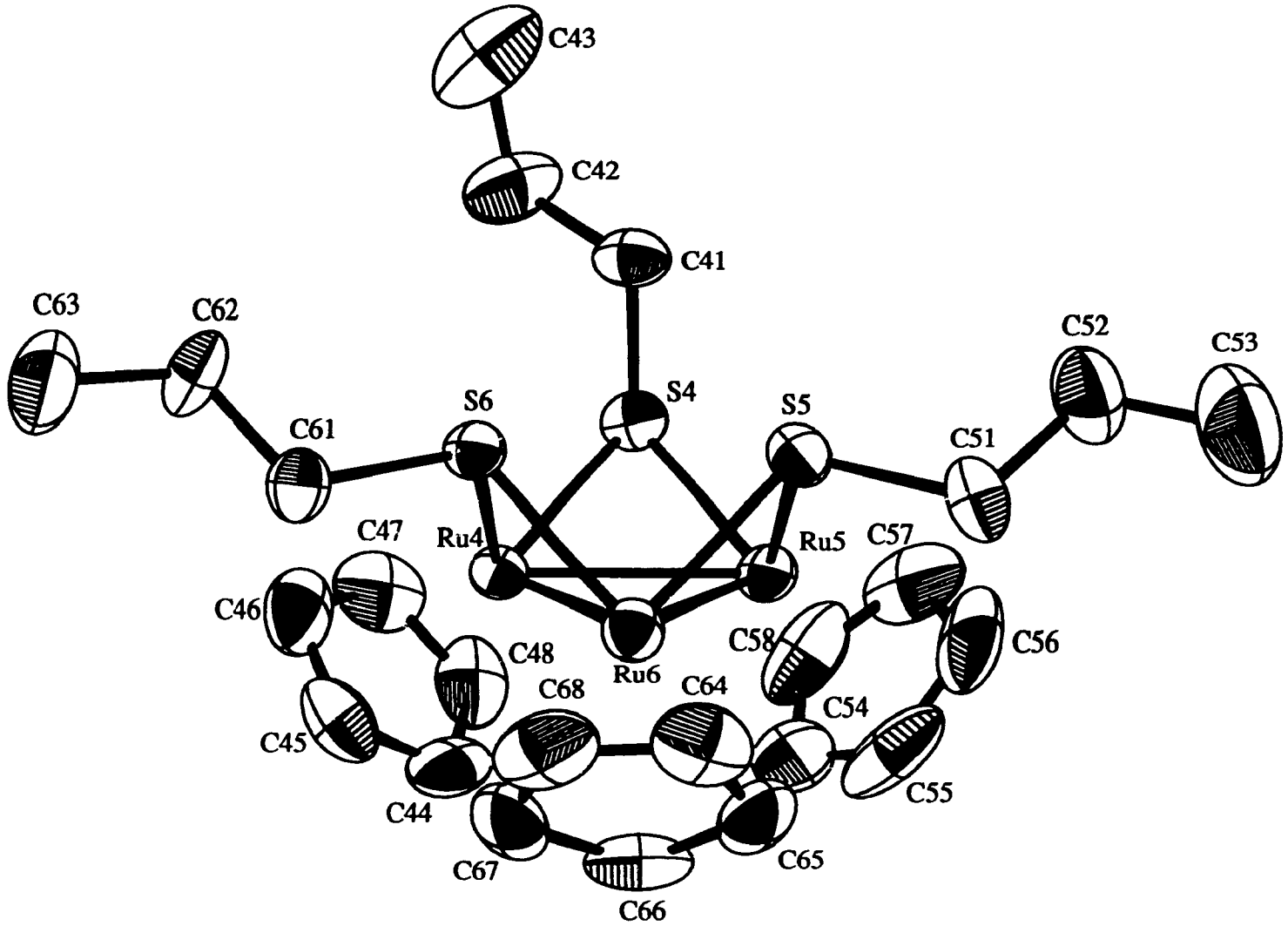

Figure 1.2 ORTEP of $[CpRuS(1\text{-}C_3H_7)]_3$, 3c.

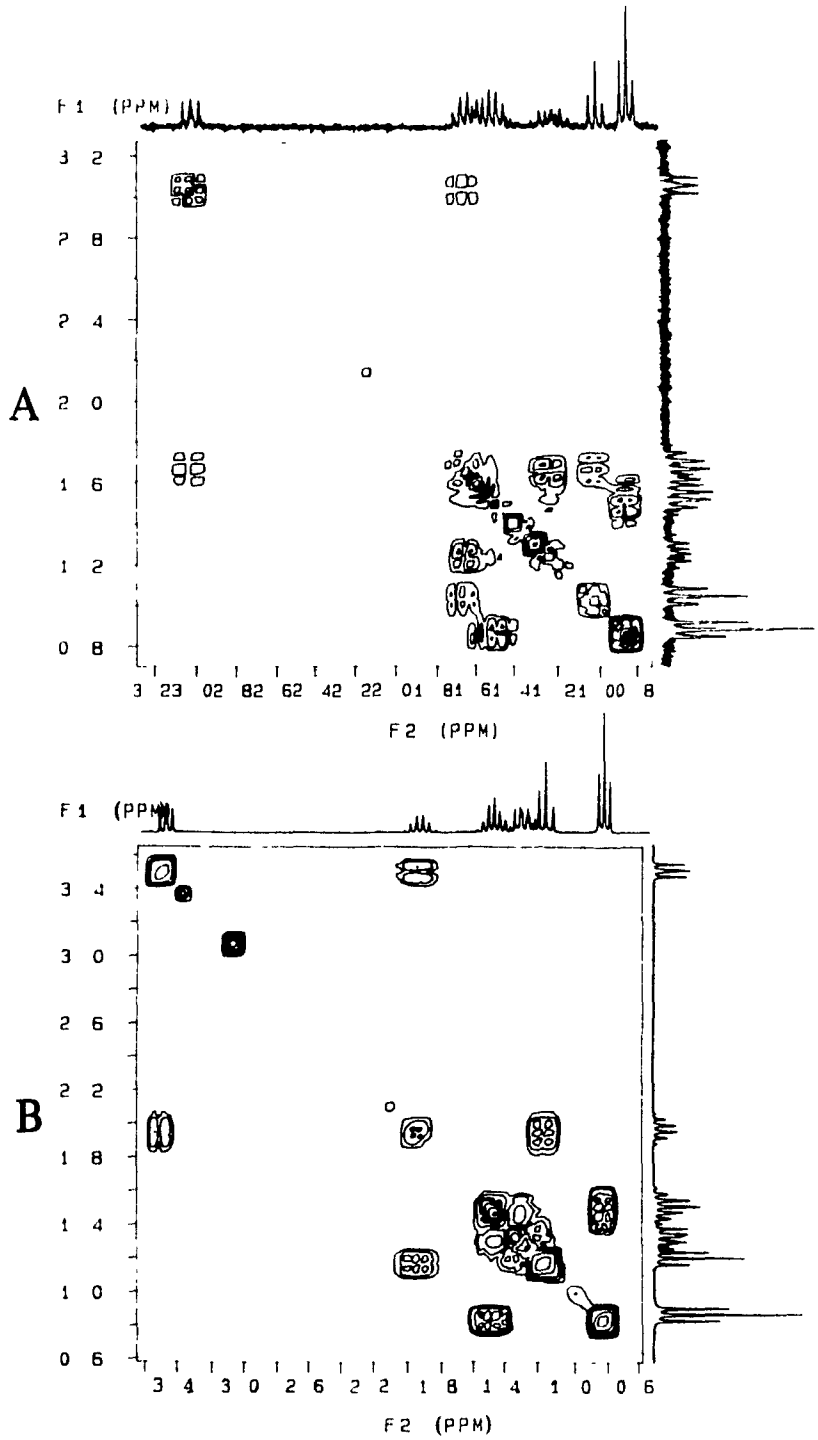

Figure 1.3 COSY spectra of $[CpRuS(1\text{-}C_3H_7)]_3$, 3c.
A) in $CDCl_3$
B) in C_6D_6

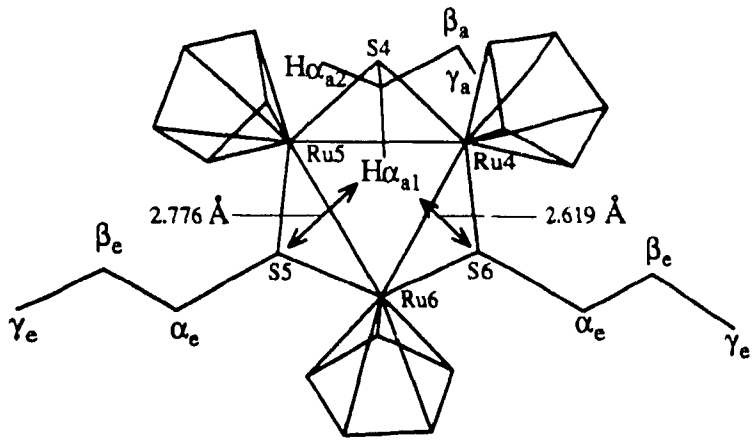

Figure 1.4 Wire model generated from x-ray determination of $[CpRuS(1\text{-}C_3H_7)]_3$, 3c, showing the ^1H NMR assigments and the proton sulfur interactions.

A COSY NMR experiment performed on 3c in $CDCl_3$ and C_6D_6 was used to assign the NMR spectrum and is displayed in Figure 1.3. In C_6D_6, the α protons on the axial R group, $H\alpha_{a1}$ and $H\alpha_{a2}$ in Figure 1.4, appeared as a multiplet at 3.50 ppm. The β_a proton appeared at 1.50 ppm, while the γ_a appeared at 1.20 ppm. The equatorial R group has two observed signals, $H\gamma_e$ an $H\beta_e$, which appeared at 0.87 and 1.50 ppm respectively. The third signal, $H\alpha_e$, appeared as diastereotopic protons at 1.33 and part of the multiplet at 1.50 ppm. The assignments between 1 and 2 ppm were confirmed by the COSY experiment in $CDCl_3$, where the coupling between the diastereotopic equatorial α protons is clearly seen at F1 = 1.62 ppm and F2 = 1.21 ppm.

The reaction of CpRu(dppe)Cl with $LiS(1\text{-}C_3H_7)$ gave a mixture of the starting chloro complex and $CpRu(dppe)S(1\text{-}C_3H_7)$, 5c, regardless of the initial ratio of the chloro complex to lithium thiolate. However, the reaction of 1c with dppe in toluene gave the light orange complex 5c in a moderate yield. A solution of this complex was

stable in air for short periods (up to 30 minutes). The NMR spectrum of **5c** under nitrogen showed no sign of ligand loss or decomposition even after 20 hours in benzene solution.

The reactions of **1a-d** with CO (one atmosphere) at room temperature in THF or toluene overnight gave $CpRu(PPh_3)(CO)SR$, **4a-d**, in excellent yields, equation 1.15.[33]

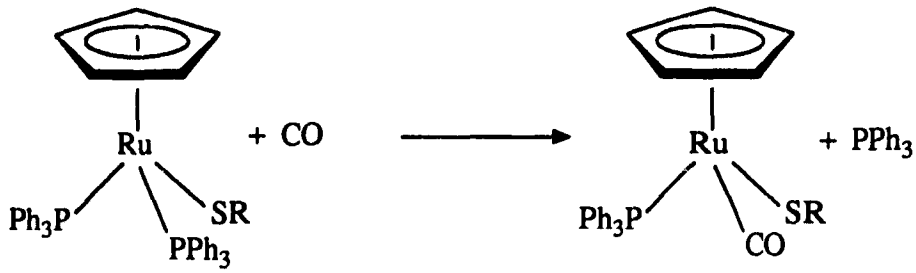

(1.15)

1a-d **4a-d**

These yellow complexes are very stable in air as solids and in solutions. Complexes **4a-d** are soluble in THF, benzene, chloroform and CS_2 without reaction, partially soluble in hexanes and insoluble in EtOH. The NMR spectra of **4a-d** each showed one Cp, one PPh_3 and the expected R group in the appropriate ratios. A small coupling between the phosphorous and the Cp protons, in the order of 0.4-0.6 Hz, was observed in both **4b** and **4d**.

The normal $\nu_{(CO)}$ range for terminal carbonyls is 1850-2125 cm^{-1}.[10] The

Table 1.2 Table of IR data for $CpRu(PPh_3)(CO)SR$, **4a-d**.

	4a	**4b**	**4c**	**4d**
$\nu_{(CO)}$	1950	1947	1942	1941

observed carbonyl stretching frequencies are listed in Table 1.2 and are within normal range. The effect of the electron-donating ability of the R group is clearly observed by the CO stretching frequencies of **4a-d**. As the R group becomes more electron donating, the metal becomes more electron rich and $\nu_{(CO)}$ decreases due to $d\pi$-$p\pi^*$ back donation. Consequently, it may be concluded that R = H in **4a** is less electron donating than R = p-tolyl, **4b**.

DISCUSSION

The preparations of **1a-d** were found to be very capricious. The problems involved are: a) the reaction did not proceed to completion at an equimolar ratio of starting materials, b) on standing, mixtures of **1a-d** and LiCl reacted to form $CpRu(PPh_3)_2Cl$, c) short reflux time gave mixture of starting materials and **1a-d**, and d) prolonged reflux gave decomposition of **1a-d**. This indicated that an equilibrium state was reached as in equation 1.16. The solution to these problems involves a short reflux

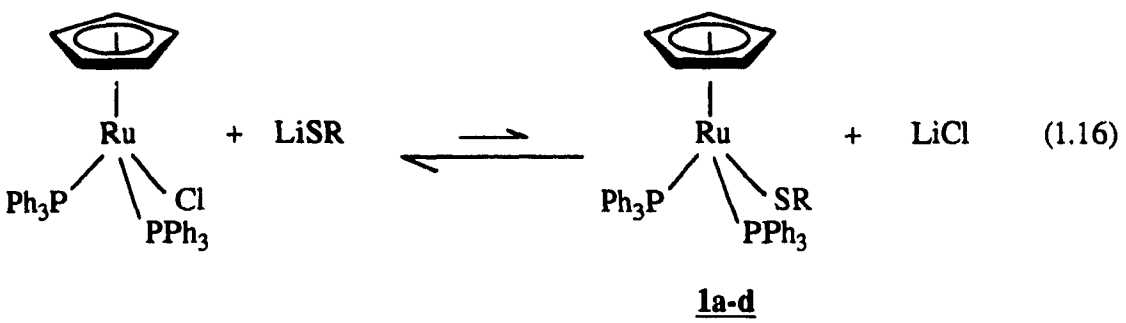

(1.16)

(15 minutes) of the chlororuthenium complex with 2 equivalents of lithium thiolate in THF, followed by rapid workup.

The metal center seemed to have a greater affinity to the chloro than the thiolato ligand. This was confirmed by the reactivity of the thiolates **1a-d** with any chlorinated aliphatic compounds as displayed in equation 1.13. This reactivity also indicates that the sulfur atom is nucleophilic.[34] Similar nucleophilic attacks have been observed in some platinum thiolates and suggest a high nucleophilicity of the coordinated sulfur atom.[30]

The compound $CpRu(PPh_3)_2SH$, **1a**, requires storage under nitrogen as a solid and is quite reactive in solution. This compound has a tendency to lose H_2S when

stored for a long period as a solid. It also loses H_2S when it is melted. The complex **1a** has been previously reported and is known to lose H_2S and PPh_3 thermally with the formation of a cubane-type tetramer $[CpRuS]_4$.[35]

When solutions of **1b-d** were heated for a prolonged period of time, loss of triphenylphosphine was observed and dimeric and trimeric complexes were formed. This type of reactivity is not surprising when one considers the bulkiness of two triphenylphosphine groups on a single metal center as shown by molecular models, as well as the sum of the cone angles of two PPh_3, 290° (Cone angle used was Tolman's cone angle, PPh_3 = 145°. The cone angle of PPh_3 derived by Immirzi and Musco from x-ray data for Ru is 123-125°)[36]

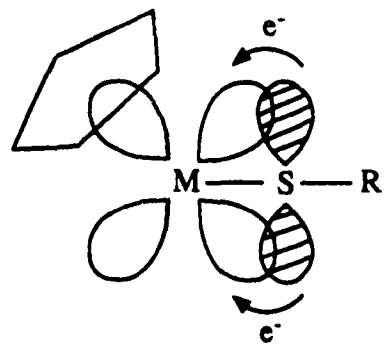

Figure 1.5 The pπ-dπ interaction between the metal and the thiolato ligand.

Fenske-Hall molecular orbital calculations carried out on CpFe(CO)SH by Ashby demonstrated that a thiolate group can stabilize a 16 electron (e^-) species through pπ-dπ bonding.[37,38] The bonding ability of a thiolate group is moderated by the electron-donating ability of the R group. The filled sulfur p orbital has the proper symmetry to overlap with an empty metal d orbital. In this way, $16e^-$ intermediates can be stabilized. Stable $16e^-$ thiolato complexes such as $CpMo(NO)(SPh)_2$ have been isolated and their stability justified by this dπ-pπ backbonding as shown in Figure 1.5.[39]

The complex $Ru(SC_{10}H_{13})_4(CH_3CN)$ is an example of a stable 14e⁻ polythiolate stabilized in part by pπ-dπ bonding and also by the bulkiness of the R group.[40]

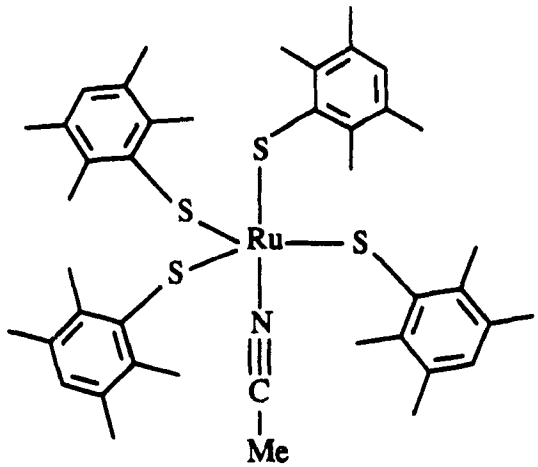

Ashby also demonstrated that the HOMO of $CpFe(CO)_2SH$ is an antibonding orbital involving the sulfur p and the metal d orbitals.[37] Consequently, the electrons in the sulfur lone pair, whose density is governed by the electron-donating ability of the R group, destabilize the molecule and therefore, make the sulfur nucleophilic.

The stability of the complexes **1a-d** was found to be governed by the tendency to lose triphenylphosphine and the reactivity of the acidic proton in the case of **1a**. The tendency to lose PPh_3 increases with the electron-donating ability of the R group. The R group donates electron density to the metal through the sulfur. The high electron density on the metal facilitates the loss of PPh_3 which acts as a strong Lewis base and a weak π-acid.[41] Consequently, **1b** is indefinitely stable as a solid and moderately stable in solution, **1c** is indefinitely stable as a solid but less stable in solution and **1d** needs to be stored under nitrogen as a solid and is quite reactive in solution. After the loss of PPh_3, the complex becomes a reactive 16e⁻ species, $CpRu(PPh_3)SR$, which is then stabilized by the electron-backdonating ability of the thiolate ligand.

R =	4-C_6H_4Me	1-C_3H_7	$CHMe_2$
	b	**c**	**d**

← Increasing stability

The complex **1b** was found to be remarkably resistant to thermal decomposition. Heating a sealed NMR sample of **1b** in C_6D_6 to 110°C for 5 hours gave no sign of decomposition. The lack of reactivity of **1b** is due to the electron-withdrawing ability of the R group which makes this SR group a less efficient stabilizer of the $16e^-$ intermediate. On the other hand, the complexes **1c-d** showed a remarkable tendency to lose PPh_3 when heated. The steric hindrance of PPh_3, the high electron density on the metal and the $p\pi$-$d\pi$ backbonding ability of the thiolate facilitated by electron-donating R groups, all favor the formation of the $16e^-$ intermediate $CpRu(PPh_3)SR$ and consequently, the sequential loss of PPh_3 followed by the formation of the dimer and finally the trimer. The same factors cause **1a-d** to react with CO to form $CpRu(PPh_3)(CO)SR$, **4a-d**, and also **1c** to react with diphenylphosphinoethane (dppe) to form CpRu(dppe)S(n-propyl), **5c**.

The dimeric complex **2c** was prepared by a very brief reflux of **1c** in toluene. According to the product distribution given in Figure 1.1, the dimer reached a maximum concentration within 5 minutes of reflux. NMR spectrum of **2c** revealed that the two Cp rings had different environments and the two R groups had only one environment. There are 6 structural possibilities for a dinuclear complex of the type $Cp_2Ru_2(SR)_2$ having a bent Ru_2S_2 ring. These isomers are shown in Figure 1.6. In addition to these, there are three more isomers having both Cp rings cis "down", as shown in Figure 1.7, however, these isomers involve excessive Cp ring interactions and therefore, are not considered further. From all possible isomers of dinuclear

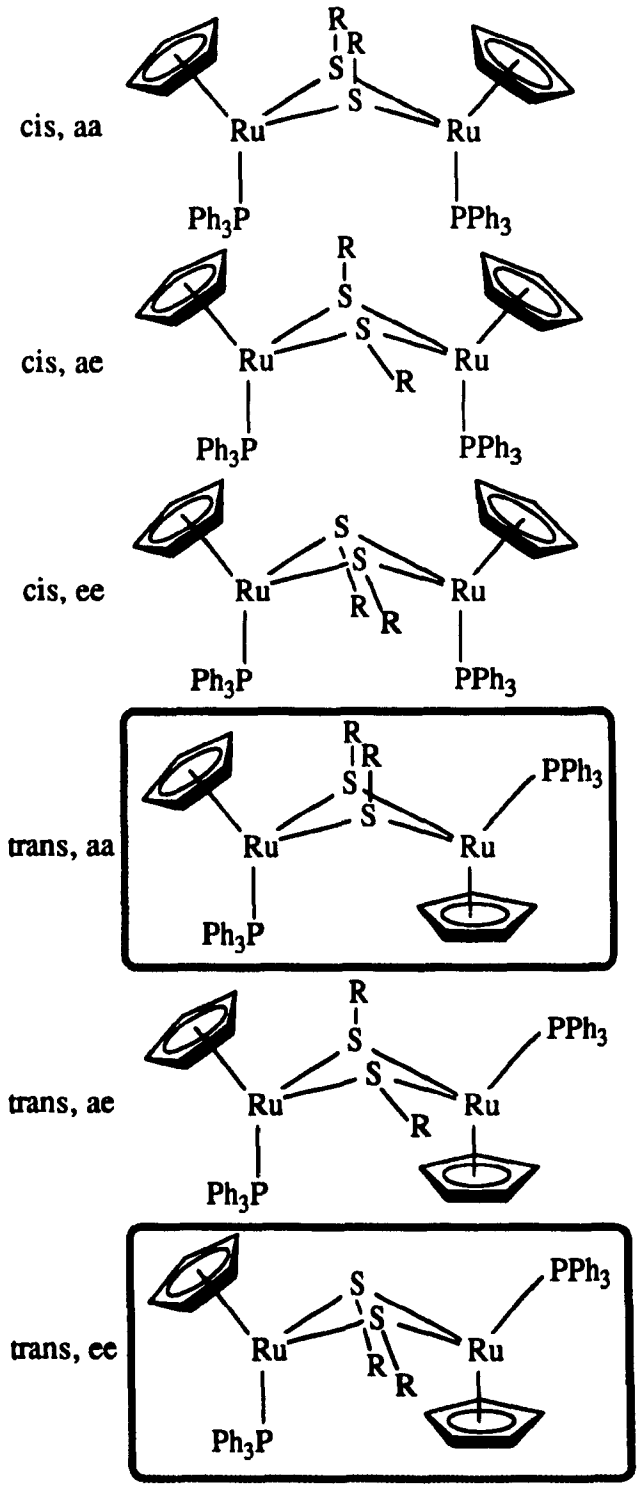

	NMR observations Number of Cp	Number of R
cis, aa	1	1
cis, ae	1	2
cis, ee	1	1
trans, aa	2	1
trans, ae	2	2
trans, ee	2	1

Figure 1.6 The expected NMR spectra of all possible isomers of $[CpRu(PPh_3)SR]_2$.

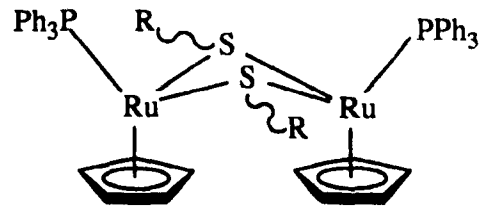

Figure 1.7 Structure of the complex $[CpRu(PPh_3)(SR)]_2$ with both Cp rings cis and "down", showing the Cp ring interactions. The R groups can occupy axial or equatorial positions on each sulfur atom.

dithiolates, two isomers are consistent with the observed NMR spectrum, trans aa and trans ee. These could not be distinguised spectroscopically. Based on models, the trans ee is assumed to be more favored due to reduced steric hindrance around the R group.

Thermal rearrangement of **1c,d** gave the dark red trimeric compounds **3c,d**. Complex **3c** has an unusual structure as described earlier (Figures 1.2 and 1.4).

The NMR spectrum of **3c** did not change with temperature even up to 100°C, thus suggesting the lack of exchange between the Cp and the R groups. COSY experiments on **3c** in C_6D_6 and $CDCl_3$ are illustrated in Figure 1.3 and show a single environment for the two protons on the α carbon of the axial R group, $H\alpha_a$ at 3.50 ppm, see Figure 1.4. Atoms $H\alpha_a$ have an unusual chemical shift which indicates a strong deshielding effect. Similarly, complex **3d** shows an unusual down field shift for the methyne proton. We conclude that the proton H1 ($H\alpha_{a1}$), which is hydrogen bonded to sulfur atoms S5 and S6, is in dynamic equilibrium with H2 ($H\alpha_{a2}$) which is not bonded to the sulfur, thus resulting in an averaged signal. This seems to be consistent with a free-rotating axial R group on the NMR time scale. The distances between $H\alpha_{a1}$ and S5 and S6 are 2.776 and 2.619 Å respectively, less than the sum of their Van der Waal

radii, which is 3.05 Å. This indicates an interaction between $H\alpha_{a1}$ and these sulfur atoms. According to Raston and White, if the distance is less than the Van der Waal distance, then hydrogen bonding is highly likely.[32] The two protons on each of the α carbons of the equatorial R groups show diastereotopicity as two multiplets; one under the large multiplet assigned to $H\beta_a$ at 1.50 ppm and the other is the multiplet at 1.33 ppm, as indicated by the strong correlation between $H\beta_e$ and $H\alpha_{e2}$, in the COSY spectrum in $CDCl_3$ (Figure 1.3).

The COSY experiments and the ^1H NMR spectra reveal that the structure of the trimer is rigid in terms of exchange between the axial and equatorial R groups, while the axial R group is free to rotate at least to the degree that each $H\alpha_a$ proton alternately interacts with the two sulfurs. This orientation may simply minimize lone pair repulsion between the sulfur atoms, since three lone pairs would likely not be able to fit inside the S_3 triangle. Having one lone pair outside the triangle reduces the steric hindrance and forces at least one of the $H\alpha_e$ atoms toward the sulfur atoms. Alternatively, the structure may be induced by hydrogen bonding alone. One or both of these factors must be important in keeping this structure in the observed orientation, since studies on molecular models suggest minimal repulsion between R groups would best be achieved when the R groups are all equatorial.

The lability of PPh_3 has been exploited previously for the complex $CpRu(PPh_3)_2Cl$, where one phosphine ligand can be replaced by a CO ligand[42a,b] or both phosphine groups can be substituted by dppe[42a]. However, this ligand exchange is difficult and requires rigorous conditions. The analogous ligand substitution reactions were performed using **1a-d** in an attempt to reduce their reactivity with respect to ligand loss and enable subsequent selective reactions at the SH bond, in the case of derivatives of **1a**. The reaction of dppe with **1c** gave **6c** in good yield. This compound

was far more stable than **1c**, and did not dissociate one end of the bidendate dppe ligand. However, the potential of this ligand to lose one end of the dppe ligand and thus afford a site of reactivity could not be ignored. Therefore, the replacement of one bulky, relatively basic PPh_3 in **1a-d** with the smaller, more acidic ligand, CO, would be a more stable alternative for reducing the reactivity of **1a-d**. Reactions of **1a-d** with CO gave $CpRu(PPh_3)(CO)SR$, **4a-d**, in very good yields. The complexes **4a-d** do not have the potential to lose a ligand as easily as **1a-d**, and are far more stable. The reaction conditions for these preparations are much milder than the CO substitution of $CpRu(PPh_3)_2Cl$ which requires high pressure of CO or 1/8 S_8 to abstract PPh_3 as PPh_3S.[42b] The ease of ligand substitution of the thiolato complexes further illustrates the activating role of the thiolato group as discussed in the previous section. The presence of an electron-donating ligand, PPh_3, and the strong π-acceptor CO ligand create a uniquely stable complex due to the reduction of the electron density at the metal.[10] The NMR spectrum of **4c** showed diastereotopic protons on the carbon α to the sulfur atom. This is consistent with the presence of a chiral metal center. The complex **4d** displayed diastereotopic methyl groups in the NMR spectrum, which is also consistent with the chiral metal center. The cyclopentadienyl NMR signal showed a very small coupling with the phosphorous in the order of 0.4-0.6 Hz. This coupling was not observed with any other derivatives of CpRu. Coupling between Cp and phosphorous is not usually observed for ruthenium since the second and third row transition metals are notoriously poorer transmitters of nuclear spin-spin coupling effects than the first row transition metals.[43]

CHAPTER 2

The Reaction of $CpRu(PPh_3)_2SR$ (R = 4-C_6H_4Me, 1-C_3H_7, $CHMe_2$) with CS_2

INTRODUCTION

The thioxanthates of several transition metals such as Cu, Cr, Mo, W, Mn, Re, Fe, and Ni are known.[44] However, thioxanthates of ruthenium have not been reported

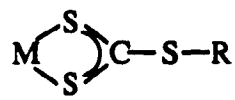

and therefore, are of interest.

There are two classical methods of preparing thioxanthates: 1) the reaction of the metal cations with the thioxanthate anions (equation 2.1) and 2) the reaction of the metal thiolates with CS_2 (equations 2.2 and 2.3).[44] The latter reaction is an insertion of

$$M^+ + x(S_2C\text{-}SR)^- \longrightarrow M(S_2C\text{-}SR)_x \qquad (2.1)$$

$$L_nM\text{-}SR + CS_2 \longrightarrow L_{n-1}M\begin{matrix}S\\S\end{matrix}C\text{-}SR + L \qquad (2.2)$$

$$LM\text{-}SR + CS_2 \longrightarrow LM\text{-}S\text{-}\underset{\underset{S}{\|}}{C}\text{-}SR \qquad (2.3)$$

$$M(S_2C\text{-}OR) \xrightarrow[CS_2]{Et_3N} M(S_2C\text{-}SR) \qquad (2.4)$$

CS_2 into the metal sulfur bond to form a bidentate[44] (equation 2.2) or a unidentate[45c,46] (equation 2.3) product. Generally, when a ligand can be easily lost, then the η^2 mode is

favored, otherwise the η^1 mode of bonding is favored. In addition, there is also a special method in which a xanthate is converted to a thioxanthate using catalytic amounts of Et_3N and excess CS_2, equation 2.4[44]

Equations 2.2 and 2.3 are directly applicable to this work as it involves a metal thiolate. While thioxanthates prepared via insertion of CS_2 have been known for quite some time,[47] no mechanistic studies can be found in the literature for this reaction. The CS_2 insertion into M-SR bond is formally a homolog of CO_2 insertion into M-OR bond. The latter being of interest in the fixation of CO_2. The mechanism of CO_2 insertion proceeds via electrophilic attack of free CO_2 on the alkoxyl group, followed by displacement of a metal ligand and insertion into the metal-alkoxy bond (see discussion).[55] It was of interest to see if CS_2 behaved in the same manner.

Complexes involving thioxanthates and other ligands on a transition metal center are not common.[44] These include $CpM(CO)_2(S_2CSR)$ where M = Mo,W[45c]; $M(CO)_4(S_2SR)$ where M = Mn, Re[49]; $Re(CO)_5(S_2CSR)$[49]; $CpFe(CO)_x(S_2CSR)$ where x = 1,2[50]; and $[M(S_2CSR)(SR)]_2$ where M = Fe[51], Co[52]. Among these, $CpFe(CO)(S_2CSR)$, is the only group 8 thioxanthate reported.[53]

The complexes $CpRu(PPh_3)_2SR$ were found to react with CS_2 to form the thioxanthate complexes $CpRu(PPh_3)(S_2CSR)$, where R = 4-C_6H_4Me, 1-C_3H_7, $CHMe_2$. The structure of $CpRu(PPh_3)(S_2CS\text{-}1\text{-}C_3H_7)$ was studied by x-ray crystallography. Since these reactions involve the Ru-S bond and the loss of one PPh_3, and both of these are of interest in this system, the mechanism was investigated by means of kinetic studies.

RESULTS

Complexes **1b-d** reacted cleanly with CS_2 in toluene or THF at room temperature to give quantitative yields of dark red thioxanthates **6b-d**, equation 2.5.

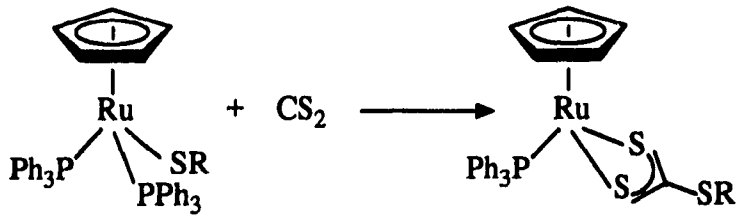

(2.5)

1b-d **6b-d**

b, R = 4-C_6H_4Me
c, R = 1-C_3H_7
d, R = $CHMe_2$

These complexes were insoluble in ethanol and hexanes and soluble in CS_2, THF, toluene, and $CHCl_3$. They were very stable as solids and also in solution. An NMR sample of **6d** was exposed to air for 5 hours with no change in the NMR spectrum. The NMR spectra of **6b-d** showed peaks due to one Cp, one PPh_3 ligand and the expected R groups in the appropriate ratios. The IR spectra showed two thioxanthate bands in the ranges 972-993 cm^{-1} and 941-962 cm^{-1}. A third band was observed in the range 803-807 cm^{-1} and was assigned to the R-S vibration.

The crystal structure of **6c** was determined and is displayed in Figure 2.1.[54] The crystal data, the tables of atom coordinates, thermal parameters, bond lengths and selected bond angles are listed in Appendix II, Tables A2.1-A2.4 respectively. The structure is a piano stool with an η^2-thioxanthate moiety, which is consistent with those structures reported for similar complexes.[44,45]

The insertion of CS_2 into the thiolate bonds was found to be irreversible. Treatment of **6b-d** with CO in C_6D_6 gave no reaction. A solution of **6b** in C_6D_6 can be refluxed for 2 hours with no sign of decomposition.

The kinetics of the CS_2 insertion reaction was studied by NMR spectroscopy in

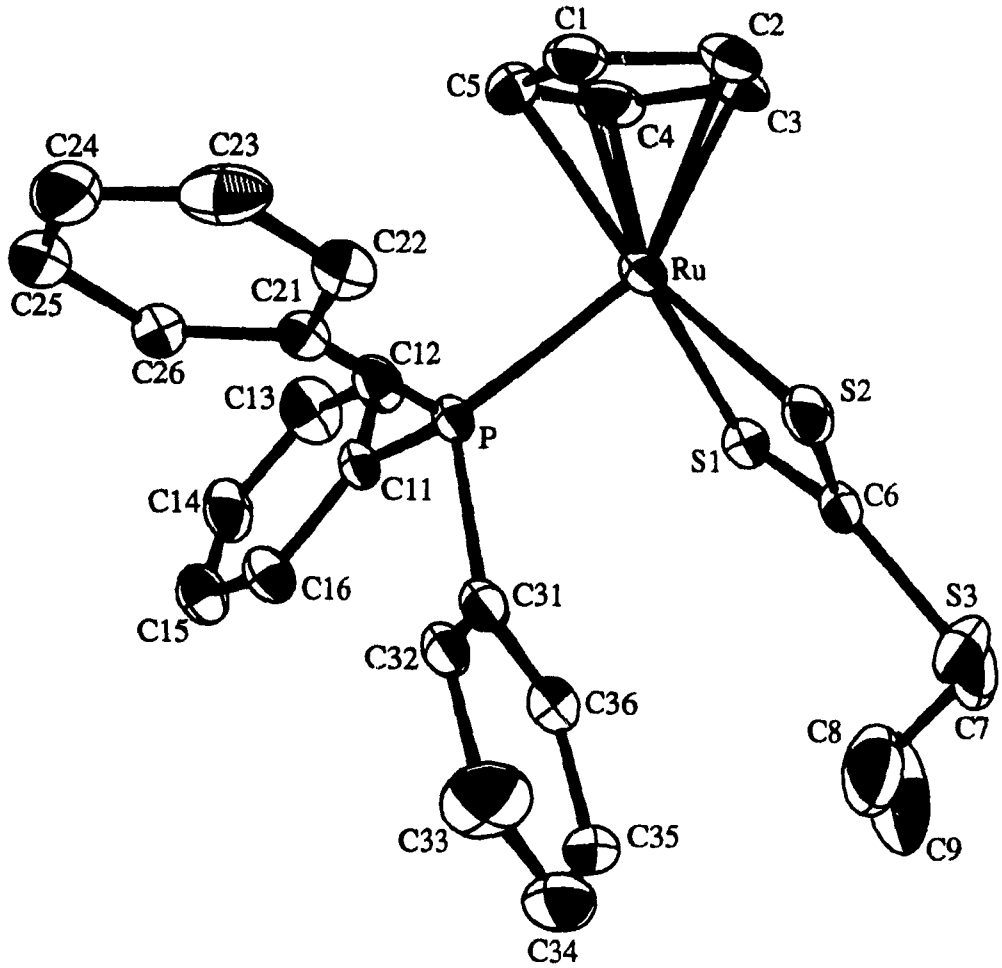

Figure 2.1 ORTEP of $CpRu(PPh_3)(S_2CS(1\text{-}C_3H_7))$, <u>**6d**</u>.

C_6D_6. It was noted that an increase in CS_2 concentration increased the rate of insertion, whereas an increase in PPh_3 concentration decreased the rate (data points of Figure 2.2). Purging an NMR sample of **1b** with CO after approximately 50 % reaction with CS_2, quickly quenched the reaction with conversion of the remaining **1b** to $CpRu(PPh_3)(CO)S\text{-}4\text{-}C_6H_4CH_3$, **4b**. The complex $CpRu(dppe)S(1\text{-}C_3H_7)$,**5c**, does not react with CS_2 even after an extended period of time. The insertion of CS_2 into the thiolate bond of $CpRu(PPh_3)(CO)S(1\text{-}C_3H_7)$,**4c**, in C_6D_6 did not occur unless the sample was treated with UV light. The rate of CS_2 insertion into the thiolato bonds increased in the order **1d** > **1c** > **1b**.

The thiol **1a** showed unusual reactivity toward CS_2 as displayed in Scheme 2.1. It was found to react slowly over 48 hours with evolution of H_2S to give the red product $Cp_2Ru_2(PPh_3)_3(CS_3)$, **6e** (ie. R = $CpRu(PPh_3)_2$). The structure was determined by spectroscopic evidence. The ^1H NMR spectrum in C_6D_6 showed two multiplets above

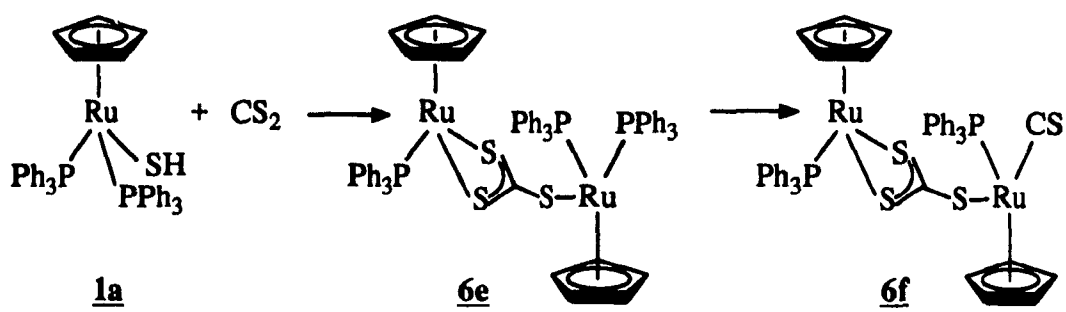

Scheme 2.1 Proposed reaction sequence for the reaction of **1a** with CS_2.

7.3 ppm in the relative ratio of 2:1, indicating the presence of three PPh_3 groups in two different environments. The Cp region had two sharp signals in a relative ratio of 1:1 at 4.66 and 4.54 ppm, which reflects 2 Cp rings in two different environments. The relative ratio of the Cp region to the PPh_3 region was 2:9, indicating 2 Cp and three

PPh_3 ligands. No other signals were observed. The proton-decoupled ^{31}P spectrum in C_6D_6 had 2 sharp signals in the ratio 2:1 at 41.28 and 52.36 ppm, confirming the interpretation of the PPh_3 region in the ^1H NMR spectrum. The IR spectrum was found to have bands at 964 and 907 cm^{-1}. These bands are also present in the thioxanthates **6b-d** which indicate the similarity between the two complexes. Persistent contaminants could not be removed by recrystallization or column chromatography and a pure sample could not be obtained for elemental analysis. However, FAB mass spectrum of **6e** gave the molecular ion and a fragmentation pattern consistent with the proposed formula $Cp_2Ru_2(PPh_3)_3(CS_3)$.

Further reaction of **6e** with CS_2 for 5 days in C_6D_6 resulted in an NMR spectrum containing two Cp signals at 4.73 ppm and 4.34 ppm of equal intensity. Only one PPh_3 environment was observed in the ^1H NMR spectrum as two bands at 7.0 ppm and 7.6 ppm in relative ratio 2:3; corresponding to the meta/para and the ortho protons respectively. The ^{31}P spectrum of **6e** indicated a contaminant containing two PPh_3, as two signals at 46.23 and 40.74 ppm in the ratio 1:1, which were tentatively assigned to $Cp_2Ru_2(PPh_3)(CS)(CS_3)$, **6f** (ie. R = $CpRu(PPh_3)(CS)$). Assuming this composition, **6f** accounted for 9% of the signals in the ^{31}P spectrum of **6e**. A nujol mull of the dried residue showed a band at 1263 cm^{-1}, consistent with the presence of a CS ligand. The reaction time, and irreproducibility made further studies difficult.

On the other hand, CO_2 was found to be unreactive toward **1b-d** at room temperature and at 1 atmosphere of CO_2. An NMR scale reaction of **1c** with SCO at -20°C for 24 hours gave 2 new peaks in the Cp region which remained unassigned. The complex **1b** did not react with SCO.

DISCUSSION

Since CS_2 is a homologue of CO_2, then the insertion of CS_2 into the metal thiolato bond is analogous to the insertion of CO_2 into the metal alkoxy bond. The latter reaction is of great interest as a potential CO_2 fixation reaction which, in the future, could become useful due to the industrial and atmospheric importance of CO_2. The mechanism of insertion of CO_2 in $W(CO)_5OR^-$ has recently been reported.[55] It proceeds via electrophilic attack of free CO_2 on the alkoxyl group, followed by displacement of metal ligand and insertion into the metal-alkoxy bond, analogous to path B in Scheme 2.2. It was of interest to determine if CS_2 reacts in the same way.

The reaction of CS_2 with a metal thiolato bond has been observed earlier.[45] Some examples of the products of these insertions include mononuclear systems with an η^1 thioxanthate ligand such as $CpNi(Bu_3P)(SC(S)SR$[45a], η^2 thioxanthates such as $CpNi(S_2CSR)$[45b], $CpM(CO)_2(S_2CSR)$[45c] (where M = Mo, W), and clusters such as $Cu_8(SR)_4(S_2CSR)_4$[45e]. No study has been reported on the mechanism of insertion of CS_2 in thiolato bonds. The two most likely modes of insertion in this case are: a) displacement of PPh_3 and precoordination of CS_2 to the metal, followed by insertion into the M-SR bond, path A in Scheme 2.2, and b) the attack of free CS_2 on the thiolate group followed by the displacement of PPh_3, path B. The reaction of **1b** with CS_2 was studied under various conditions in an attempt to determine which mechanism applied in this case. The reason for selection of **1b** for the kinetic study was that under identical conditions, its rate of reaction was the slowest followed in order by **1c** and **1d**.

The observations include: 1) rate acceleration with increasing CS_2 concentration; 2) rate reduction by addition of PPh_3 or CO; 3) conversion of **1b** to $CpRu(PPh_3)(CO)S(4\text{-}C_6H_4Me)$ in the presence of CS_2 and CO; 4) failure of the

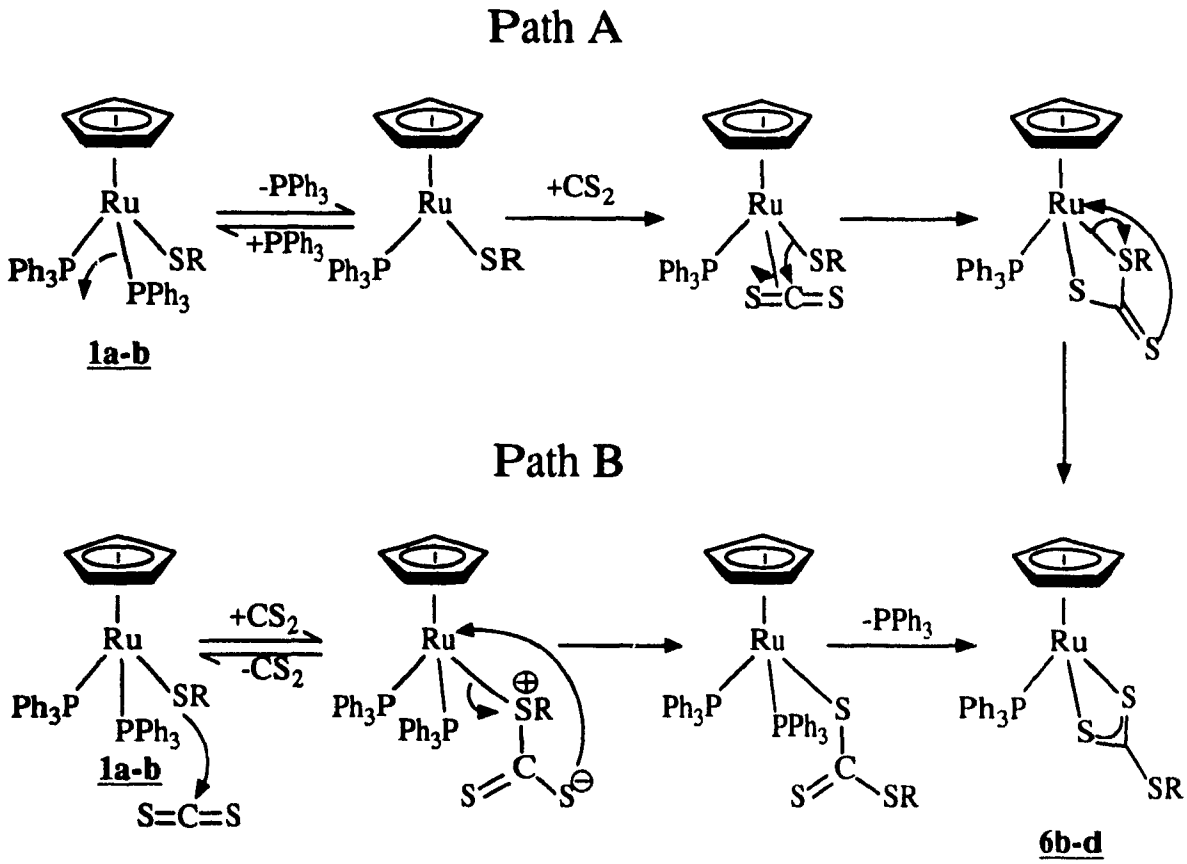

Scheme 2.2 Possible mechanism for the formation of **6b-d**.

carbonyl complexes **4b-d** to react with CS_2 unless irradiated with UV light and 5) failure of the dppe complex **5c** to react with CS_2. The first observation is consistent with both mechanisms proposed. On the other hand, the second observation seems to imply the reaction path A. If excess PPh_3 or CO is added to the reaction medium, then the concentration of the coordinatively unsaturated intermediate would be drastically reduced and therefore, the reaction would be inhibited. Under the same conditions, the reaction path B should not be affected by excess ligand since the displacement of PPh_3 is intramolecular. In comparison, the insertion of CO_2 into the metal alkoxy bond of

$W(CO)_5OR^-$ is insensitive to the concentration of CO.[55b] Furthermore, if path B was effective, then the reactions of **4b-d** with CS_2 would likely form the sulfur-bonded CS_2 intermediates (η^1-thioxanthate), even if subsequent reactions were inhibited by the lack of an available leaving group. It was observed that **4b-d** did react with CS_2 under UV light. It is likely that UV light forced the reaction to proceed via path A by photolytically producing the coordinatively unsaturated intermediate. The complexes $CpRu(PPh_3)_2H$ and CpRu(dppe)H, for example, give $CpRu(PPh_3)_2(\eta^1\text{-}SC(S)H)$ and $CpRu(dppe)(\eta^1\text{-}SC(S)H)$ respectively.[56] As observed by NMR spectroscopy, the conversion of **1b** to **6b** showed no sign of an intermediate containing a monodendate thioxanthato ligand, as one would expect if the reaction mechanism was similar to that of $CpRu(PPh_3)_2H$. If insertion of CS_2 occured before ligand loss, as in path B, then an η^1-complex should be formed as an intermediate. The monodendate complex $CpRu(PPh_3)(CO)(S\text{-}C(S)\text{-}SR)$ could not be trapped by CO treatment during the reaction, nor could it be induced by bubbling CO through solutions of **6b-d** or by heating solutions of **6b-d** with excess PPh_3.

The results suggest precoordination of CS_2 followed by insertion, path A. In this mechanism, the intermediate is the coordinatively unsaturated $CpRu(PPh_3)SR$. This species is stabilized by $p\pi$-$d\pi$ donation of the thiolate group to the metal. As discussed in section I, the stability of this unsaturated species is greatest when the R group is electron donating. Thus, the trend of reactivity is also in the order of electron-donating ability of the R group as expected for path A. Since the unsaturated intermediate is effectively stabilized by electron-donating R groups, then it would exist at a higher concentration and therefore, be more prone to attacks by CS_2. Consequently, the observed rate of reaction would be proportionally greater.

A kinetic analysis of path A shown in Scheme 2.3 led to the derivation of a rate

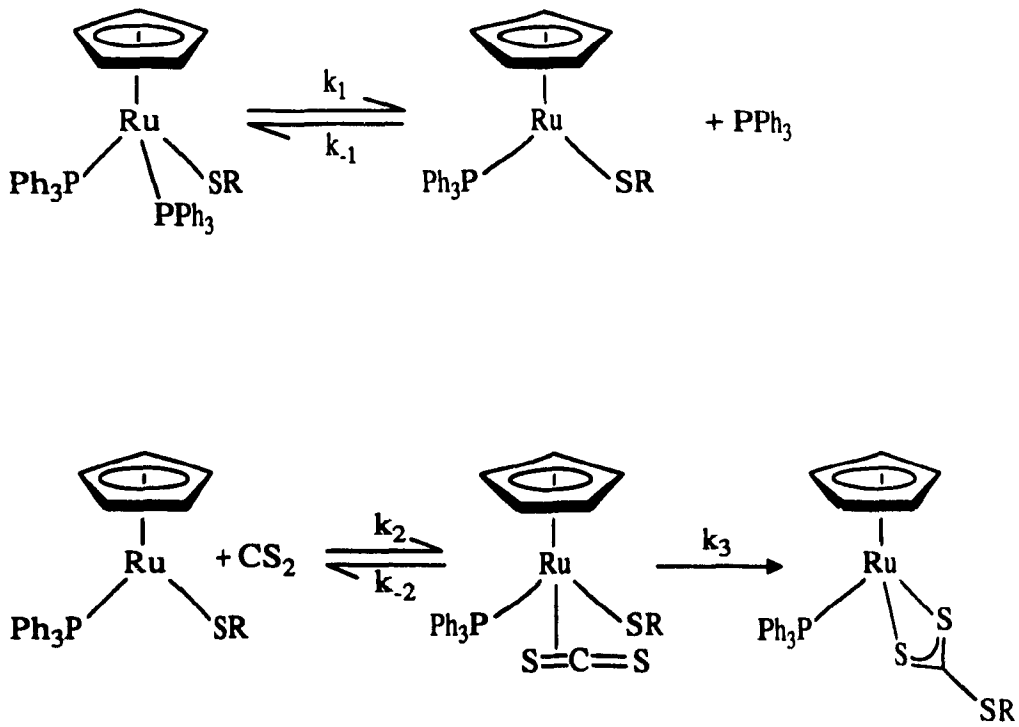

Scheme 2.3 Mechanism of insertion of CS_2 into Ru-SR bonds of **1b-d**.

law based on inhibited enzyme kinetics[57] shown in equation 2.6. Integration of this equation gives an expression of time as a function of concentration shown in equation 2.7. Since X in equation 2.7 appears as a logarithmic term and a linear term, the concentration term within X cannot be isolated and therefore, the standard form of the integrated kinetic equation could not be derived. Equation 2.7 can be simplified to equation 2.8 by introducing constants C_1, C_2 and C_3 as defined in equation 2.8. When $C_3 = [CpRu(PPh_3)_2SR]_o$, which is the initial concentration of **1b** (i.e. $[PPh_3]_o = 0$), and using the observed rate in the absence of added PPh_3, then the value of C_1 and C_2 can be calculated by computer iteration[58] to fit curve A with the data in Figure 2.2 ($C_1 = 1.2 \times 10^4$, $C_2 = -1.00$). If C_1 is multiplied by four to simulate a four fold decrease in $[CS_2]$, and the previous values of C_2 and C_3 are used, then the curve B is obtained.

$$\frac{d\,[CpRu(PPh_3)S_2CSR]}{dt} = \frac{V_S}{\dfrac{K_S\,[PPh_3]}{K_I\,[CpRu(PPh_3)_2SR]} + 1} \qquad (2.6)$$

where $V_S = k_3[CS_2]$

$$K_I = \frac{[CpRu(PPh_3)SR][PPh_3]}{[CpRu(PPh_3)_2SR]}$$

$$K_S = \frac{k_{-2} + k_3}{k_2} \quad \text{(Michaelis constant)}$$

$$t = \frac{K_S}{V_S K_I}\left\{\left(\frac{K_I}{K_S} - 1\right)[CpRu(PPh_3)_2SR]_o X - \left([CpRu(PPh_3)_2SR]_o + [PPh_3]_o\right)\ln(1-X)\right\} \qquad (2.7)$$

where $X = \dfrac{[CpRu(PPh_3)S_2CSR]}{[CpRu(PPh_3)S_2CSR] + [CpRu(PPh_3)_2SR]}$

$$t = C_1\{C_2[CpRU(PPh_3)_2SR]_o X - C_3 \ln(1 - X)\} \qquad (2.8)$$

where: $C_1 = \dfrac{K_S}{V_S K_I}$ $\quad C_2 = \dfrac{K_I}{K_S} - 1$ $\quad C_3 = [CpRu(PPh_3)_2SR]_o + [PPh_3]_o$

Finally multiplying C_3 by three to simulate addition of two equivalents of PPh_3 gave curve C. These calculated curves agree very well with the data collected by NMR

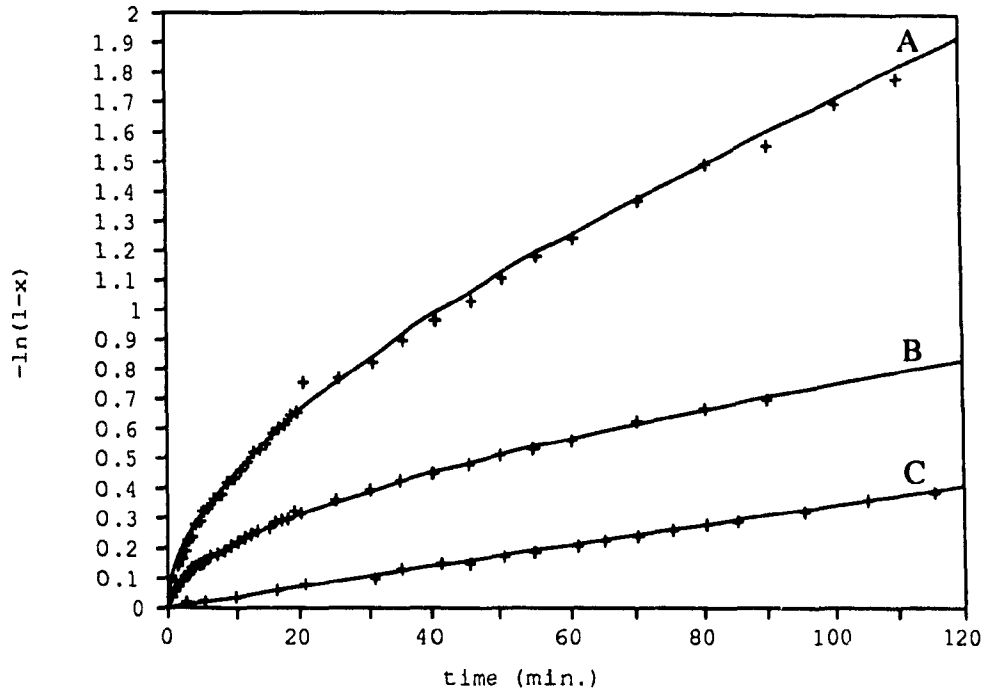

Figure 2.2 Calculated curves and experimental rate data for the reaction of **1b** with CS_2:
A) [**1b**]$_o$: [CS_2] = 1 : 385 with no PPh_3
B) as in a) [**1b**]$_o$: [CS_2] = 1 : 96
C) as in a) with [PPh_3]$_o$ = 2[**1b**]$_o$

studies. Using the values of C_1, C_2 and C_3, one can estimate $\frac{K_I}{K_S} = 2\text{x}10^{-4}$ and $k_3 = 0.12$ sec^{-1}; however, these values are subject to large uncertainties because small errors in measurements of initial concentrations of the reagents result in large errors in measurements of these values.

Based on the observations and the success in the prediction of the kinetic model, one may be confident that the mechanism involved in the insertion of CS_2 into the ruthenium thiolato bonds of **1b-d** is path A (Scheme 2.3). This is in contrast with the observed mechanism of insertion of CO_2 into the metal alkoxy bond which proceeds via an electrophilic attack analogous to path B.[55] The most likely reason for

the difference is that the thiolato ligand is a better pπ-dπ donor than the alkoxy ligand and therefore, the $16e^-$ intermediate in path A is more effectively stabilized. For the alkoxides, the only available mechanism is path B. Two factors also contribute to the different mechanisms of these reactions: 1) CO_2 is a better electrophile than CS_2 and 2) CS_2 is expected to be a better ligand than CO_2.

The reaction of **1a** with CS_2 did not give simple analogs of **6b-d**. While the colour change and the changes in the NMR spectrum suggested incorporation of CS_2, evolution of H_2S suggested further reaction. The presence of the S_2CSR moiety was confirmed by IR spectroscopy; the bands at 964 and 907 cm^{-1} were, by comparison with **6b-d**, **1b-d** and literature values[44], assigned to the delocalized C-S bond stretching modes. The mass spectra detected a parent ion and a fragmentation pattern consistent with the formulation $Cp_2Ru_2(PPh_3)_3(CS_3)$. NMR spectroscopy clearly indicated the presence of two different CpRu moieties, one with two PPh_3, the other with one PPh_3. By analogy to Scheme 2.3, it is reasonable to propose initial CS_2 insertion into the Ru-SH bond to give $CpRu(PPh_3)(CS_3)SH$, **6a**, followed by the rapid reaction of **6a** with **1a** to give **6e** as in Scheme 2.4. The CS_3^{-2} moiety has been observed as a bidendate ligand on one metal[60] and also as a tridendate bridge between two metal centers[59] as proposed for **6e**. Careful monitoring of the NMR spectrum of **1a** in C_6D_6/CS_2 gave no evidence of **6a**. Perhaps the concentration of **6a** never reached detectable limits due to its high reactivity toward **1a**. Further reaction of **6e** with CS_2 was observed after 5 days. The new complex, **6f**, was found to have 2 Cp signals, and two PPh_3 in different environments. A new IR band at 1263 cm^{-1} indicated the presence of a terminal thiocarbonyl group. A likely structure of **6f** is given in Scheme 2.4. It is conceivable that **6e** reacted with CS_2 to form a thiocarbonyl complex and PPh_3S.[61] The complex $CpRu(PPh_3)_2Cl$ has previously been observed to react with CS_2 at 130°C (toluene) to

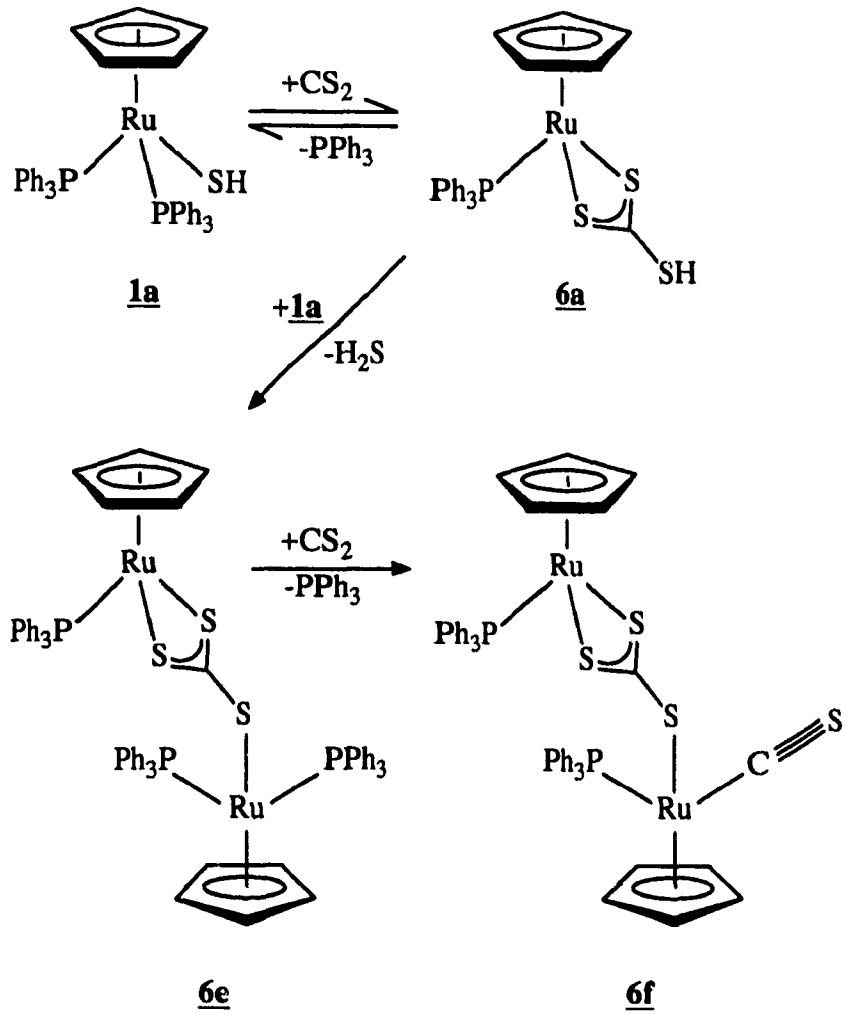

Scheme 2.4 Proposed reaction scheme for the reaction of 1a with CS_2.

form $CpRu(PPh_3)(CS)Cl$.[62] Reactions of CS_2 with transition metal complexes in the presence of PPh_3 have been studied and are known to proceed via π-bonded CS_2 followed by sulfur abstraction by PPh_3.[63] The presence of PPh_3S could not be confirmed due to overlap with the bonded PPh_3 in the ^1H NMR spectrum. It is possible that one of the contaminants observed in the NMR spectra of 6e was due to 6f. The

contaminants appeared late in the course of the reaction which is consistent with this interpretation. The slow rate of the reaction from **6e** to **6f** has made further investigation difficult.

CHAPTER 3

The Reaction of $CpRu(PPh_3)_2SR$ (R = 4-C_6H_4Me, 1-C_3H_7, $CHMe_2$) with SO_2

INTRODUCTION

Environmental concerns about SO_2 in the atmosphere have prompted interest in its reaction with metal complexes with respect to potential fixing reactions for the removal of SO_2 from stack emission and to also supply insight into the mechanism of the Claus process.

Sulfur dioxide can bond directly to the metal via ligand displacement reactions.[65,66,67,68] Metal-bonded SO_2 occurs in a variety of geometries.[65,68] It has

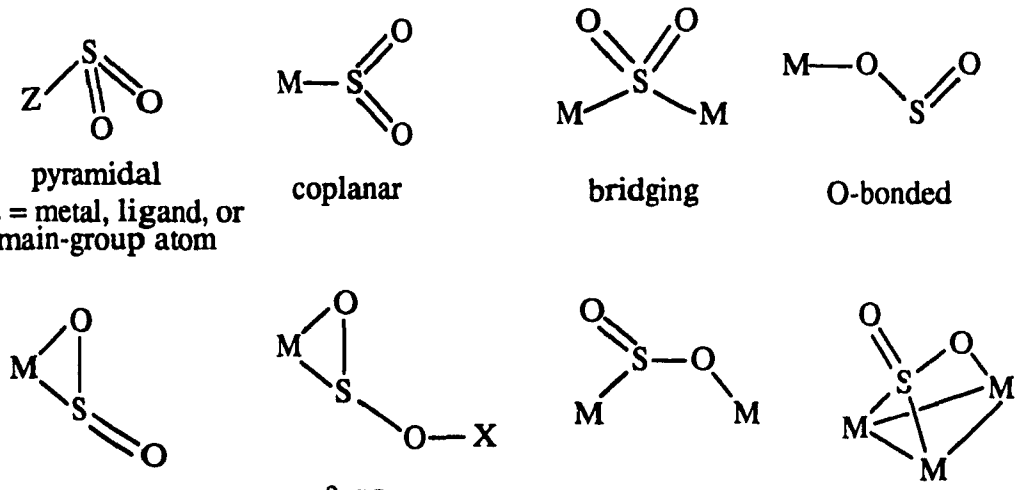

been shown that coplanar metal-bonded SO_2 can donate electron density through its HOMO while accepting electrons by back donation from the metal d orbital into its LUMO, the SO_2 $3b_1$ orbital which has the appropriate symmetry for interaction with

the metal d orbital.[67] The electron-accepting ability of SO_2 is superior to that of CO.[69]

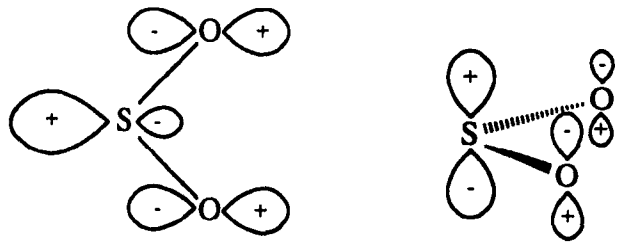

$8a_1$ (HOMO) $3b_1$ (LUMO)

Figure 3.1 The frontier orbitals of SO_2.

Sulfur dioxide can also form adducts to metal ligands. Pyramidal SO_2 is the preferred type of bonding for all ligand-bonded SO_2 and some electron rich metal-bonded SO_2.[66] In this geometry, SO_2 uses its LUMO to accept electron density from a donor atom such as I, N or S.[70] In the case of inorganic thiolates, only

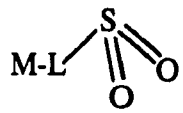

Ligand-bonded
M-L = $Pt(CH_3)(PPh_3)_2I$

$Cu(PMe_3)_2(SPh)(SO_2)$[70a], $Pt(PPh_3)_2(SPh)_2(SO_2)_2$[70a] and $CpW(CO)_2(PPh_3)S(SO_2)R$[23] have been reported, and only $Cu(PPh_2Me_3)_3(SPh)(SO_2)$ has been characterized by x-ray chrystallography. Interestingly, organic sulfides and disulfides have not been reported to interact with SO_2. Consequently, further studies of ligand interaction with SO_2 seem to be a natural progression of the study of metal thiolates.

In this work, the complexes $CpRu(PPh_3)_xSR{\bullet}(SO_2)_{3-x}$, where x = 1,2, were prepared from $CpRu(PPh_3)_2SR$ and observed by NMR spectroscopy. Using kinetic experiments, the mechanism of the reaction has been determined. The structure of $CpRu(PPh_3)(SO_2)S(SO_2)(4\text{-}C_6H_4Me)$ was determined by x-ray crystallography.

Sulfur dioxide was found to insert in metal alkyl bonds[25,64], as well as in metal hydride bonds[65].

$$M\text{-}CR_3 + SO_2 \longrightarrow M\text{-}\overset{\overset{O}{\|}}{\underset{\underset{O}{\|}}{S}}\text{-}CR_3 \qquad (3.1)$$

Where M = Fe, Re, Ru, Mn, Mo, W, Cr

$$CpM(CO)_3H + SO_2 \longrightarrow CpM(CO)_3(\text{-}\underset{\underset{O}{\|}}{S}\text{-}O\text{-}H) \qquad (3.2)$$

Where M = Mo,W

RESULTS

The complexes $CpRu(PPh_3)_2S(SO_2)R$, **7b-d**, and $CpRu(SO_2)(PPh_3)S(SO_2)R$, **8b-d**, where R = 4-$C_6H_4Me$, 1-$C_3H_7$ and $CHMe_2$, were observed through a series of experiments monitored by ^1H NMR spectroscopy. Monitoring the reaction by IR spectroscopy in solution was attempted but failed due to the strong free SO_2 stretching band which masked the bonded SO_2 bands. Due to their instabilities, only the complex $CpRu(SO_2)(PPh_3)S(SO_2)(4\text{-}C_6H_4Me)$, **8b**, was isolated. The following is a description of the relevant NMR-scale experiments and their results.

NMR samples of **1b-d** were prepared (7-10 mg of **1b**, **1c** or **1d** in 0.7 mL of C_6D_6). A rapid stream of SO_2 was bubbled through the sample for 15 minutes, at which time the solution became darker red. The NMR spectra showed peaks due to two Cp signals corresponding to intermediates **7b** and **7c** and final products **8b** and **8c**, see equation 3.3. When **1d** was reacted with SO_2, only one Cp signal was observed in

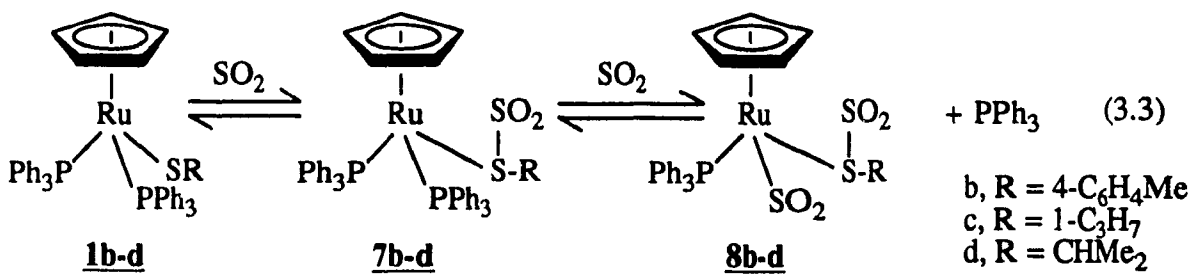

the NMR spectrum and was assigned to the final product **8d**. The NMR data are listed in Table 3.1. Following the treatment of **1b-d** with SO_2, the phenyl region of the NMR spectra always displayed a complicated pattern of three bands in the ranges 6.82-7.24 ppm, 7.04-7.40 ppm and 7.40-7.65 ppm. The band at 7.27-7.40 ppm corresponds to the ortho protons of free PPh_3 and the band at 7.40-7.65 ppm corresponds to the ortho protons of bonded PPh_3. The third band at 6.82-7.24 ppm was assigned to a mixture of

Table 3.1 ^1H NMR spectra after 15 minutes of rapid SO_2 flow through solutions of **1b-d**. The relative intensities are listed in parentheses.

	4-C_6H_4Me		1-C_3H_7		$CHMe_2$	
	7b	**8b**	**7c**	**8c**	**7d**	**8d**
Cp	4.48 (s, 5)	5.01 (s, 15)	4.60 (s, 25)	4.95 (s, 5)	Not observed	5.06(s, 5)
CH	—	—	—	—	Not observed	2.85 (sept, 1)
CH_2	—	—	1.50 (m, 10) 2.20 (m, 10)	1.52 (m, 1) 2.33 (m, 1) 2.46 (m, 2)	—	—
CH_3	2.13 (s, 3)	2.09 (s, 9)	0.70 (t, 15, J_{H-H}= 7.2 Hz)	0.80 (t, 3, J_{H-H}= 7.4 Hz)	Not observed	1.26 (d, 3, J_{H-H}= 6.6 Hz) 1.32 (d, 3, J_{H-H}= 6.8 Hz)
Bonded PPh_3	6.82 - 7.22 (m, 80) 7.40 - 7.65 (m, 30)		6.90 - 7.04 (m, 108) 7.25 - 7.65 (m, 22)		Not observed	7.05 - 7.24 (m, 18) 7.43 - 7.65 (m, 6)
Free PPh_3	7.27 - 7.40 (m, 18)		7.04 - 7.20 (m, 66)		Not observed	7.26 - 7.40 (m, 6)
4-C_6H_4Me	Not observed	6.94 (d, 1, J_{H-H}= 8.4 Hz)	—	—	—	—

resonances corresponding to the meta and para protons of free and bonded PPh_3. With the integrals of the bands at 7.27-7.40 ppm and 7.40-7.65 ppm, one can obtain the ratio of free PPh_3 to bonded PPh_3. These ratios were 3:5 and 1:1 for **1b** and **1d** respectively. It was impossible to measure this ratio for **1c** due to overlap of the bands. The corresponding ratios of Cp signals were 1:3, 1:5 and 0:1 for **7b**:**8b**, **7c**:**8c** and **7d**:**8d** respectively. By comparing the integrals of the Cp peaks and the PPh_3 peaks, one can assign two PPh_3 for **7b-d** and 1 PPh_3 for **8b-d**.

Further bubbling of SO_2 produced more **8b** and **8c** at the expense of **7b** and **7c**. A complete conversion of **1b** to **8b** was achieved by continued bubbling for 4 hours, while bubbling for 15 minutes through the solution of **7c** gave enrichment of **8c** for a final ratio of **7c**:**8c** of 1:6. Eventually, in all cases, one equivalent of free PPh_3 was observed at the end of the reaction. A signal was observed for **8b** at 6.94 ppm (J_{H-H}= 8.6 Hz) which was assigned to one of the doublets arising from the AB quartet of the 4-C_6H_4Me group. The spectra of the complexes **8b-d** are listed in Table 3.1. It must be pointed out that the chemical shifts of this series are dependent on the SO_2 concentration. In all the experiments, PPh_3S was observed in trace amounts as a distinctive band at 7.56-7.66 ppm.

Excess PPh_3 was added to NMR samples of **1b** and **1d**, 30 and 13 equivalents respectively, before addition of SO_2 for 15 minutes. The results are illustrated in Table 3.2. In both cases, **8b** or **8d** was not observed. In the case of **1b**, a mixture of **1b** and **7b** was observed in the ratio of 1.5:1. In the case of **1d**, only peaks due to **7d** were observed. The phenyl region of **1d** showed a ratio of bonded to free PPh_3 of 2:13 before addition of SO_2, and did not change after the reaction, indicating no loss of PPh_3. The reaction was followed for 1 hour with no further change.

When a solution of **1b** (10 mg) in C_6D_6 (0.7 mL) was treated with SO_2 gas for 10 minutes, an orange precipitate formed. The NMR spectrum of the slurry showed a

Table 3.2 ^{1}H NMR data for the reactions of **1b,d** with SO_2 in the presence of free PPh_3 The relative intensities are shown in parentheses.

	4-C_6H_4Me		$CHMe_2$	
	1b	**7b**	**1d**	**7d**
Cp	4.27 (s, 7.5)	4.64 (s, 5)	Not observed	4.77(s, 5)
CH	—	—	Not observed	2.83(sept, 1)
CH_3	2.15 (s, 4.5)	2.08 (s, 3)	Not observed	1.48 (d, 3, J_{H-H}= 8.4 Hz) 1.51 (d, 3, J_{H-H}= 6.0 Hz)
Bonded PPh_3	6.82-7.13(m, 315) 7.51-7.71(m, 30)		Not observed	6.90 - 7.10(m, 135) 7.50 - 7.82 (m, 12)
Free PPh_3	7.30-7.53(m, 180)		Not observed	7.32 - 7.46 (m, 78)
1-C_6H_4Me	7.84 (d, 1, J_{H-H}= 8.6 Hz)	Not observed	—	—

mixture of **7b** and **8b** in ratio of 1:1 and no **1b**. Rapidly evaporating the slurry to dryness under vacuum and dissolving the residue in C_6D_6 showed no **7b** and a 1:1 ratio of **8b** and **1b**. The true chemical shifts of **8b** may be evaluated in the absence of SO_2. Two singlets due to the methyl group and the Cp ring were observed at 2.09 ppm (s, 3H) and 4.63 ppm (s, 5H). Two bands at 6.84-7.08 ppm and 7.46-7.74 ppm were assigned to the meta/para protons and otho protons of the PPh_3. A doublet at 7.87 ppm (J_{H-H}= 7.6 Hz, 2H) was assigned to the aromatic protons of the 4-C_6H_4Me group. The other protons of this AB quartet are assumed to be part of the PPh_3 bands. When SO_2 was bubbled again through the solution, **1b** disappeared and **7b** reappeared with **8b** unchanged, in the ratio 1:1. The resulting slurry of deep red solution and orange precipitate was filtered. The NMR spectrum of the filtrate was enriched in **8b** at the expense of **7b**, indicating that the orange precipitate was mostly the latter. The NMR spectrum of the orange precipitates showed a mixture of **8b** and **1b**. Upon resting, the orange precipitate darkened as **1b** reformed. These experiments indicate the facile

reversibility of the reaction from **1b** to **7b** and the slow reversibility **1b** or **7b** with **8b**, equation 3.4.

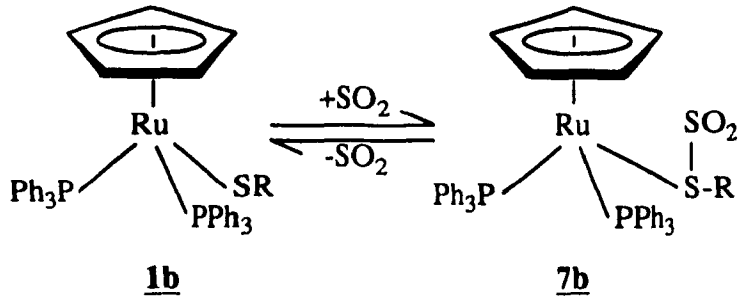

(3.4)

The reaction of **1b** with SO_2 was monitored as a function of time at high and at low concentrations of SO_2. The resulting spectra are shown in Figures 3.2 and 3 3. At high concentrations of SO_2 (continuous rapid flow of SO_2), the reaction was observed to proceed from **1b** to a mixture of **7b** and **8b** (1:1) in 10 minutes, spectrum *ii*. After 1 hour, the reaction mixture consisted of a ratio of **7b**:**8b** of 1:9, spectrum *iv*. On the other hand, at low concentration of SO_2 (0.5 mL SO_2 gas in 0.7 mL of solution), the reaction mixture consisted of **1b** and **8b** (1:6) after only 2 minutes, spectrum *ii*. After 10 minutes, the spectrum had not changed further. Addition of another 0.5 mL SO_2 at 12 minutes from the beginning of the reaction gave enrichment of **8b** at the expense of **1b** without the presence of **7b**, spectrum *iii*. Purging the resulting product with N_2 for 20 minutes gave a ratio of **1b**:**8b** of 3:2 with no sign of **7b**, indicating reversibility of reaction **7b** to **8b** as in equation 3.5, spectrum *iv*.

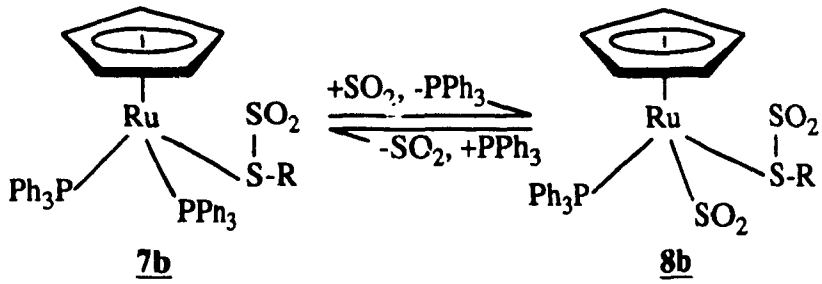

(3.5)

The complex **8b** was isolated by reacting a concentrated solution of **1b** in THF

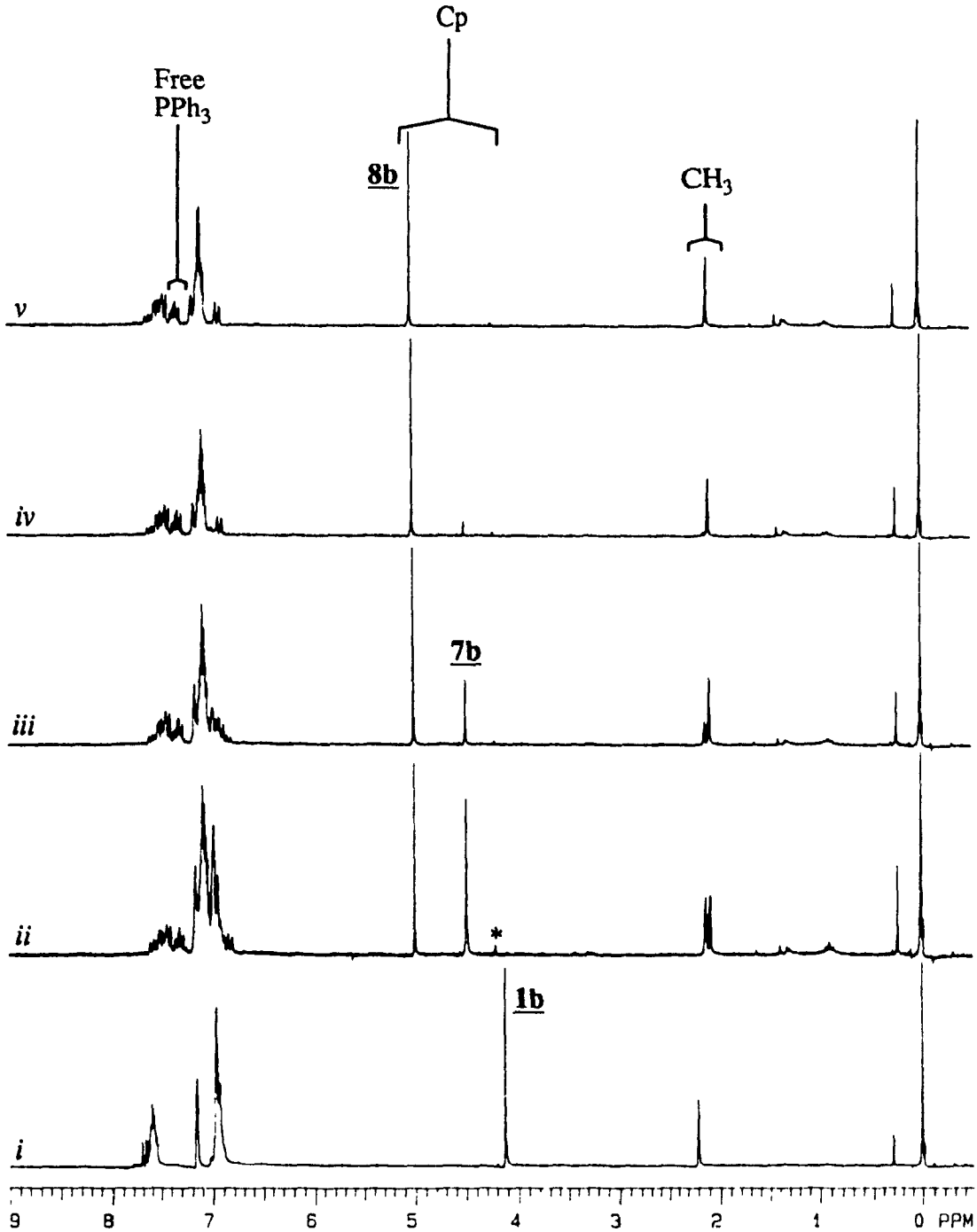

Figure 3.2 Reaction of SO_2 with **1b** at high concentration of SO_2;
(*i*) before beginning of reaction;
(*ii*) 10 minutes after beginning of reaction;
(*iii*) 30 minutes after beginning of reaction;
(*iv*) 1.0 hour after beginning of reaction;
(*v*) 3.5 hours after beginning of reaction.
* = contaminant

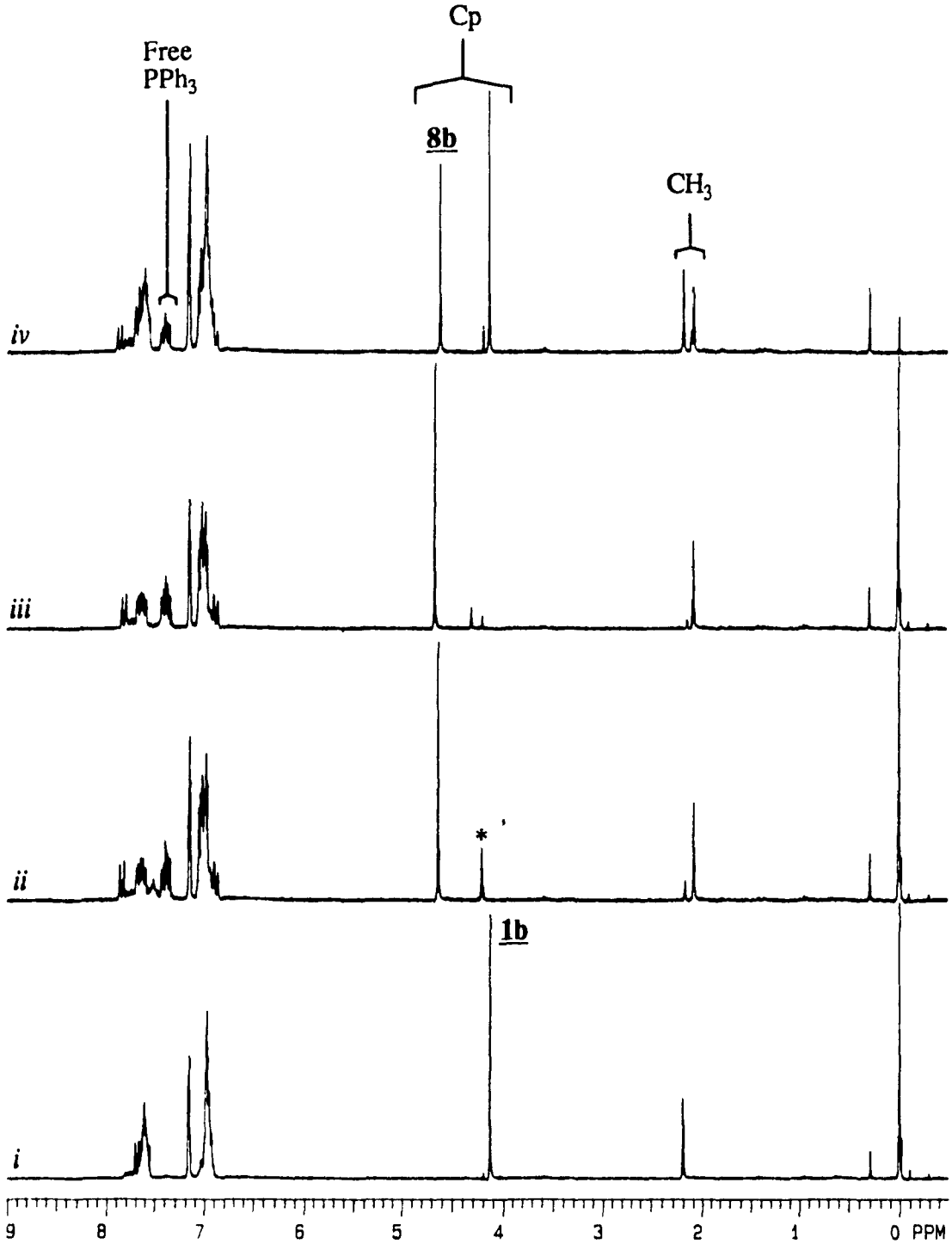

Figure 3.3 Reaction of SO_2 with **1b** at low concentration of SO_2;
(*i*) before beginning of reaction;
(*ii*) 2 minutes after addition of 0.5 cc SO_2;
(*iii*) 12 minutes after addition of initial 0.5 cc SO_2 and 2 minutes after addition of a further 0.5 cc SO_2;
(*iv*) sample from spectra *iv* after 20 minutes of purging with N_2.
* = contaminant

with SO_2 at room temperature and pouring the solution into Et_2O which had been previously saturated with SO_2. The complex **8b** is not very soluble, however, PPh_3 is very soluble in ether. In this way, air stable purple crystallographic grade crystals of **8b** could be obtained by decanting the mother liquor containing PPh_3. The yield of this process was rather low, 34%, and was not optimized. Elemental analysis of **8b** indicated the empirical formula $CpRu(SO_2)_2(PPh_3)S(4\text{-}C_6H_4Me)$. The IR spectrum showed two $\upsilon_{(SO)}$ stretches at 1258 and 1283 cm^{-1}. The crystal structure was determined and is displayed in Figure 3.4.[71] The crystal data, atom coordinates, anisotropic thermal factors and selected bond lengths and angles are listed in Appendix III, Tables A3.1-A3.4. The structure is a piano stool with two SO_2 moieties, one bonded pyramidally to the thiolate ligand and the other coplanarly bonded to the metal. The thiolate sulfur lies 2.719(18) Å out of the plane of the SO_2 bonded to it. This geometry is normal for ligand-bonded SO_2 fragments.[70a,b] The Ru metal lies 0.053(19) Å out of the plane of the metal-bonded SO_2 and is considered coplanar. This geometry of bonding is common in metal-bonded SO_2.[24,66,70a] The Ru-S2 bond length is 2.121(3) Å and is close to the range observed for similar complexes (2.0-2.1 Å).[66] The Ru-S1 bond length is 2.382(3) Å and is normal for a Ru-S bond in an $18e^-$ system.[72,73] The Ru-P bond length is 2.3517(25) Å and is slightly longer than for analogous compounds.[74] The S1-S3 bond length is 2.844(5) Å, much longer than that in the copper complex, $Cu(PPh_2Me)_3(SPh)(SO_2)$, whose S-S bond length is 2.530 Å.[70a]

The Cp resonance of pure **8b** in the NMR spectrum showed no broadening when cooled to -65°C. Addition of one and two equivalents of optically pure europium-shift reagent, tris[3-trifluoromethylhydroxymethylene-(+)-camphormato]europium(III) (Eu-Opt), showed no splitting of the Cp resonance in deuterated toluene.

Upon melting, **8b** showed an apparent phase change above 125°C and melting

occured at 138°C. The pungent odor of $SO_2$was detected upon melting. When **8b** was heated to near melting, 130-138°C for 20 minutes, **9b** was produced quantitatively. The NMR spectrum of **9b** showed 1 Cp, one PPh_3 and one 4-C_6H_4Me group. The IR spectrum of **9b** showed only one $\upsilon_{(SO)}$ stretch at 1261 cm^{-1}. These observations imply the loss of an SO_2 fragment as shown in equation 3.6.

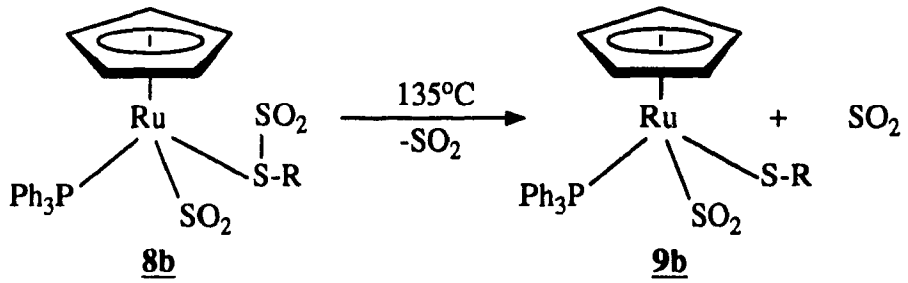

(3.6)

An NMR sample of CpRu(dppe)S(1-C_3H_7), **5d**, was prepared in C_6D_6. A strong stream of SO_2 was bubbled through the sample for 30 minutes. An immediate colour change from yellow to beige was observed. The Cp region had one signal at 4.81 ppm (s, 5H). The phenyl region now had three major bands at 6.85-7.05 ppm (m, 8H), 7.10-7.32 ppm (m, 8H) and 7.38-7.60 ppm (m, 4H) which correspond to the ortho, metha and para protons respectively. The aliphatic region showed four multiplets and one triplet at 2.43 (m, 2H), 1.78 (m, 2H), 1.57 ppm (m, 2H), 1.05 ppm (m, 2H), and 0.60 ppm (t, 3H, J_{H-H}= 7.1 Hz). Further exposure to SO_2 for up to 20 hours gave no further reaction. Apparently, the reaction stopped at the ligand-S adduct and did not proceed further.

The reaction of CpRu(PPh_3)(CO)S(1-C_3H_7), **4d**, with SO_2 gave a new thiolato-adduct **4d**•SO_2 as indicated by the NMR spectrum. After evaporation to dryness under vacuum and redissolving, the complex **4d**•SO_2 remained intact as indicated by the resulting NMR spectrum which did not correspond to **4d**. The NMR spectrum showed a single Cp resonance at 4.86 ppm. The isopropyl R group showed a methyne septet at 2.87 ppm, and the methyl groups were a doublet of doublets at 1.46

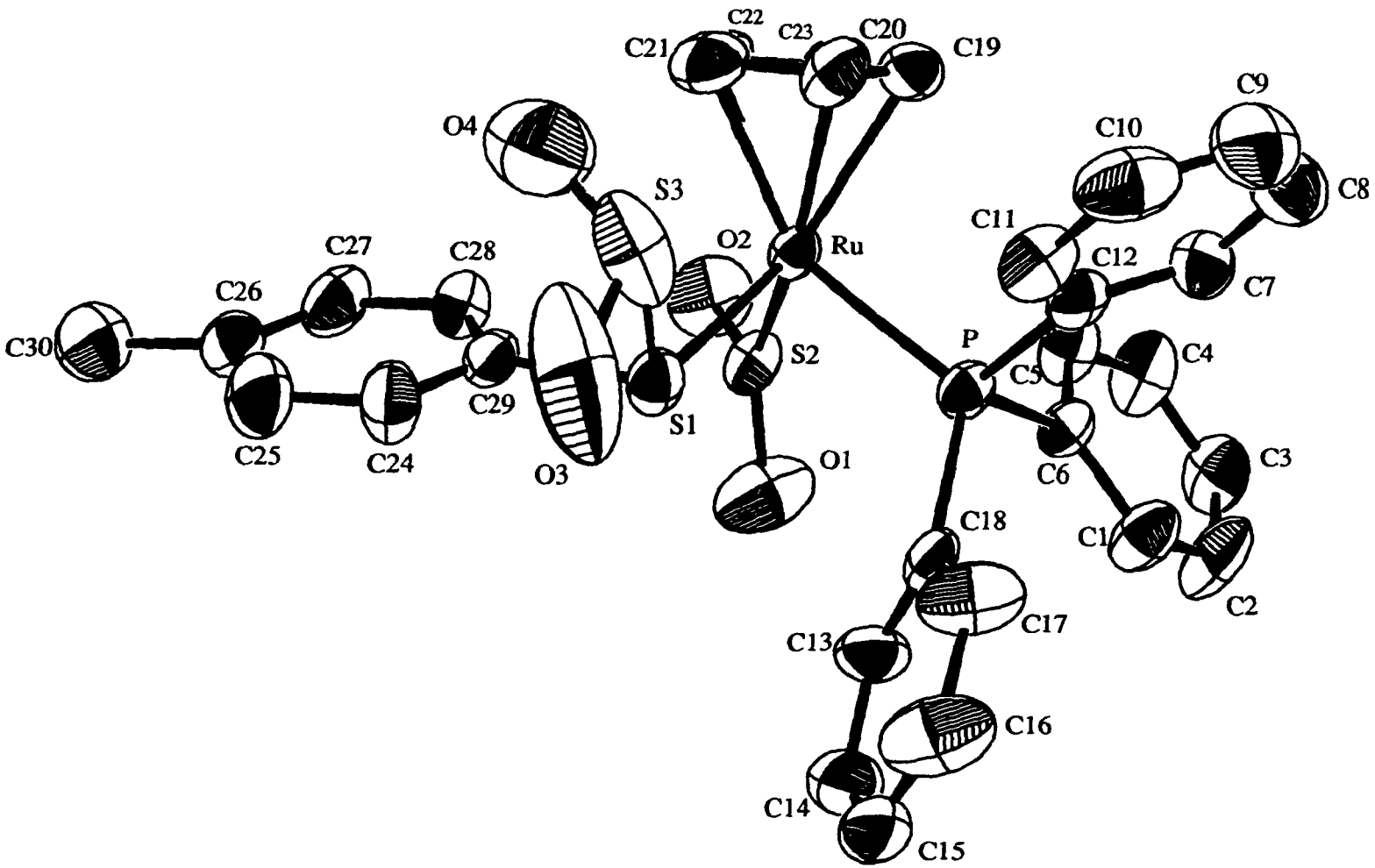

Figure 3.4 ORTEP of $CpRu(PPh_3)(SO_2)S(SO_2)(4\text{-}C_6H_4Me)$, **8b**.

and 1.44 ppm (J_{H-H}= 6.74 Hz). The PPh_3 showed two bands at 7.02 and 7.61 ppm. The Cp resonance showed no broadening when the NMR was recorded at -70°C. The IR spectrum (in C_6D_6) showed a $\nu_{(CO)}$ stretch at 1945 cm^{-1} and the $\nu_{(SO2)}$ stretch band was assigned to the broad band at 1254 cm^{-1}.

DISCUSSION

The insertion of SO_2 into metal alkyls[67,75,76,77] and hydrides[26,78] has previously been reported, as depicted by equations 3.1 and 3.2 (here reproduced). However, the

$$M\text{-}CR_3 + SO_2 \longrightarrow M\text{-}\overset{\overset{O}{\|}}{\underset{\underset{O}{\|}}{S}}\text{-}CR_3 \qquad (3.1)$$

Where M = Fe, Re, Ru, Mn, Mo, W, Cr

$$CpM(CO)_3H + SO_2 \longrightarrow CpM(CO)_3(\text{-}\underset{\underset{O}{\|}}{S}\text{-}O\text{-}H) \qquad (3.2)$$

Where M = Mo,W

reaction of thiolates with SO_2 has only been documented twice, for $Cu(PPh_2Me)_3SR$ and for $CpW(CO)_3SR$, equations 3.7 and 3.8 respectively.[23,70] In the case of the reactions of $Cu(PPh_2Me)_3SR$ with SO_2, the products are pyramidal SO_2 fragments reversibly bonded to the thiolato sulfur.[70a] Equation 3.8 is believed to be under fast

$$(PPh_2Me)_3Cu\text{-}S\text{-}R + SO_2 \rightleftharpoons (PPh_2Me)_3Cu\text{-}\overset{\overset{O}{\|}}{\underset{\underset{O}{|}}{S}}\text{-}R \qquad (3.7)$$

$$CpW(CO)_2(PPh_3)(S\text{-}R) + SO_2 \rightleftharpoons CpW(CO)_2(PPh_3)(\overset{\overset{O}{\|}}{\underset{\underset{O}{|}}{S}}\text{-}R) \qquad (3.8)$$

exchange condition in the NMR time scale, so that the NMR observed is an averaged spectrum of the two species.[23] However, the products of the reactions between **1b-d** and SO_2 were found to be unique, differing sharply with previously known reactions.

The reactions were monitored by NMR spectroscopy, whereby intermediates,

7b-d, were first observed and the final products, 8b-d, were eventually formed. The ^1H NMR study at high concentration of SO_2 showed that intermediates 7b-c contain two PPh_3 groups as well as a chiral center, as shown by diastereotopic methyl protons for 7c. The IR spectra could not be obtained because 7b-d could not be isolated as pure products, as they only survived in the presence of free SO_2. The observation of the $\nu(SO_2)$ bands during the course of the reaction was prevented by the strong free SO_2 band which lies in the same region. The complexes 8b-c were found to increase in concentration at the expense of 7b-c as the reaction proceeded. Also, the production of free PPh_3, as detected in the NMR spectrum, was found to parallel the production of 8b-c. It was therefore concluded that 8b-c were produced from 7b-d through the loss of PPh_3. In the case of 8d, there was no evidence of 7d in the NMR spectra. Paths **A** and **B** are proposed (Scheme 3.1) to account for these observations. The SO_2 moiety on the thiolates of 7b-d is assumed to be pyramidally bonded based on the similarity with the Cu complex. The observed reversibility of reaction **A** for 1b supports the assignment of 7b-d because such $MS(SO_2)R$ adducts readily and reversibly lose SO_2, although in the case of 7b-d and in contrast with $CpW(CO)_2(PPh_3)SR$, the rate of exchange is slow in the NMR time scale as shown by the chiral sulfur.[23,66] In step **B**, loss of PPh_3 was concomitant with formation of 8b-c; presumably the intermediate in this step is the $16e^-$ species $CpRu(PPh_3)S(SO_2)R$ which quickly binds SO_2 to form 8b-d. Addition of excess PPh_3 before addition of SO_2, should inhibit the formation of the $16e^-$ intermediate between 7b-d and 8b-d in path **B**, and consequently, the reaction cannot proceed and, as observed, 8b-d do not form. Exploitation of this led to the trapping of 7d which was observed in the NMR spectrum. If ligand loss is not possible, as in the cases $CpRu(dppe)S(1\text{-}C_3H_7)$ and $CpRu(PPh_3)(CO)S(1\text{-}C_3H_7)$, then only adducts form, and further reaction does not proceed, in agreement with the proposed

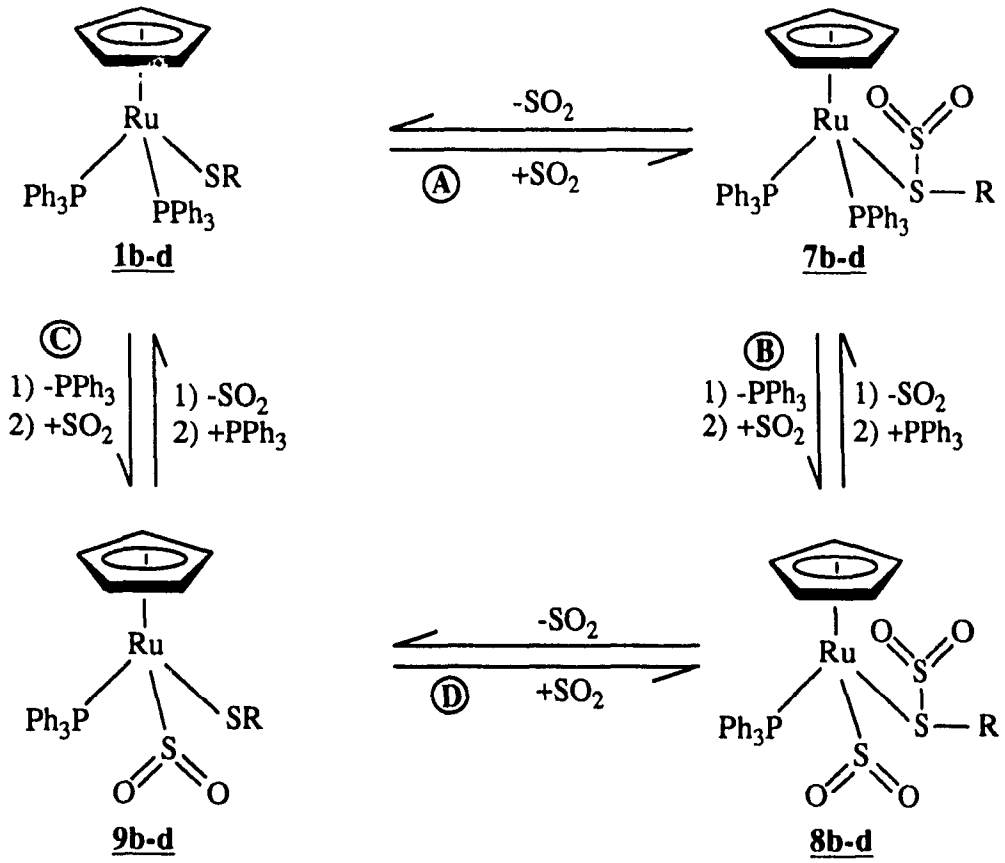

Scheme 3.1 Proposed mechanism of the reactions between **1b-d** and SO_2.

scheme. Furthermore, the carbonyl complex **4d** reacted with SO_2 to form a stable SO_2 adduct, **4d**•SO_2.

Observations in the early stage of the reaction of **1b** with low concentration of SO_2 suggested that complex of **8b** was produced rapidly at first, followed by slower production as the SO_2 concentration increased. To resolve this apparent paradox, the reaction was monitored under conditions of low concentration and at high concentration of SO_2 and the results are shown in Figures 3.2 and 3.3. Because the spectra remained unchanged from 2 to 10 minutes (see Figure 3.3), and further addition

of SO_2 was required to change the spectra, we may conclude that the conversions of **1b** to **8b** is very rapid at low concentration of SO_2. The product distribution is dependent on SO_2 concentration and not on time (that is, the reaction reaches equilibrium within 2 minutes). The concentration of **7b** was never high because at low concentrations of SO_2, equilibrium **A** lies far toward **1b**. The reaction appeared to proceed directly to **8b** possibly via an unobserved intermediate **9b**, as indicated by paths **C** and **D** in Scheme 3.1.

Contributions of both pathways (**A-B** and **C-D**) may be invoked to resolve the results from the high concentration SO_2 experiment. As the concentration of SO_2 increases, the SO_2 molecule will bind to all available sites as quickly as possible. We know from the results of the CS_2 reactions that **1b-d** exist in equilibrium with the $16e^-$ species $CpRu(PPh_3)SR$. When the solutions of **1b-d** are first exposed to low concentrations of SO_2, they will bind to this unsaturated species to form **9b-d** through path **C**. As soon as **9b-d** are formed, they react further with SO_2 to form **8b-d**. At the same time, SO_2 will bind to **1b-d** to form **7b-d**, via path **A**. The low concentration experiment indicates that paths **C** and **D** are favored at low concentrations of SO_2. The concentrations of **8b-d** will therefore rise quickly through paths **C** and **D** as **1b-d** are depleted through both paths. Eventually, **1b-d** will be consumed and some **7b-d** and much **8b-d** will be observed. If the concentration of SO_2 rises very quickly, as in the case of the high concentration experiments, then the reverse reaction of path **A** becomes negligible. When **7b-d** are formed, the SO_2 moiety acts as a Lewis acid and attacks the electrons in the filled p orbital of the thiolato sulfur for bonding. Through rehybridization of the thiolato sulfur, the ability to donate electron density to the metal through $p\pi$-$d\pi$ donation (Figure 1.5) should be reduced because the filled sulfur p orbital is no longer available. The $16e^-$ intermediate, $CpRu(PPh_3)S(SO_2)R$, which is

implied in path **B** should be less well stabilized and consequently, step **B** should be inherently slower than step **C**.

In the case of **1d**, the $CHMe_2$ group is more electron donating than the other R groups and tends to better stabilize the $16e^-$ species $CpRu(PPh_3)S(CHMe_2)$ which consequently should exist at higher concentrations. When SO_2 is added, **8d** could be formed so quickly through paths **C** and **D** that **7d** is not observed. Alternately, if **7d** was formed, then the electron-donating R group might stabilize the intermediate formed from **7d**, i.e. $CpRu(PPh_3)S(SO_2)(CHMe_2)$, such that reaction **B** proceeds rapidly and **7d** is not observed.

The reverse reactions of **A** and **D** were observed. When a mixture of **7b** and **8b** was stripped to dryness, a mixture of **1b** and **8b** was observed. This indicated that **7b** lost SO_2 via path **A** much faster than **8b** did via paths **D** and **C** or path **B**. Consequently, it may be concluded that thiolate-bonded SO_2 in **7b** is more labile than the thiolate-bonded SO_2 in **8b**. In the absence of PPh_3 and SO_2, **8b** was found to be stable in solution.

By separating free PPh_3 from **8b-d**, one would eliminate the reverse reactions of paths **C** and **B**. When a saturated ether solution of **7b** and **8b** was filtered and left under SO_2, **7b** slowly converted to **8b**. Diethyl ether is a poor solvent for **7b** and **8b** but is an excellent solvent for PPh_3. The presence of free PPh_3 in solution was desired so as to slow the reaction path **B**. As the concentration of **8b** slowly increased, it crystallized to give crystallographic-grade crystals which were quickly isolated by decanting the solvent along with free PPh_3 produced in the reaction.

X-ray studies of **8b** indicated two SO_2 moieties, a pyramidal ligand-bonded SO_2 and a coplanar metal-bonded SO_2, as shown in Figure 3.4. The dual mode of bonding makes this complex quite unique. The ligand-bonded SO_2 is typical of other

ligand-bonded SO_2 groups, where the SO_2 fragment acts as a Lewis acid.[70a] In complex **8b**, the angle (α) between the S1→S3 vector and the SO_2 plane is 17°. The

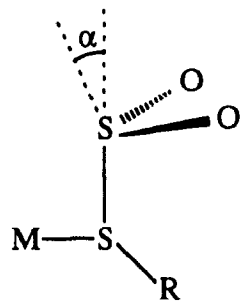

only other structurally determined analog is $Cu(PPh_2Me)_3(S(SO_2)Ph)$, where α is 35°.[70] In amine-bonded SO_2 complexes, α was measured as 15-22°.[79] The Lewis acid character of SO_2 may be defined as the contribution of the empty $3b_1$ orbital of the SO_2 fragment in bonding, see Figure 3.1 (here reproduced). Therefore, the extent of the

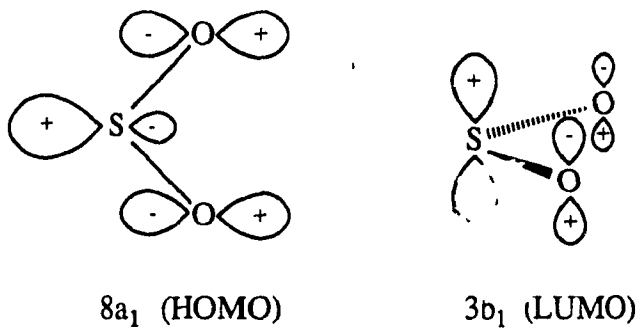

Figure 3.1 The frontier orbitals of SO_2.

Lewis acid character of SO_2 is inversely proportional to α. At the extreme, when α is 0, then the SO_2 moiety utilizes exclusively its $3b_1$ orbital in bonding and may then be considered a pure Lewis acid. Consequently, compared to other examples such as the Cu complex, the ligand-bonded SO_2 in **8b** has a strong Lewis acid character. The SO_2 $3b_1$ orbital has a high p character, whereas the $8a_1$ orbital is sp^2 hybridized. Ligand-SO_2 bonds involving a large $3b_1$ contribution (small α) would have greater p

character, and therefore might be expected to be longer than if the bond involved less $3b_1$ contribution (large α). Since the ligand-bonded SO_2 in **8b** has a strong Lewis acid character, then a long sulfur-sulfur bond may not be suprising (2.844(5) Å for **8b** versus 2.530 Å for the Cu complex[70]).

The observed loss of the thiolato-bonded SO_2 in **8b** is expected since this bond is much longer than the organic covalent S-S bond length (2.03-2.08 Å[4,82]) and S1-S3 is also much longer than that in the Cu analog. Surprisingly, **8b** retains the thiolate-bonded SO_2 even in the absence of SO_2 in solution, whereas **7b**, $CpW(CO)_2(PPh_3)S(SO_2)R$, and the Cu complex lose SO_2 in solution under the same conditions. Therefore, in this case, the sulfur-sulfur bond length does not seem to be proportional to its bond strength.

The coplanar SO_2 bonded to the ruthenium atom is typical of an SO_2 molecule acting as a Lewis base.[66] The large Lewis base character is shown by the near planarity of the SO_2 moiety with respect to the Ru-S2 bond (i.e. α = 88.6°). The Ru-S2 bond length is 2.121(3) Å. This is unusually short compared to that of $[Ru(NH_3)_4(SO_2)Cl]^+$ (2.223 Å[80]) but within the normal range of other irreversibly-bonded coplanar M-SO_2 bond lengths (2.0-2.1 Å[66]). Also of interest is the S2-Ru-S1-S3 dihedral angle of 171.82°. This angle makes the metal-bonded SO_2 moiety's plane nearly parallel to the S1→S3 vector. Furthermore, the two SO_2 planes are mutually orthogonal (91.1(11)°) This may reflect a long range covalent interaction. Calculations by Ashby of $CpFe(CO)_2SR$ found that the HOMO involves primarily the thiolato-sulfur 3p lone pair, and the metal d_{xz} orbital.[38] This orbital also delocalized into the carbonyl π antibonding orbital. In **8b**, the metal-bonded SO_2 moiety has an empty π orbital, the $3b_1$ orbital, in the proper orientation for interaction in the same manner as a carbonyl, see Figure 3.5.[67,69] These electronic factors may account for the orientation of the

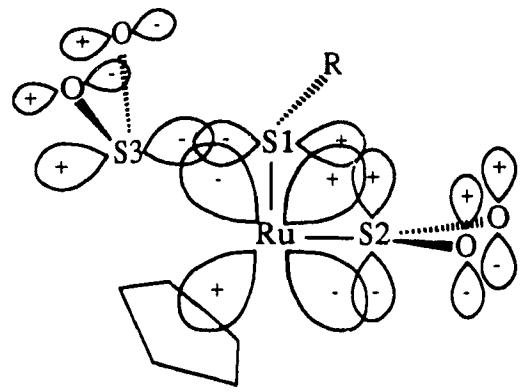

Figure 3.5 The xy plane showing the interaction between the metal d_{xz}, the thiolate-bonded SO_2 LUMO, the metal-bonded SO_2 HOMO, and the 3p orbital on the thiolate.

metal-SO_2 moiety relative to the metal thiolate bond and the thiolate SO_2. Such a delocalization may also account for the unusual stability of the thiolate-bonded SO_2 in **8b**. The complex **4d**•SO_2 can be regarded as an electronic homologue of **8b**, where CO replaces the metal-bonded SO_2 in **8b**. Accordingly, **4d**•SO_2 is also unusually stable with respect to SO_2 loss, even under vacuum.

Another way of looking at **8b** is to mix the LUMO of the thiolate-bonded SO_2, the HOMO of the metal-bonded SO_2, the filled thiolato-sulfur 3p orbital and the empty metal d orbital to generate the simplified MO diagram shown in Figure 3.6. The four orbitals should form four molecular orbitals; two bonding and two antibonding. The four available electrons occupy the 2 lower bonding orbitals which makes an overall stable system.

The structure of **8b** also shows the presence of two chiral centers, one at the metal center and the other at S1. Consequently, there should be a pair of diastereomers observable in the NMR spectrum. The NMR spectra of **8b-d** showed only one Cp resonance each and diastereomeric methyls in the case of **8d**. It might be postulated

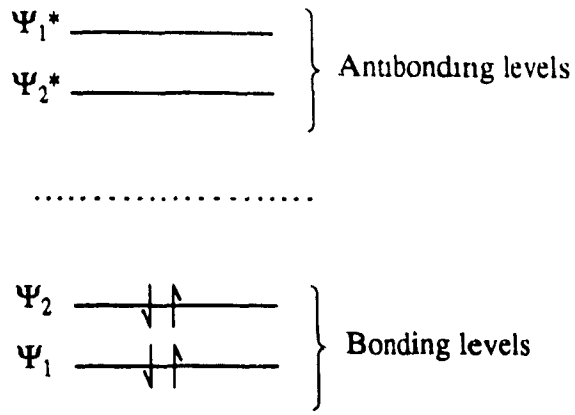

Figure 3.6 General MO diagram of 4 electrons in 4 orbitals.

that the chiral center at S1 does not show chirality in the NMR time scale due to rapid inversion. It is known that when sulfur uses pπ-dπ bonding in its bonding mode with metals, its pyramidal inversion rate is greatly increased.[81] However, variable temperature NMR spectroscopy shows no broadening of the Cp resonance of **8b** at -65°C. Alternately, if strong asymmetric induction occured during the preparations of **8b-d**, then only one of the diastereomers might be produced. The driving force for this asymmetric induction could be a combination of steric and electronic factors. However, in the case of $CpRu(PPh_3)_2S(SO_2)(CHMe_2)$, **7d**, the NMR showed diastereotopic methyls thus indicating a slow thiolate sulfur inversion rate. Since there is no compelling reason to assign a lower barrier to S1 inversion for **8b** than **7d**, the tentative conclusion is that the single set of peaks for the NMR spectrum of **8b** is due to the presence of one diastereomer. It is notable that **4b**•SO_2 should also show diastereomers, however, only one set of peaks was observed in the NMR spectrum of the complex too. The Cp resonance of **4d**•SO_2 also did not broaden at -65°C.

In the IR spectrum of **8b**, each SO_2 moiety should display two bands[66], however, only one band was observed for each SO_2 (1283, 1258 cm^{-1}). The other

bands are presumed to be under the band at 1100 cm^{-1} which corresponds to PPh_3. The intensity and the width of that band increased on going from **1b** to **8b**. When the complex **8b** was heated above 125°C, SO_2 was evolved and the complex **9b** was formed; only one band was observed (1261 cm^{-1}). Since all thiolate-bonded SO_2 groups can be reversibly removed and, in most cases, coplanar metal-bonded SO_2 ligands cannot[66], it was concluded that the remaining band at 1258 cm^{-1} corresponded to the metal-bonded SO_2 ligand.

CHAPTER 4

The Preparation and Structures of Polysulfano Complexes Containing the $CpRu(PPh_3)(CO)$ Moiety

INTRODUCTION

Catenating elements bond to themselves to form chains and rings such as those found in organic chemistry. In particular, sulfur has a high tendency to catenate, second only to carbon.[83] In the early 1900's, elemental sulfur itself was found to consist of rings of eight sulfur atoms crystallizing orthorhombically (S_α).[4,84] Other cyclic structures of S_X (x = 6, 7, 8, 9, 10, 12 and 18) have been obtained in crystalline form and characterized.[4] Upon melting, α-sulfur is converted into a viscous polymeric sulfur via sulfur ring cleavage and formation of polymers containing > 100 000 helical units of S_8 (M.W. > 10^6).[4,85] Consequently, sulfur does not have a melting point in the strict sense of the term.

Inorganic catenated sulfur compounds are well known and include various number of sulfur atoms. These include sulfanes, halosulfanes, sulfur amines, polythionate dianions, and cyanogen polysulfides (Table 4.1).[86] Polysulfide anions of the type S_x^{-2} (x = 1-6) have been studied and found industrial application in high-density sodium or lithium batteries.[10] The higher polysulfide ions (eg. S_6^{-2}) are stable in acid solutions, whereas the lower sulfide ions (eg. S_2^{-2}) are more stable in basic solutions. Intermediate polysulfide ions are stable at intermediate pH.

Organic catenated sulfur systems, RS_xR where x > 2, are called polysulfanes. It is arguable that disulfides should be included in this group however, most authors seem

Table 4.1 List of known inorganic acyclic polysulfides.

$X—S_y—X$

X	y	Names
H	1-8	Sulfanes
F	1,2	Halosulfanes
Cl, Br	1-8	Halosulfanes
R_2N	1-4,	Sulfur amines (R = Alkyl)
SO_3^-	1-4	Polythionate dianions
CN	1-8	Cyanogen polyfides

to keep disulfides separate. There are several reviews published on the preparation of disulfides and polysulfides.[4,87] The preparation of disulfides can be achieved by the oxidation of thiol (equation 4.1), by the reduction of sulfonyl chlorides or sulfenyl chlorides (equations 4.2) or via the reaction of alkyl halides with disulfide ions (equation 4.3). The interchange of thiols with disulfides and interchange between disulfides can be used, in some circumstance, for the preparation of unsymmetrical disulfides as in equations 4.4 and 4.5. However, the most useful method is based on the thioalkylation of a thiol by various sulfur transfer agents.[4] Several leaving groups, Z,

$$R^1SH + R^2S^{\delta+}-Z^{\delta-} \rightleftharpoons R^1SSR^2 + ZH$$

may be used, and among the most common are phthalimido, imidazolo, benzimidazolo, 1,2,4-trizolo, 1,2,3-benzotriazolo, maleimido and succinimido.[88,89,90] The advantages of using phthalimide-based transfer agents are their unlimited shelf-life, the variety of possible R^2 groups and their facile reactivity.[89] Various sulfur linkages such as monosufides, R^2S-, disulfides, R^2SS-, and sulfinyls, $R^2S(O)$- have been prepared.

$$2RSH \xrightarrow{[O]} RSSR \qquad (4.1)$$

$$RS(O)_XCl \xrightarrow{[H]} RSSR \qquad x = 0, 2 \qquad (4.2)$$

$$2\,RX + S^{-2} \longrightarrow RSSR + 2\,X^- \qquad (4.3)$$

$$RSSR + R'SH \longrightarrow RSSR' + RSH \qquad (4.4)$$

$$RSSR + R'SSR' \longrightarrow 2\,RSSR' \qquad (4.5)$$

$$\diagdown\!\!\diagup NS_XR + R'SH \longrightarrow RS_XSR' + \diagdown\!\!\diagup N\text{-}H \qquad X = 1 \qquad (4.6)$$

$$X = 2 \qquad (4.7)$$

$$\diagdown\!\!\diagup NSR + R'SSH \longrightarrow RSSSR' + \diagdown\!\!\diagup N\text{-}H \qquad (4.8)$$

$$RSSX + R'SY \longrightarrow RSSSR' + XY \qquad X,Y = H, Cl;\ X \neq Y \qquad (4.9)$$

$$RSSH \longrightarrow RSSSSR \qquad (4.10)$$

$$2RSSH + SCl_2 \longrightarrow RSSSSSR + 2\,HCl \qquad (4.11)$$

$$2RSSH + S_2Cl_2 \longrightarrow RSSSSSSR + 2\,HCl \qquad (4.12)$$

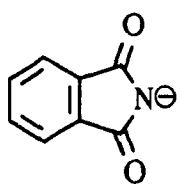
phthalimido (phth)

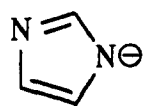
inidazolo

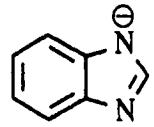
benzimidazolo

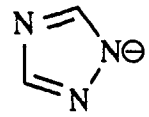
1,2,4-triazolo

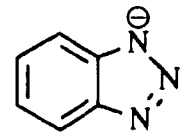
1,2,3-benzimidazolo

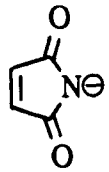
maleimido

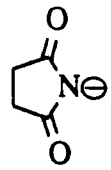
succinimido

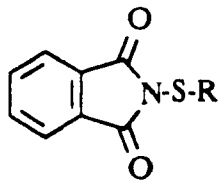

sulfinylphthalimide

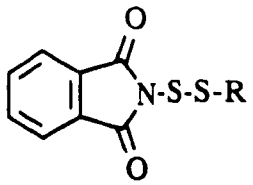

sulfinylthiophthalimide

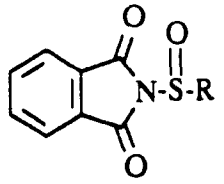

sulfenylphthalimide

Unsymmetrical organic disulfides and trisulfides can be prepared in high yields via the use of mono and disulfur transfer agents as in equations 4.6 and 4.7.[92] Alternately, addition of hydridodisulfides to a monosulfur transfer agent also gives a trisulfide, see equation 4.8.[89] However, hydridodisulfides typically are difficult to handle as they tend to be decomposed by surface reactions with glass and therefore, quartz must be used for their manipulation.[4] The preparation of higher sulfides is restricted to symmetrical polysulfides summarized in equations 4.10-4.12.

One way to prepare thiosulfinates is by the oxidation of organic disulfides.[4] However, this route has shown to be difficult to control because the oxidation of disulfides has proven to be far more complicated than the simple stepwise coordination of oxygen. The process is complicated by the homolytic rearrangement of the expected product to give rearrangement of the R group and the oxygen, (i.e. formation of RS(O)SR′, $RS(O)_2SR$, $R'S(O)_2SR'$, $RS(O)_2SR'$, $RSS(O)_2R'$, RSSR, and R′SSR′) resulting in double oxidation of the starting disulfide to give thiosulfonates and symmetrical disulfides.[4] The result of any particular oxidation is dependent on the disulfide, the oxidant and possibly catalysts and solvents.[4] A more selective oxidizing agent is m-chloroperbenzoic acid. Oxidation by peracids has been suggested to be equivalent to electrophilic attack by OH^+ which would tend to occur at the most electronegative sulfur.

Alternaternatively, a more specific route to unsymmetrical organic

thiosulfinates is the reaction of a thiol with a sulfinyl phthalimide.[88] The oxidation of

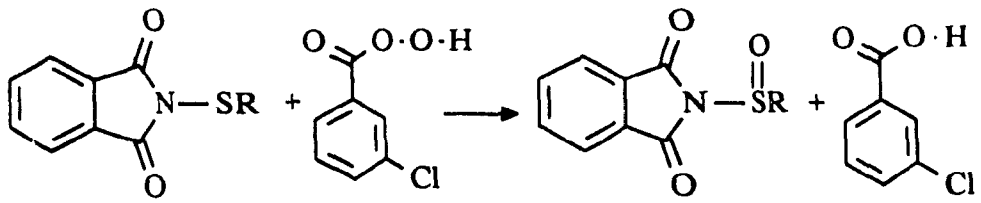

(4.13)

(4.14)

the sulfur transfer agent, phthalimide sulfide, with m-chloroperbenzoic acid gives the corresponding sulfinyl phthalimide, equation 4.13, which can then react with thiols to give the thiosulfinates in good yield, equation 4.14. The stability of organic thiosulfinates is dependent on the R group.[4] They tend to decompose thermally and photolytically to give total scrambling of the R groups and oxygen as in the case of the oxidation of disulfides. Generally, long alkyl groups are more stable than short alkyl groups, which are more stable than aryl groups.[4,93] Cyclic thiosulfinyls tend to be more stable than non-cyclic systems.[82]

Organometallic catenated sulfides, MS_xR where $x > 1$, are far more scarce than their organic counterparts. To date only a handful of these complexes have been reported.

The complexes $CpW(CO)_3ER$, where E = S (**IV**), SS (**V**) and S(O) (**VI**), were prepared by the reaction of the metal thiol with phthalimido sulfur transfer agent, Scheme 4.1.[94] Similarly, $Cp_2Ti(SH)_2$ reacted with the monosulfur transfer reagent, phth-SR, to give $Cp_2Ti(SSR)_2$ which rearranges, when R = aryl, to give CpTi(SR)(SSSR), **VII** (see Scheme 4.2). Complex **VII** is the only previously reported

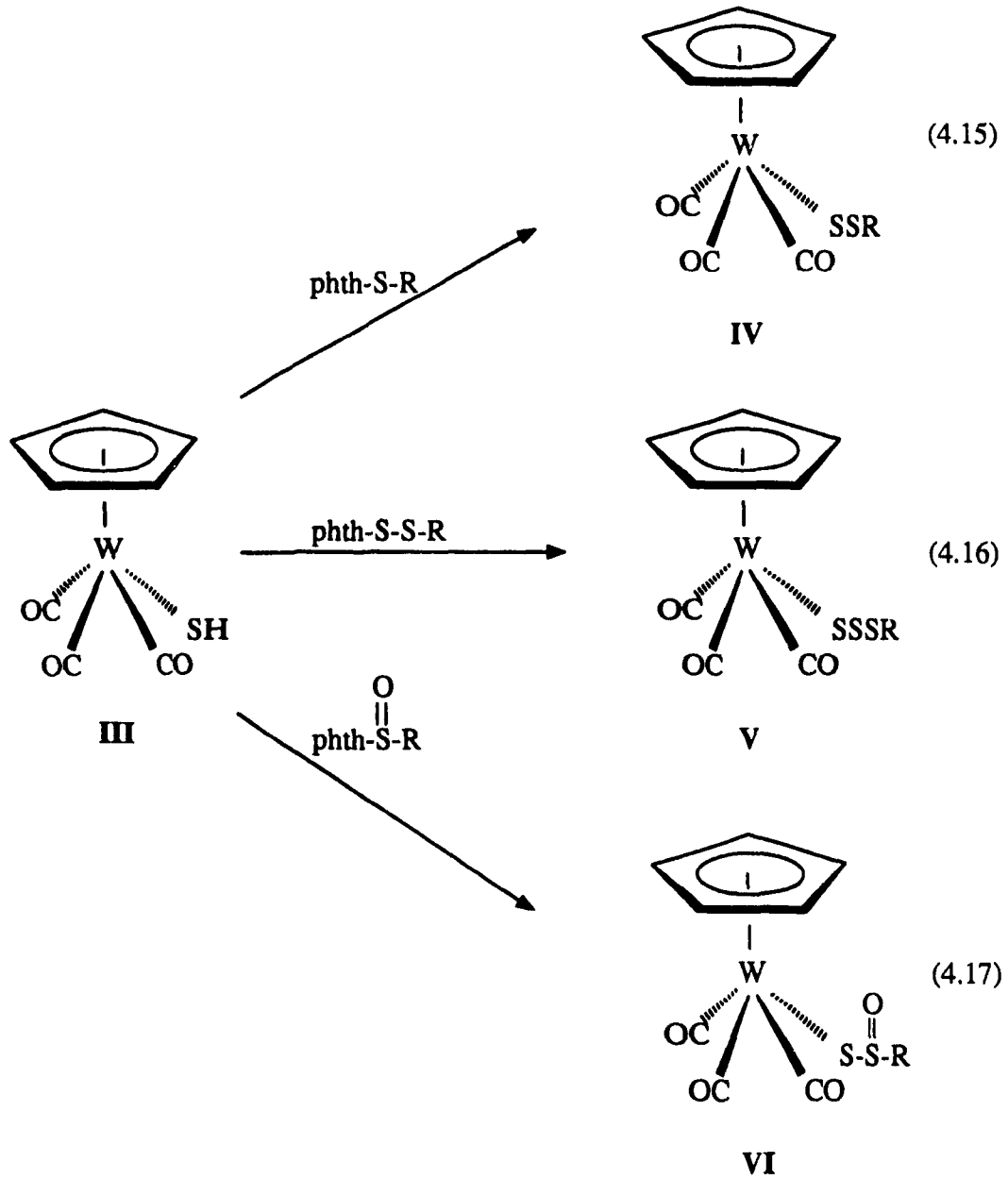

Scheme 4.1 Preparation of catenated sulfur derivatives of $CpW(CO)_3SH$, **III**.

crystal structure of a metallic trisulfide.[95]

Another route to the preparation of organometallic disulfides is by oxidative addition of RSSX to $Cp_2Ti(CO)_2$ to form $Cp_2Ti(SSR)(X)$, where X = Cl or phth.[96] Similarly, the complex cis-$(PPh_3)_2Pt(SSR)(phth)$ was prepared by the oxidative

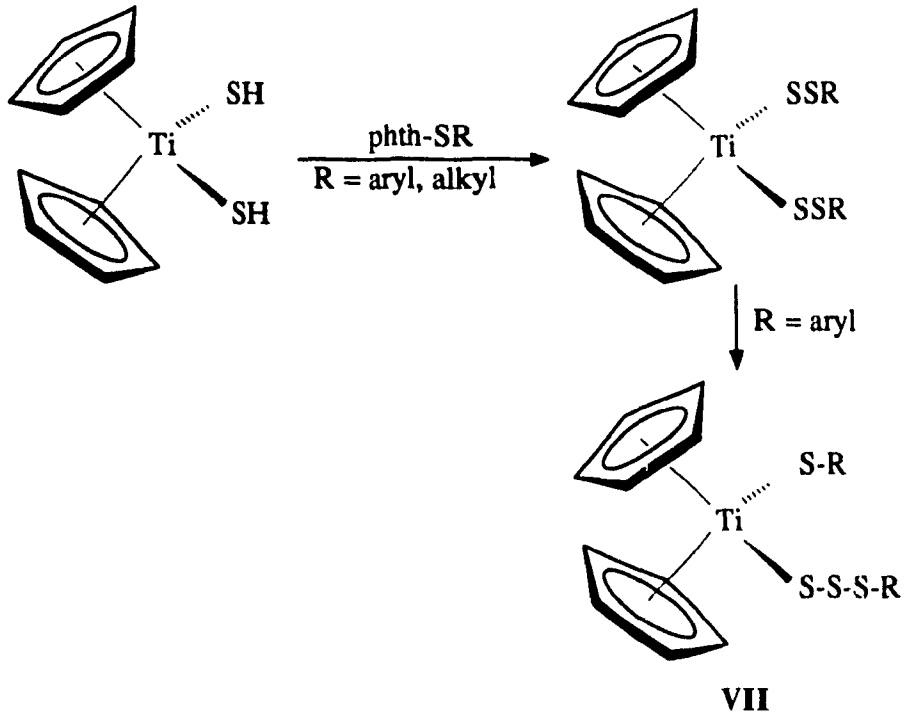

Scheme 4.2 Preparation of $Cp_2Ti(SR)(SSSR)$, **VII**.

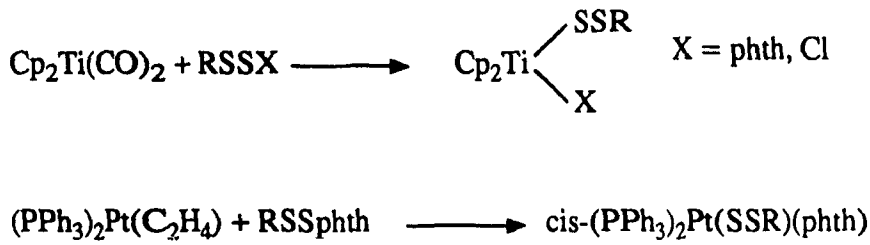

addition of phth-SSR to $(PPh_3)_2Pt(C_2H_4)$.[24]

In general, all metallic disulfides and trisulfides lose elemental sulfur in solution and are readily desulfurized by PPh_3 to yield the corresponding thiolate. Some disulfides have been structurally determined and these are; $CpW(CO)_3SSR$ (**IV**)[97]; cis-$(PPh_3)_2Pt(SSR)(phth)$[97]; and $Cu(tet\text{-}b)SSCH_2CO_2$ (**VIII**)[98]. There are some

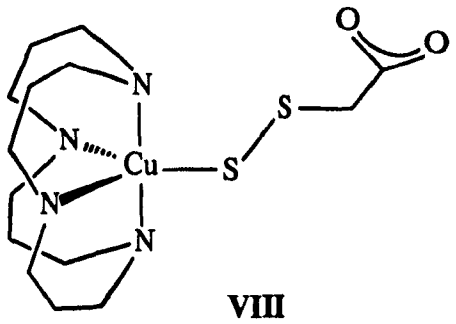

VIII

non-linear organometallic disulfides which include $CpW(NO)(\eta^2\text{-}S_2R)(R)$[26]; $[Fe_2S_2(S\text{-}CMe_3)(CO)_6]^-$[127]; $[Mo_2(N\text{-}4\text{-}C_6H_4Me)_2(S_2P(OC_2H_5)_2)_2S_2(OCMe)(SSR)]$[128].

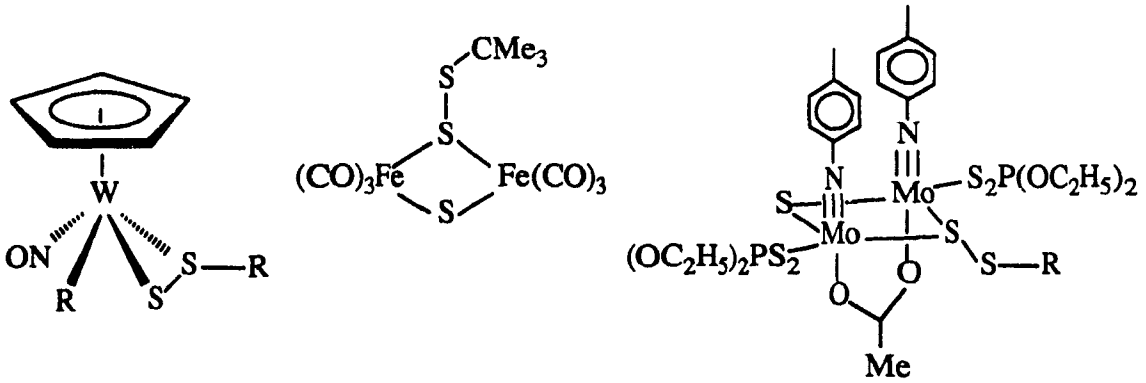

Of those, only the latter was not reported crystallographically.

Organometallic thiosulfinates, MSS(O)R, are virtually unknown and therefore, of great interest. Only one of these systems, $CpW(CO)_3SS(O)R$, has been prepared by Hartgerink (VI) as an air stable solid and was characterized, although not by x-ray crystallography.[99] Rauchfuss *et al.* prepared a thiosulfinate ether (IX) and Welker *et al.* prepared a disulfur monoxide (X)[100] both of which have a S_2O moiety.

Organic thiosulfonates, $RS(O)_2SR'$, are well known and very stable.[4,93] A few crystal structures of organic thiosulfonates have been determined, namely

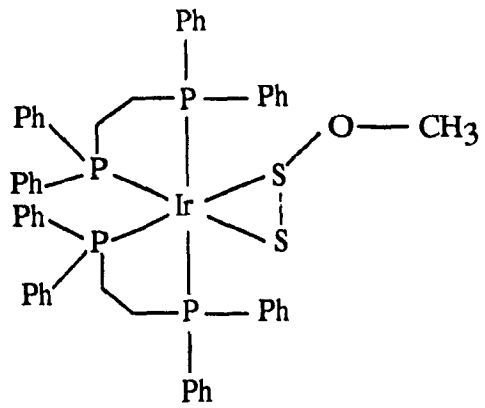

IX

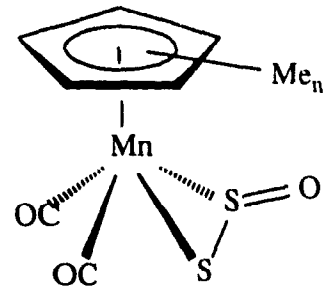

n = 1,5

X

$(4\text{-}BrC_6H_4)SS(O)_2(4\text{-}BrC_6H_4)$ (**XI**)[101] and compound **XII**[102]. However, metal thiosulfonates, $MSS(O)_2R$, are unknown. Some tellurium thiosulfonate complexes such as **XIII** and **XIV** have been structurally determined.[103,104] A close analog is the

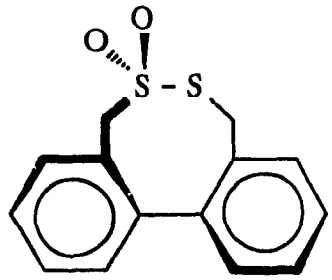

XII

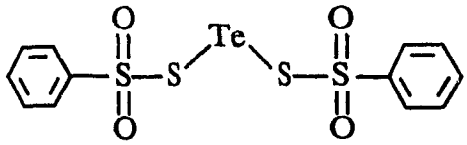

XIII

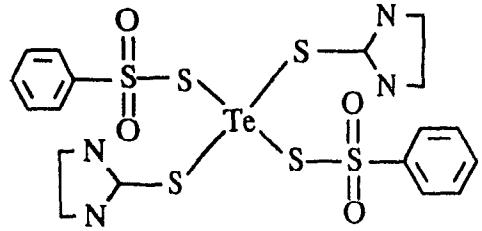

XIV

sulfonate $MS(O)_2R$. Most of these are prepared by insertion of SO_2 into a metal alkyl bond, as discussed in chapter 3.[25,64] Recently, Abrahamson *et al.* prepared

$CpW(CO)_3S(O)_2R$ via the oxidation of the thiolate.[105]

In this chapter, several polysulfano complexes based on the $CpRu(PPh_3)(CO)$ moiety will be discussed. These were prepared by the reaction of $CpRu(PPh_3)(CO)SH$ with phthER, where E = S, SS and S(O). A representative x-ray crystal structure of each of these rare classes of organometallic complexes has been obtained. In addition, a novel intermolecular oxygen transfer between two molecules of $CpRu(PPh_3)(CO)SS(O)R$ was observed and the product, $CpRu(PPh_3)(CO)SS(O)_2R$, was structurally determined. The latter is a unique example of an organometallic thiosulfone.

I Preparation of $CpRu(PPh_3)(CO)SSR$ ($R = 4\text{-}C_6H_4Me, 1\text{-}C_3H_7, CHMe_2$)

RESULTS

The treatment of $CpRu(PPh_3)(CO)SH$, **4a**, with phth-SR where R = p-tolyl, n-propyl, i-propyl, in toluene or THF gave the complexes $CpRu(PPh_3)(CO)SSR$, **10b-d**, see equation 4.18. These complexes are yellow air-stable solids soluble in THF,

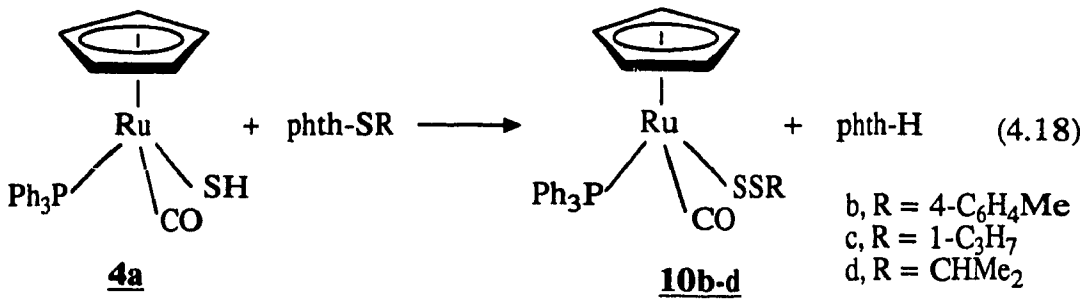

benzene and CCl_4, but insoluble in ethanol and hexanes. Solutions of **10b-d** decomposed within 10 minutes in air to form green paramagnetic solutions containing triphenylphosphinesulfide. Under nitrogen, **10b-d** were far more stable. The NMR sample solutions prepared under nitrogen were stable for up to 10 hours. The NMR spectra of **10b-d** contain peaks due to one Cp ring, one PPh_3 group and the appropriate R group, observed in the proper multiplicity and intensity, Table 4.2. The IR spectra in toluene showed one sharp $\nu_{(CO)}$ stretching frequency at 1954, 1941 and 1942 cm^{-1} for **10b**, **10c** and **10d** respectively, Table 4.3.

The x-ray structure of **10d** is depicted in Figure 4.1.[124] All crystallographic data, atom coordinates, bond angles and bond lengths are located in Appendix IV, Tables A4.1-A4.4. The structure is a piano stool with one PPh_3, one CO, and one RSS

Table 4.2 ^{1}H NMR for $CpRu(PPh_3)(CO)S_xR$, where x = 1,2,3 and $CpRu(PPh_3)(CO)SS(O)_yR$ where y = 1,2.[a,b]

Number	Cp	$C\underline{H}_2CH_2CH_3$	$CH_2C\underline{H}_2CH_3$	$C\underline{H}Me_2$	CH_3	$4\text{-}C_6\underline{H}_4Me$
10b	4.64				2.12	7.86[c]
10c	4.73	2.74[d] 2.92[d]	1.93[d]		1.04[e]	
10d	4.73			3.20[m]	1.56[g] 1.41[f]	
11b	4.71				2.01	6.88[h] 7.82[i]
11c	4.820	2.892[d]	1.820[d]		0 884[e]	
11d	4.82			3.35[m]	1.41[k] 1.38[k]	
12b	5.00 4.80				2.04 1.95	6.87[o] 7.81[n] 7.96[o]
12c	4.82 4.79	3.25[d]	2.03[d]		1.44[f] 0.75[p]	
12d	4.96			3.00[r]	1.24[f]	
13b	4.73				1.89	6.81[s] 8.20[s]

a) In C_6D_6 solution; reported in ppm relative to internal TMS b) Phenyl resonances of PPh_3 appeared as two multiplets in the range 6.98-7.18 ppm and 7.45-7.60 ppm in the ratio 3:2 c) d, J_{H-H}= 8.3 Hz d) multiplet e) t, J_{H-H}= 7.3 Hz f) t, J_{H-H}= 6.8 Hz g) d, J_{H-H}= 6.6 Hz h) d, J_{H-H}= 7.9 Hz i) d, J_{H-H}= 8.5 Hz j) t, J_{H-H}= 7.7 Hz k) d, J_{H-H}= 6.1 Hz l) d, J_{H-H}= 2.4 Hz m) septet n) d, J_{H-H}= 4.2 Hz o) d, J_{H-H}= 4.0 Hz p) t, J_{H-H}= 7.5 Hz q) d, J_{H-H}= 6.0 Hz r) t, J_{H-H}= 6.8 Hz, s) d, J_{H-H}= 8.2 Hz.

Table 4.3 $\nu_{(CO)}$ stretching frequency (cm^{-1}) for $CpRu(PPh_3)(CO)S_XR$, where x = 1,2,3 and $CpRu(PPh_3)(CO)SS(O)_yR$, where y = 1,2, recorded in toluene.

complex \ R group	4-C_6H_4Me	1-C_3H_7	$CHMe_2$
$CpRu(PPh_3)(CO)SR$	1947	1942	1941
$CpRu(PPh_3)(CO)SSR$	1954	1941	1942
$CpRu(PPh_3)(CO)SSSR$	1957	1956	1956
$CpRu(PPh_3)(CO)SS(O)R$	1960	1978 1959	1958
$CpRu(PPh_3)(CO)SS(O)_2R$	1971*		

* in C_6D_6

ligand. The cyclopentadienyl ring shows rotational disorder which was resolved. Each carbon atom of the Cp ring has a partial occupancy of 0.5 and between each resides another partial atom. For simplicity, only one ring of partial atoms is shown in Figure 4.1. It was found that the crystal was racemic. The dihedral angle about the sulfur-sulfur bond was found to be 77.95° which is significantly less than the normal dihedral bond angle of 90° observed for organic disulfides.[4,82] However, dihedral angles of organometallic polysulfides range from 63-99° and thus, the observed angle falls within this range.[91,97,98,106] The sulfur-sulfur bond length of 2.038(4) Å is in the normal range of organic analogs (2.03-2.08 Å)[4,82] and also organometallic analogs (2.01-2.05 Å)[91,97,98,106]. There is some disorder at S2 which was resolved as two partial atoms, S2A and S2B. These two sulfur sites should impose a reorientation of the R group, however, although several residual peaks were observed in the difference map, the disorder in this area could not be resolved satisfactorily and thus, C26 and C27 were both left as single atoms with large thermal factors. When **10d** was irradiated with UV light in an NMR tube (C_6D_6) for 2 hours, the major product was **4d**.

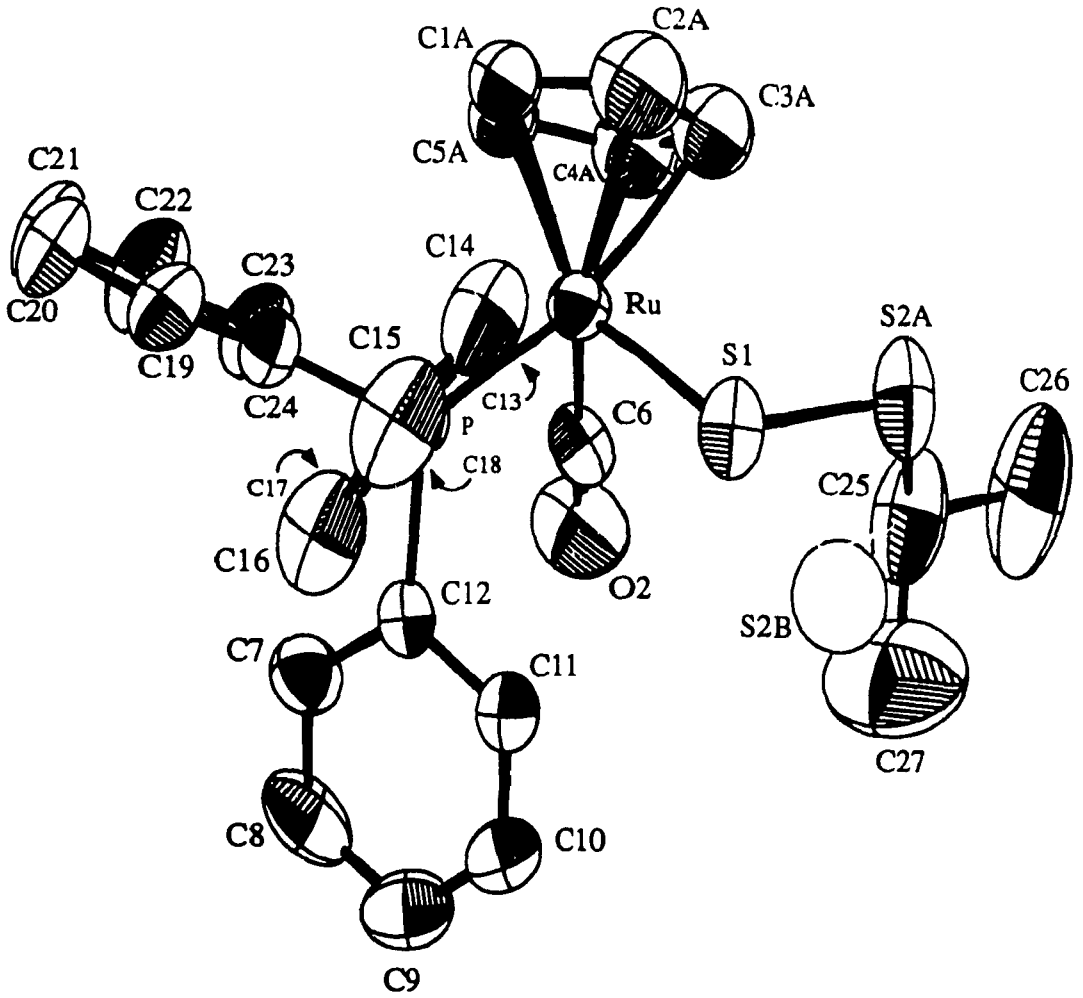

Figure 4.1 ORTEP of $CpRu(PPh_3)(CO)SS(CHMe_2)$, **10d**.

Substantial amounts of isopropyl disulfide and PPh_3 were also detected.

The complex **10d** did not insert sulfur when it was mixed with elemental sulfur in an NMR tube in C_6D_6. The complex **10b** did not react with excess PPh_3 for 30 minutes in an NMR tube in C_6D_6.

DISCUSSION

The reactions of the phthalimide monosulfur transfer agents with the thiol **4a** gave the novel unsymmetrical disulfides **10b-d**, equation 4.18 (here reproduced). The

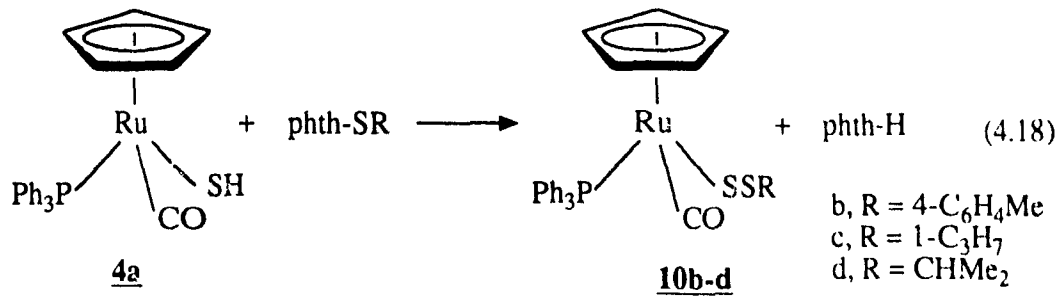

sulfur transfer agent selected was (alkyl or aryl)thiophthalimide due to its success in other organometallic systems.[24,89,91,96,99]

The disulfides **10b-d** are very stable in the solid state and in solution under nitrogen. In air, solutions of **10b-d** decompose to form green solutions and triphenylphosphinesulfide which indicates that in air, oxidation of **10b-d** decreases the sulfur chain length. The complexes **10b-d** do not react with PPh_3 under nitrogen. Analogous organic disulfides are not attacked by triphenylphosphine unless they are "activated" by an acyl or a 2-alkenyl terminal group.[4,108] Such a reaction involves the breaking of a carbon-sulfur bond which is known to be relatively strong. Treatment of **10d** with UV light gives the product distribution consistent with the free radical reaction. The presence of substantial amounts of $Me_2CHSSCHMe_2$ supports the free radical disproportionation via RS•.

The crystal structure of **10d** was determined. The bond length S1-S2 was found to be 2.042(4) Å compared to 2.053(4) Å for $CpW(CO)_3SS$(p-tolyl).[94] Standard S-S bond lengths in organic systems are generally thought to be in the range of 2.03 Å

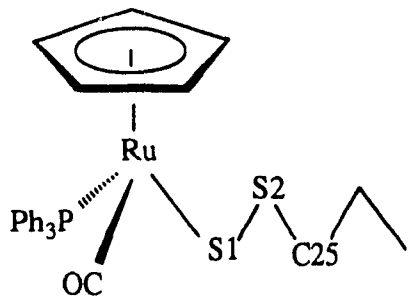

10d

to 2.08 Å.[4,82]

A more striking point of interest is the unusually small dihedral angle RuS1S2C25 of 77.95°. From molecular models, there seems to be no significant steric reason for this small angle. This is in contrast with organic disulfides whose dihedral angles are closer to 90°.[4] The complex $CpW(CO)_3SS$(p-tolyl) was also found to have an even smaller dihedral angle of 63.1°.[94]

The main reason for the dihedral angle in organic disulfides is minimization of repulsion between adjacent sulfurs. It was suggested by Pauling that the bivalent sulfur

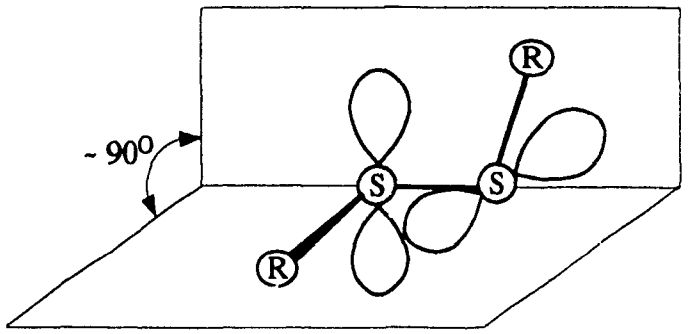

Figure 4.2 Repulsion between adjacent sulfur lone pairs.

bonds are nearly pure p in character.[4,82] In contrast to carbon, sulfur does not hybridize significantly. This is supported by observed dihedral angles about organic sulfur-sulfur

bonds. Figure 4.2 illustrates that the dihedral angle is result of minimal lone pair repulsion, the lobes representing non-bonding 3p-orbitals. For clarity, the spherical non bonding 3s orbital is not illustrated.

As observed in organic[109] and other organometallic[106] systems, the dihedral angle is inversely proportional to the bond length (Table 4.4). This trend was attributed

Table 4.4 Bond lengths and dihedral angles of known metal disulfides.

Complex	S-S bond length (Å)	Torsion angle
$CpW(CO)_3SS(4\text{-}C_6H_4Me)$	2.053(4)	63.1
$CpRu(PPh_3)(CO)SS(CHMe_2)$	2.038(4)	77.95
$cis\text{-}(PPh_3)_2Pt(SSCHMe_2)(phth)$	2.037(4)	89.5
$Cu(tet\text{-}b)SSCH_2CO_2$	2.017(7)	98.6

to lone pair repulsion between adjacent sulfur atoms. However, if this was the only factor, then the graph would be expected to reach a minimum bond length at 90° and reverse direction; this was not observed. Consequently, other unknown factors must be involved.

II Preparation of $CpRu(PPh_3)(CO)SSSR$ ($R = 4\ C_6H_4Me$, $1\text{-}C_3H_7$, $CHMe_2$)

RESULTS

The complexes $CpRu(PPh_3)(CO)SSSR$, **11c-d**, were prepared by reaction of **1a** with phth-SS-R as shown by equation 4.19. The resulting yellow compounds were

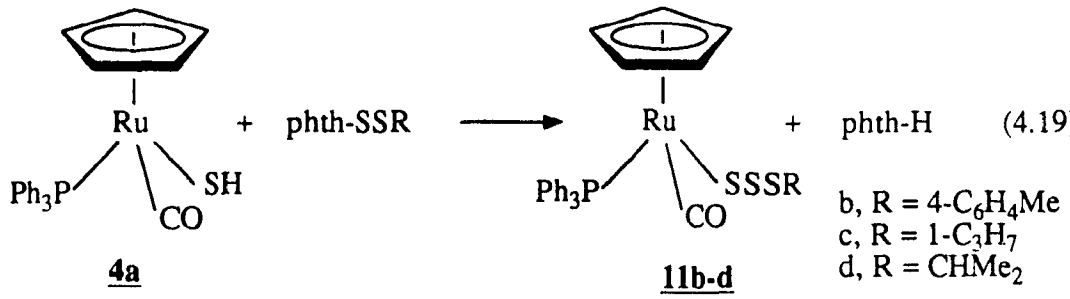

stable in air, soluble in THF, benzene, and CCl_4 and insoluble in ethanol and hexanes. In solution, they were remarkably stable even when exposed to air for hours. The ^1H NMR and the IR spectral results are listed in Tables 4.2, 4.3 and 4.5.

Solutions of analytical samples of **11b-d** showed extra Cp peaks in their ^1H NMR spectra in addition to the main peaks due to **11b-d**. A solution of **11b** gave three peaks in the Cp region in the NMR spectrum at 4.73, 4.71(**11b**) and 4.68 ppm in the ratio 1.3:10:1 respectively, see Figure 4.3. The two minor peaks do not correspond to the thiolate **4b**, the disulfide **10b**, nor any other known complex. A solution of **11c** gave four peaks at 4.820, 4.767, 4.728 and 4.725 ppm in the ratio 5.4:3.1:1:1 respectively, see Figure 4.4. The peak at 4.82 ppm is due to **11c** while that at 4.728 ppm corresponds to **10c**. This identification was confirmed by TLC analysis on Alumina in CCl_4, wherein two spots with an $R_f = 0.37$ and 0.63, corresponding to **10c**

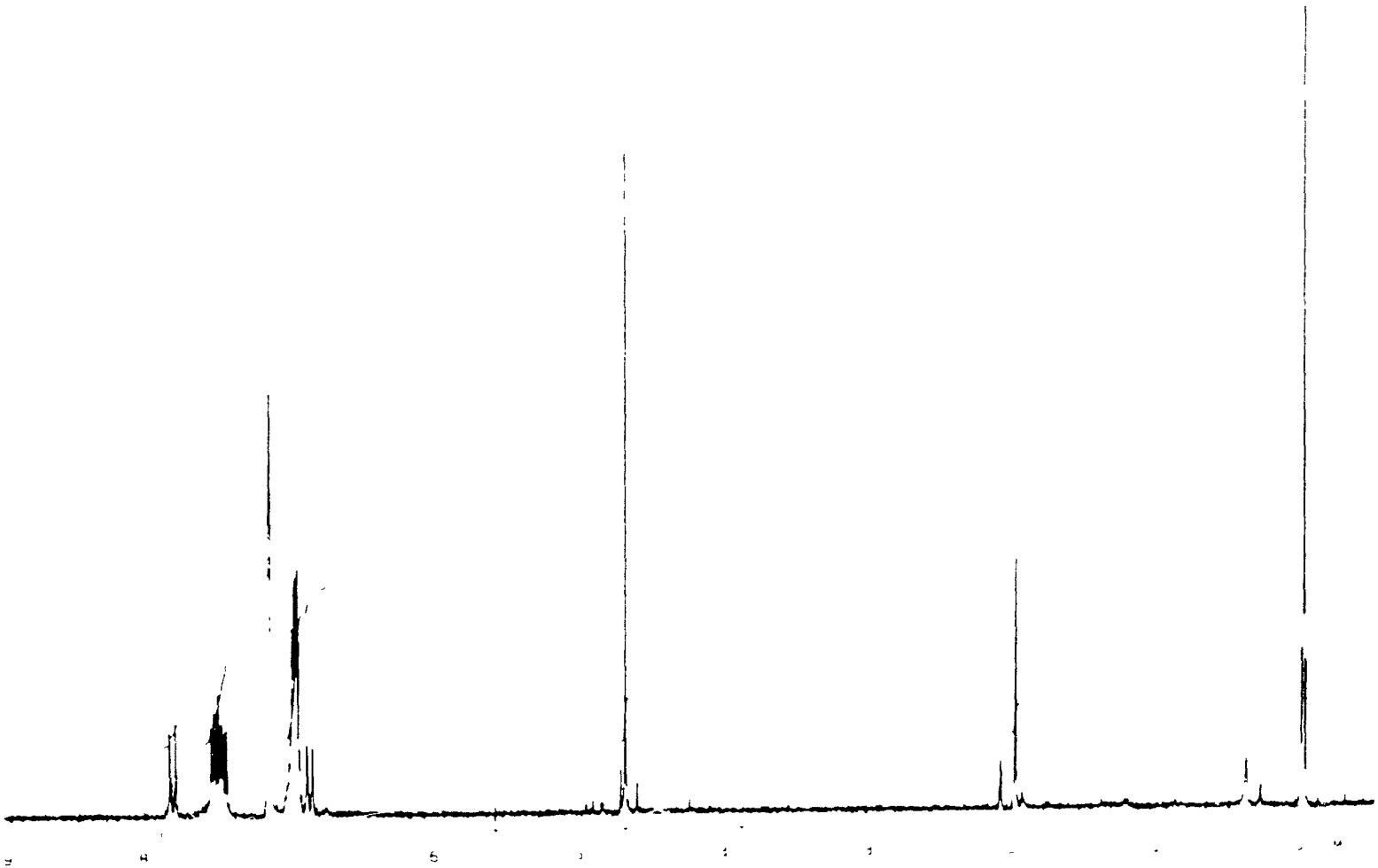

Figure 4.3 ^{1}H NMR spectrum of $CpRu(PPh_3)(CO)SSS(4\text{-}C_6H_4Me)$, **11b**.

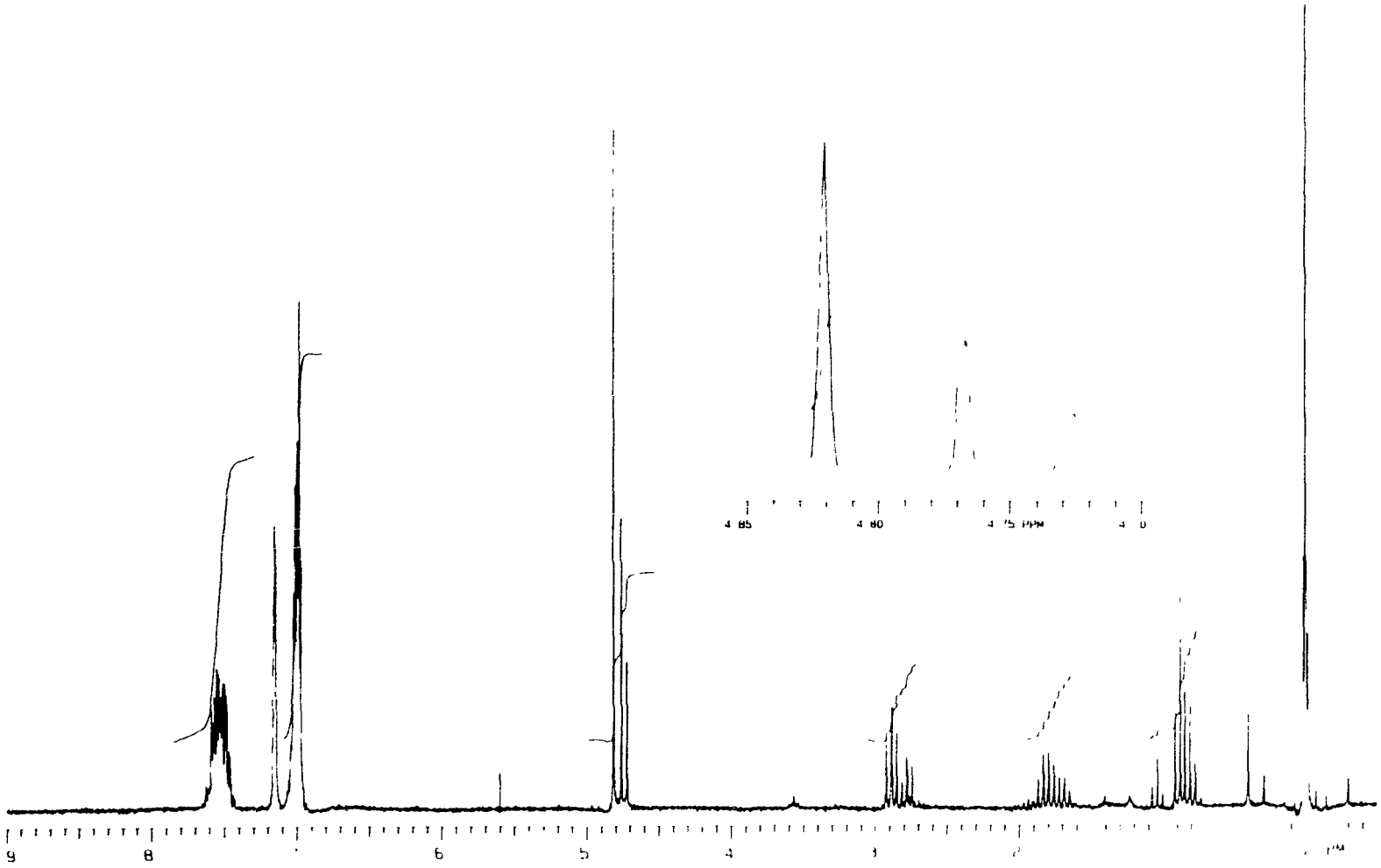

Figure 4.4 ^{1}H NMR spectrum of $CpRu(PPh_3)(CO)SSS(1\text{-}C_3H_7)$, **11c**.

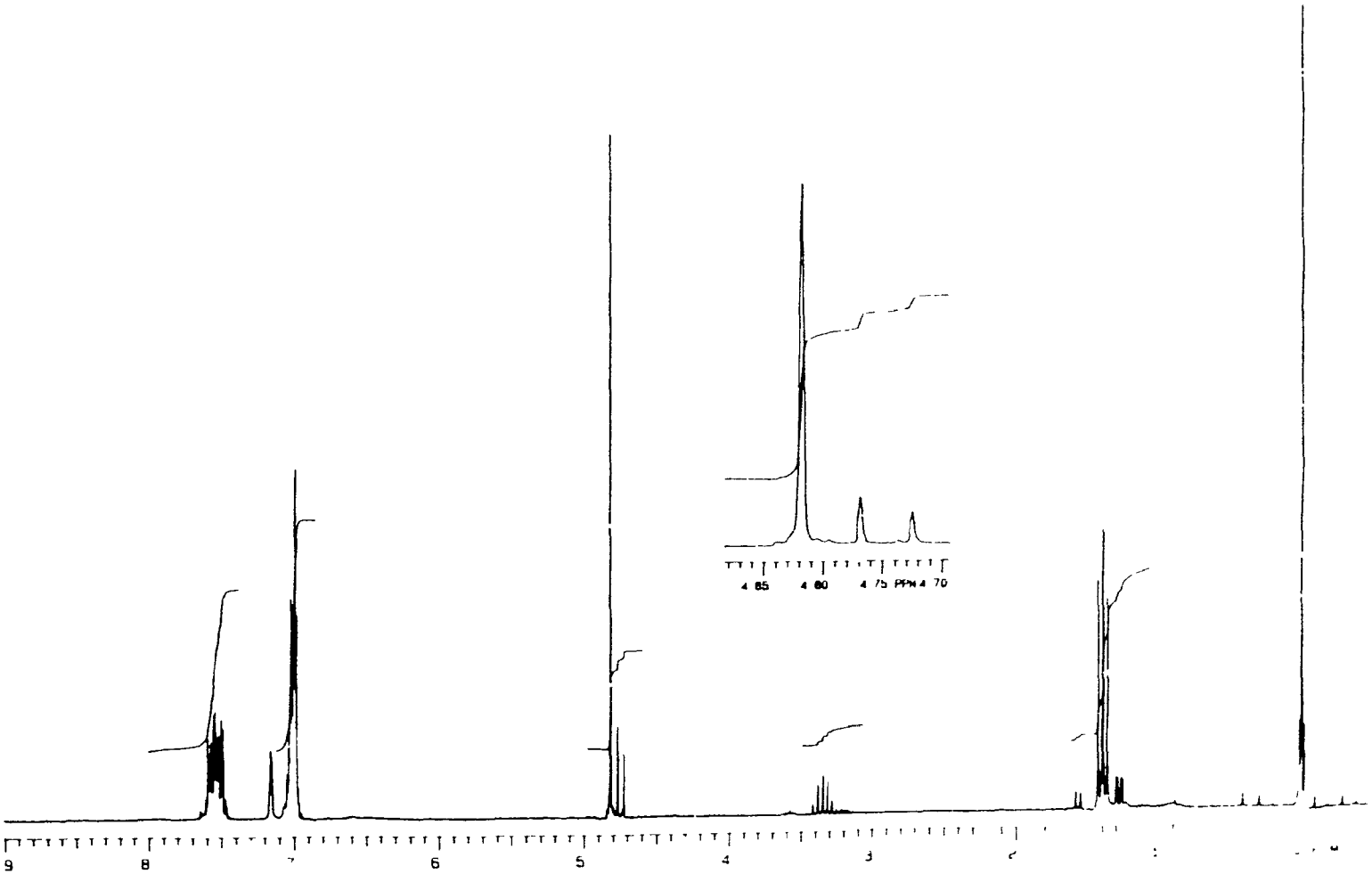

Figure 4.5 ^{1}H NMR spectrum of $CpRu(PPh_3)(CO)SSS(CHMe_2)$, **11d**.

and **11c** respectively, were detected. The other Cp peaks did not correspond to the thiolate **4c** and remain unassigned. A solution of **11d** gave three Cp peaks at 4.82, 4.77, and 4.72 ppm in the ratio 10.9:1.4:1 repectively, see Figure 4.5. The peak at 4.82 ppm is due to **11d** while that at 4.72 ppm is due to the disulfide **10d**; the latter assignment being confirmed by TLC analysis wherein two spots at $R_f = 0.39$ and 0.61 were detected (Alumina in CCl_4) which were assigned to **10d** and **11d** respectively. The remaining peaks do not correspond to the thiolate **4d** and remain unassigned. Each Cp peak in the NMR spectra of **11b-d** showed peaks due to the appropriate companion R groups with the expected intensity. Variable temperature NMR of **11c** showed no change in intensity or line width of the various Cp signals in the range -60°C to +60°C. NOE experiments showed no exchange between the Cp signals. The pattern of Cp peaks observed for **11c** was invariant with solvent (C_6D_6, $(CD_3)_2CO$, toluene-d_8, CD_2Cl_2) and did not change after further purification by column chromatography and recrystallization. A powdered sample of **11c** was dissolved at -78°C and a spectrum was taken within 10 minutes showing four signals at the same intensity as the spectra at room temperature, within experimental error. The presence of added elemental sulfur or triphenylphosphine did not change the peak ratio of the Cp region of **11c** even after 2 hours. When **11c** was treated with excess tris(diethylamine)phosphine in C_6D_6 in an NMR tube, peaks due to **10c** and **4c** slowly formed. The reaction was monitored over time and it was observed that the two unknown contaminants disappeared before **11c** was consumed. The half life of the reaction was estimated to be 6 hours. The IR spectra of **11b-d** in toluene each showed one sharp υ_{CO} band with no apparent shoulders or broadening. However, the IR spectra recorded in CCl_4 showed shoulders that indicate the presence of other similar complexes, see Table 4.5. The NMR peaks due to the minor species did not increase in intensity when NMR samples of **11b-d**

Table 4.5 $\nu_{(CO)}$ stretching frequency (cm^{-1}) for $CpRu(PPh_3)(CO)S_3R$, $CpRu(PPh_3)(CO)SS(O)R$ recorded in CCl_4.

complex \ R group	4-C_6H_4Me	1-C_3H_7	$CHMe_2$
$CpRu(PPh_3)(CO)SSSR$	1950sh 1962s	1941sh 1946sh 1950sh 1961s	1950sh 1961s
$CpRu(PPh_3)(CO)SS(O)R$	1964s 1976sh	1982sh 1958m 1942m	1965s 1957sh 1950sh 1943sh

were allowed to stand for several days.

The crystal structure of **11c** was determined and is shown in Figure 4.6.[110a] Appendix V, Tables A5.1-A5.4 contain the crystallographic data, atom coordinates, bond lengths and bond angles respectively. The structure of **11c** is a piano stool with PPh_3, CO and RSSS as ligands. Disorder at S3 and C25 were observed as indicated by large thermal parameters at these atoms and residual electron density in the difference map in this area indicated further disorder. However, this disorder could not be modeled accurately. The presence of some **10c** within the crystal of **11c** was tested as a model of the disorder but this did not improve the R factor. The disorder was observed in three independent crystallographic determinations on different crystals from the same batch.[110] The bond lengths S1-S2 and S2-S3 are 2.042(4) Å and 2.005(5) Å respectively, with corresponding dihedral angles of 71.5(2)° and 65.2(4)° respectively. The former bond length is considered normal while the latter is abnormally short.[4,82] Both dihedral angles are abnormally small compared to organic trisulfides.[4,82]

When **11c** was irradiated with UV light in an NMR tube for 15 minutes, no reaction was observed. After further photolysis for 20 hours, all the Cp peaks

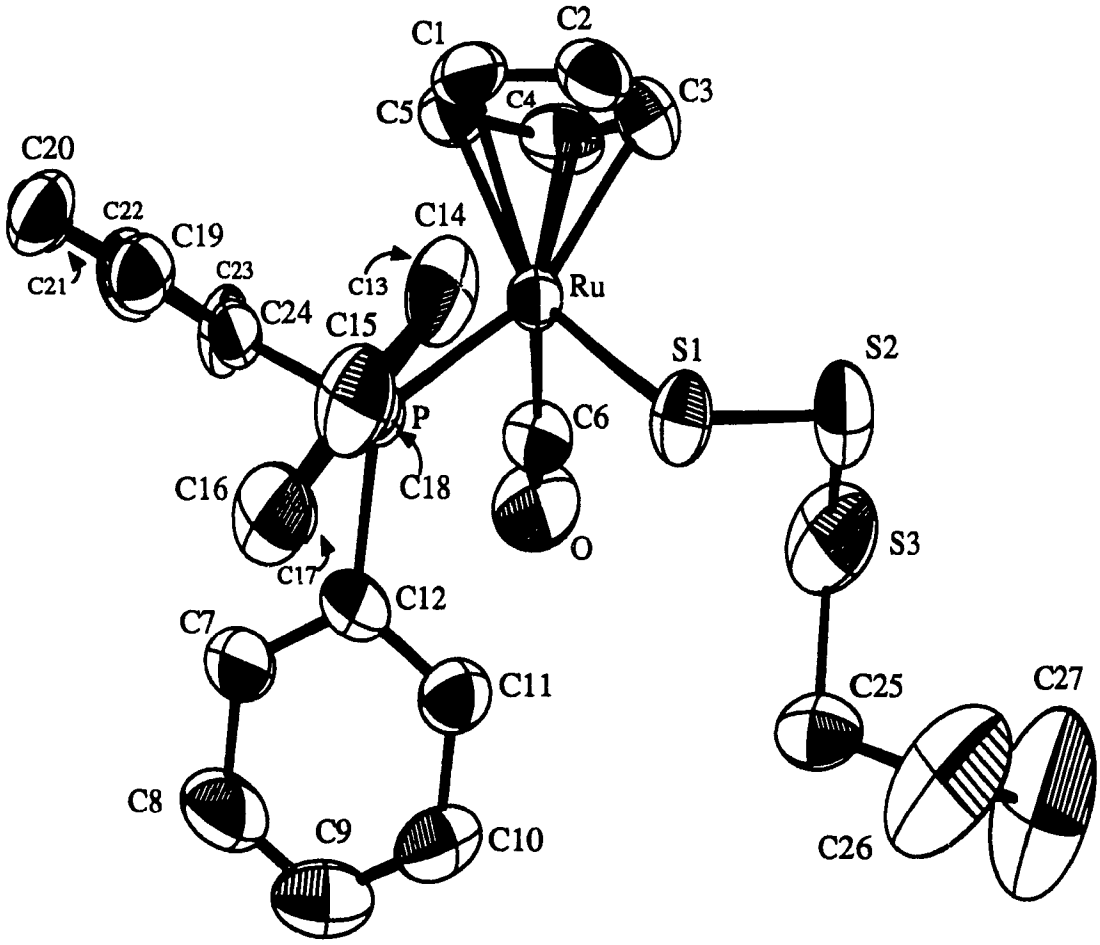

Figure 4.6 ORTEP of $CpRu(PPh_3)(CO)SSS(1\text{-}C_3H_7)$, **11c**.

originally present were still present at a different ratio, 1:1:1.5 for the peaks at 4.82(**11c**), 4.73 and 4.73(**10c**) ppm respectively. In addition, several new Cp resonances were observed including four major signals at 4.74, 4.70, 4.64 and 4.03 ppm in the ratio 1.0:3.6:1.2:0.9 respectively. No sign of the thiolate **4c** was observed in the NMR spectrum. The new Cp peaks accounted for 45 % of the integral of the total Cp pattern while the old Cp peaks accounted for 28 %, the remaining 27 % was due to a complex pattern of minor products. Due to the complexity of the NMR pattern, the mixture was not separated for further analysis.

DISCUSSION

The reactions of **4a** with the disulfur transfer agents gave the trisulfides **11b-d**, equation 4.19 (here reproduced). The organometallic trisulfides previously known (i.e.

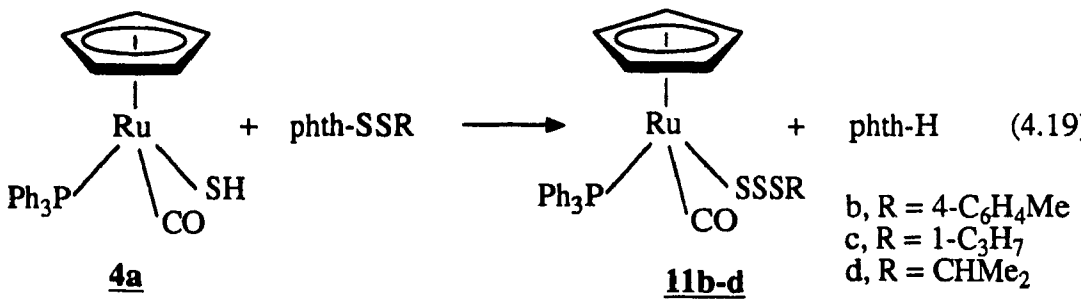

based on Cp_2Ti and $CpW(CO)_3$ moieties) are unstable toward spontaneous loss of sulfur.[24,95,97] However, the complexes **11b-d** seem to be remarkably stable in that respect.

During characterization of the compounds **11b-d**, the NMR spectra of the pure products each showed several extra sets of peaks. One of these sets corresponded to those of the appropriate disulfides **10b-d**. The presence of the other cyclopentadienyl peaks may be due to the presence of rotomers, branched isomers analogous to the thiosulfinyls **12b-d**, or some other as yet unidentified sulfur compounds. The former two possibilities will be discussed in detail while the latter possibility, being too speculative, will not be discussed further.

The disulfides **10b-d** do not originate from monosulfur transfer agents present in the disulfur transfer agents; the NMR spectra of the latter showed their purities to be at least 95%. The trisulfides **11b-d** do not lose sulfur spontaneously nor do they react with triphenylphosphine. Consequently, the disulfides had to originate in the preparation step, possibly via the branched by-products, **XVII**, postulated below.

These would normally be expected to easily lose sulfur; being metastable as postulated by both Morris[24] and Harpp[111].

Unsymmetrical trisulfides can exist in a total of four rotomers. Two are the cis (*d* and *l*) and two are trans (*d* and *l*). If R or R' is chiral, then diastereomers should be

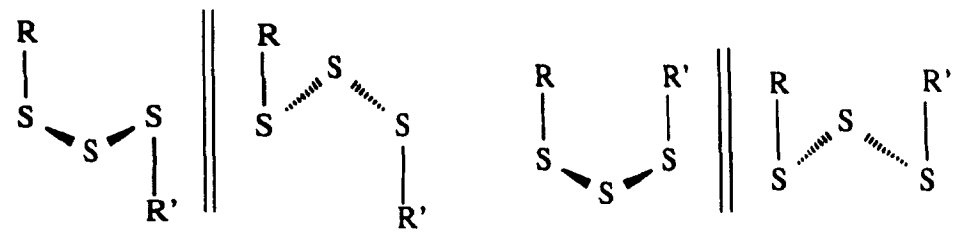

trans (*d* and *l*) cis (*d* and *l*)

present and detectable by their different NMR or IR spectra. Fairly high barriers to rotation about the sulfur-sulfur bond, in excess of 16 Kcal/mole, would be required to make these rotomers observable on the NMR time scale at room temperature. This estimate is based on the observation of sharp signals at +60°C i.e. slow exchange. One can assume that at +60°C, the rate of exchange is slower than if coalescence was observed, which implies that ΔG^* is greater than the value required for coalescence. If we assume coalescence at the highest observed temperature, then a minimum ΔG^* can be calculated using equation 4.20.[112] Thus, to explain the source of the extra Cp

$$\Delta G^* = aT_C[9.972 + \log(T_C/\Delta\nu)] \qquad (4.20)$$

Where $a = 1.914 \times 10^{-2}$ (ΔG in kJ mol^{-1})
$= 4.575 \times 10^{-3}$ (ΔG in kcal mol^{-1})

Based on assumption: $T_c = 333°K$
$\Delta\nu = 20$ Hz

signals in the NMR spectra of **11b-d**, one could propose that restricted rotation gives

rise to rotomers observable in NMR spectra, see Scheme 4.3. This explanation is

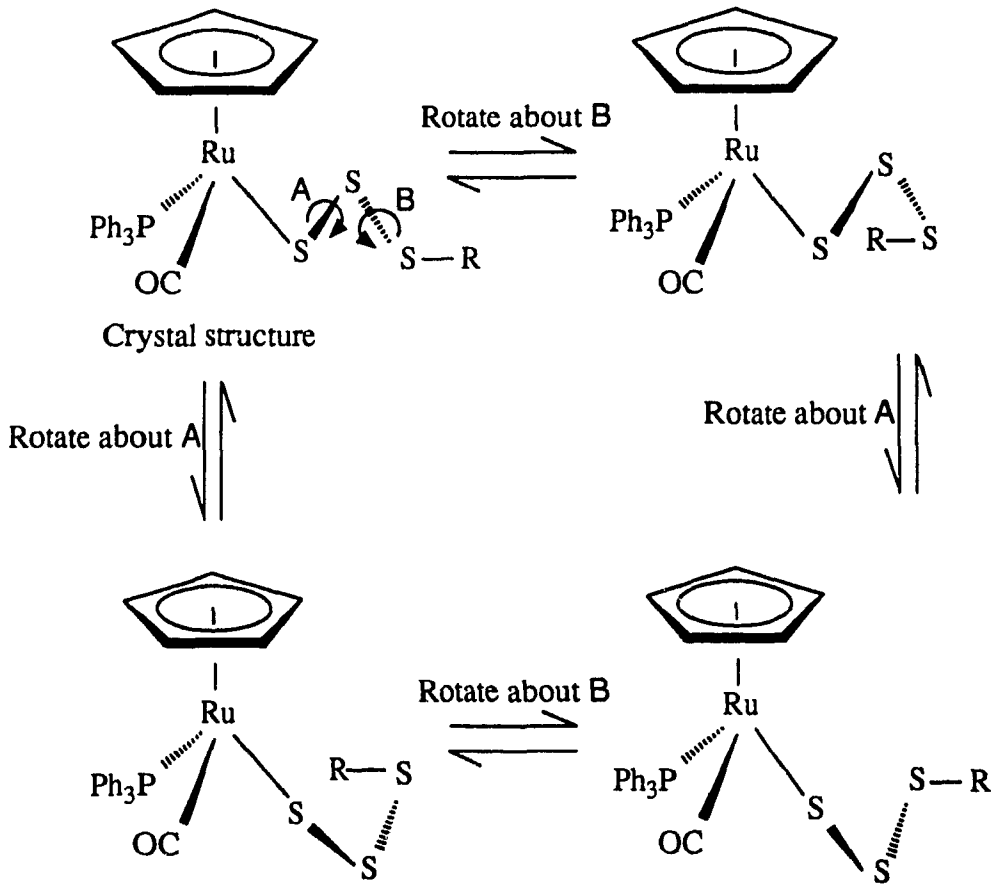

Scheme 4.3 Possible rotomers of $CpRu(PPh_3)(CO)SSSR$, **11b-d**.

supported by an abnormally short bond length of S2-S3 in **11c** (2.005(5) Å). This short bond distance may indicate a substantial π bond contribution in the order of about 0.4.[109] The barrier to rotation about a sulphur-sulphur bond can be quite large in sterically-hindered organic disulfides, being 15.5 Kcal/mole for bis(2,6-di-t-butylphenyl)disulfide.[113] In the case of cyclic organic disulfides, values of 28.8 Kcal/mole have been reported.[4] It is believed that the contribution to the barrier

due to lone pair repulsion is 7.0 Kcal/mole and higher barriers are due mainly to steric hindrance.[82,113,114] The presence of the $CpRu(PPh_3)(CO)$ moiety could cause substantial hindrance which may result in a high barrier to rotation thus giving the observed NMR spectrum. However, since the R group on the other end of the sulfur chain is small, then steric hindrance is unlikely. The IR data shows only one CO stretching frequency which could be due to overlap or more likely, to the other minor compounds detected in the NMR spectra which are in such low concentration that they are not observable in the IR spectra.

Several attempts were made to determine if the multiple peaks were actually due to a single compound. Variable temperature NMR from -60°C to +60°C showed no change in relative peak intensity and no sign of coalescence was observed. Polarization transfer experiments (NOE) in one dimension showed only experimentally insignificant magnetization transfer between the various Cp signals.

An alternate possible explanation comes from the dissolution of a powdered sample of the trisulfide **11c**. An NMR sample was prepared at -78°C and observed at that temperature. The shortest time that the sample could be prepared was 10 minutes. At that time 4 Cp signals were observed which did not change with time. This seems to indicate that the sample reached equilibrium distribution during the preparation time. The low temperature dissolution of **11d** showed the pattern observed at room temperature. This observation implies that if an equilibrium distribution is reached, then it is reached in less than 10 minutes at -78°C. This observation indicates a fairly rapid rate of exchange at that temperature. On the other hand, the signals remain sharp at +60°C which indicates a slow rate of exchange, slow in the NMR chemical shift time scale at +60°C (in this case the chemical shift time scale is less then 20Hz). There seems to be a profound contradiction in the observations here, which points to an error

in the proposed model.

It is known that F_2S_2 exists as a branched isomer (**XV** in Figure 4.7).[115] To

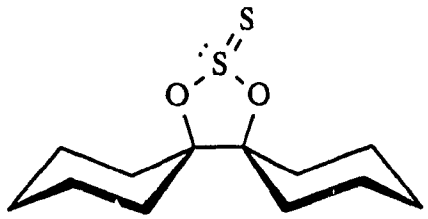

XVI

our knowledge, the only other branched sulfur system characterized by x-ray is **XVI**.[116] It is believed that an electron-withdrawing atom, such as fluorine or the bridging oxygen, enables the adjoining sulphur to utilize its 3-d orbital. There are several reactions that indicate that the branched isomer of organic polysulfides may be involved during a reaction.[4] Similarly, it is conceivable that the ruthenium center forces the adjacent sulphur to use its 3-d orbital in forming a branched sulphur chain, **XVII**, analogous to the thiosulfinyls **12b,d**. Calculations in organic systems indicate that the heat of formation of the branched isomer may lie at only 10 Kcal above the linear isomer.[117] The branched sulphur chain would introduce a second chiral center and thus two other Cp signals would be observed. As a result, the four Cp signals in the NMR spectrum of **11c** could be assigned as follows: the major Cp would be due to all the rotomers of the linear trisulphide, 2 Cp would be due to the branched isomer and the fourth Cp signal would be due to the disulfide. A proposed mechanism[99] for the formation of **11b-d** is shown in Scheme 4.4. A possible mechanism for the production of **XVII** differs only slightly from this, Scheme 4.5.

The trisulfides **11b-d** were found to be remarkably stable to air oxidation in organic solvents. They were also found to be resistant to loss of sulfur as they do not react with PPh_3 within 2 hours and react slowly with $(Et_2N)_3P$. This is in sharp

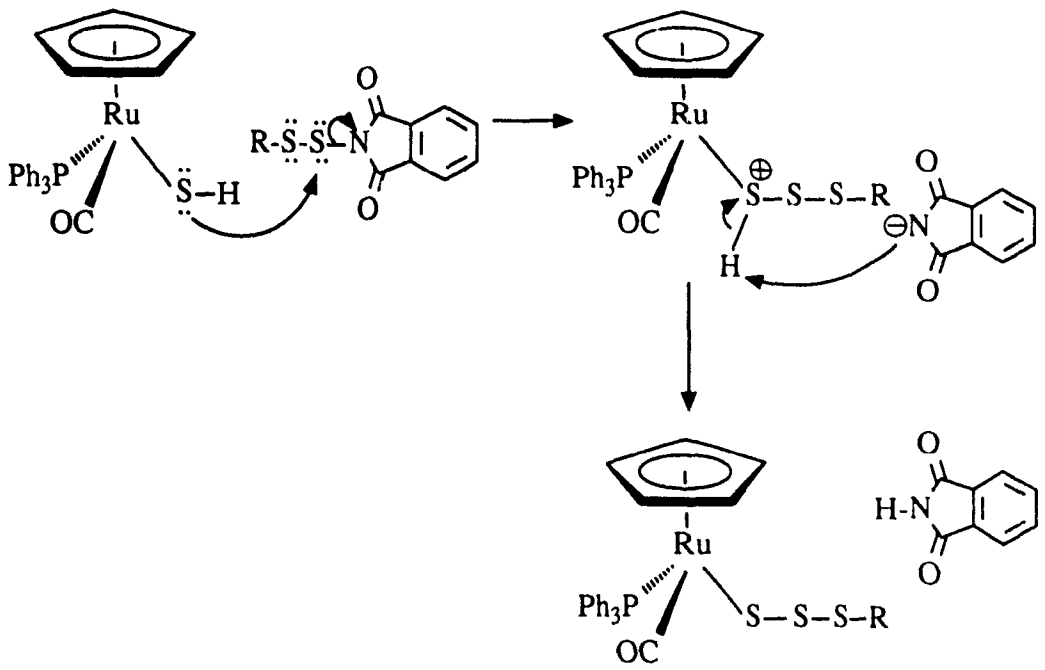

11b-d

Scheme 4.4 Proposed mechanism for the production of $CpRu(PPh_3)(CO)SSSR$[99], **11b-d**

contrast with $CpW(CO)_3SSR$ and $Cp_2Ti(SPh)(SSSPh)$.[95,96,97,99,106] Under UV irradiation, **11d** decomposed to two major and several unknown compounds. One of the major new Cp signals is **10d** which is the result of the expected desulfurization. The loss of a second sulfur to form **4d** was not observed. The other Cp signals remained unassigned. The intended product was the cyclic trisulfide **XVIII**. If this was formed, then the expected NMR spectrum would reflect diastereomers arising from the two chiral centers; one at the sulfur attached to both the metal and the R group and the other at the metal center. The complex **XVIII** could not be identified due to the complexity of the spectrum.

The crystal structure of **11c** (Figure 4.6) is consistent with the presence of the disulfide **10c** in the single crystal of the trisulfide **11c** used for the x-ray analysis.

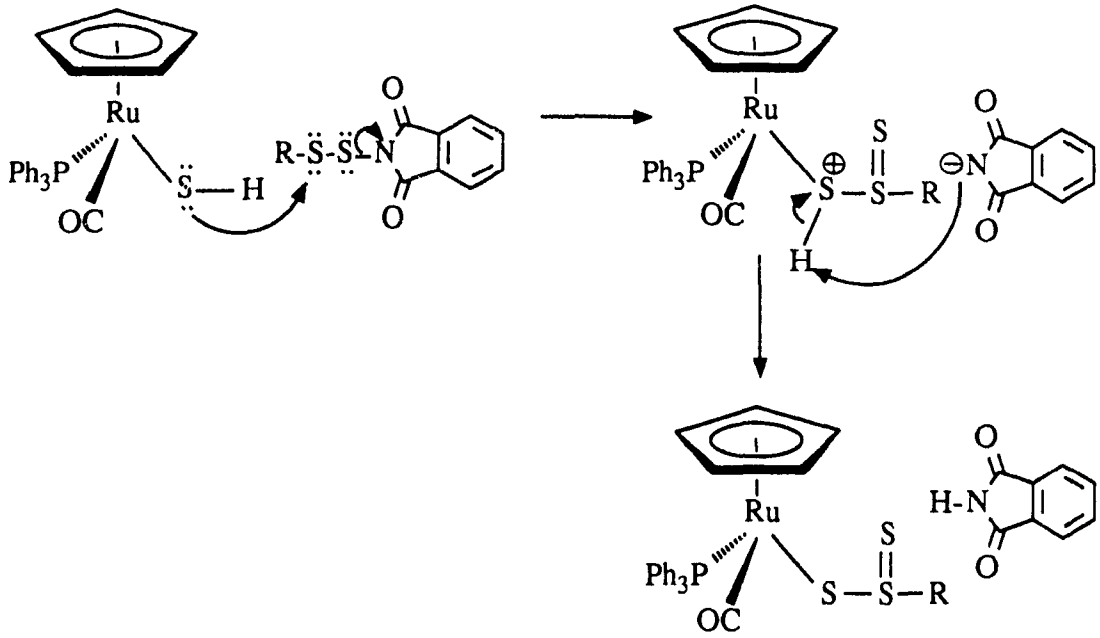

Scheme 4.5 Proposed mechanism for the production of $CpRu(PPh_3)(CO)SS(S)R$, **XVII**.

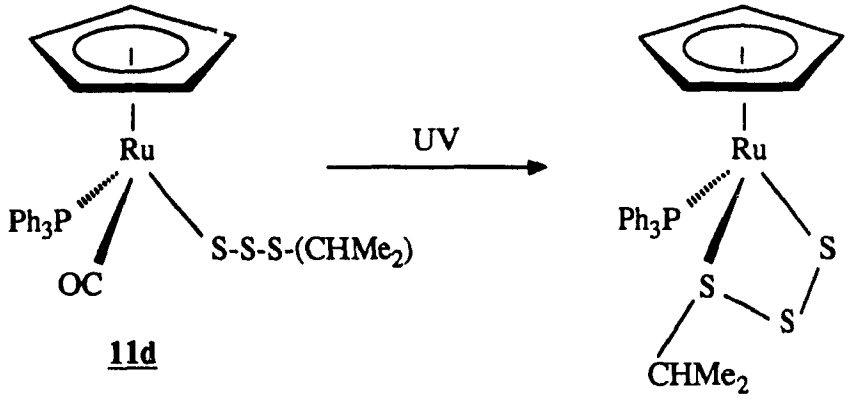

11d **XVIII**

When the crystal structures of **10d** and **11c** are compared, all the atom positions are found to correspond to within 0.2 Å. Since the space groups are different, packing constraints are unlikely to be similar and the structures are therefore near their

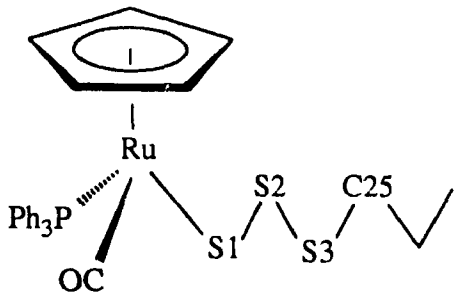

11c

energetic minima relative to intramolecular repulsion. The positions of S1 and S2 are the same for both compounds. Carbon atom C25 of the disulfide lies in the same position as S3 of the trisulfide and carbon atom C26A of the disulfur compound lies in the same position as C25 of the trisulfide. If one imagines changing the R group in **10d** to that in **11c** (i.e. 1-C_3H_7), then it would be reasonable to assume that C27 of the disulfide would lie in the same position as C26 of the trisulfide. In other words, little disruption to the lattice of **11c** would occur if some of the molecules of **11c** were replaced by those of **10c** such that C25 ,C26 and C27 of the latter occupied the position of S3, C25 and C26 of the former, respectively. In this case, the electron densities at the positions of S3 and C27 in the lattice of **11c** should be lower than expected. The temperature factors of S3 and C27 are somewhat large, consistent with this proposal Therefore, it is reasonable to conclude that the presence of **10c** in solutions of **11c** is due to the co-crystallization. This also suggests that the other contaminants in **11b-d** may be present in the crystal and that all these minor species were produced during the synthesis of **11b-d**.

The most interesting structural features of the trisulfide are the S-S bond lengths. The bond length for S1-S2 is normal (2.042(4) Å) while that for S2-S3 is

unusually short (2.005(5) Å) compared to the organic S-S bond length. However, the short S2-S3 bond length is not unique as other unusual bond lengths have been reported as shown in Figure 4.7 [118,119] In the only other organometallic trisulfide whose

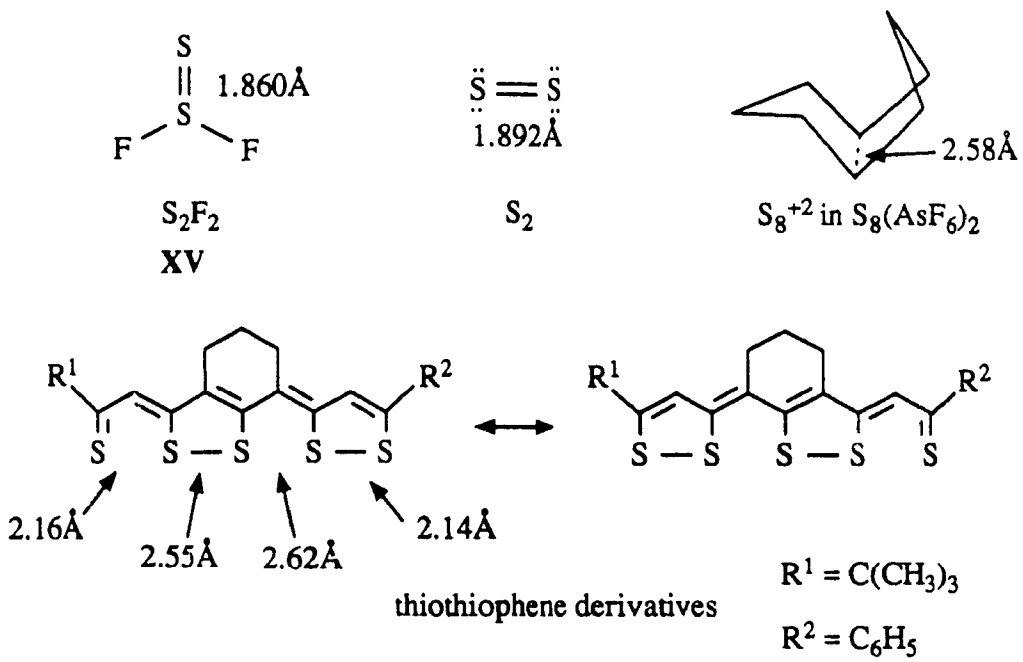

Figure 4.7 Selected bond lengths from organic and inorganic sulfur compounds.

structure has been determined, $Cp_2Ti(S(p\text{-Tolyl}))(SSS(p\text{-tolyl}))$[106], the S1-S2 distance was 2.053(3) Å and the S2-S3 distance was 2.011(3) Å. The same trend was observed in the bond lengths of both complexes as one travels away from the metal along the catenated sulfur chain. The alternating bond lengths have been observed in other polysulfides.[82,118] Steudel *et al.* suggested that neighboring sulfur bonds within a long chain interact with each other.[82,118] Consequently, steric and electronic factors which induce an abnormally long bond length create a deformation of one bond, which would cause the opposite deformation in the next bond and so on along the chain.

The dihedral angles in <u>11c</u> are 71.5(2)° for Ru-S1-S2-S3 and 65.2(4)° for

S1-S2-S3-C25. Both these dihedral angles are small compared to organic trisulfur analogs.[4,82,107,119] The minimum energy structure of organic trisulfides does not have a sulfur-sulfur dihedral angle of 90°. This is a result of the lone pair interaction between the first sulfur and the third sulfur atom as shown in Figure 4.8.[82] If the dihedral angle

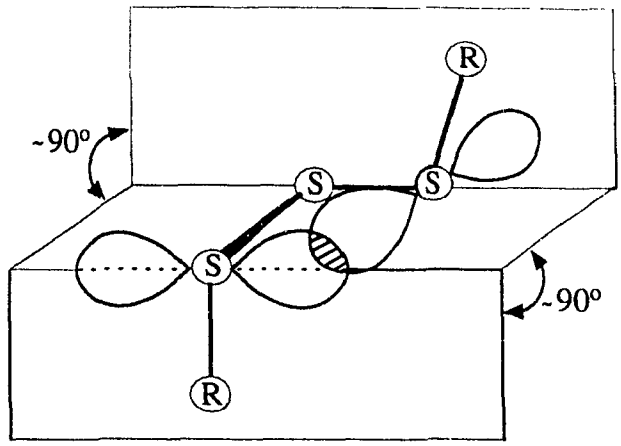

Figure 4.8 Interaction of lone pairs between first and third sulfurs in trisulfides.

changes slightly from 90° then this lone pair interaction will be substantially reduced. Consequently, the preferred dihedral angle in polysulfides is usually 5° to 15° greater or less than 90°.[107,119]

Following the same logic, the small dihedral angle may reflect the large size of the sulfur lobes, thus indicating that the sulfur atoms are very nucleophilic. The loss of sulfur induced by trivalent phosphines proceeds via nucleophilic attack by the phosphine at the sulfur atom.[108] This tendency would be substantially reduced if the sulfur atom was itself nucleophilic. If the nucleophilicity is truly reflected by the dihedral angle, then this would account for the greater stability of the trisulfides **11b-d** compared to the disulfides **10b-d**, as we would expect by comparing their respective dihedral angles. Consequently, one may speculate that the smaller the dihedral angle, the more stable the compound would be relative to loss of sulfur. This trend has been

empirically observed previously.[24,91,96,99] Note also that in the ruthenium system, the dihedral angle is directly proportional to the bond length. However, when one

Table 4.6 Bond lengths and dihedral angles of ruthenium systems.

Complex	S-S bond length (Å)	Dihedral angle
10d	2.038(4)	77.95
11c	2.042(4) 2.005(5)	71.5 65.2

considers the first S-S bond of the trisulfides as analogous to the disulfides, the opposite trend is observed, as discussed in conjuction to Table 4.4. If the bond lengths of metallic disulfides and trisulfides are plotted against the dihedral angles, one notices that the first sulfur-sulfur bond of metallic trisulfides follows the previous trend while the second sulfur-sulfur bond does not, Graph 4.1. It appears that in the case of trisulfides, the first S-S bond closest to the metal tends to be longer and thereby lies on the right side of the graph, while the second S-S bond from the metal tends to be short and thereby lies on the left side of the graph.

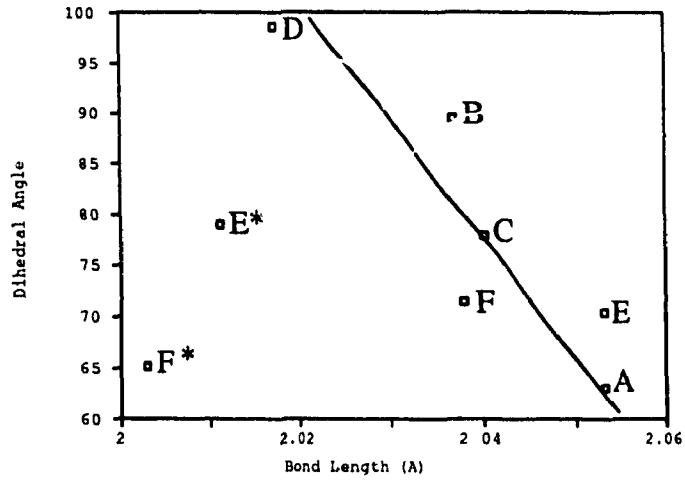

A $CpW(CO)_3SS(4\text{-}C_6H_4Me)$[97]

B cis-$(PPh_3)_2Pt(SSCHMe_2)(Phth)$[97]

C $CpRu(PPh_3)(CO)SS(CHMe_2)$

D $Cu(tet\text{-}b)SSCH_2CO_2$[98]

E $Cp_2Ti(SPh)(SSSPh)$[95]

F $CpRu(PPh_3)(CO)SSS(1\text{-}C_3H_7)$

* second S-S bond from the metal

Graph 4.1 Relation between dihedral angle about an S-S bond and bond length of metal disulfanes and trisulfanes.

III Preparation of $CpRu(PPh_3)(CO)SS(O)R$ ($R = 4\text{-}C_6H_4Me, 1\text{-}C_3H_7, CHMe_2$)

RESULTS

Treatment of **4a** with phthS(O)R in toluene gave $CpRu(PPh_3)(CO)SS(O)R$, **12b-d**, as air-stable yellow solids soluble in benzene, CH_2Cl_2 and THF, and insoluble in ethanol and hexanes, equation 4.21. Complexes **12b-d** seemed to be moderately

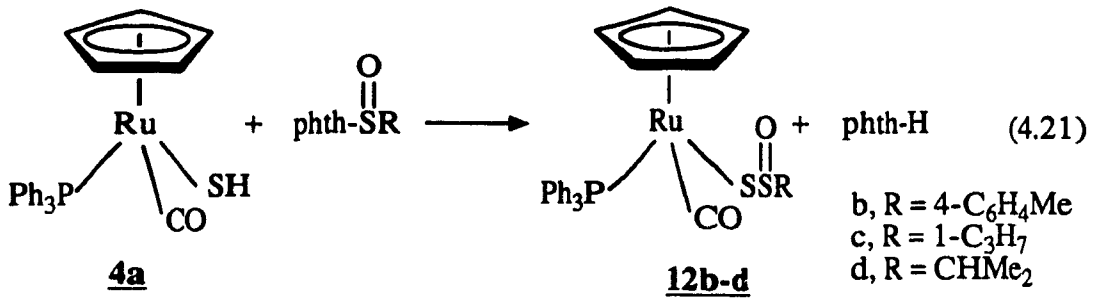

(4.21)

stable in organic solvents, surviving in solutions in air for up to 30 minutes before noticeable decomposition was observed by colour change.

A solution of **12b** gave four signals in the Cp region in the NMR spectrum at 5.00(**12b**(A)), 4.80(**12b**(B)), 4.73(**13b**) and 4.62(**10b**) ppm in the ratio 10.7:5.2:1.0:1.4 respectively, see Figure 4.9. The two major Cp signals were assigned to the diastereomers arising from the presence of two chiral centers: one at the metal, the other about the sulfur bonded to the oxygen. One of the remaining signals in the NMR spectrum was assigned to the disulfide **10b** while the other signal did not correspond to the thiolate **4b**, nor to any other known complexes and was assigned to **13b** (see below). The diastereomers of complex **12b** were separated yielding four crops of various ratios of **12b**(A):**12b**(B):**13b**:**10b**, see Experimental. Each crop of crystals had

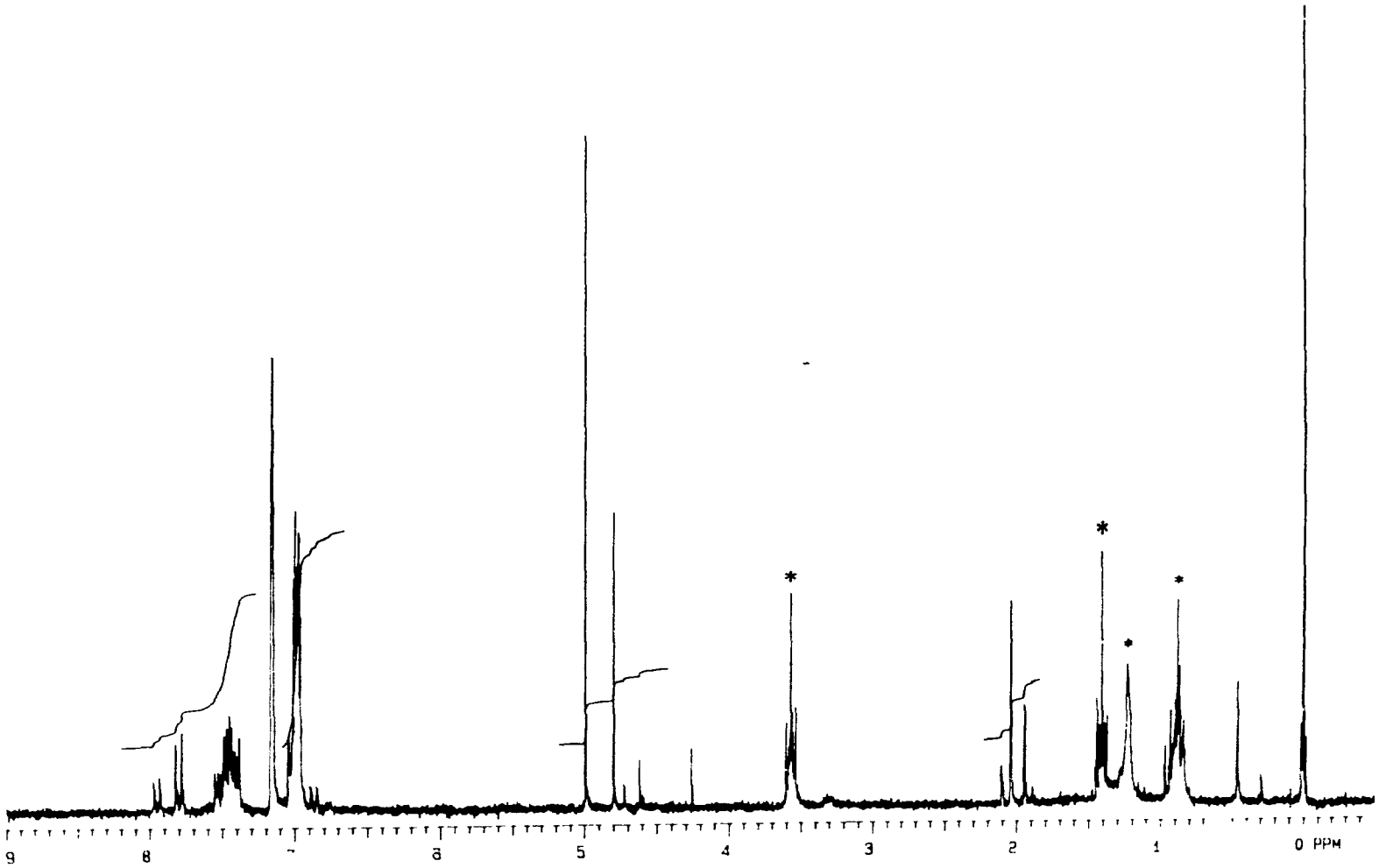

Figure 4.9 ^{1}H NMR spectrum of $CpRu(PPh_3)(CO)SS(O)(4\text{-}C_6H_4Me)$, **12b**.
* Residual THF
* Residual hexanes

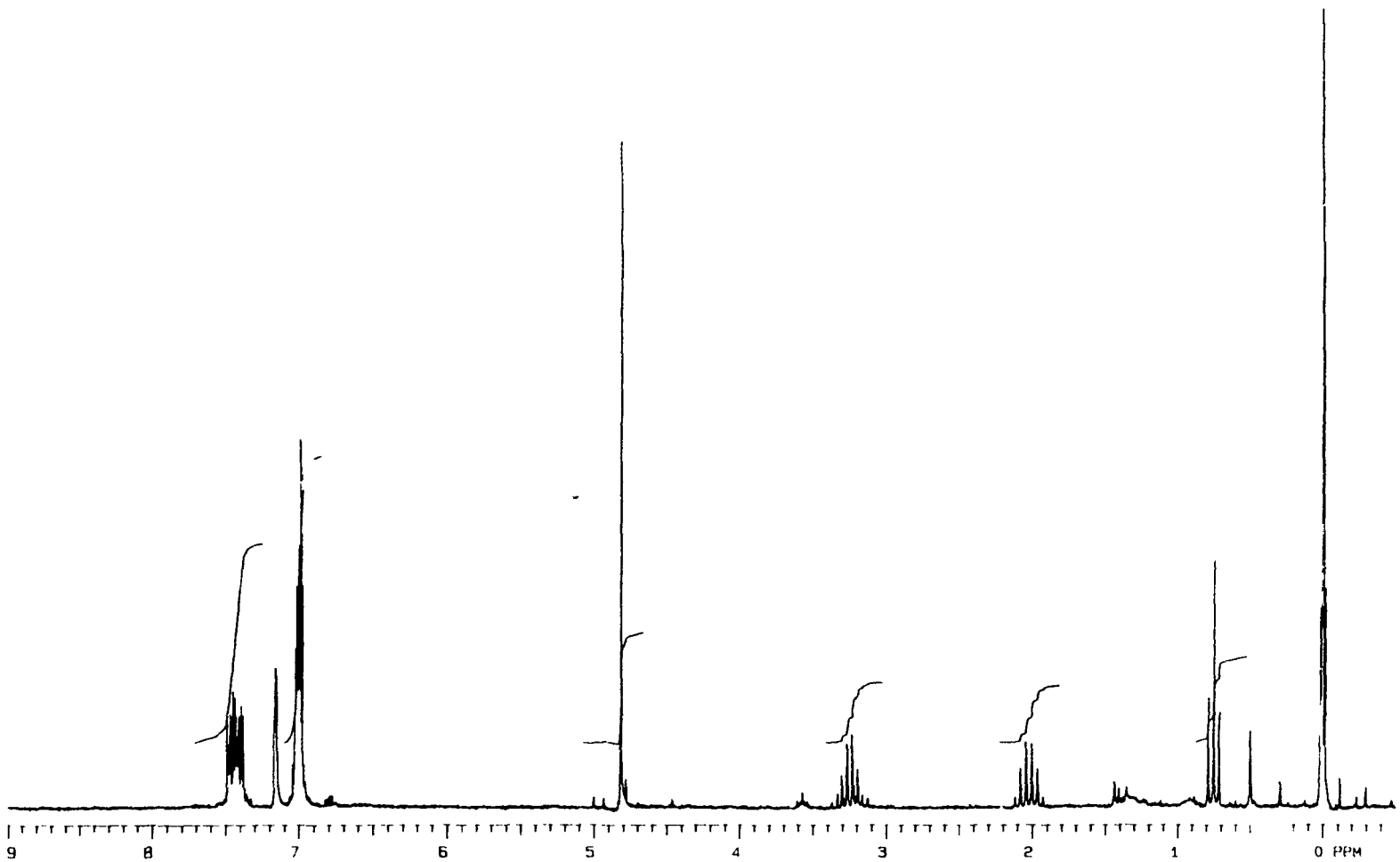

Figure 4.10 ^{1}H NMR spectrum of $CpRu(PPh_3)(CO)SS(O)(1\text{-}C_3H_7)$, **12c**.

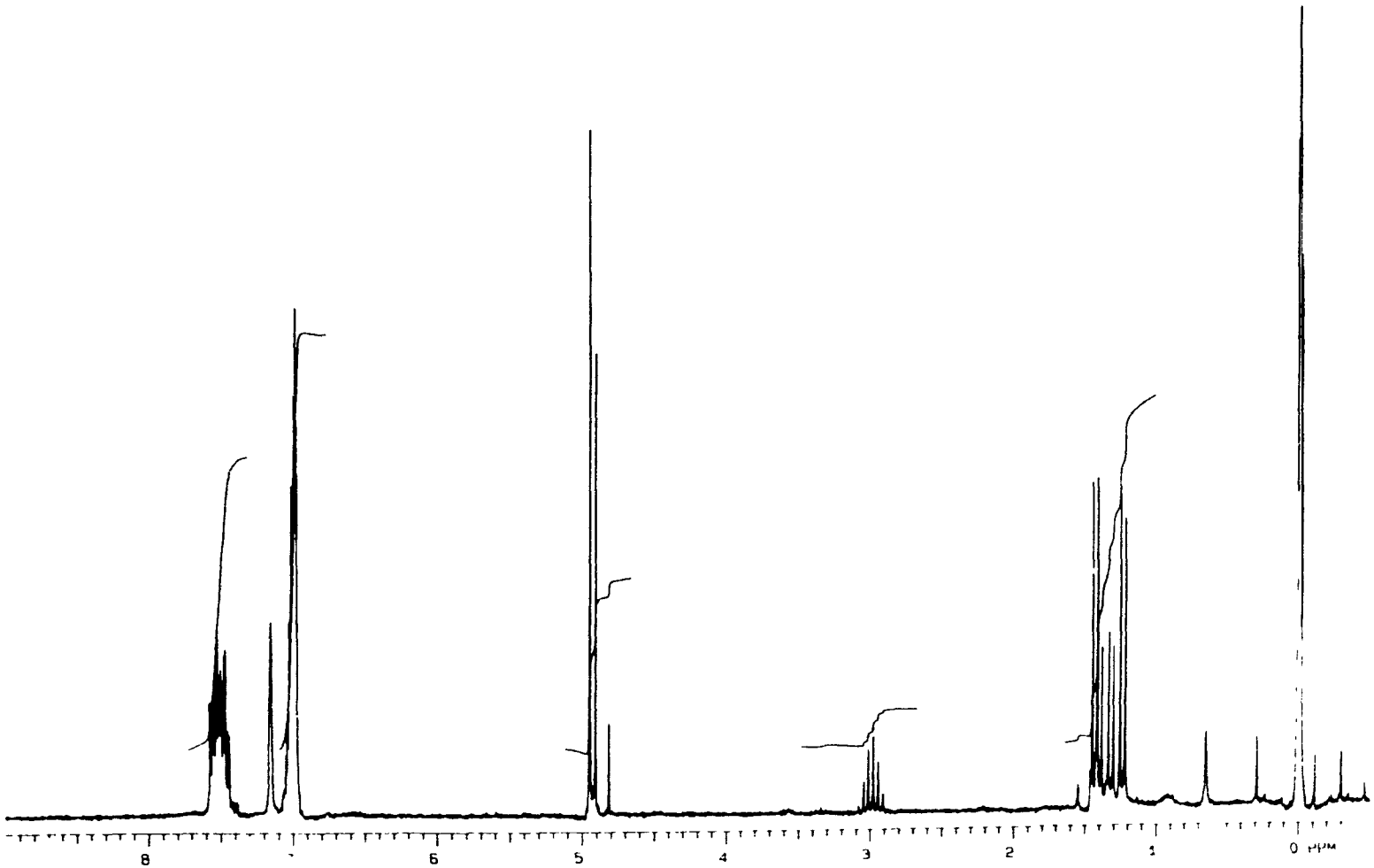

Figure 4.11 ^{1}H NMR spectrum of $CpRu(PPh_3)(CO)SS(O)(CHMe_2)$, **12d**.

a different melting point but the IR spectrum, in toluene and nujol, of each showed comparable bands due to $\nu_{(CO)}$ and $\nu_{(SO)}$ at 1960-1961 cm^{-1} and 1029-1044 cm^{-1} respectively, see Experimental section Table E.1. The crop whose NMR spectrum showed nearly pure **12b**(A), crop 3, and the crop whose NMR spectrum showed the most homogeneous mixture, crop 1, gave the same elemental analysis, suggesting similar composition. The NMR spectrum of **12b** was recorded at 100°C with no apparent change. A solution of **12c** gave four signals in the Cp region in the NMR spectrum at 5.00, 4.93, 4.82 and 4.78 ppm in the ratio 1:1:60:7 respectively, see Figure 4.10. The peak at 4.82 ppm was assigned to one of the diastereomers of **12c**, the other diastereomer was not assigned. The remaining minor Cp signals did not correspond to the thiolate **4c**, the disulfide **10c** nor any known complexes, and remained unassigned. Complex **12c** displayed two strong IR bands due to $\nu_{(CO)}$ bands in toluene at 1978 and 1959 cm^{-1}, Table 4.3. In addition to these bands, a third band was observed as a shoulder when the spectrum was recorded in CCl_4, see Table 4.5. The $\nu_{(SO)}$ was observed in toluene as two moderate bands at 1108 and 1082 cm^{-1}. In nujol, the $\nu_{(SO)}$ was observed as one weak band at 1054 cm^{-1}. A solution of **12d** gave three signals in the Cp region in the NMR spectrum at 4.96, 4.91 and 4.82 ppm in the ratio 7.2:4.1:1 respectively, see Figure 4.11. The two major signals were assigned to the diastereomeric pair. The remaining Cp signal did not correspond to the thiolate **4d**, the disulfide **10d** nor any known complexes, and remains unassigned. Each Cp peak in the NMR spectra of **12b-d** showed peaks due to the appropriate companion R groups with the expected intensities. Complex **12d** displayed one strong band for $\nu_{(CO)}$ in toluene at 1958 cm^{-1}. In toluene, the $\nu_{(SO)}$ was not observable, however, in nujol, a moderate band was noted at 1031 cm^{-1}.

When a sealed NMR sample of crop 4 of **12b** was heated to 100°C for 8 hours

and cooled to room temperature, the NMR spectrum showed an enrichment of the minor species **13b** and **10b** at the expense of **12b**(A) and **12b**(B), see Table 4.7. This indicates that at elevated temperatures, there is a conversion from one set of diastereomers, **12b**, into **10b** and **13b**, along with the formation of some **4b**. The

Table 4.7 Table indicating results of thermal treatment of **12b** using crop 4.

	Cp resonance (ppm) (Intensity in percent)	
Before	**12b**(A) **12b**(B)	5.00(92) 4.80(3.2)
	13b **10b**	4.73(2.6) 4.62(2.0)
After heating 100°C, for 10 hours	**12b**(A) **12b**(B)	5.00(2) 4.80(3)
	13b **10b**	4.73(48) 4.62(31)
	4b	4.64(16)

corresponding p-tolyl resonances were also observed at the appropriate intensities. The IR spectra in toluene showed that the bands at 1031 and 1045 cm^{-1} were significantly reduced while the band at 810 cm^{-1} grew. Complex **13b** was characterized and will be discussed below.

The compounds **12b-d** were unreactive toward triphenylphosphine. However, an NMR sample in C_6D_6 of **12d** decomposed readily when exposed to a UV light for 2.5 hours, to form isopropyl disulfide (10 % of all methyls present) along with substantial amounts of **4d** (29 % of all Cp signals), PPh_3S (34 % of all phenyl resonances) and two unknown compounds whose Cp signals lie at 4.82 and 4.51 ppm (67 % and 5 % of all Cp signals respectively).

The crystal structure of **12d** was determined and is shown in Figure 4.12.[120]

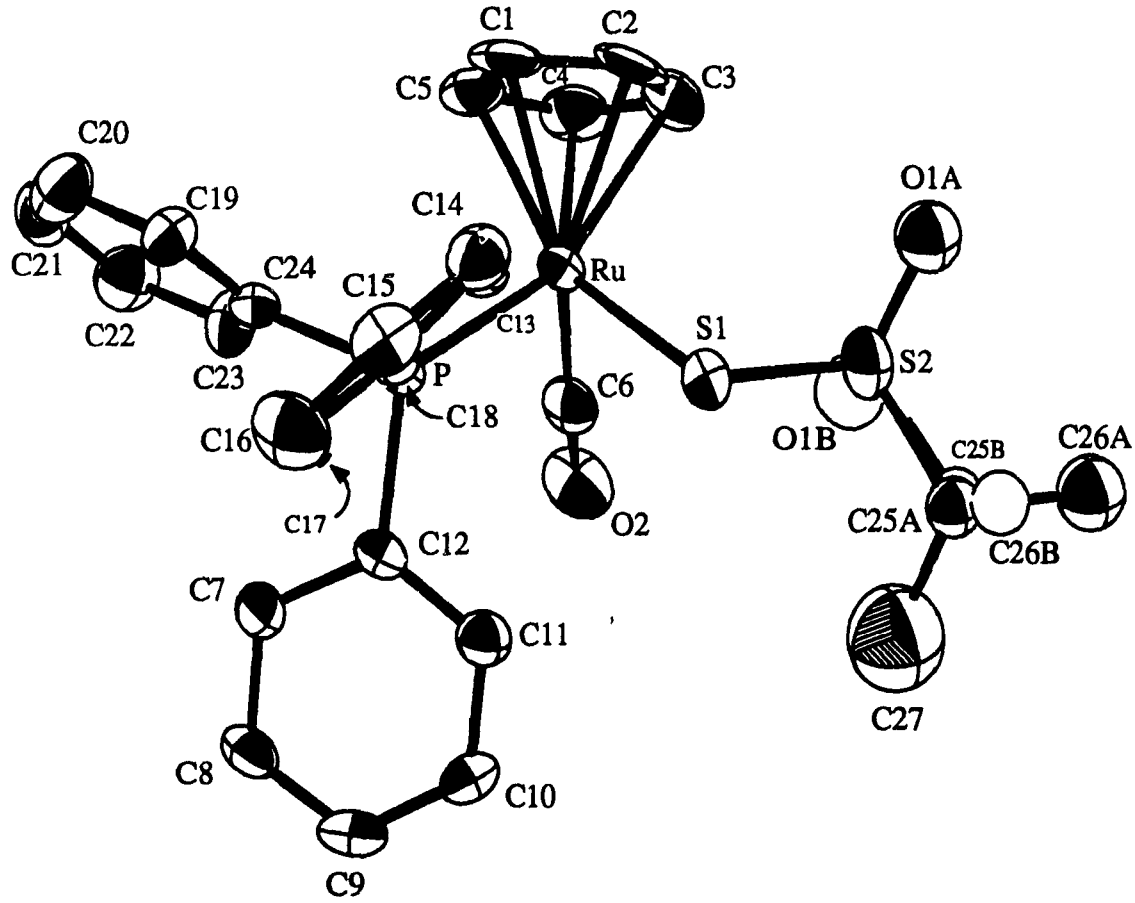

Figure 4.12 ORTEP of $CpRu(PPh_3)(CO)SS(O)(CHMe_2)$, **12d**.
Atoms labeled "A" are 60% occupancy
Atoms labeled "B" are 40% occupancy

Appendix VI, Tables A6.1-A6.4, contains the crystallographic data, atom coordinates, bond lengths and bond angles, respectively. The structure of **12d** is a piano stool with one PPh_3, one CO and one RS(O)S ligand. The oxygen on the sulfinyl sulfur, O1, was located in two different positions, O1A and O1B, while the remainder of the molecule remained essentially in the same position, with the exception of the R group. This disorder is not consistent with a simple rotation about the S1-S2 bond but rather an inversion at S2, see Figure 4.13. The ratio of diastereomers observed in the crystal

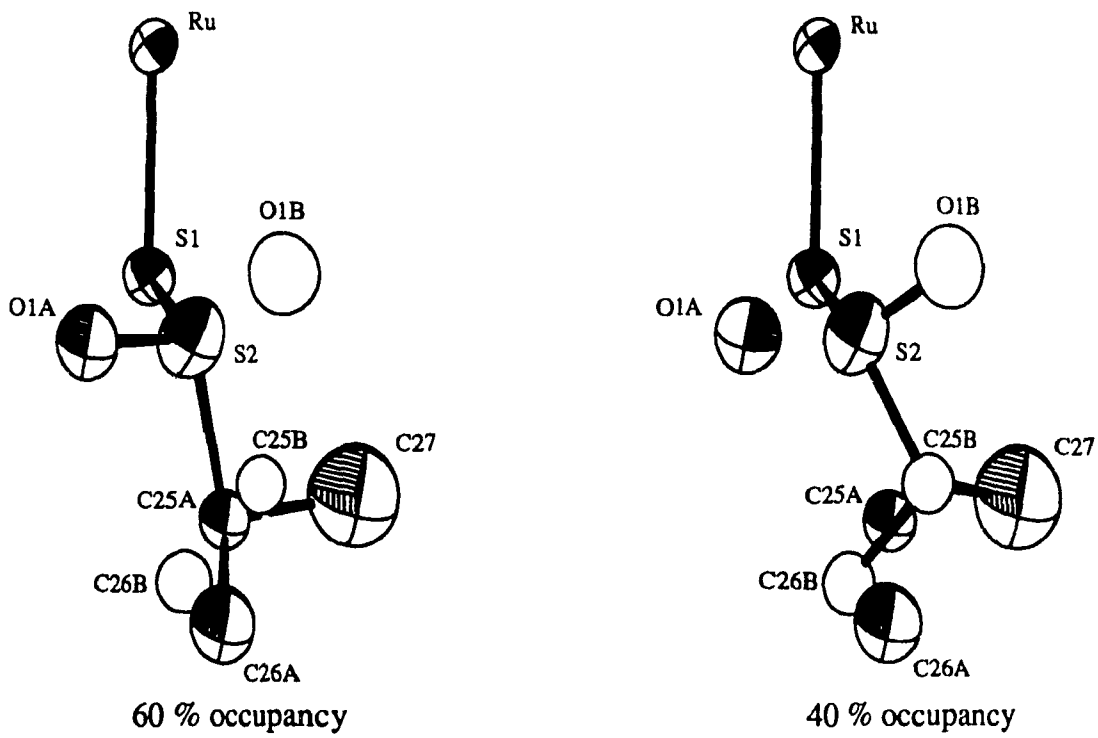

Figure 4.13 ORTEP of the thiosulfinate ligand showing the disorder.

structure through a ratio of partial occupancy of the O1A to O1B, is exactly the same as the ratio of the two Cp signals observed in the NMR spectrum. The disorder in the area

of the R group results from a rotation about S2-C25 bond. The sulfur-sulfur bond length was found to be 2.076(3) Å which is considered normal when compared to the organic thiosulfinate sulfur-sulfur bond length of 2.108 Å.[121]

DISCUSSION

Organometallic thiosulfinyl, MSS(O)R, has been postulated earlier[100] but to our knowledge, only one has been prepared[94,97]. Hartgerink's $CpW(CO)_3SS(O)R$ (**6**) were rather unstable but were still characterized although not by x-ray crystallography. In general, organic analogs are also not very stable, and tend to disproportionate to thiolsulfonates, $R\text{-}\overset{\overset{\displaystyle O}{\|}}{\underset{\underset{\displaystyle O}{\|}}{S}}\text{-}S\text{-}R$.[4,93] The reaction between **4a** and a sulfinyl transfer agent appeared to be a suitable route to the preparation of the thiosulfinyls **12b-d**, equation 4.20 (here reproduced). The sulfinyl transfer agent selected was N-(alkyl and

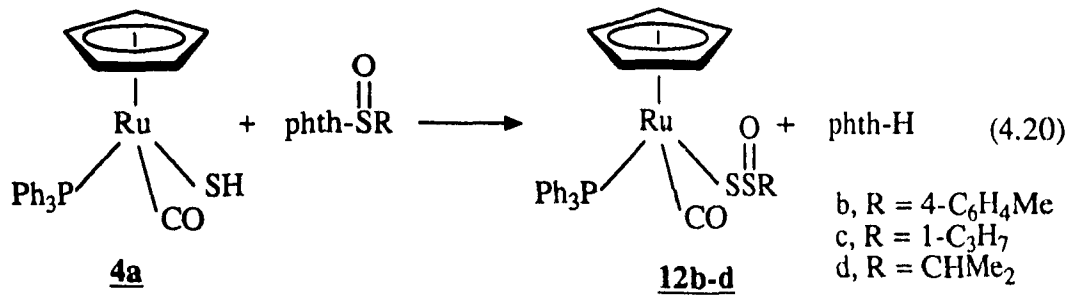

(4.20)

arylsulfinyl)phthalimide prepared by Harpp's method[88], since this was successfully used by Hartgerink[99]. The yields of these preparations are somewhat low, due in large part to unidentified side reactions. Some of the by-products were triphenylphosphenesulfide and **10b-d**. The presence of **10b-d** indicates either oxygen transfer or disproportionation occurs during the preparations. Both these decomposition modes have been observed in the oxidation of organic disulfides.[4]

The NMR spectra of **12b-d** show 2 major products and two minor contaminants. The presence of two major products is consistent with diastereomeric pairs arising from the presence of two chiral centers, one at the metal and one at the

sulfinyl center. At elevated temperatures, the major pair of Cp signals in **12b** gave way to the minor contaminants along with a small amount of **4b**. One of the mimor contaminants has been identified by NMR as **10b**.

The S-S bonds in organic thiosulfinate esters are quite weak and prone to homolitic cleavage[122] and intermolecullar oxygen transfer[4]. Thermal disproportionation and recombination are not the likely mechanisms of interchange between the observed species. If this was the case, then recombination of the free radicals would lead to the formation of organic disulfides and disulfur bridged metal, however, these were not observed. Since the elemental analyses for the cleanest and the most contaminated crops of **12b** (crop 1 and crop 3) were identical, then a mixture of isomers is the likely source of the contaminants.

The crystal structure of **12d** indicated the presence of two diastereomeric compounds within the same crystal in the ratio of 2:3 (see ORTEP in Figures 4.12 and 4.13). The corresponding NMR spectrum also shows the presence of two diastereomeric species in the ratio of 2:3. Consequently, the NMR signals can be assigned to the specific structure. The most intense NMR spectra can be assigned to the shaded ORTEP in Figure 4.13, while the weaker NMR spectra can be assigned to the ORTEP shown as ghost atoms.

The product distribution upon treatment with UV light is consistent with a free radical pathway. The presence of $Me_2CHSSCHMe_2$ in the product supports the free radical pathway with concurrent intermolecular or intramolecular oxygen migration. A Cp-containing compound was observed in this reaction in reasonable yield (67%). The R group shows diastereotropic methyls. This compound could not be identified as any compound already characterized and remaines unassigned.

IV Preparation of $CpRu(PPh_3)(CO)SS(O)_2R$ ($R = 4\text{-}C_6H_4Me$)

RESULTS

Prolonged thermal treatment of **12b** gave $CpRu(PPh_3)(CO)SS(O)_2(4\text{-}C_6H_4Me)$, **13b**, along with **10b**, see equation 4.21. In addition to **13b** and **10b**, the presence of **4b**

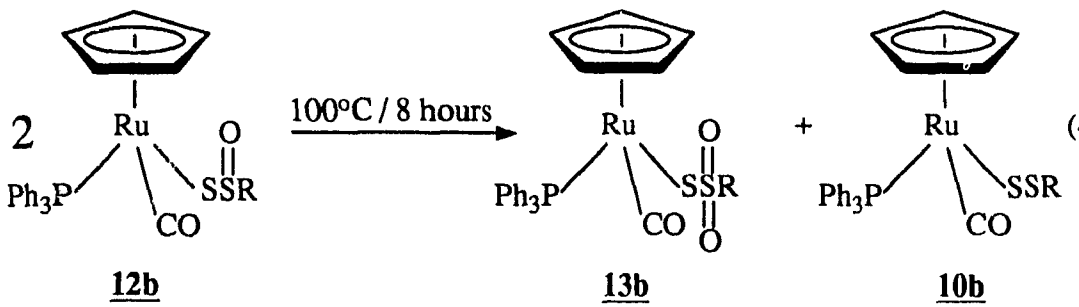

(4.21)

was also observed in the ratio of 1 : 0.65 : 0.35 respectively. The air-stable yellow brown needles of **13b** were soluble in benzene and THF, and insoluble in hexanes. The NMR spectrum of **13b** showed one Cp resonance at 4.73 ppm and the expected R group in the appropriate intensity. The IR spectrum showed one $\nu_{(CO)}$ at 1971 cm^{-1}.

The crystal structure of **13b** was determined and is shown in Figure 4.14.[126] All crystallographic data, atom coordinates, bond angles and lengths are listed in Appendix VII, Tabes A7.1-A7.4. The structure is a piano stool with one PPh_3, one CO and one SS(O)2R ligand. The latter is a thiosulfonyl ligand which, to our knowledge, has never been reported on a metal. The crystal was found to be optically resolved. The general R factors of the two possible enantiomers are 0.044 and 0.046. Since these R factors are statistically different[123], the absolute configuration corresponding to the lower R factor was selected and is shown in Figure 4.14. The S1-S2 bond length is 2.023(8) Å

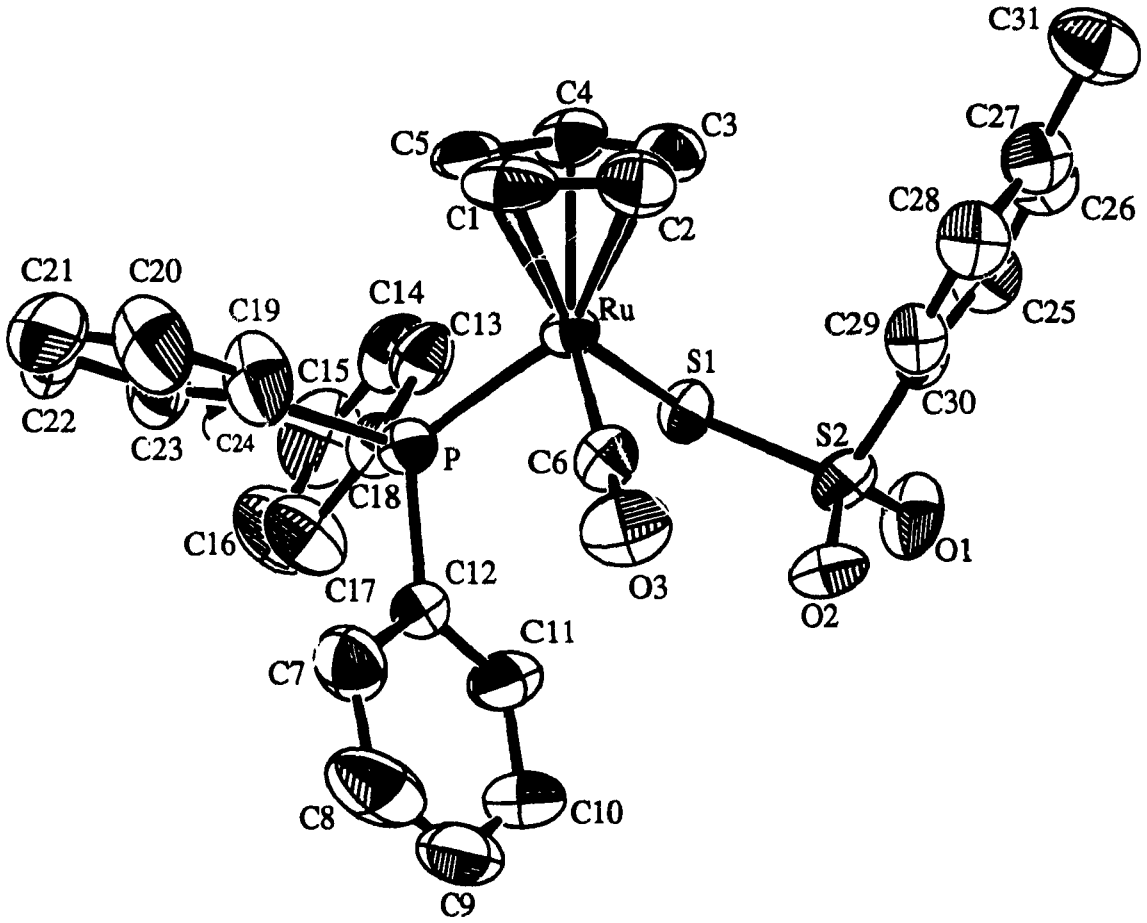

Figure 4.14 ORTEP of $CpRu(PPh_3)(CO)SS(O)_2(4\text{-}C_6H_4Me)$, **13b**.

which is slightly shorter than for organic thiosulfonates (2.0919(6) Å (**XI**)[101], 2.048(2) Å (**XII**)[102]). The Ru-S1 distance is 2.383(2) Å, which is identical to the Ru-S1 bond distances in **10d** and **12d**.

DISCUSSION

Organometallic thiosulfonyls have not been reported in literature. The thermal rearrangement of **12b** formed the thiosulfonyl $CpRu(PPh_3)(CO)SS(O)_2(4\text{-}C_6H_4Me)$, **13b**, as shown in equation 4.21 (here reproduced). The observed ratio of **13b**:**10b** was

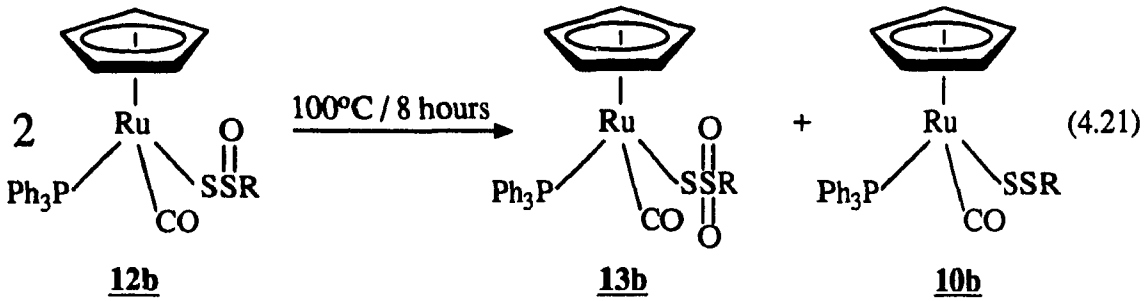

1:0.65. The stoichiometry of the reaction 4.21 shows that the ratio should have been 1:1, however, one third of **10b** apparently disproportionated to **4b** through the loss of elemental sulfur. Since the reaction proceeds cleanly, intermolecular oxygen transfer is the likely mechanism in this reaction. A similar reaction mechanism has been proposed in the decomposition of metal sulfonates to thiolates.[105]

The crystal structure of **13b** confirmed the presence of the thiosulfonyl group as shown in Figure 4.14. This is the first reported metal thiosulfonyl. The crystal is optically pure and the absolute configuration has been determined. The observed S1-S2 bond length in **13b** is midrange when compared to other known thiosulfonates.

Table 4.8 List of known organic thiosulfonate S-S bond lengths.

Complex	S-S bond Length (Å)
$^{-}S\text{-}S(O)_2\text{-}Me$[85]	1.954(1)
$[(C_3H_6N_2)S]_2Te[SS(O)_2(C_6H_5)]_2$, **XIV**[104]	2.016(5)
$CpRu(PPh_3)(CO)SS(O)_2(4\text{-}C_6H_4Me$, **13b**	2.023(8)
$C_{14}H_{12}S_2O_2$, **XII**[102]	2.048(2)
$Te[SS(O)_2(C_6H_5)]_2$, **XIII**[103]	2.080(2)
$(4\text{-}BrC_6H_4)SS(O)_2(4\text{-}BrC_6H_4)$, **XI**[101]	2.091(6)

V FINAL ADDRESS

At this point, it is appropriate to draw some conclusions regarding the relation between the various catenated sulfur chains. One can observe that the $\nu_{(CO)}$ stretching frequencies increased as follows: SR ≤ SSR < SSSR < $\overset{O}{\overset{\|}{S}}SR$ < $\underset{\underset{O}{\|}}{\overset{O}{\overset{\|}{S}}}SR$, see Table 4.3. It follows then that the SR group is more electron donating than the $SS(O)_2R$ group and consequently, the electronegativity of these groups may be arranged as follows:

$$SR \quad SSR \quad SSSR \quad \overset{O}{\overset{\|}{S}}SR \quad \underset{\underset{O}{\|}}{\overset{O}{\overset{\|}{S}}}SR$$

$$\longrightarrow$$

Increasing electronegativity

The inherent instability of the S_XR groups as x increases, may reflect the less effective $p\pi$-$d\pi$ donation from the α sulfur to the metal for SSSR, as opposed to SR.

As one proceeds from the disulfide (**10d**) to the thiosulfinyl (**12d**) to the thiosulfonyl (**13b**), one observes that the ruthenium sulfur bond length remains constant (2.395(3) Å, 2.379(2) Å and 2.383 (2) respectively). In contrast, the S1-S2 bond length increases from **10d** to **12d** (2.038(4) Å and 2.076(3) Å respectively) however, when the second oxygen is added on S2, the S1-S2 bond length decreases to 2.023(3) Å. This last decreased bond length may be misleading due to the different R groups.

EXPERIMENTALS

All experiments were performed under nitrogen in appropriately-sized Schlenk tubes or appropriately sized three-necked round bottom flasks. Tetrahydrofuran, hexanes and toluene were distilled over sodium/benzophenone prior to use. Absolute ethanol was degassed by repeated cycles of evacuation and purging with nitrogen (3x) prior to use. Bis(1,2-diphenylphospheno)ethane (Strem), methyllithium, 2-propylthiol, 1-propylthiol, triphenylphosphine (Aldrich) and 4-methylbenzenethiol (Fairfield) were used as received. The complex $CpRu(PPh_3)_2Cl$ was prepared as reported[125] using $RuCl_3 \cdot 3H_2O$ (Aldrich or kindly supplied by PGM Chemicals Ltd.). The compounds 1-propylthiophthaimide, 2-propylthiophthalimide, p-tolylthiophthalimide, 1-propylsulfonylphthalimide, 2-propylsulfonylphthalimide and p-tolylsulfonylphthalimide were prepared using methods by Bach and Harpp.[88,89,125] Solvents and other liquid reagents were transferred by means of appropriately sized syringes. Syringes and containers exposed to thiols were decontaminated by rinsing with commercial bleach prior to cleaning.

<u>Caution</u>: Preparations involving the use of H_2S must be performed with extreme care. This gas is very toxic and has a very unpleasant odor even at extremely low concentrations. The reactions were conducted in a well ventilated fume hood and H_2S was handled by means of a gas manifold shown in Figure E.1. The H_2S emanating from an H_2S cylinder (Matheson) via Tygon tubing was dried by means of a calcium chloride column and passed trough a Nujol bubbler before entering the reaction vessel; a 3-neck round bottomed flask fitted with a stopcock, a gas inlet bubbler, a stopper and a magnetic stir bar. After passing through the reagents, unreacted H_2S was passed through three washing towers containing successively, 5 M NaOH, saturated aqueous

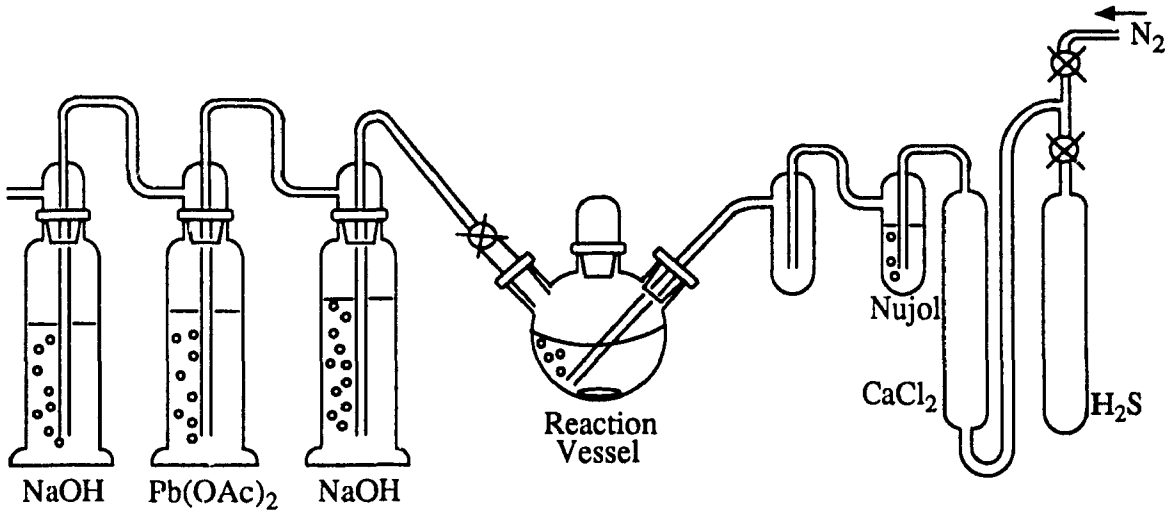

Figure E.1 Apparatus used for the manipulation of H_2S.

lead acetate and 5 M NaOH. A nitrogen line (Tygon) was connected to the H_2S manifold prior to the calcium chloride drying column by means of a T-connector attached to a stopcock. This permitted the system to be purged before and, most importantly, after the reaction, which significantly reduced exposure to residual H_2S during the work up.

Nuclear magnetic resonance (NMR) spectra were recorded on a Varian XL-200 or XL-300 spectrometer. All NMR samples were prepared under N_2 atmosphere using benzene-d_6, degassed by freeze-thaw degassing under vacuum. Chemical shifts are reported in ppm relative to tetramethylsilane, used as an internal standard, and the multiplicities are reported as m, d, t and ABq (multiplet, doublet, triplet and AB quartet respectively). The ^{31}P NMR spectra were performed on Varian XL-300 using 85 % phosphoric acid as the external reference. COSY and NOE experiments were performed at 300 MHz in 5mm tubes. Infrared spectra were recorded on an Analect AQS-20 fourier-transform infrared (FT-IR) spectrometer calibrated using a He/Ne laser (632.8 nm). The detector used was a triglicine sulfate (TGS) detector with a standard

resolution of 4 cm^{-1}. All bands are reported in cm^{-1} with an accuracy of ± 1 cm^{-1} and the intensities are reported as sh, w, m, s and vs (shoulder, weak, moderate, strong and very strong respectively). All mass spectra were obtained by fast atom bombardment (FAB) on a ZAB-HS mass spectrometer at the McGill University Biomedical Mass Spectrometry unit. The specific conditions employed are reported as a footnote. Elemental analyses were performed by Spang Microanalytical Laboratories, Eagle Harbor, Michigan. Melting points were obtained on a Thomas Hoover capillary melting point apparatus in a sealed capillary tube under a nitrogen atmosphere and are uncorrected.

Cyclopentadienylbis(triphenylphosphine)mercaptoruthenium(II), $CpRu(PPh_3)_2SH$, 1a

Caution:

This experiment requires H_2S: use extreme care. Follow all precautions and use the apparatus described earlier. At the end of the experiment, there will be a substantial amount of H_2S condensed in the liquid nitrogen trap of the vacuum line used. It is desirable to neutralize it by removing the trap while still frozen in liquid nitrogen, in a fume hood, and pouring commercial bleach into it. The reaction will be strongly exothermic and will rapidly melt most of the solvent. Complete neutralization requires 5-10 minutes.

Sodium metal (0,10 g, 4.43 mmole) was dissolved in absolute ethanol (20 mL) and H_2S was bubbled through the solution at a steady rate for 30 minutes. The solution was then purged with N_2 for 20 minutes, and THF (50 mL) followed by $CpRu(PPh_3)_2Cl$ (1.00 g, 1.31 mmole) were added. The resulting slurry was brought rapidly to reflux (heating mantle) and maintained for 15 minutes. The best yield was obtained by very carefully purging the refluxing solution by closing the system, and very briefly opening the system to vacuum, followed by opening to nitrogen. This cycle was repeated 2-3 times for each purging before resuming normal reflux. The purging was repeated 3-4 times during reflux. This procedure removes unwanted H_2S from the reaction flask. After reflux, the solution was cooled to room temperature in a water bath. The brown solution was stripped to dryness (vacuum pump) and extracted with toluene (4 x 15 mL). Each extract was filtered under nitrogen through Celite (1

inch). The combined filtrates were stripped to dryness and the resulting dark oil recrystallized from THF/ethanol, washed with ethanol followed by hexanes and pumped on overnight to give the analytical sample as orange-brown microcrystals (0.600 g, 0.83 mmole). Yield = 63% mp. = 171-174°C

^{1}H NMR (C_6D_6): -3.11(t, 1H, J_{H-P} = 6.15 Hz, S<u>H</u>), 4.28(s, 5H, Cp), 6.94(m, 9H, PPh_3), 7.57(m, 6H, PPh_3).

Anal. calcd. for $C_{41}H_{36}P_2RuS$: 68.04%C, 5.01%H, 4.43%S

found: 67.96 %C, 5.01 %H, 4.39 %S

<u>Cyclopentadienylbis(triphenylphosphine)-4-methylbenzenethiolatoruthenium(II), $CpRu(PPh_3)_2S$-4-C_6H_4Me, 1b</u>

A Schlenk tube was charged with THF (200 mL) and cooled to -78°C in an ethanol/dry ice bath. Methyllithium (3.73 mL, 1.4 M in ether, 5.22 mmole) was added followed by 4-methylbenzenethiol (0.574 g, 5.22 mmole). The cooling bath was removed and the solution was allowed to warm to room temperature over 15 minutes and while stirring, a white precipitate formed. The complex $CpRu(PPh_3)_2Cl$ (2.00 g 2.87 mmole) was added as a solid and the resulting slurry was rapidly brought to reflux within 7 minutes by means of a water bath on a hot plate. A gentle reflux was maintained for 15 minutes after which the volume of the deep red solution was immediately reduced to 50 mL under vacuum, and ethanol (50 mL) was added. Further evaporation under vacuum to 50 mL gave red-orange microcrystals which were collected by decanting the mother liquors. The bright red solid was washed successively with ethanol, hexanes and pumped on overnight to give the analytical sample (1.58 g, 1.94 mmole). Yield = 74% mp. = 207-210°C

IR (Nujol): $\upsilon_{(CS\ of\ S\text{-}R)}$= 748(m)

^{1}H NMR (C_6D_6): 2.21(s, 3H, $C\underline{H}_3$), 4.14(s, 5H, Cp), 6.98(m, 11H, PPh_3 and 4-$C_6\underline{H}_4CH_3$), 7.64(m, 8H, PPh_3 and 4-$C_6\underline{H}_4CH_3$)

Anal. Calcd. for $C_{48}H_{42}P_2RuS$: 70.83%C, 5.20%H, 3.94%S

found: 70.76 %C, 5.21 %H, 3.90 %S

Cyclopentadienylbis(triphenylphosphine)-1-propylthiolatoruthenium(II), $CpRu(PPh_3)_2S\text{-}1\text{-}C_3H_7$, 1c

A Schlenk tube was charged with THF (110 mL) and cooled to -78°C in an ethanol/dry ice bath. Methyllithium (2.05 mL, 1.4 M in ether, 2.87 mmole) was added followed by 1-propylthiol (0.26 mL, 2.87 mmole), the cooling bath was removed and while stirring, the solution was allowed to warm to 0°C. The Schlenk tube was then immersed in a water bath at 40°C for 15 minutes. The complex $CpRu(PPh_3)_2Cl$ (1.00 g 1.44 mmole) was added and the resulting slurry rapidly brought to reflux within 7 minutes by means of a water bath on a hot plate. A gentle reflux was maintained for 15 minutes after which the volume of the red solution was rapidly concentrated under vacuum to 50 mL and ethanol (100 mL) was added. Further concentration to 50 mL followed by standing, gave the product as red crystals which were collected by decanting the mother liquors. The crystals (0.87g, 1.14 mmole) were washed successively with ethanol and hexanes and pumped on overnight. Yield = 79% mp. = 167-169°C

IR (Nujol): $\upsilon_{(CS\ of\ S\text{-}R)}$= 761(m)

^{1}H NMR (C_6D_6): 1.19(t, 3H, $J_{H\text{-}H}$ = 6.9 Hz, $CH_2CH_2C\underline{H}_3$), 1.98(m, 2H, $CH_2C\underline{H}_2CH_3$), 2.41(t, 2H, $C\underline{H}_2CH_2CH_3$, $J_{H\text{-}H}$ = 7.2 Hz), 4.36(s, 5H, Cp), 6.95(m, 9H, PPh_3), 7.62(m,

6H, PPh_3)

Anal. Calcd. for $C_{26}H_{42}P_2RuS$: 69.00%C, 5.53%H, 4.19%S

found: 68.84%C, 5.45%H, 4.16%S

Cyclopentadienylbis(triphenylphosphine)-2-propylthiolatoruthenium(II), $CpRu(PPh_3)_2S$-2-$CHMe_2$, 1d

A Schlenk tube was charged with THF (100 mL) and cooled to -78°C in an ethanol/dry ice bath. Methyllithium (1.14 mL, 1.4 M in ether, 1.60 mmole) was added followed by 1-propylthiol (0.149 mL, 1.60 mmole). The cooling bath was removed and the stirred solution was allowed to warm to 0°C. The Schlenk tube was then immersed in a water bath at 40°C for 15 minutes. The complex $CpRu(PPh_3)_2Cl$ (1.00 g 1.44 mmole) was added and the resulting slurry rapidly brought to reflux within 7 minutes by heating the water bath with a hot plate. A gentle reflux was maintained for 15 minutes after which the dark red reaction solution was rapidly concentrated under vacuum to 20 mL and ethanol (50 mL) was added. Further concentration to 10 mL followed by standing, gave the product as a beige powder which was collected by decanting the mother liquors. The solid was washed successively with ethanol and hexanes and pumped on overnight to give the analytical sample as orange-beige microcrystals (0.744 g, 0.972 mmole). Yield = 68% mp. = 161-163°C

IR (Nujol): $\upsilon_{(CS\ of\ S\text{-}R)}$= 821(w)

^1H NMR (C_6D_6): 1.58(d, 6H, $J_{H\text{-}H}$= 6.6 Hz, $CH\underline{Me}_2$), 2.52(sept, 1H, $J_{H\text{-}H}$= 6.6 Hz, $C\underline{H}Me_2$), 4.73(s, 5H, Cp), 6.98(m, 9H, PPh_3), 7.64(m, 6H, PPh_3)

Anal. Calcd. for $C_{26}H_{42}P_2RuS$: 69.00%C, 5.53%H, 4.19%S

Found: 68.83%C, 5.55%H, 4.23%S

Kinetic studies of the reaction of CS_2 with 1b

In each experiment, an NMR tube was charged with **1b** (0.0070 g) and the appropriate amount of PPh_3 was added. The tube was purged with nitrogen and C_6D_6 (0.40 mL) was added followed by TMS (1 μL). At time zero, the appropriate amount of CS_2 was added to the solution through a septum using a gas tight syringe. The reaction was followed by automatically acquiring spectra at appropriate intervals by means of an array of preacquisition delays. The rate was determined by comparing the relative integrals of the Cp peaks due to **1b** and **6b**. The total solvent volume was assumed to be the sum of the volumes of C_6D_6 and CS_2. Variations in solvent volumes were accounted for in subsequent calculations so that various amounts of CS_2 could be compared directly.

1,1′-Bis(cyclopentadienyl)-1,1′-bis(triphenylphosphene)-bis (μ-1-propylthiolato)diruthenium(II), $[CpRu(PPh_3)\text{-}\mu\text{-}S\text{-}1\text{-}C_3H_7]_2$, 2c

A Schlenk tube was charged with **1c** (0.17 g, 0.22 mmole) and toluene (2 mL). The tube was immersed in refluxing toluene for 5 minutes and immediately stripped to dryness under vacuum. The residue was suspended in hexanes and deposited on top of a chromatography column (Alumina, 2.5 cm x 25 cm). Elution with hexanes gave a band containing PPh_3. Eluting with THF in hexanes (1:1) gave an orange band. This band was collected and reduced under vacuum to about 3 mL and cooled at -20°C overnight. Three types of crystals formed, yellow translucent (PPh_3), orange ($CpRu(PPh_3)_2Cl$, which is a minor contaminant in **1c**) and dark red, **2c**. Identification

of the crystals was confirmed by NMR. The dark red crystals were separated and collected manually as well formed crystals (30 mg, 0.065 mmole). Yield = 30% mp. = 91-92°C

^{1}H NMR (C_6D_6): 0.89,(t, 6H, J_{H-H}= 5.7 Hz, $CH_2CH_2C\underline{H}_3$), 1.70(m, 4H, $CH_2C\underline{H}_2CH_3$), 2.54, 2.78(diastereotropic multiplet, 2H, $C\underline{H}_2CH_2CH_3$), 4.16(s, 5H, Cp), 4.41(s, 5H, Cp), 7.01(m, 18H, PPh_3), 7.49(m, 12H, PPh_3)

1,1′,1″-Tris(cyclopentadienyl)-tris(μ-1-propylthiolato)triruthenium(II), [CpRu-μ-S-1-C_3H_7]$_3$, 3c

A solution of **1c** (0.694 g, 0.960 mmole) in toluene (40 mL) was prepared in a three-necked flask fitted with a water condenser. The solution was brought to reflux by means of a heating mantel. A gentle reflux was maintained for four hours. The cool solution was reduced in volume under vacuum to 3 mL and placed on a column of activated Alumina (2.5 cm x 23 cm). Elution with hexane gave a fraction containing PPh_3. Elution with THF in hexanes (3:7) gave an orange band which was collected and dried under vacuum. Recrystallization from hot THF in hexanes (3:7) gave crystallographic-grade dark purple crystals which were washed with cold hexanes (2 mL, -78°C) and dried in vacuum overnight (0.110 g, 0.153 mmole). Yield = 51% mp. = 125-127°C

^{1}H NMR (C_6D_6): 0.87(t, 6H, ,J_{H-H}= 7.2 Hz, $CH_2CH_2C\underline{H}_3$(e)), 1.20(t, 3H, J_{H-H}= 7.3 Hz, $CH_2CH_2C\underline{H}_3$(a)), 1.33(diastereotropic multiplet, 3.8H, $C\underline{H}_2CH_2CH_3$(e)), 1.50(m, 4.2H, $C\underline{H}_2CH_2CH_3$(e)(diastereomer), $CH_2C\underline{H}_2CH_3$(e)), 1.97(m, 2H, $CH_2C\underline{H}_2CH_3$(a)), 3.50(m, 1.5H, $C\underline{H}_2CH_2CH_3$(a)), 4.55(s, 10H, Cp), 4.59(s, 5H, Cp)

Anal. Calcd. for $C_{24}H_{36}Ru_3S_3$: 39.82%C, 5.01%H, 13.29%S

Found: 40.07%C, 5.08%H, 13.15%S

1,1′,1″-Tris(cyclopentadienyl)-tris(μ-2-propylthiolato)triruthenium(II), [CpRu-μ-S-CHMe$_2$]$_3$, 3d

A solution of **1d** (1.879 g, 2.45 mmole) in toluene (50 mL) was prepared in a three-necked flask fitted with a water condenser and was refluxed for 4.5 hours. The cool solution was stripped to dryness and dissolved in the minimum amount THF. This solution was chromatographed on Alumina (25 x 200 mm) using hexanes as the eluent (300 mL). A brown band eluted first and was collected. The eluent was changed to THF in hexanes (1:4) which eluted a second band. The first band was stripped to dryness, washed with hexanes (5 x 2 mL) and pentane (1 x 2 mL) and recrystallized from THF/hexanes (1:1) to give analytically-pure dark red crystals of **3d** (0.0195 g, 0.027 mmole). The second band was stripped to dryness to give a nearly pure **3d** (>90 % pure by NMR, 0.2720g, 0.376 mmole). Combined yield = 49.2% mp. = 260-261°C

^{1}H NMR (C_6D_6): 0.78(sept, 2H, C<u>H</u>Me$_2$, 1.09, 1.51(diastereiotropic doublet, 12H, J_{H-H}= 6.5 Hz, CH<u>Me$_2$</u>),1.55(d, 6H, J=6.7 Hz, CH<u>Me$_2$</u>), 4.50(s, 10H, Cp), 4.58(s, 5h, Cp), 4.97(sept, 1H, C<u>H</u>Me$_2$)

Anal. Calcd. for $C_{24}H_{36}Ru_3S_3$: 39.82%C, 5.01%H, 13.29%S

Found: 39.89%C, 5.12%H, 13.27%S

Cyclopentadienylcarbonyltriphenylphosphinemercaptoruthenium(II), $CpRu(PPh_3)(CO)SH$, 4a

A suspension of **1a** (0.34 g, 0.47 mmole) in THF (20 mL) was prepared. The flask was evacuated and refilled with CO. The suspension was stirred for 3 hours, at which time **1a** had dissolved and the solution was clear yellow-brown in colour. The solution was reduced in volume under vacuum to about 3 mL and placed on a column of Alumina (20 mm x 40 cm). Elution with hexanes removed PPh_3. Elution with THF in hexanes (2:3) gave a yellow band which was collected and reduced to dryness under vacuum. The resulting brown powder was pumped on for 1 hour to give analytically pure **4a** (0,154 g, 0.31 mmole) Yield = 67 % mp. = decomposition between 190 and 194°C with formation of dark red liquid and H_2S gas.

IR (toluene): $\nu_{(CO)}$= 1950(s)

^1H NMR (C_6D_6): -3.10(d, 1H, J_{H-H}= 7.4 Hz, S<u>H</u>), 4.56(d,, 5H, J_{H-P}= 0.6 Hz, Cp), 7.00(m, 9H, PPh_3), 7.66(m, 6H, PPh_3)

Anal. Calcd. for $C_{24}H_{21}OPRuS$: 58.89%C, 4.32%H, 6.55%S

Found: 58.79%C, 4.22%H, 6.62%S

Cyclopentadienylcarbonyltriphenylphosphine-4-methylbenzenethiolato-ruthenium(II), $CpRu(PPh_3)(CO)S\text{-}4\text{-}C_6H_4Me$, 4b

A dark red suspension of **1b** (0,51 g, 0.63 mmole) in THF (2 mL) was prepared. Carbon monoxide was bubbled through the solution. After 10 minutes, the colour became less intense and **1b** dissolved. The solution was stirred under CO overnight.

The resulting orange solution was reduced in volume to 1 mL under vacuum and ethanol (1 mL) was added. The solution was further reduced in volume until a yellow precipitate formed and allowed to stand for 30 minutes. The solution was slowly reduced in volume to 0.5 mL. The mother liquors were removed using a pipette and the solids were washed with ethanol (4 x 2 mL) and hexanes (6 x 2 mL). After drying in vacuo, a crude yellow powder was obtained (0.35 g, 0.57 mmole). Analytically pure sample was obtained by recrystallization from THF/hexanes as bright yellow microcrystals containing THF in the ratio **4b**:THF = 2:1; peaks due to THF were detected in the NMR spectrum in the appropriate intensity. Yield = 91% mp. = 166-168°C

IR toluene): $\nu_{(CO)}$= 1947(s)

^{1}H NMR (C_6D_6): 2.15(s, 3H, 4-$C_6H_4C\underline{H}_3$), 4.63(s, 5H, Cp), 6.99,(m, 11H, PPh_3 and 4-$C_6\underline{H}_4CH_3$), 7.64(m, 6H, PPh_3), 7.87(d, 2H,J_{H-H}= 8.2 Hz, 4-$C_6\underline{H}_4CH_3$)

Anal. Calcd. for $C_{33}H_{31}O_{1.5}PRuS$: 64.37%C, 5.07%H, 5.21%S

Found: 64.46%C, 5.14%H, 5.29%S

Cyclopentadienylcarbonyltriphenylphosphine-1-propylthiolatoruthenium(II), CpRu(PPh_3)(CO)S-1-C_3H_7, 4c

A suspension of **1c** (0.49 g, 0.64 mmole) in THF (70 mL) was stirred under CO, overnight, as for **1a**. The solution was reduced in volume to 1.5 mL and chromatographed on Alumina (20 mm x 40 cm). Elution with hexanes removed PPh_3. Elution with THF in hexanes (2:3) gave a yellow band which was collected and reduced in volume under vacuum until an orange oil formed. This oil was left overnight at room temperature whereupon clusters of analytically pure orange crystals

formed. The mother liquor was decanted and the crystals (0.139 g, 0.26 mmole) were washed with hexanes and pumped on overnight. Yield = 41 % mp. = 133-134°C

IR (toluene): $\nu_{(CO)}$= 1942(s)

^{1}H NMR (C_6D_6): 1.14(t, 3H,J_{H-H}= 7.3 Hz, $CH_2CH_2C\underline{H}_3$), 1.87(m, 2H, $CH_2C\underline{H}_2CH_3$), 2.61(m, 2H, $C\underline{H}_2CH_2CH_3$), 4.67(d, 5H, J_{H-P}= 0.4 Hz, Cp), 7.02(m, 9H, PPh_3), 7.71(m, 6H, PPh_3)

Anal. Calcd. for $C_{27}H_{27}OPRuS$: 61.00%C, 5.12%H, 6.03%S

Found: 61.13%C, 5.[illegible]0%H, 6.04%S

Cyclopentadienylcarbonyltriphenylphosphine-2-propylthiolatoruthenium(II), CpRu(PPh_3)(CO)S-2-CHMe$_2$, 4d

A solution of **1d** (0,72 g, 0.94 mmole) in THF (70 mL) was stirred under CO overnight. The solution was evaporated under vacuum to 3 mL and chomatographed on Alumina. Elution with hexanes removed PPh_3. Elution with THF in hexanes (2:3) gave a yellow band which was collected and reduced in volume under vacuum to 15 mL, at which point, analytically-pure crystals slowly formed. The mother liquors were decanted and the orange-brown crystals (0.24 g, 0.45 mmole) were washed with hexanes (2 x 2 mL) and dried under vacuo. Yield = 48 % mp. = 157-158°C

IR (toluene): $\nu_{(CO)}$= 1941(s)

^{1}H NMR (C_6D_6): 1.54, 1.58(diastereotropic doublet, 6H, J_{H-H}= 6.6 Hz, CH$\underline{Me}_2$), 2.77(septet, 1H, C$\underline{H}$Me$_2$), 4.67(d, 5H, J_{H-P}= 0.4 Hz, Cp), 7.02(m, 9H, PPh_3), 7.72(m, 6H, PPh_3)

Anal. Calcd. for $C_{27}H_{27}OPRuS$: 61.00%C, 5.12%H, 6.03%S

Found: 61.18%C, 5.22%H, 6.04%S

Cyclopentadienyl(diphenylphosphenoethane)-1-propylthiolatoruthenium(II)

CpRu(dppe)S-1-C_3H_7, 5c

A solution of 1c (0.60 g, 0.78 mmole) in toluene (10 mL) was prepared. To that solution, diphenylphosphenoethane (dppe, 0.312 g, 0.783 mmole) was added and stirred overnight. The orange solution was reduced in volume under vacuum to 2 mL and placed on a column of Alumina (20 mm x 40 cm). Using toluene as the eluent, the major product was eluted as a light orange band which was collected and evaporated to dryness (0.3430 g, 0.536 mmole). Recrystallization from THF/EtOH and washing with hexanes gave the product as orange microcrystals (0.280 g, 0.438 mmole). Yield = 36 % mp = 147-150°C

^{1}H NMR (C_6D_6): 0.82(t, 3H, J_{H-H}= 9.2 Hz, $CH_2CH_2C\underline{H}_3$), 1.47(m, 4H, $C\underline{H}_2$), 1.86(m, 2H, $C\underline{H}_2$), 2.71(m, 2H, $C\underline{H}_2$), 4.71(s, 5H, Cp), 7.00(m, 8H, $P\underline{Ph}_2CH_2CH_2P\underline{Ph}_2$), 7.18(m, 8H, $P\underline{Ph}_2CH_2CH_2P\underline{Ph}_2$), 7.87(m, 4H, $P\underline{Ph}_2CH_2CH_2P\underline{Ph}_2$)

Cyclopentadienyltriphenylphosphine-4-methylbenzenethioxanth atoruthenium(II),

CpRu(PPh_3)S_2CS-4-C_6H_4Me, 6b

A solution of 1b (0.1576 g, 0.194 mmole) in THF (3 mL) was treated with CS_2 (5 mL), stirred for 1 hour and then stripped to dryness. The residue was redissolved in THF (3 mL). Ethanol was added (5 mL) and the solution was reduced in volume under vacuum, until turbid and allowed to stand at -16°C overnight. The mother liquors were decanted and the solids were washed with hexanes and pumped on overnight to give deep red crystals. (0.0846 g, 0.135 mmole). Yield = 83% mp. = 173-176°C

IR (KBr) $\upsilon_{(CS\ of\ CS3)}$= 993(s), 941(vs); $\upsilon_{(CS\ of\ S\text{-}R)}$= 805(s)

^{1}H NMR (C_6D_6): 1.95(s, 3H, 4-$C_6H_4C\underline{H}_3$), 4.28(s, 5H, Cp), 6.82, 7.21(ABq, 4H, $J_{H\text{-}H}$= 8.0 Hz, 4-$C_6\underline{H}_4CH_3$), 7.06(m, 9H, PPh_3), 7.62(m, 6H, PPh_3)

Anal. Calcd. for $C_{27}H_{27}PRuS_3$: 59.31%C, 4.33%H, 15.31%S

found: 59.42%C, 4.43%H, 15.24%S

Cyclopentadienyltriphenylphosphine-1-propylthioxanthatoruthenium(II), $CpRu(PPh_3)S_2CS\text{-}1\text{-}C_3H_7$, 6c

A solution of **1c** (0.500 g, 0.65 mmole) in toluene (100 mL) was treated with CS_2 (40 mL) and stirred for 30 minutes. The solution was stripped to dryness under vacuum and the residue dissolved in toluene (5 mL). This solution was placed on a column of activated Alumina (25 mm x 23 cm). Elution with hexanes gave a band containing PPh_3. Elution with THF in hexanes (1:4) gave an orange band which was collected, concentrated under vacuum to 30 mL and stored at -16°C overnight. The mother liquors were decanted and the red crystals were washed with cold hexanes (-78°C) and pumped on overnight to give **6c** (0.2158 g, 0.373 mmole). The mother liquors were stripped to dryness and the residue recrystallized to give more **6c** (0.0467 g, 0.080 mmole). Combined yield = 69% mp. = 120-122°C

IR (Nujol): $\upsilon_{(CS\ of\ CS3)}$= 972(s), 962(vs); $\upsilon_{(CS\ of\ S\text{-}R)}$= 807(m)

^{1}H NMR (C_6D_6): 0.67(t, 3H, $J_{H\text{-}H}$= 7.4 Hz, $CH_2CH_2C\underline{H}_3$), 1.38(m, 2H, $CH_2C\underline{H}_2CH_3$), 2.76(t. 2H, $J_{H\text{-}H}$= 7.3 Hz, $C\underline{H}_2CH_2CH_3$), 4.31(s, 5H, Cp), 7.05(m, 9H, PPh_3), 7.63(m, 6H, PPh_3)

Anal. Calcd. for $C_{27}H_{27}PRuS_3$: 55.94%C, 4.69%H, 16.59%S

found: 56.03%C, 4.69%H, 16.67%S

Cyclopentadienyltriphenylphosphine-2-propylthioxanthatoruthenium(II), $CpRu(PPh_3)S_2CS\text{-}CHMe_2$, 6d

A solution of **1d** (0.3953 g, 0.516 mmole) in THF (18 mL) was treated with CS_2 (10 mL) and stirred for 45 minutes. The resulting red solution was reduced in volume to 10 mL under vacuum and ethanol (15 mL) was added. Further concentration and cooling to -78°C gave dark red crystals of **6d**, which were washed with cold ethanol (-78°C) followed by hexanes and pumped on overnight. (0.2187 g, 0.377 mmole).

Yield = 73% mp. = 162-164°C

IR (KBr): $\upsilon_{(CS\ of\ CS3)}$= 975(vs), 958(s); $\upsilon_{(CS\ of\ S\text{-}R)}$= 803(s)

^1H NMR (C_6D_6): 1.089(d, 6H, $J_{H\text{-}H}$= 6.8 Hz, CH$\underline{Me}_2$), 3.70(sept, 1H, C$\underline{H}$Me$_2$), 4.33(s, 5H, Cp), 7.07(m, 9H, PPh_3), 7.66(m, 6H, PPh_3)

Anal. Calcd. for $C_{27}H_{27}PRuS_3$: 55.94%C, 4.69%H, 16.59%S

Found: 56.08%C, 4.73%H, 16.26%S

1,1′-Bis(cyclopentadienyl)-1,1,1′-tris(triphenylphosphine)-μ-trithiocarbonatodi~ruthenuim(II)

$CpRu(PPh_3)_2(CS_3)RuCp(PPh_3)$, 6e

Carbon disulfide (2 mL) was added to a suspension of **1a** (0.25 g, 0.345 mmole) in toluene (3 mL). The complex dissolved and a rapid colour change from brown to red was observed. The solution was stirred for 48 hours and stripped to dryness under vacuum. The residue was redissolved in the minimum amount of THF and chromatographed on Alumina (20 mm x 40 cm). Eluting with hexanes removed PPh_3. Eluting with THF in hexanes (3:7) gave a red band that was collected, reduced in

volume until turbid and cooled at -20°C to give red microcrystals (0.0865 g, 0.0705 mmole). The mother liquor was decanted, further reduced in volume and cooled at -20°C to give an oil. The mixture was warmed to room temperature and allowed to stand, whereupon red crystals (0.0689 g, 0.0561 mmole) slowly formed. Repeated attempts to further purify **6a** did not succeed in ridding it of persistent contaminants. Combined yield = 37% mp. = 150-154°C

IR (Nujol): $\upsilon_{(CS\ of\ CS3)}$= 964(vs), 907(m)

^{1}H NMR (C_6D_6): 4.66(s, 5H, Cp), 4.54(s, 5H, Cp), 6.86-7.04(m, 18H, PPh_3), 7.06-7.14(m, 9H, PPh_3), 7.36-7.48(m, 12H, PPh_3), 7.75-7.86(m, 6H, PPh_3)

^{31}P NMR (C_6D_6) (In ppm relative to external standard of H_3PO_4): 52.36(s, 1P), 41.28(s, 2P)

Mass Spectrum: 1227($M^{\cdot+}$+H)(1.5), 966($M^{\cdot+}$-PPh_3)(2.1), 704($M^{\cdot+}$-2PPh_3)(2.0), 691($M^{\cdot+}$-CpRu(PPh_3)CS_3)(20.5), 441($M^{\cdot+}$-3PPh_3)(10.1), 429($^+$-CpRu(PPh_3)CS_3-PPh_3)(100)

Cyclopentadienyltriphenylphosphine(Ru-η^1-sulfurdioxide)-4-methylbenzene~thiolato(S-sulfurdioxide)ruthenium(II), CpRu(SO_2)(PPh_3)S(SO_2)-4-C_6H_4Me, 8b

A Schlenk tube was charged with **1b** (0.3710 g, 0.456 mmole) and THF (4 mL). Sulfur dioxide was bubbled through the solution for 1 hour during which, an orange precipitate in a red supernatant formed. The slurry was poured into 40 mL diethyl ether which had been previously saturated with SO_2. The slurry was filtered and the filtrate was left to stand under SO_2, whereupon deep red crystals slowly formed. The mother liquors were decanted and cooled to -78°C while the crystals were washed with cold

hexanes (2 x 2 mL, -78°C) and briefly dried in vacuum. Upon standing, a second crop of **8b** formed from the mother liquors as crystallographic grade crystals. Yield = 34% mp. Loss of crystallinity occurred at 125°C followed by melting at 138°C. Bubbles evolved from the melted residue and the pungent smell of SO_2 was detected when the capillary was subsequently opened.

IR (Nujol): $\nu_{(SO)}$= 1258(m), 1283(m)

^{1}H NMR (C_6D_6): 2.09(s, 3H, 4-$C_6H_4C\underline{H}_3$), 4.61(s, 5H, Cp), 6.88, 7.87(ABq, 4H, J_{H-H}= 8.0 Hz, 4-$C_6\underline{H}_4CH_3$), 6.95(m, 9H, PPh_3), 7.65(m, 6H, PPh_3)

Anal. Calcd. for $C_{30}H_{27}O_4PRuS_3$: 53.01%C, 4.00%H, 14.15%S

Found: 53.49%C, 3.70%H, 12.92%S

Cyclopentadienyltriphenylphosphine-Ru-η^1-sulfurdioxide-4-methylbenzene~ thiolatoruthenium(II),

$CpRu(SO_2)(PPh_3)S$-4-C_6H_4Me, 9b

A solid sample of **8b** (10-20 mg) was heated under nitrogen at 130°C (±5°C) by means of a glycerin bath for 20 minutes. The sample remained solid but lost its crystallinity. The pungent odor of SO_2 was detected.

IR (Nujol): $\nu_{(SO)}$= 1261(m)

^{1}H NMR (C_6D_6): 1.89(s, 3H, 4-$C_6H_4C\underline{H}_3$), 4.66(s, 5H, Cp), 6.59, 7.26(ABq, 4H, J_{H-H}= 8.3 Hz, 4-$C_6\underline{H}_4CH_3$), 6.98(m, 9H, PPh_3), 7.63(m, 6H, PPh_3)

Cyclopentadienylcarbonyltriphenylphosphine-4-methylbenzenedisulfino-ruthenium(II),

$CpRu(PPh_3)(CO)SS\text{-}4\text{-}C_6H_4Me$, 10b

To a solution of $CpRu(PPh_3)(CO)SH$ (0.062 g, 0.13 mmole) in THF (25 mL) was added p-methylbenzenethiophthalimide(0.034 g, 0.13 mmole). The solution was stirred for 1 hour, then reduced in volume under vacuum to 2 mL and placed on a column of Alumina (20 mm X 30 cm). Elution with hexanes (1.5 column length) followed by THF in hexanes (1:4) gave a yellow band which was collected and concentrated under vacuum until a precipitate formed. Yellow clumps of microcrystals were isolated (0.033g, 0.054 mmole). Yield = 42 % MP. = 162-163°C

IR (toluene): $\upsilon_{(CO)}$ = 1954(s)

IR (Nujol): $\upsilon_{(CO)}$ = 1936(s)

^1H NMR (C_6D_6): 2.12(s, 3H, $C_6H_4C\underline{H}_3$), 4.64(s, 5H, Cp), 7.18(m, 11H, PPh_3 and 4-$C_6\underline{H}_4CH_3$), 7.60(m, 6H, PPh_3), 7.86(d, 2H, $J_{H\text{-}H}$= 8.26 Hz, $C_6\underline{H}_4CH_3$)

Anal. Calcd. for $C_{31}H_{27}OPRuS_2$: 60.87%C, 4.45%H, 10.48 %S

Found: 60.74 %C, 4.28 %H, 10.52 %S

Cyclopentadienylcarbonyltriphenylphosphine-1-propyldisulfanoruthenium(II),

$CpRu(PPh_3)(CO)SS\text{-}1\text{-}C_3H_7$, 10c

To a solution of $CpRu(PPh_3)(CO)SH$ (0.194 g, 0.40 mmol) in THF (3 mL), 1-propylthiophthalamide (0.088 g, 0.40 mmole) was added. The resulting solution was stirred overnight, concentrated under vacuum to 3 mL and chromatographed on a column of Alumina (20 mm X 30 cm). Elution with hexanes (1.5 column length)

followed by THF in hexanes (1:4) gave a yellow band was recovered and reduced to 20 mL to give a yellow crystalline product. A second crop was recovered by concentrating the mother liquor to give a combined yield of 0.101g (0.18 mmole).

Yield = 45% MP. = 155-156°C

IR (toluene): $\upsilon_{(CO)}$ = 1941(s)

IR (Nujol): $\upsilon_{(CO)}$ = 1932(s), 1940(s)

^{1}H NMR (C_6D_6): 1.04(t, 3H, J_{H-H}= 7.34 Hz, $CH_2CH_2C\underline{H}_3$), 1.93(m, 2H, $CH_2C\underline{H}_2CH_3$), 2.74, 2.92(diastereotropic multiplet, 2H, $C\underline{H}_2CH_2CH_3$), 4.73(s, 5H, Cp), 7.01(m, 9H, PPh_3),7.59(m, 6H, PPh_3)

^{13}C NMR (C_6D_6): 48.73($CH_2CH_2\underline{C}H_3$), 13.79($CH_2\underline{C}H_2CH_3$), 22.39($\underline{C}H_2CH_2CH_3$), 41.83(Cp), 89.20(para $P(\underline{C}_6H_6)_3$), 128.25(d, J_{C-P}= 10.2 Hz, meta $P(\underline{C}_6H_6)_3$), 133.87(d, J_{C-P}= 11.0 Hz, ortho $P(\underline{C}_6H_6)_3$), 135.84(d, J_{C-P}= 48.3 Hz, quaternary $P(\underline{C}_6H_6)_3$)

Anal. Calcd. for $C_{27}H_{27}OPRuS_2$: 57.53%C, 4.83%H, 11.38%S

Found: 57.69%C, 4.73%H, 11.41%S

<u>Cyclopentadienylcarbonyltriphenylphosphine-2-propyldisulfanoruthenium(II), CpRu(PPh$_3$)(CO)SS-CHMe$_2$, 10d</u>

To a solution of CpRu(PPh_3)(CO)SH (0.159 g 0.325 mmol) in THF (3 mL) was added isopropylthiophthalamide (0.072 g, 0.325 mmol). The solution was stirred overnight, reduced in volume under vacuum to 1.5 mL, and placed on a column of Alumina (20 mm X 30 cm). Elution with hexanes (1.5 column length) followed by THF in hexanes (1:4) gave a yellow band which was collected and concentrated under vacuum until turbid and left overnight. Crystallographic grade crystals were isolated. Concentration of the mother liquors under vacuum gave two more crops of crystallographic grade

crystals. The combined weight of product was 0.120 g (0.213 mmol). Yield = 66%

MP. = 145-147°C

IR (toluene): $\upsilon_{(CO)}$ = 1942(s)

IR (Nujol): $\upsilon_{(CO)}$ = 1935(m), 1942(s), 1956(m)

IR (CCl_4): $\upsilon_{(CO)}$ = 1944(s)

^1H NMR (C_6D_6): 1.41, 1.56(diastereotropic doublet, 6H, J_{H-H}= 6.7Hz, CH<u>Me</u>$_2$), 3.20(septet, 1H, C<u>H</u>Me$_2$), 4.73(s, 5H, Cp), 7,01(m, 9H, PPh_3), 7.60(m, 6H, PPh_3)

Anal. Calcd. for $C_{27}H_{27}OPRuS_2$: 57.53%C, 4.83%H, 11.38%S

Found: 57.36%C, 4.79%H, 11.32%S

<u>Cyclopentadienylcarbonyltriphenylphosphine-4-methylbenzenetrisulfano-ruthenium(II),</u>

<u>CpRu(PPh_3)(CO)SSS-4-C_6H_4Me, 11b</u>

A sample of CpRu(PPh_3)(CO)SH (0.370 g, 0.756 mmole) was combined with p-methylbenzenedisulfanophthalimide (0.228 g, 0.756 mmole) in an appropriately sized Schlenk and then dissolved in toluene (5 mL) The solution was stirred for 1 hour and stripped to dryness. The residue was dissolved in THF (3 mL) and placed on an Alumina column (20 mm X 30 cm). The column was eluted with hexanes (150 mL) followed by THF in hexanes (1:4). A yellow band was collected, concentrated to 40 mL and cooled overnight at -16°C. Yellow microcrystals (0.209 g, 0.325 mmole) were collected, washed with hexanes (2 X 2 mL) and dried under vacuum. The analytical sample was obtained by recrystallization from CH_2Cl_2/hexanes. Yield = 43% mp. = 141-144°C

IR (toluene): $\upsilon_{(CO)}$= 1957(s)

IR (CCl_4): $\upsilon_{(CO)}$ = 1950(sh), 1962(s)

^{1}H NMR (C_6D_6): 2.01(s, 3H, 4-$C_6H_4C\underline{H}_3$), 4.71(s, 5H, Cp), 6.88, 7.82(ABq, 4H, J_{H-H}= 8.2 Hz, 4-$C_6\underline{H}_4CH_3$), 7.0(m, 9H, PPh_3), 7.5(m, 6H, PPh_3)

Additional signals due to contaminant **A**: 2.10(s, 3H, 4-$C_6H_4C\underline{H}_3$), 4.68(s, 5H, Cp), 7.0(m, 9H, PPh_3), 7.5(m, 6H, PPh_3)

Additional signals due to contaminant **B**: 1.96(s, 3H, 4-$C_6H_4C\underline{H}_3$), 4.73(s, 5H, Cp), 7.0(m, 9H, PPh_3), 7.5(m, 6H, PPh_3)

Ratio of **11b**:**A**:**B** = 10:2:1

Anal. Calcd. for $C_{31}H_{27}OPRuS_3$: 57.84%C, 4.23%H, 14.94%S

Found: 58.45%C, 4.15%H, 14.65%S

Cyclopentadienylcarbonyltriphenylphosphine-1-propyltrisulfanoruthenium(II), CpRu(PPh_3)(CO)SSS-1-C_3H_7, 11c

A sample of CpRu(PPh_3)(CO)SH (0.560 g, 1.14 mmole) was combined with 1-propyltrithiophthalamide (0.290 g, 1.14 mmole) in an appropriately sized Schlenk tube, dissolved in toluene (5 mL) and stirred for 1 hour. The solution was stripped to dryness, the residue dissolved in THF (3 mL) and placed on an Alumina column (20 mm X 30 cm). The column was eluted with hexanes (150 mL) followed by THF in hexanes (1:4). A yellow band was collected, reduced in volume under vacuum to 40 mL and left in the dark at room temperature overnight. Crystallographic grade yellow crystals were obtained (0.295 g, 0.496 mmole). Yield = 44% mp. = 144-147°C

IR (toluene): $\upsilon_{(CO)}$ = 1949(sh), 1956(s)

IR (CCl_4): 1941(sh),1946(sh), 1950(sh), 1961(s)

^{1}H NMR (C_6D_6, 300 MHz): 0.884(t, 3H, J_{H-H}= 7.3 Hz, $CH_2CH_2C\underline{H}_3$), 1.820(m, 2H,

$CH_2C\underline{H}_2CH_3$), 2.892(t, 2H, J_{H-H}= 7.2 Hz, $C\underline{H}_2CH_2CH_3$), 4.820(s, 5H, Cp), 7.05(m, 9H, PPh_3), 7.54(m, 6H, PPh_3)

Additional signals due to contaminant **A**: 0.813(t, 3H, J_{H-H}= 7.7 Hz, $CH_2CH_2C\underline{H}_3$), 1.709(m, 2H, $CH_2C\underline{H}_2CH_3$), 2.785(t, 2H, J_{H-H}= 7.1 Hz, $C\underline{H}_2CH_2CH_3$), 4.767(s, 5H, Cp), 7.05(m, 9H, PPh_3), 7.54(m, 6H, PPh_3)

Additional signals due to contaminant **B**: 1.042(t, 3H, J_{H-H}= 7.3 Hz, $CH_2CH_2C\underline{H}_3$), 1.92(m, 2H, $CH_2C\underline{H}_2CH_3$), 4.727(d, 5H, J_{H-P}= 0.6 Hz, Cp), 7.05(m, 9H, PPh_3), 7.54(m, 6H, PPh_3)

Ratio of **11c**:**A**:**B** = 2.5:1.4:1

Anal. Calcd. for $C_{27}H_{27}OPRuS_3$: 54.44%C, 4.57%H, 16.14%S

Found: 54.11%C, 4.57%H, 16.21%S

Cyclopentadienylcarbonyltriphenylphosphine-2-propyltrisulfanoruthenium(II), $CpRu(PPh_3)(CO)SSS\text{-}CHMe_2$, 11d

A sample of $CpRu(PPh_3)(CO)SH$ (0.314 g, 0.640 mmole) was combined with 2-propyltrithiophthalamide (0.162 g, 0.640 mmole) in an appropriately sized Schlenk tube, dissolved in toluene (5 mL) and the solution stirred for 1 hour. The solution was stripped to dryness under vacuum, the residue was dissolved in THF (4 mL) and placed on an Alumina column (20 mm X 30 cm). The column was eluted with hexanes (150 mL) followed by THF in hexanes (1:4). A yellow band was collected, concentrated under vacuum until a small amount of precipitate formed and then left overnight in the dark. Yellow crystals (0.205 g, 0.344 mmole) were isolated, washed with THF in hexanes (10:19, 4 X 2mL) and dried in a nitrogen stream. Yield = 54 % mp. = 154-156°C

IR (toluene): $\upsilon_{(CO)}$ = 1956(s)

IR (CCl_4) $\upsilon_{(CO)}$ = 1950(sh),1961(s)

^{1}H NMR (C_5D_6): 1.41, 1.38(diastereotropic doublet, 6H, J_{H-H}= 6.1 Hz, CH<u>Me</u>$_2$), 3.35(septet, 1H, C<u>H</u>Me$_2$), 4.82(s, 5H, Cp), 7.00(m, 9H, PPh_3), 7.54(m, 6H, PPh_3)

Additional signals due to contaminant **A**: 1.26, 1.30(diastereotropic doublet, 6H, J_{H-H}= 2.4 Hz, CH<u>Me</u>$_2$), 3.20(m, 1H, C<u>H</u>Me$_2$), 4.77(s, 5H, Cp), 7.00(m, 9H, PPh_3), 7.54(m, 6H, PPh_3)

Additional signals due to contaminant **B**: 1.57(d, 6H, J_{H-H}= 6.6 Hz, CH<u>Me</u>$_2$), 3.20(m, 1H, C<u>H</u>Me$_2$), 4.72(s, 5H, Cp), 7.00(m, 9H, PPh_3), 7.54(m, 6H, PPh_3)

Ratio of **<u>11d</u>:A:B** = 11:1.4:1

Anal. Calcd. for $C_{27}H_{27}OPRuS_3$: 54.44%C, 4.57%H, 16.14%S

Found: 54.33%C, 4.58%H, 16.25%S

<u>Cyclopentadienylcarbonyltriphenylphosphine-4-methylbenzene-2-oxodisulfano-ruthenium(II),</u>

<u>CpRu(PPh$_3$)(CO)SS(O)-4-C$_6$H$_4$Me, 12b</u>

To a solution of CpRu(PPh_3)(CO)SH (0.291 g, 0.59 mmole) in THF (4 mL) was added p-methylbenzenesulfinylphthaimide (0.169 g, 0.59 mmole). The solution was stirred for 2 hours then concentrated to 2 mL under vacuum and chromatographed on Alumina (15 mm X 20 cm). Elution with hexanes (300 mL) followed by THF in hexanes (1:1) gave a yellow band which was collected and concentrated to 2 mL under vacuum. Hexanes (10 mL) were added to produce brown clumps (0.025 g, 0.040 mmole). Further concentration under vacuum gave more brown microcrystals (0.050 g, 0.080 mmole). Another crop of yellow microcrystals (0.063 g, 0.10 mmole) was obtained by

filtering the mother liquor and concentrating further. A final crop of fluffy yellow-green powder (0.068 g, 0.11 mmole) was obtained by futher concentration of the mother liquors.

Table E.1 Melting points, yields and IR bands observed for each crop of **12b**.

			Toluene		Nujol	
Crop	M.P.(°C)	Yield (%)	$\nu_{(CO)}$	$\nu_{(SO)}$	$\nu_{(CO)}$	$\nu_{(SO)}$
1	172-175	6.8	1961(s) 1937(sh)	1029(m) 1044(m)	1991(w) 1967(s) 1959(s) 1950(sh)	1034(m)
2	170-172	13	1961(s)	1031(w) 1045(m)	1991(m) 1966(s) 1952(s)	1034(m)
3	150-151	17	1960(s)	1032(sh) 1045(m)	1957(m) 1932(s)	1032(m)
4	139-145	19	1960(s)	1029(m) 1045(m)	1966(m) 1959(m) 1933(s)	1033(m)

^{1}H NMR (C_6D_6): Diastereomers **12b(A)** and **12b(B)** were observed: **12b(A)**) 2.04(s, 3H, $C_6H_4C\underline{H}_3$), 5.00(s, 5H, Cp), 6.98(m, 9H, PPh_3), 7.51(m, 6H, PPh_3), 7.81(d, 2H, $J_{H\text{-}H}$= 4.2Hz); **12b(B)**) 1.95(s, 3H, $C_6H_4C\underline{H}_3$), 4.80(s, 5H, Cp), 6.87, 6.98(m, 9H, PPh_3), 7.51(m, 6H, PPh_3), 7.96(ABq, 4H, $J_{H\text{-}H}$= 4.0 Hz, 4-$C_6H_4CH_3$)

Other signals observed **13b** and **10b** were observed: **13b**: 1.89(s, 3H, $C_6H_4C\underline{H}_3$), 4.73(s, 5H, Cp), 6.98(m, 9H, PPh_3), 7.51(m, 6H, PPh_3); **10b**: 2.10(s, 3H, $C_6H_4C\underline{H}_3$), 4.62(s, 5H, Cp), 6.98(m, 9H, PPh_3), 7.51(m, 6H, PPh_3)

Table E.2 Relative intensity of the Cp signals in the ^1H NMR of **12b**.

Crop	Ratio of **12b**(A) : **12b**(B) : **13b** : **10b**
immediately from the column	11:5:1:1.4
1	15:60:6:1
2	8:17:2:1
3	98:4:3:1
4	12:4:1:1

Anal. Calcd. for $C_{31}H_{27}O_2PRuS_2$: 59.32%C, 4.34%H, 10.21%S

Found: Crop 1; 59.18%C, 4.50%H, 10.31%S

Crop 3; 59.40%C, 4.49%H, 10.14%S

Cyclopentadienylcarbonyltriphenylphosphine-1-propyl-2-oxodisulfano-ruthenium(II),

$CpRu(PPh_3)(CO)SS(O)$-1-C_3H_7, 12c

To a solution of $CpRu(PPh_3)(CO)SH$ (0.214 g, 0.44 mmole) in THF (4 mL), 1-propylsulfinylphthaimide (0.253 g, 1.07 mmole) was added. The sample was stirred for 1 hour, stripped to dryness under vacuum, then dissolved in THF (2 mL) and chromatographed on Alumina (15 mm X 20 cm). Elution with hexanes (300 mL) followed by THF in hexanes (65:35) gave a yellow band which was collected and stripped to dryness under vacuum. A greenish-yellow, foul smelling crude product was recovered (0.1240 g, 0.21 mmole). Analytical sample was obtained by recrystallization from toluene/hexanes. Yield = 48% mp. = 204-205°C

IR (Nujol): $\upsilon_{(CO)}$= 1964(s), 1955(s), 1950(sh), 1942(sh), 1937(sh)

$\upsilon_{(SO)}$= 1054(w)

IR (toluene): $\upsilon_{(CO)}$= 1978(m), 1959(m)

$\upsilon_{(SO)}$= 1108(m), 1082(m)

IR (CCl_4): $\upsilon_{(CO)}$= 1982(sh), 1958(m), 1942(m)

$\upsilon_{(SO)}$= 1107(w), 1081(w), 1030(w)

IR (CS_2): $\upsilon_{(CO)}$= 1980(m), 1959(m)

^{1}H NMR (C_6D_6): 0.75(t, 3H, J_{H-H}= 7.48 Hz, $CH_2CH_2C\underline{H}_3$), 2.03(m, 2H, $CH_2C\underline{H}_2CH_3$), 3.25(m, 2H, $C\underline{H}_2CH_2CH_3$), 4.82(s, 5H, Cp), 6.99(m, 9H, PPh_3), 7.45(m, 6H, PPh_3)

Additional signals due to contaminant **A**: 5.01(s, Cp)

Additional signals due to contaminant **B**: 4.93(s, Cp)

Additional signals due to contaminant **C**: 4.79(s, Cp)

Ratio of **12c**:**A**:**B**:**C** is 1:1:95:5

^{13}C NMR (C_6D_6): 12.91(s, $CH_2CH_2\underline{C}H_3$), 18.65(s $CH_2\underline{C}H_2CH_3$), 64.21(s, Cp), 87.55(s, para $P(\underline{C}_6H_5)_3$), 128.48(d, J_{C-P}= 10.7Hz, meta $P(\underline{C}_6H_5)_3$), 133.66(d, J_{C-P}= 11.1 Hz, ortho $P(\underline{C}_6H_5)_3$), 135.22(d, J_{C-P}= 48.6 Hz, quaternary $P(\underline{C}_6H_5)_3$)

Anal. Calcd. for $C_{27}H_{27}O_2PRuS_2$: 55.94%C, 4.69%H, 11.06%S

Found: 55.15%C, 4.87%H, 11.02%S

Cyclopentadienylcarbonyltriphenylphosphine-2-propyl-2-oxodisulfano-ruthenium(II),

$CpRu(PPh_3)(CO)SS(O)$-$CHMe_2$, 12d

To a solution of $CpRu(PPh_3)(CO)SH$ (0.299 g, 0.61 mmole) in THF (2 mL) was added 2-propylsulfinylphthaimide (0.155 g, 0.65 mmole). The solution was stirred for 1 hour

and stripped to dryness under vacuum. The residue was dissolved in THF (2 mL) and chromatographed on Alumina (15 mm X 20 cm). Elution with hexanes (300 mL) followed by THF in hexanes (1:1) gave two yellow bands which were collected and concentrated under vacuum until a solid formed in the first band and a orange-yellow oil formed in the second band. The oil from the second band was left to stand, whereupon a yellow solid formed. The second band was recrystallized from THF/hexanes to form yellow crystallographic grade crystals (0.114 g, 0.20 mmole). The first band was found to contain an unidentified mixture of products. Yield = 33% mp. = 171°C-phase change from yellow to orange; 177°C-onset of melting was noted by loss of crystallinity; 188°C-decomposition to a liquid and gas evolved.

IR (Nujol): $\upsilon_{(CO)}$= 1966(m), 1954(m), 1939(s)

$\upsilon_{(SO)}$= 1031(m)

IR (toluene): $\upsilon_{(CO)}$= 1958(s)

IR (CCl_4): $\upsilon_{(CO)}$= 1965(s), 1957(sh), 1950(sh), 1943(sh)

^{1}H NMR (C_6D_6): 1.24(d, 3H, J_{H-H}= 6.8 Hz, CH<u>Me</u>$_2$), 1.44(d, 3H, J_{H-H}= 6.0 Hz, CH<u>Me</u>$_2$), 3.00(q, 0.6H, J_{H-H}= 6.8 Hz, C<u>H</u>Me$_2$), 4.96(s, 2.9H, Cp), 7.00(m, 9H, PPh$_3$), 7.53(m, 6H, PPh$_3$)

Additional signals due to contaminant **A**: 1.32(d, 3H, J_{H-H}= 6.8 Hz, CH<u>Me</u>$_2$), 1.40(d, 3H, J_{H-H}= 6.0 Hz, CH<u>Me</u>$_2$), 2.97(septet, 1H, J_{H-H}= 6.8 Hz, C<u>H</u>Me$_2$), 4.91(s, 5H, Cp), 7.00(m, 9H, PPh$_3$), 7.53(m, 6H, PPh$_3$)

Additional signals due to contaminant **B**: 1.45(d, 6H, J_{H-H}= 7.0 Hz, CH<u>Me</u>$_2$), 3.35(m, 1H, C<u>H</u>Me$_2$), 4.82(s, 5H, Cp), 7.00(m, 9H, PPh$_3$), 7.53(m, 6H, PPh$_3$)

Ratio of **<u>12d</u>:A:B** is 7:4:1

Anal. Calcd. for $C_{27}H_{27}O_2PRuS_2$: 55.94%C, 4.69%H, 11.06%S

Found: 56.01%C, 4.87%H, 10.93%S

Cyclopentadienylcarbonyltriphenylphosphine-4-methylbenzene-2-dioxodisulfano-ruthenium(II),

$CpRu(PPh_3)(CO)SS(O)_2$-4-C_6H_4Me, 13b

A solution of **12b** (crop 4) (0.0425g, 0.0677mmole) in toluene (40 mL) was prepared in a three-neck flask fitted with a water condenser. The solution was brought to reflux by means of a heating mantel. A gentle reflux was maintained for 9 hours and 45 minutes. The solution was cooled, evaporated to dryness, redissolved in THF (3 mL), and placed on a column of activated Alumina (1 cm x 20 cm). Elution with hexanes followed by THF in hexanes (1:5) gave a yellow-brown band which was collected and evaporated to dryness under vacuum leaving a dark oil (0.0173g). The oil was recrystallized from THF/hexanes which produced a dark oil which was left undisturbed for 24 days. A single crystallographic grade yellow-brown crystal formed along with few other lower grade crystals (0.0014 g). Yield = 6.4 % mp. 188-191°C.

^1H NMR (C_6D_6): 1.89(s, 3H, 4-$C_6H_4C\underline{H}_3$), 4.73(s, 5H, Cp), 6.81, 8.20(ABq, 4H, J_{H-H}= 8.2 Hz, 4-$C_6\underline{H}_4CH_3$), 6.95(m, 9H, PPh_3), 7.39(m, 6H, PPh_3)

IR (C_6D_6): $\nu_{(CO)}$= 1971 cm^{-1}

CONTRIBUTION TO ORIGINAL KNOWLEDGE

1. The complexes $CpRu(PPh_3)(L)SR$, where R = $4\text{-}C_6H_4Me$, $1\text{-}C_3H_7$, and $CHMe_2$; L = PPh_3 and CO, are among the few monomeric thiolate complexes of ruthenium.

2. The aggregation of $CpRu(PPh_3)_2SR$, in the cases where R is an alkyl, to give first dimeric and then trimeric complexes, is unusual in that each ruthenium sequentially loses two PPh_3 ligands.

3. The structure of $[CpRuS(1\text{-}C_3H_7)]_3$ is unprecedented and suggests the possibility of an previously unknown type of interaction between the protons on the α carbon of the axial R-group and the adjacent sulfur atoms.

4. The kinetics of CS_2 insertion into the metal thiolato bond of $CpRu(PPh_3)_2SR$ was studied. The mechanism was shown to be different than that of the insertion of CO_2 into a metal alkoxyl bond, in that precoordination of CS_2 is indicated.

5. The complexes $CpRu(SO_2)(PPh_3)S(SO_2)R$ (R = $4\text{-}C_6H_4Me$, $1\text{-}C_3H_7$, and $CHMe_2$) were prepared by the unusual stepwise reaction of SO_2 with $CpRu(PPh_3)_2SR$. The complex $CpRu(SO_2)(PPh_3)S(SO_2)(4\text{-}C_6H_4Me)$ was isolated and structurally determined. It is the only known complex which combines both thiolate-bonded and metal-bonded SO_2 moieties. The stable complex $CpRu(PPh_3)(CO)S(SO_2)(CHMe_2)$ was also observed spectroscopically. These two complexes are the only known ligand-bonded SO_2 complexes which are stable with respect to SO_2 loss. A possible molecular orbital is proposed to account for their stability.

6. The complexes $CpRu(PPh_3)(CO)SSR$, $CpRu(PPh_3)(CO)SSSR$ and $CpRu(PPh_3)(CO)SS(O)R$ (R = $4\text{-}C_6H_4Me$, $1\text{-}C_3H_7$, and $CHMe_2$) are examples of rare classes of compounds a containing catenated polysulfano ligand. The x-ray structure of

$CpRu(PPh_3)(CO)SSS(1\text{-}C_3H_7)$ is only the second linear trisulfane determined. The structure of $CpRu(PPh_3)(CO)SS(O)(CHMe_2)$ is the first reported for a metal thiosufinate.

7. The complex $CpRu(PPh_3)(CO)SS(O)(4\text{-}C_6H_4Me)$ undergoes a previously unknown intermolecular oxygen transfer to give $CpRu(PPh_3)(CO)SS(O)_2(4\text{-}C_6H_4Me)$, the first metal thiosulfonate to be reported and structurally characterized.

REFERENCES

1 Handbook of Chemistry and Physics, 62th edition, Weast, R.C. ed., CRC Press, Boca Raton, Florida, **1981**

2 The Bible, American Bible Society, New York, **1973**

3 Sagan, C., Cosmos, Random House, New York, **1980**

4 Oae, S., Organic Chemistry of Sulfur, Plenum Press, N. Y., **1977**, pp 304-382

5 Fenwick, G.R., Hanley, A.B., Sulfur-Containing Drugs and Related Organic Compounds, Vol. 1, Part B, Damani, L.A. ed., Halsted Press: a division of John Wiley & Sons, New York, **1989**

6 Block, E., Ashmed, S., Jain, M.K., *J. Am. Chem. Soc.*, **1984**, 106, 8295

7 Block, E., Ashmad, S., Catalfamo, I.L., Jian, M.K., Apitz- Castro, R, *J. Am. Chem. Soc.*,, **1986**, 108, 7045

8 Fessenden, R.J., Fessenden, J.S., Organic Chemistry, 2nd ed., Willard Grant Press, Boston, **1982**

9 Huxtable, R.J., Lafranconi, W.M., Biochemistry of Sulfur, Plenum Press, New York, **1986**

10 Cotton, F.A., Wilkinson, G., Advanced Inorganic Chemistry, 4th ed., John Wiley & Sons, New York, **1980**

11 Beck, R.J., *Oil & Gas Journal*, July 30, **1990**, OGJ Special, 49

12 Sulfur and its Inorganic Derivatives in the Canadian Enviroment, Publication No. NRCC 15015, Publications, NRCC/CNRC, Ottawa, Canada, **1977**

13 Angelici, R.J., *Accounts of Chemical Research*, **1988**, 21, 387

14 Gates, B.C., Katzer, J.R., Schuit, G.C.A., Chemistry of Catalytic Process, McGraw-Hill Book Company, New York, **1979**

15 Grancher. P., *Hydrocarbon Processing*, **1978**, 57, 155

Grander, P., *Hydrocarbon Processing*, **1978**, 57, 25

16 Hachgenei, J.W., Angelici, R.J., *Organometallics*, **1989**, 8, 14

17 Berg, J.M., Holm, R.H., Metal Ions in Biology, Wiley, New York, **1982**, vol. 4, pp 1-66

18 Dev, S., Imagawa, K., Mizobe, Y., Cheng, G., Wakatsuki, Y., Yamazaki, H., Hidai, M., *Organometallics*, **1989**, 8, 1232

19 Schmidt, M.S, Ph.D. Thesis, University of Wisconsin-Madison, **1984**

20 a) Knox, G.R., Pryde, A., *J. Organometal. Chem.*, **1974**, 74, 105

b) Killops, S.D., Knox, S.A.R., *J. Chem. Soc., Dalton trans.* **1978**, 1260

21 Amarasekera, J., Rauchfuss, T.B., Wilson, S.R., *Inorg. Chem.*, **1987**, 26, 3328

22 Amarasekera, J., Rauchfuss, T.B., *Inorg. Chem.*, **1989**, 28, 3875

23 Soo Lum, B., Ph.D. Thesis, McGill University, Montreal, Quebec, Canada, **1990**

24 Morris, S., Ph.D. Thesis, McGill University, Montrreal, Quebec, Canada, **1987**

25 Bennett, M.A., Bruce, M.I., Matheson, T.W., Comprehensive Organometallic Chemistry, vol. 4, Wilkinson, G. ed., Pergamon Press, Toronto, **1982**, p. 778

26 a) Evans, S.V., Legzdins, P., Rettig, S.J., Sánchez, L., Trotter, J., *Organometallics*, **1987**, 6, 7

b) Legzdins, P., Rettig, S.J., Sánchez, L., *Organometallics*, **1988**, 7, 2394

27 Jeannin, S., Jeannin, Y., Lavigne, G., *Inorg. Chem.*, **1978**, 17, 2103

28 Fompeyrine, P., Lavigne, G., Bonnet, J.-J., *J. Chem. Soc., Dalton trans.*, **1987**, 91

29 a) Singleton, E., Lyles, D.C., private communication

b) Shaver, A.G., Plouffe, P.Y., Singleton, E., Lyles, D.C., manuscript in preparation

30 Shaver, A., Lai, R.D., Bird, P.H., Wickramasinghe, W., *Can. J. Chem.* **1985**, 63,

2555 and reference therein

31 Singleton, E., Liles, D.C., National Chemical Research Laboratory, Council for Scientific and Industrial Research, Pretova, South Africa

32 Raston and White, *J. Chem. Soc. Dalton Trans.*, **1975**, 2405

33 Compound **4a** was reported in Amarasekera, J., Rauchfuss, T.B., *Inorg. Chem.*, **1989**, 28, 3875 and was also mentioned in ref. **21**

34 Shaver, A., Lai, R.D., Bird, P.H., Wickramasinghe, W., *Can. J. Chem.*, **1985**, 63, 2555

35 Rauchfuss, T., University of Illinois at Urbana-Champaign, personal communication

36 McAuliffe, C.A., Comprehensive Organometallic Chemistry, vol. 2, Wilkinson, G. ed., Pergamon Press, Toronto, **1982**, p. 1015

37 Ashby, M.T., Enemark, J.H., Lichtenberger, D.L., *Inorg. Chem.*, **1988**, 27, 191

38 Ashby, M.T., Ph.D. Thesis, University of Arisona, **1986**

39 Ashby, M.T., Enemark, J.H., *J. Am. Chem. Soc.*, **1986**, 108, 730

40 Koch, S.A., Millar, M., *J. Am. Chem. Soc.* **1983**, 105, 3362

41 a) McAuliffe, C.A., Comprehensive Organometallic Chemistry, vol. 2, Wilkinson, G. ed., Pergamon Press, Toronto, **1982**, p. 1033

b) Marynick, D.S., *J. Am. Chem. Soc.*, **1984**, 106, 4064

42 a) Albers, M.O., Robinson, D.J., Singleton, E., *Coord. Chem. Rev.*, **1987**, 79, 1

b) Davies, S.G., Simpson, S.J., *J. Chem. Soc. Dalton Trans.* **1984**, 993

43 Ashby, G.S., Bruce, M.I., Tomkins, I.B., Wallis, R.C., *Aust. J. Chem.*, **1979**, 32, 1003

44 Gatton, G., Behrendt, W., Topics in Sulfur Chemistry, Georg Thieme, Struttgart, vol. 2, Senning, A. ed., **1977**, p. 183

45 a) Stato, F., Lida, K., Sato, M., *J. Organomet. Chem.* **1972**, 39, 197

b) Bladon, P., Bruce, R., Knox, G.R., *J. Chem. Commun.* **1965**, 557

c) Havlin, R., Knox, G.R., *Z. Naturforsch.* **1966**, 21b, 1108

d) Bruce, R., Knox, G.R., *J. Organometal. Chem.* **1966**, 6, 67

e) Chandha, R.K., Kumar, R., Tuck, D.G., *Polyhedron* **1988**, 7, 1121

f) Avdeef, A., Fackler, Jr., J.P., *J. Coord. Chem.* **1975**, 4, 211

46 a) Sato, F., Iida, K., Sato, M., *J. Organometal. Chem.*, **1972**, 39, 197 b) Kim, Y.-J., Osakada, K., Sugita, K., Yamamoto, T., Yamamoto, A., *Organomatallics*, **1988**, 7, 2182

47 Mylius, I., *Ber.* **1873**, 6, 312.

48 a) Iwasaki, I., Cooke, S.R B., *Chem. Eng.*, **1957**, 9, 1267

b) Havlin, R., Knox, G.R., *Z. Naturforsch.*, **1966**, B 21, 1108

49 Hunt, J., Knox, S.A.R., Oliphant, V., *J. Organometal., Chem.*, **1974**, 80, C50

50 Bruce, R., Knox, G.R., *J. Organometal. Chem.*, **1966**, 6, 67

51 Coucouvanis, D., Lippard, S.J., Zubieta, J.A., *J. Am. Chem. Soc.*, **1970**, 92, 3342

52 Lewis, D.F., lippard, S.J., Zubieta, J.A., *J. Am. Chem. Soc.*, **1972**, 94, 1563

53 The periotic table numbering used labels every colunm as 1 through 18 from left to right.

54 Bird, P., Livingstone, E., Department of Chemistry, Concordia University, Montreal, Quebec, Canada

55 a) Darensbourg, D.J., Sanchez, K.M., Rheingold, A.L., *J. Am., Chem., Soc.*, **1987**, 109, 290

b) Darensbourg, D.J., Sanchez, K.M., Reibenspies, J.H., Rheingold, A.L. *J. Am. Chem. Soc.*, **1989**, 111, 7094

56 a) Bruce, M.I., Humphrey, M.G., Swincer, A.G., Wallis, R.C., *Aust. J. Chem.*,

1984, 37, 1747

b) Mishra, A.G., Agarwala, U.C., *Inorg. Chim. Acta*, **1988**, 145, 191

57 Alberty, R.A., Daniels, F M., Physical Chemistry, fith edition, John Wiley and Sons, N. Y. **1980**, pp 541-545

58 Program was kindly supplied by Dr. Jik Chin of McGill University, Montreal, Quebec, Canada

59 a) Fehlhammer, V.W.P, Mayr, A., Stoizenberg, H., *Angew. Chem.*, **1979**, 91, 661.

b) Forniés, J., Usón, M.A., Gil, J.I., *J. Organomet. Chem.*, **1986**, 311, 243

60 ref. **44**, pp 161-171

61 Butler, I.S., *Acc. Chem. Res.*, **1970**, 10, 359

62 Unpublished results.

63 Butler, I.S., *Acc. Chem. Res.*, **1977**, 10, 359

64 Kubas, G.J., Ryan, R.R., *Polyhedron*, **1986**, 5, 473

65 Kubas, G.J., Wasserman, H.J., Ryan, R.R., *Organometallics*, **1985**, 4, 2012

66 Kubas, G.J., *Inorg. Chem.*, **1979**, 18, 182

67 Schenk, W.A., *Angew. Chem. Int. Ed. Engl.*, **1987**, 26, 98

68 Schenk, W.A., *Angew. Chem. Int. Ed. Ingl.*, **1987**, 26, 98

69 Conway, P., Grant, S.M., Manning, A.R., Stephens, F.S., *Inorg. Chem.*, **1983**, 22, 3714

70 a) Eller, P.G., Kubas, G.J., *J. Am. Chem. Soc.*, **1977**, 99, 4346

b) Snow, M.R., Ibers, J.A., *Inorg. Chem.*, **1973**, 12, 224

71 Data purchassed by Crystalytics Company, Lincoln, Nebraska, U.S.A.

Data processing by Dr. J. Britten, McGill University, Montreal, Quebec, Canada

72 Osakada, K., Yamamoto, T., Yamamoto, A, Takenaka, A, Sasada, Y., *Inorg. Chim. Acta*, **1985**, 105, L9

73 Shaver, A., Plouffe, P.Y., Bird, P., Livingstone, E., *Inorg. Chem.*, **1990**, 29, 1826

74 a) Wilczewski, T, Dauter, Z, *J. Organometal. Chem.*, **1986**, 312, 349

b) Bleeke, J.R., Rauscher, D.J., *Organometallics*, **1988**, 7, 2328

c) Cesarotti, E., Angoletta, M., Walker, N.P.C., Hursthouse, M.B.,Vefghi, R., Schofield, P.A., White, C., *J. Organometal. Chem.*, **1985**, 286, 343

75 Wojcicki, A., *Advan. Organometal. Chem.*, **1974**, 12, 31

76 Bennet, M.A., Bruce, M.I., Matheson, T.W., Comprehensive Organometallic Chemistry, vol. 4, Wilkinson, G. ed., Pergamon Press, Toronto, **1982**, pp. 777

77 a) Young, D., Kitching, W., *Organometallics*, **1988**, 1196

b) Jacobson, S.E., Wojcicki, A., *J. Am. Chem. Soc.*, **1973**, 95, 6921

78 a) Kubat-Martin, K.A., Kubas, G.J., Ryan, R.R., *Organometallics*, **1988**, 7, 1657

b) Kubat-Martin, K.A., Kubas, G.J., Ryan, R.R., *Organometallics*, **1989**, 8, 1910

79 Childs, J.D., van der Helm, D., Christian, S.D., *Inorg. Chem.*, **1975**, 14, 1386

80 Vogt, L.H., Katz, J.L., Wiberley, S.E., *Inorg. Chem.*, **1965**, 4, 1157

81 Orrell, K.G., *Coord. Chem. Rev.*, **1989**, 96, 1

82 Kice, J.L., Sulfur in Organic and Inorganic Chemistry, vol. 1, Senning, A. ed., Marcel Dekker, Inc., New York, New York, **1971**, pp 153-207

83 Schmidt, M., *Angrew. Chem. Int. Ed. Engl.*, **1973**, 12, 45

84 Warren, B.E., Burwell, J.T., *J. Chem. Phys.*, **1935**, 3, 6

85 Tobolsky, A.V., McKnight, W., Polymer Sulfur and Sulfur Polymers, Interscience Publisher, New York, **1966**

86 a) Foss, O., Adv. Inorg. Chem. Radiochem., **1960**, 2, 237

b) von Halasz, S.P., Glemser, O., Sulfur in Organic and Inorganic Chemistry, vol. 1, Senning, A. ed., Marcel Dekker Inc., New York, **1971**, pp.209-237

87 March, J., Advanced Organic Chemistry, 2nd ed., McGraw-Hill Book Company,

New York, **1977**

88 Harpp, D.N., Back, T.G., J. *Org. Chem.* **1973**, 38, 4328

89 Harpp, D.N., Ash, D.K., Back, T.G., Gleason, J.G., Orwig, B.A., VanHorn, W.F., Snyder, J.P., *Tetrahedron Letters*, **1970**, 41, 3551

90 Harpp, D.N., Ash, D.K., *Int. J. Chem., A*, **1971**, 1, 57

91 Marmolejo, G., Ph. D. Thesis, McGill University, Montreal, Quebec, Canada, 1985

92 a) Lau, P.T.S., *Eastman Organic Chemical Bulletin*, **1975**, 46, No.2

b) Harpp, D.N., Back, T.G., *Tetrehedron Letters*, **1972**, 15, 1481

c) Harpp, D.N., Steliou. K., Chan, T.H., *J. Chem. Soc.*, **1978**, 100, 1222

93 Reid, E.E., Organic Chemistry of Bivalent Sulfur, vol. 1, Chemical Publishing Co., N. Y., **1958**

94 Shaver, A., Hartgerink, J., *Can. J. Chem.*, **1987**, 65, 1190

95 Shaver, A., McCall, J.M., Bird, P.H., Ansari, N., *Organometallics*, **1983**, 2, 1894

96 Lai, R.D., Ph. D. Thesis, McGill University, Montreal, Quebec, Canada, **1981**

97 Shaver, A.G., Hartgerink, J., Lai, R.D., Bird, P., Ansari, N., *Organometallics*, **1983**, 2, 938

98 John, E., Baradwaj, P.K., Krogh-Jespersen, K., Potenza, J.A., [illegible]gar, H.J., *J. Am. Chem. Soc.*, **1986**, 108, 5015

99 Hartgerink, J., Masters Thesis, McGill University, Montreal, Quebec, Canada, 1981

100 Urove, G.A., Welker, M.E., *Organometallics*, **1988**, 7, 1013

101 Noordick, J.H., Vos, A., *Rec. Trav. Chim. Pays-Bas*, **1967**, 86, 156

102 Wahl, G.H., Bordner, J., Harpp, D.N., Gleason, J.G., *Acta Cryst.*, **1973**, B29, 2272

103 Åse, K., *Acta chem. Scand.*, **1971**, 25, 838

104 Åse, K., Naartmann-Moe, K., Solheim, J.O., *Acta Chem. Scand.*, **1971**, 25, 2467

105 Weinmann, D.J., Abrahamson, H.B., *Inorg. Chem.*, **1987**, 26, 3034 and references therein

106 McCall, J.M., Ph. D. Thesis, McGill University, Montreal, Quebec, Canada, 1983

107 Snyder J.P., Harpp, D.N., *Tettrahedron Letters*, **1978**, 2,197

108 a)Moore, C.G., Trego, B.R., *Tetrahedron*, **1962**, 18, 205

b)Mukaiyama, T., Takei, H., *Topics in Phospherous Chemistry*,**1976** , 8, 587

109 Hordvik, A., *Acta Chem. Scand.*, **1966**, 20, 1885-1891

110 a) Data collected by Molecular Structure Co., Woodland, Texas, U.S.A. (Rigaku diffractometer)

b) Data collected by Siemens X-Ray, Madison, Wisconsin, U.S.A. (Siemens-Nicolet diffractometer)

c)Data collected by Dr. André Michel, Université de Sherbrooke, Sherbrooke, Quebec, Canada (ENRAF-NONIUS CAD4 diffractometer)

All data processing by Dr. J. Britten, McGill University, Montreal, Quebec, Canada

111 Harpp, D.N., *International Symposium on Organic Chemistry of Sulfur*, Nijmegen, The Netherlands, 29 June-4July **1986**

112 a) Sandström, J., Dynamic NMR Spectroscopy, Academic Press, N. Y., N. Y., **1982**

b) Sanders, J.K.M., Hunter, B.K., Modern NMR Spectroscopy, Oxford University Press, Oxford, N. Y., **1987**

113 Fraser, R.R., Boussard, G., Saunders, J.B. Lambert, J.B., Mixan, C. E., *J. Amer Chem. Soc.*, **1971**, 93, 3822

114 Fraser, R.R., Boussard, G., Saunders, J.K., Lambert, J.B., Mixan, C.E. *J. Am.*

Chem. Soc **971**, 93, 3822

115 Tobolsky, A.V. Sulfur in Organic and Inorganic Chemistry, vol. 3, Senning, A. ed., Marcel Dekker, Inc., New York, 1971, pp 19-38

116 Harpp, D.N., Skuliou, K., *J. Chem. Soc., Chem. Commun.*, **1980**, 825

117 a) Benson, S., *Chem. Rev.*, **1978**, 78, 23

b) Tebbe, F.N., Wasserman, E., Peet, W.G., Vatvars, A., Hayman, A.C., *J. Am. Chem Soc*, **1982**, 104, 4971.

118 Steudel, R., *Angrew. Chem. Internat. Edit.*, **1975**, 14, 655

119 a) Steudel, R., Reinhardt, R., Schuster, F., *Angrew. Chem. Int. Ed. Engl.*, **1977**, 16, 715

b) Steudel, R., *Angew. Chem. internat Edit.*, **1975**, 14, 655

120 Data purchassed from Molecular Structure Co., Woodland, Texas, U.S.A.
Data processing by Dr. J. Britten, McGill University, Montreal, Quebec, Canada

121 Kiers, C T., Vos, A, Recueil, *J Royal Netherlands Chem. Soc.*, **1978**, 97, 166

122 Freeman, F., Angeletakis, C.N., Maricich, T.J., *J. Org. Chem.* **1982**, 47, 3403

123 Hamilton, W.C., *Acta Chryst.*, **1965**, 18, 502

124 Data collection by Crystalytics Company, Lincoln, Nebraska, U.S.A.
Data processing by Dr. J. Britten, McGill University, Montreal, Quebec, Canada

125 Back, T.G., Ph.D. Thesis, McGill University, Montreal, Quebec, Canada, 1974

126 Data acquisition and processing by Dr. J.F. Britten, McGill University, Montreal, Quebec, Canada

127 Wu, X., Bose, K.S., Sinn, E., Averill, B.A., *Organometallics*, **1989**, 8, 251

128 Noble, M.E., *Inorg. Chem.*, **1986**, 25, 3311

Appendix I

Structural Analysis of $[CpRuS(1\text{-}C_3H_7)]_3$, **3c**.

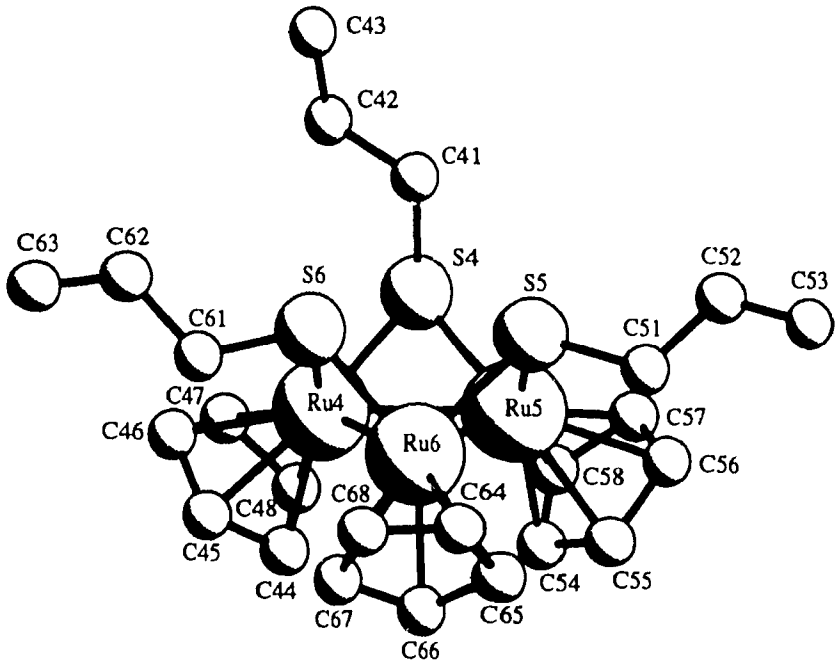

Table A1.1 Crystal data for $[CpRuS(1\text{-}C_3H_7)]_3$.

Space Group: Triclinic, $P\bar{1}$

Cell Dimensions.

a = 10.554(1)	b = 14.033(2)	c = 18.243(2)
α = 76.977(10)	β = 87.299(8)	γ = 89.009(11)

Volume = 2629.4(9) $Å^3$

Empirical formula : $C_{24}H_{36}Ru_3S_3$

Cell dimensions were obtained from 25 reflections with 2Θ angle in the range 15.42 - 39.5°.

Crystal dimensions: 0 .34 × 0.27 × 0.06 mm

FW = 723.95 Z = 4 F(000) = 1440

D_{calc} = 1.829 Mg m^{-3}, μ = 1.897 mm^{-1}, λ = 0.71069 Å, $2\Theta_{(max)}$= 54°

The intensity data were collected on an Enraf-Nonius CAD4F using the $\omega/2\Theta$ scan mode.
The h,k,l ranges are: 0 13, -17 17, -23 23

No. of reflections measured	11430
No. of reflections with Inet > 3.0 σ (Inet)	9276

Semiempirical absorption correction, based on azimuth scans of 9 reflections were applied to the data

Data set was solved by direct method using SHELXS-86 and refined using SHELX-76. The last least squares cycle was calculated with 60 atoms, 545 parameters and 9276 out of 11430 reflections.
Weights based on counting-statistics were used.

For significant reflections, R = 0.0304, Rw = 0.0268

where $R = \Sigma|Fo-Fc|/\Sigma|Fo|$,
$Rw = \sqrt{[\Sigma w(Fo-Fc)^2)/\Sigma(wFo^2)]}$ and
$GoF = \sqrt{[\Sigma(w(Fo-Fc)^2)/(\text{No. of reflns - No. of params.})]}$

The maximum shift/σ ratio was 0.068

In the last D-map, the deepest hole was -0.69 $e^-/Å^3$, and the highest peak 0.80 $e^-/Å^3$.

Table A1.2 Atomic coordinates, x,y,z and B_{iso} for $[CpRuS(1\text{-}C_3H_7)]_3$. E.S.Ds. refer to the last digit printed.

	x	y	z	U_{eq}
Ru1	0.11997(3)	0.33684(2)	0.29335(2)	0.0322(1)
Ru2	0.27144(3)	0.46145(3)	0.19233(2)	0.0372(1)
Ru3	0.15007(3)	0.52374(2)	0.30754(2)	0.0322(1)
S1	0.12172(1)	0.36062(8)	0.16475(6)	0.0408(3)
C11	-0.0204(4)	0.4155(4)	0.1198(3)	0.0056(1)
C12	-0.1192(6)	0.3366(6)	0.1251(5)	0.0144(3)
C13	-0.2349(8)	0.3589(7)	0.1173(6)	0 0230(5)
S2	0.13350(1)	0.59240(8)	0.18152(6)	0.0401(3)
C21	0.2230(4)	0.7058(3)	0.1526(2)	0.0048(1)
C22	0.2278(5)	0.7389(4)	0.0669(3)	0.0067(1)
C23	0.3050(6)	0.8282(4)	0.0389(3)	0 100(2)
S3	-0.03832(9)	0.45060(7)	0.29392(6)	0 0341(2)
C31	-0.1338(4)	0.4202(3)	0.3823(2)	0.038(1)
C32	-0.2512(4)	0.3648(3)	0.3700(3)	0.055(1)
C33	-0.3447(5)	0.3508(4)	0.4372(3)	0.073(2)
C14	0.2503(4)	0.2565(3)	0.3763(3)	0.053(1)
C15	0.2489(5)	0.2072(3)	0.3163(3)	0 061(1)
C16	0.1246(5)	0.1723(3)	0.3149(3)	0.063(2)
C17	0.0517(5)	0.1984(3)	0.3723(3)	0.058(1)
C18	0.1274(5)	0.2509(3)	0.4104(3)	0 052(1)
C24	0.4588(4)	0.4059(5)	0.2315(3)	0 070(2)
C25	0.4688(4)	0.5044(5)	0.2090(4)	0.071(2)
C26	0.4478(4)	0.5321(4)	0.1324(4)	0.075(2)
C27	0.4254(5)	0.4489(6)	0.1064(4)	0.086(2)
C28	0.4309(5)	0.3680(4)	0.1693(4)	0 077(2)
C34	0.2892(5)	0.6170(4)	0.3417(3)	0.058(1)
C35	0.3052(5)	0.5217(4)	0.3844(3)	0.060(1)
C36	0.1954(5)	0.4947(4)	0.4291(3)	0.061(1)
C37	0.1109(5)	0.5743(4)	0.4151(3)	0.062(1)
C38	0.1672(5)	0.6499(4)	0.3617(3)	0.059(1)
Ru4	0.38489(3)	0.00935(2)	0.70247(2)	0.0345(1)
Ru5	0.23537(3)	0.07453(3)	0.80648(2)	0.0377(1)
Ru6	0.35556(3)	0.20413(2)	0.69274(2)	0 0330(1)
S4	0.38687(10)	-0.04577(8)	0.83082(6)	0.0415(3)
C41	0.5297(4)	-0.0198(3)	0.8749(3)	0.049(1)
C42	0.6339(5)	-0.0940(4)	0.8650(4)	0.078(2)
C43	0.7572(5)	-0.0723(4)	0.8887(4)	0 110(2)
S5	0.37282(10)	0.19483(8)	0.81905(6	0.0405(3)
C51	0.2832(4)	0.2933(3)	0.8492(2)	0.050(1)
C52	0.2772(5)	0.2758(4)	0.9341(3)	0.073(2)
C53	0.2021(6)	0.3484(5)	0.9616(3)	0.118(3)
S6	0 54421(9)	0.11844(7)	0.70332(6)	0.0348(2)
C61	0.6372(4)	0.1423(3)	0.6142(2)	0.041(1)
C62	0.7555(4)	0.0771(4)	0.6217(3)	0.063(1)
C63	0.8465(5)	0.1032(4)	0.5537(3)	0.079(2)

C44	0.2523(5)	-0.0165(4)	0.6209(4)	0.073(2)
C45	0.3728(6)	-0.0028(4)	0.5853(3)	0.066(2)
C46	0.4512(5)	-0.0787(4)	0.6193(3)	0.069(2)
C47	0.3833(6)	-0.1389(4)	0.6757(4)	0.079(2)
C48	0.2595(5)	-0.1042(4)	0.6798(4)	0.073(2)
C54	0.0484(5)	0.0432(7)	0.7688(4)	0.086(2)
C55	0.0360(5)	0.1284(5)	0.7909(5)	0.090(2)
C56	0.0590(5)	0.1113(6)	0.8682(5)	0.092(2)
C57	0.0843(5)	0.0138(7)	0.8929(4)	0.098(2)
C58	0.0783(5)	-0.0285(5)	0.8300(6)	0.087(2)
C64	0.3243(5)	0.3635(3)	0.6448(3)	0.060(1)
C65	0.2074(5)	0.3156(4)	0.6584(3)	0.062(1)
C66	0.2055(5)	0.2482(4)	0.6128(3)	0.063(1)
C67	0.3225(6)	0.2549(4)	0.5722(3)	0.069(2)
C68	0.3931(5)	0.3272(4)	0.5918(3)	0.067(1)
H1	0.5113(4)	-0.0245(3)	0.9271(3)	0.095(4)
H2	0.5580(4)	0.0444(3)	0.8521(3)	0.095(4)

$U_{eq} = \frac{1}{3} \Sigma_i \Sigma_j U_{ij} a_i^* a_j^* (a_i a_j)$

Table A1.3 Anisotropic thermal factors for $[CpRuS(1\text{-}C_3H_7)]_3$. U(i,j) values ×100. E.S.Ds. refer to the last digit printed.

	U11	U22	U33	U23	U13	U12
Ru1	13.35(2)	3.30(2)	3.09(2)	-0.88(2)	-0.17(1)	-0.21(1)
Ru2	3.28(2)	4.30(2)	3.65(2)	-1.17(2)	0.51(2)	-0.46(2)
Ru3	33.33(2)	3.40(2)	3.06(2)	-0.98(2)	-0.02(1)	-0.47(1)
S1	4.42(6)	4.76(7)	3.42(6)	-1.66(5)	-0.01(5)	-0.43(5)
C11	5.2(3)	7.9(4)	4.4(3)	-2.6(3)	-1.5(2)	0.2(3)
C12	14.4(3)					
C13	23.0(5)					
S2	4.11(6)	4.08(6)	3.65(6)	-0.48(5)	0.01(5)	-0.43(5)
C21	5.9(3)	3.9(3)	4.0(3)	0.2(2)	0.7(2)	-0.5(2)
C22	8.5(4)	6.4(4)	4.5(3)	0.1(3)	0.61(3)	-0.19(3)
C23	12.9(6)	9.7(5)	5.8(4)	1.5(4)	0.73(4)	-0.36(4)
S3	3.15(5)	3.94(6)	3.14(6)	-0.82(5)	0.04(4)	-0.2(4)
C31	3.4(2)	4.5(3)	3.5(2)	-1.1(2)	0.4(2)	-0.2(2)
C32	4.9(3)	5.6(3)	5.9(3)	-1.5(3)	1.2(2)	-1.7(2)
C33	5.9(3)	8.4(4)	6.8(4)	-0.5(3)	1.8(3)	-1.9(3)
C14	5.3(3)	4.5(3)	5.8(3)	-0.1(2)	-2.4(3)	-0.1(2)
C15	6.4(3)	4.2(3)	7.2(4)	-0.4(3)	0.5(3)	1.9(3)
C16	8.9(4)	3.0(3)	7.4(4)	-1.6(3)	-1.7(3)	-0.3(3)
C17	5.8(3)	4.4(3)	6.4(4)	0.7(3)	-0.3(3)	-0.9(2)
C18	6.7(3)	4.4(3)	4.1(3)	-0.2(2)	-0.3(2)	0.3(2)
C24	3.0(3)	0.1(5)	7.4(4)	-1.2(4)	0.0(3)	-0.1(3)
C25	4.4(3)	8.3(4)	9.5(5)	-4.5(4)	1.5(3)	-2.2(3)
C26	3.7(3)	6.8(4)	10.4(5)	0.9(4)	2.3(3)	-0.9(3)
C27	4.7(3)	5.6(7)	6.7(4)	-5.6(5)	2.7(3)	-1.7(4)
C28	4.5(3)	6 7(4)	12.3(6)	-3.8(4)	2.8(4)	-0.2(3)
C34	5.9(3)	5.8(3)	5.9(3)	-2.0(3)	0.4(3)	-2.6(3)
C35	5.3(3)	6.6(4)	7.3(4)	-3.4(3)	-2.8(3)	1.2(3)
C36	8.9(4)	5.9(3)	3.8(3)	-1.4(3)	-0.4(3)	-2.1(3)
C37	5.6(3)	9.2(4)	5.0(3)	-4.1(3)	0.3(3)	-0.3(3)
C38	8.0(3)	4.5(3)	6.1(4)	-2.7(3)	-1.9(3)	0.1(3)
Ru4	3.39(2)	3.37(2)	3.70(2)	-0.97(2)	-0.26(2)	-0.34(1)
Ru5	3.09(2)	4.24(2)	3.86(2)	-0.68(2)	0.28(2)	-0.45(2)
Ru6	3.38(2)	3.32(2)	3.11(2)	-0.50(2)	-0.26(1)	0.06(1)
S4	3.96(6)	3.92(6)	4.16(7)	-0.02(5)	-0.17(5)	-0.51(5)
C41	4.6(3)	5.4(3)	4.4(3)	0.1(2)	-0.9(2)	-0.6(2)
C42	6.1(4)	6.4(4)	10.9(5)	-1.3(3)	-3.2(3)	1.2(3)
C43	6.4(4)	9.8(5)	15.3(7)	0.2(5)	-0.2(4)	1.5(4)
S5	4.23(6)	4.43(7)	3.54(6	-1.15(5)	-0.09(5)	-0.32(5)
C51	6.3(3)	5.0(3)	4.3(3)	-2.2(2)	0.6(2)	-0.5(2)
C52	9.3(4)	8.0(4)	4.8(3	-2.1(3)	1.3(3)	0.5(3)
C53	15.1(7)	14.4(7)	6.6(5)	-4.4(5)	1.4(4)	3.0(5)
S6	3.16(5)	3.72(6)	3.42(6	-0.49(5)	-0.05(4)	-0.35(4)
C61	3.9(2)	4.2(3)	4.1(3)	-0.7(2)	0.8(2)	-0.5(2)
C62	3.5(3)	6.2(3)	7.1(4)	-1.2(3)	1.8(3)	0.6(2)
C63	5.7(3)	10.0(5)	8.8(5)	-4.1(4)	2.5(3)	-0.4(3)

C44	6.4(4)	7.8(4)	9.7(5)	-5.7(4)	-4.4(4)	2.0(3)
C45	9.5(5)	6.4(4)	4.5(3)	-2.4(3)	-0.1(3)	-1.8(3)
C46	6.3(4)	7.6(4)	8.2(5)	-4.9(4)	0.3(3)	-0.3(3)
C47	11.1(5)	4.3(3)	9.4(5)	-3.6(3)	-2.9(4)	0.1(3)
C48	6.6(4)	7.7(4)	9.2(5)	-5.2(4)	1.1(3)	-3.3(3)
C54	3.2(3)	14.5(7)	8.9(5)	-4.1(5)	-0.6(3)	-0.7(4)
C55	3.3(3)	8.5(5)	2.6(7)	2.8(5)	2.2(4)	1.1(3)
C56	3.8(3)	12.4(7)	13.4(7)	-7.7(6)	3.0(4)	-1.3(4)
C57	4.4(3)	14.7(7)	7.3(5)	3.4(5)	2.4(3)	-0.3(4)
C58	3.7(3)	6.5(4)	15.4(7)	-1.8(5)	2.8(4)	-1.6(3)
C64	8.3(4)	3.4(3)	6.2(4)	-0.2(2)	-1.9(3)	0.0(3)
C65	6.0(3)	6.4(4)	5.4(3)	0.3(3)	-0.1(3)	2.9(3)
C66	6.3(3)	5.1(3)	7.0(4)	0.6(3)	-3.5(3)	-0.4(3)
C67	10.1(5)	6.8(4)	3.4(3)	-0.4(3)	-1.1(3)	3.6(3)
C68	5.6(3)	6.4(4)	6.3(4)	2.8(3)	-0.4(3)	0.2(3)
H1	9.5(4)					
H2	9.5(4)					

Anisotropic Temperature Factors are of the form:

$$\text{Temp} = -2\pi^2(h^2a^{*2}U_{11} + k^2b^{*2}U_{22} + l^2c^{*2}U_{33} + 2hka^*b^*U_{12} + 2hla^*c^*U_{13} + 2klb^*c^*U_{23})$$

Table A1.4 Selected bond length and angles for $[CpRuS(1\text{-}C_3H_7)]_3$.

Ru(1)-Ru(2)	2.7159(6)	S(1)-C(11)	1.818(5)
Ru(1)-Ru(3)	2 7183(6)	C(11)-C(12)	1.518(9)
Ru(1)-S(1)	2.2932(12)	C(12)-C(13)	1.262(11)
Ru(1)-S(3)	2.2920(11)	S(2)-C(21)	1.825(4)
Ru(1)-C(14)	2.197(5)	C(21)-C(22)	1.526(6)
Ru(1)-C(15)	2 227(5)	C(22)-C(23)	1.484(8)
Ru(1)-C(16)	2.253(4)	S(3)-C(31)	1.830(4)
Ru(1)-C(17)	2.249(4)	C(31)-C(32)	1.526(6)
Ru(1)-C(18)	2.207(5)	C(32)-C(33)	1 516(7)
Ru(2)-Ru(3)	2.7125(6)	C(14)-C(15)	1.421(8)
Ru(2)-S(1)	2.2859(12)	C(14)-C(18)	1.407(7)
Ru(2)-S(2)	2.3036(12)	C(15)-C(16)	1.412(7)
Ru(2)-C(24)	2.204(5)	C(16)-C(17)	1.382(8)
Ru(2)-C(25)	2.232(5)	C(17)-C(18)	1.403(8)
Ru(2)-C(26)	2.242(5)	C(24)-C(25)	1.355(9)
Ru(2)-C(27)	2.237(6)	C(24)-C(28)	1.402(10)
Ru(2)-C(28)	2.199(6)	C(25)-C(26)	1.391(10)
Ru(3)-S(2)	2.2974(11)	C(26)-C(27)	1.383(11)
Ru(3)-S(3)	2.3023(11)	C(27) C(28)	1.423(9)
Ru(3)-C(34)	2.186(6)	C(34)-C(35)	1.400(7)
Ru(3)-C(35)	2.201(6)	C(34)-C(38)	1.420(8)
Ru(3)-C(36)	2.236(5)	C(35)-C(36)	1.392(7)
Ru(3)-C(37)	2.251(6)	C(36)-C(37)	1.402(8)
Ru(3)-C(38)	2.227(6)	C(37)-C(38)	1.389(7)
Ru(4)-Ru(5)	2.716(1)	C(41)-C(42)	1.534(7)
Ru(4)-Ru(6)	2.712(1)	C(41)-H(1)	1.080()
Ru(4)-S(4)	2.295(1)	C(41)-H(2)	1.080()
Ru(4)-S(6)	2.296(1)	C(42)-C(43)	1.449(8)
Ru(4)-C(44)	2.182(7)	S(5)-C(51)	1.832(5)
Ru(4)-C(45)	2.192(6)	C(51)-C(52)	1.511(7)
Ru(4)-C(46)	2.244(7)	C(52)-C(53)	1.443(9)
Ru(4)-C(47)	2.242(6)	S(6)-C(61)	1.826(4)
Ru(4)-C(48)	2.210(6)	C(61)-C(62)	1.528(6)
Ru(5)-Ru(6)	2.712(1)	C(62)-C(63)	1.513(7)
Ru(5)-S(4)	2.289(1)	C(44)-C(45)	1.397(8)
Ru(5)-S(5)	2.302(1)	C(44)-C(48)	1.443(8)
Ru(5)-C(54)	2.203(6)	C(45)-C(46)	1.387(8)
Ru(5)-C(55)	2.233(5)	C(46)-C(47)	1 359(8)
Ru(5)-C(56)	2.243(7)	C(47)-C(48)	1.391(9)
Ru(5)-C(57)	2.227(6)	C(54)-C(55)	1.348(13)
Ru(5)-C(58)	2.181(6)	C(54)-C(58)	1.369(11)
Ru(6)-S(5)	2.294(1)	C(55)-C(56)	1.408(13)
Ru(6)-S(6)	2.301(1)	C(56)-C(57)	1.366(12)
Ru(6)-C(64)	2.235(4)	C(57)-C(58)	1.410(13)
Ru(6)-C(65)	2.202(5)	C(64)-C(65)	1.400(7)
Ru(6)-C(66)	2.190(5)	C(64)-C(68)	1.366(8)
Ru(6)-C(67)	2.196(5)	C(65)-C(66)	1.394(8)
Ru(6)-C(68)	2.248(5)	C(66)-C(67)	1.403(8)

S(4)-C(41)	1.821(5)	C(67)-C(68)	1.388(9)

Ru(2)-Ru(1)-Ru(3)	59.888(16)	Ru(2)-Ru(3)-C(36)	129.60(14)
Ru(2)-Ru(1)-S(1)	53.50(3)	Ru(2)-Ru(3)-C(37)	162.27(14)
Ru(2)-Ru(1)-S(3)	93.85(3)	Ru(2)-Ru(3)-C(38)	136.03(13)
Ru(2)-Ru(1)-C(14)	104.48(11)	S(2)-Ru(3)-S(3)	83.54(4)
Ru(2)-Ru(1)-C(15)	99.06(12)	S(2)-Ru(3)-C(34)	102.83(13)
Ru(2)-Ru(1)-C(16)	126.12(13)	S(2)-Ru(3)-C(35)	131.94(13)
Ru(2)-Ru(1)-C(17)	159.84(13)	S(2)-Ru(3)-C(36)	164.22(14)
Ru(2)-Ru(1)-C(18)	137.98(14)	S(2)-Ru(3)-C(37)	135.33(13)
Ru(3)-Ru(1)-S(1)	100.40(3)	S(2)-Ru(3)-C(38)	105.07(13)
Ru(3)-Ru(1)-S(3)	53.90(3)	S(3)-Ru(3)-C(34)	161.84(15)
Ru(3)-Ru(1)-C(14)	101.63(13)	S(3)-Ru(3)-C(35)	143.54(13)
Ru(3)-Ru(1)-C(15)	131.54(14)	S(3)-Ru(3)-C(36)	110.25(14)
Ru(3)-Ru(1)-C(16)	162.60(14)	S(3)-Ru(3)-C(37)	102.07(14)
Ru(3)-Ru(1)-C(17)	133.97(14)	S(3)-Ru(3)-C(38)	124.56(14)
Ru(3)-Ru(1)-C(18)	103.14(13)	C(34)-Ru(3)-C(35)	37.21(19)
S(1)-Ru(1)-S(3)	92.07(4)	C(34)-Ru(3)-C(36)	61.71(19)
S(1)-Ru(1)-C(14)	131.44(14)	C(34)-Ru(3)-C(37)	61.40(20)
S(1)-Ru(1)-C(15)	98.03(15)	C(34)-Ru(3)-C(38)	37.52(20)
S(1)-Ru(1)-C(16)	94.96(14)	C(35)-Ru(3)-C(36)	36.57(19)
S(1)-Ru(1)-C(17)	123.27(15)	C(35)-Ru(3)-C(37)	60.89(20)
S(1)-Ru(1)-C(18)	155.86(13)	C(35)-Ru(3)-C(38)	61.72(20)
S(3)-Ru(1)-C(14)	135.45(14)	C(36)-Ru(3)-C(37)	36.43(19)
S(3)-Ru(1)-C(15)	166.74(13)	C(36)-Ru(3)-C(38)	61.12(19)
S(3)-Ru(1)-C(16)	134.05(14)	C(37)-Ru(3)-C(38)	36.14(18)
S(3)-Ru(1)-C(17)	106.30(13)	Ru(1)-S(1)-Ru(2)	72.76(4)
S(3)-Ru(1)-C(18)	106.06(14)	Ru(1)-S(1)-C(11)	116.20(18)
C(14)-Ru(1)-C(15)	37.47(20)	Ru(2)-S(1)-C(11)	118.44(19)
C(14)-Ru(1)-C(16)	61.64(19)	S(1)-C(11)-C(12)	109.1(4)
C(14)-Ru(1)-C(17)	61.46(17)	C(11)-C(12)-C(13)	120.6(8)
C(14)-Ru(1)-C(18)	37.27(18)	Ru(2)-S(2)-Ru(3)	72.25(3)
C(15)-Ru(1)-C(16)	36.72(19)	Ru(2)-S(2)-C(21)	109.19(14)
C(15)-Ru(1)-C(17)	60.87(18)	Ru(3)-S(2)-C(21)	111.77(13)
C(15)-Ru(1)-C(18)	61.93(19)	S(2)-C(21)-C(22)	109.6(3)
C(16)-Ru(1)-C(17)	35.75(19)	C(21)-C(22)-C(23)	112.7(5)
C(16)-Ru(1)-C(18)	60.99(19)	Ru(1)-S(3)-Ru(3)	72.55(3)
C(17)-Ru(1)-C(18)	36.68(20)	Ru(1)-S(3)-C(31)	110.30(13)
Ru(1)-Ru(2)-Ru(3)	60.100(15)	Ru(3)-S(3)-C(31)	112.10(15)
Ru(1)-Ru(2)-S(1)	53.75(3)	S(3)-C(31)-C(32)	108.7(3)
Ru(1)-Ru(2)-S(2)	94.83(3)	C(31)-C(32)-C(33)	111.6(4)
Ru(1)-Ru(2)-C(24)	99.68(14)	Ru(1)-C(14)-C(15)	72.4(3)
Ru(1)-Ru(2)-C(25)	126.61(17)	Ru(1)-C(14)-C(18)	71.8(3)
Ru(1)-Ru(2)-C(26)	159.99(14)	C(15)-C(14)-C(18)	107.5(4)
Ru(1)-Ru(2)-C(27)	136.67(21)	Ru(1)-C(15)-C(14)	70.1(3)
Ru(1)-Ru(2)-C(28)	103.43(14)	Ru(1)-C(15)-C(16)	72.6(3)
Ru(3)-Ru(2)-S(1)	100.77(3)	C(14)-C(15)-C(16)	107.2(4)
Ru(3)-Ru(2)-S(2)	53.77(3)	Ru(1)-C(16)-C(15)	70.64(24)
Ru(3)-Ru(2)-C(24)	106.93(16)	Ru(1)-C(16)-C(17)	72.0(3)
Ru(3)-Ru(2)-C(25)	99.04(19)	C(15)-C(16)-C(17)	108.5(5)
Ru(3)-Ru(2)-C(26)	122.92(18)	Ru(1)-C(17)-C(16)	72.3(3)

Ru(3)-Ru(2)-C(27)	158.32(21)	Ru(1)-C(17)-C(18)	70.05(25)
Ru(3)-Ru(2)-C(28)	141.12(19)	C(16)-C(17)-C(18)	108.8(5)
S(1)-Ru(2)-S(2)	93.39(4)	Ru(1)-C(18)-C(14)	71.0(3)
S(1)-Ru(2)-C(24)	121.71(19)	Ru(1)-C(18)-C(17)	73.3(3)
S(1)-Ru(2)-C(25)	154.44(19)	C(14)-C(18)-C(17)	107.9(5)
S(1)-Ru(2)-C(26)	134.52(19)	Ru(2)-C(24)-C(25)	73.3(3)
S(1)-Ru(2)-C(27)	100.90(21)	Ru(2)-C(24)-C(28)	71.2(3)
S(1)-Ru(2)-C(28)	93.69(16)	C(25)-C(24)-C(28)	108.8(5)
S(2)-Ru(2)-C(24)	143.99(19)	Ru(2)-C(25)-C(24)	71.1(3)
S(2)-Ru(2)-C(25)	111.39(18)	Ru(2)-C(25)-C(26)	72.3(3)
S(2)-Ru(2)-C(26)	102.04(14)	C(24)-C(25)-C(26)	108.9(6)
S(2)-Ru(2)-C(27)	123.89(19)	Ru(2)-C(26)-C(25)	71.5(3)
S(2)-Ru(2)-C(28)	161.15(15)	Ru(2)-C(26)-C(27)	71.8(3)
C(24)-Ru(2)-C(25)	35.56(24)	C(25)-C(26)-C(27)	108.5(5)
C(24)-Ru(2)-C(26)	60.30(19)	Ru(2)-C(27)-C(26)	72.2(4)
C(24)-Ru(2)-C(27)	61.43(21)	Ru(2)-C(27)-C(28)	69.8(4)
C(24)-Ru(2)-C(28)	37.1(3)	C(26)-C(27)-C(28)	107.0(6)
C(25)-Ru(2)-C(26)	36.23(25)	Ru(2)-C(28)-C(24)	71.6(3)
C(25)-Ru(2)-C(27)	60.5(3)	Ru(2)-C(28)-C(27)	72.7(3)
C(25)-Ru(2)-C(28)	60.80(25)	C(24)-C(28)-C(27)	106.8(6)
C(26)-Ru(2)-C(27)	36.0(3)	Ru(3)-C(34)-C(35)	72.0(3)
C(26)-Ru(2)-C(28)	61.08(20)	Ru(3)-C(34)-C(38)	72.8(3)
C(27)-Ru(2)-C(28)	37.42(24)	C(35)-C(34)-C(38)	107.4(4)
Ru(1)-Ru(3)-Ru(2)	60.012(16)	Ru(3)-C(35)-C(34)	70.8(3)
Ru(1)-Ru(3)-S(2)	94.91(3)	Ru(3)-C(35)-C(36)	73.1(3)
Ru(1)-Ru(3)-S(3)	53.55(3)	C(34)-C(35)-C(36)	108.7(5)
Ru(1)-Ru(3)-C(34)	140.82(14)	Ru(3)-C(36)-C(35)	70.4(3)
Ru(1)-Ru(3)-C(35)	107.01(15)	Ru(3)-C(36)-C(37)	72.4(3)
Ru(1)-Ru(3)-C(36)	99.50(15)	C(35)-C(36)-C(37)	107.7(4)
Ru(1)-Ru(3)-C(37)	124.30(13)	Ru(3)-C(37)-C(36)	71.2(3)
Ru(1)-Ru(3)-C(38)	159.73(13)	Ru(3)-C(37)-C(38)	71.0(3)
Ru(2)-Ru(3)-S(2)	53.98(3)	C(36)-C(37)-C(38)	108.8(5)
Ru(2)-Ru(3)-S(3)	93.70(3)	Ru(3)-C(38)-C(34)	69.7(3)
Ru(2)-Ru(3)-C(34)	103.82(15)	Ru(3)-C(38)-C(37)	72.9(4)
Ru(2)-Ru(3)-C(35)	101.50(15)	C(34)-C(38)-C(37)	107.5(5)
S(4)-Ru(4)-S(6)	91.57(4)	Ru(4)-S(4)-C(41)	116.0(2)
S(4)-Ru(4)-C(44)	131.3(2)	Ru(5)-S(4)-C(41)	117.7(2)
S(4)-Ru(4)-C(45)	156.3(1)	S(4)-C(41)-C(42)	109.6(4)
S(4)-Ru(4)-C(46)	124.3(1)	S(4)-C(41)-H(1)	109 4(4)
S(4)-Ru(4)-C(47)	96.1(2)	S(4)-C(41)-H(2)	109.4(4)
S(4)-Ru(4)-C(48)	97.5(2)	C(42)-C(41)-H(1)	109.4(5)
S(6)-Ru(4)-C(44)	136.1(2)	C(42)-C(41)-H(2)	109.4(4)
S(6)-Ru(4)-C(45)	106.4(2)	H(1)-C(41)-H(2)	109.5(6)
S(6)-Ru(4)-C(46)	105.8(1)	C(41)-C(42)-C(43)	114.3(5)
S(6)-Ru(4)-C(47)	132.8(2)	Ru(5)-S(5)-Ru(6)	72.3(4)
S(6)-Ru(4)-C(48)	166.5(2)	Ru(5)-S(5)-C(51)	109.4(1)
C(44)-Ru(4)-C(45)	37.2(2)	Ru(6)-S(5)-C(51)	111.3(1)
C(44)-Ru(4)-C(46)	61.4(2)	S(5)-C(51)-C(52)	110.2(3)
C(44)-Ru(4)-C(47)	61.6(2)	C(51)-C(52)-C(53)	112.9(4)
C(44)-Ru(4)-C(48)	38.4(2)	Ru(4)-S(6)-Ru(6)	72.3(3)

C(45)-Ru(4)-C(46)	36.4(2)	Ru(4)-S(6)-C(61)	110.7(1)
C(45)-Ru(4)-C(47)	60.4(2)	Ru(6)-S(6)-C(61)	111.5(1)
C(45)-Ru(4)-C(48)	62.3(2)	S(6)-C(61)-C(62)	109.8(3)
C(46)-Ru(4)-C(47)	35.3(2)	C(61)-C(62)-C(63)	112.6(4)
C(46)-Ru(4)-C(48)	60.8(2)	Ru(4)-C(44)-C(45)	71.8(4)
C(47)-Ru(4)-C(48)	36.4(2)	Ru(4)-C(44)-C(48)	71.9(4)
S(4)-Ru(5)-S(5)	93.2(4)	C(45)-C(44)-C(48)	106.6(5)
S(4)-Ru(5)-C(54)	120.4(3)	Ru(4)-C(45)-C(44)	71.0(4)
S(4)-Ru(5)-C(55)	153.3(2)	Ru(4)-C(45)-C(46)	73.8(3)
S(4)-Ru(5)-C(56)	134.7(2)	C(44)-C(45)-C(46)	108.6(5)
S(4)-Ru(5)-C(57)	101.2(2)	Ru(4)-C(46)-C(45)	69.8(3)
S(4)-Ru(5)-C(58)	93.7(2)	Ru(4)-C(46)-C(47)	72.3(4)
S(5)-Ru(5)-C(54)	145.6(2)	C(45)-C(46)-C(47)	108.6(5)
S(5)-Ru(5)-C(55)	112.9(2)	Ru(4)-C(47)-C(46)	72.4(4)
S(5)-Ru(5)-C(56)	102.3(2)	Ru(4)-C(47)-C(48)	70.5(4)
S(5)-Ru(5)-C(57)	123.3(2)	C(46)-C(47)-C(48)	110.0(5)
S(5)-Ru(5)-C(58)	160.5(3)	Ru(4)-C(48)-C(44)	69.8(3)
C(54)-Ru(5)-C(55)	35.4(3)	Ru(4)-C(48)-C(47)	73.1(4)
C(54)-Ru(5)-C(56)	60.5(3)	C(44)-C(48)-C(47)	106.1(5)
C(54)-Ru(5)-C(57)	61.3(3)	Ru(5)-C(54)-C(55)	73.5(4)
C(54)-Ru(5)-C(58)	36.4(3)	Ru(5)-C(54)-C(58)	70.9(4)
C(55)-Ru(5)-C(56)	36.7(3)	C(55)-C(54)-C(58)	108.2(8)
C(55)-Ru(5)-C(57)	60.3(3)	Ru(5)-C(55)-C(54)	71.1(3)
C(55)-Ru(5)-C(58)	59.8(2)	Ru(5)-C(55)-C(56)	72.1(3)
C(56)-Ru(5)-C(57)	35.6(3)	C(54)-C(55)-C(56)	108.7(6)
C(56)-Ru(5)-C(58)	60.5(3)	Ru(5)-C(56)-C(55)	71.3(4)
C(57)-Ru(5)-C(58)	37.3(4)	Ru(5)-C(56)-C(57)	71.6(4)
S(5)-Ru(6)-S(6)	84.1(4)	C(55)-C(56)-C(57)	107.7(8)
S(5)-Ru(6)-C(64)	103.7(2)	Ru(5)-C(57)-C(56)	72.8(4)
S(5)-Ru(6)-C(65)	104.5(2)	Ru(5)-C(57)-C(58)	69.6(4)
S(5)-Ru(6)-C(66)	134.9(2)	C(56)-C(57)-C(58)	106.7(7)
S(5)-Ru(6)-C(67)	164.0(2)	Ru(5)-C(58)-C(54)	72.7(4)
S(5)-Ru(6)-C(68)	131.5(2)	Ru(5)-C(58)-C(57)	73.1(4)
S(6)-Ru(6)-C(64)	128.2(1)	C(54)-C(58)-C(57)	108.6(7)
S(6)-Ru(6)-C(65)	163.7(1)	Ru(6)-C(64)-C(65)	70.3(3)
S(6)-Ru(6)-C(66)	139.9(2)	Ru(6)-C(64)-C(68)	72.8(3)
S(6)-Ru(6)-C(67)	107.6(2)	C(65)-C(64)-C(68)	108.6(5)
S(6)-Ru(6)-C(68)	103.3(1)	Ru(6)-C(65)-C(64)	72.9(3)
C(64)-Ru(6)-C(65)	36.8(2)	Ru(6)-C(65)-C(66)	71.0(3)
C(64)-Ru(6)-C(66)	61.3(2)	C(64)-C(65)-C(66)	107.7(5)
C(64)-Ru(6)-C(67)	60.5(2)	Ru(6)-C(66)-C(65)	72.0(3)
C(64)-Ru(6)-C(68)	35.5(2)	Ru(6)-C(66)-C(67)	71.6(3)
C(65)-Ru(6)-C(66)	37.0(2)	C(65)-C(66)-C(67)	107.1(5)
C(65)-Ru(6)-C(67)	61.5(2)	Ru(6)-C(67)-C(66)	71.1(3)
C(65)-Ru(6)-C(68)	60.6(2)	Ru(6)-C(67)-C(68)	73.8(3)
C(66)-Ru(6)-C(67)	37.3(2)	C(66)-C(67)-C(68)	108.2(5)
C(66)-Ru(6)-C(68)	61.2(2)	Ru(6)-C(68)-C(64)	71.8(3)
C(67)-Ru(6)-C(68)	36.4(2)	Ru(6)-C(68)-C(67)	69.8(3)
Ru(4)-S(4)-Ru(5)	72.7(3)	C(64)-C(68)-C(67)	108.4(5)

Appendix II

Structural Analysis of $CpRu(PPh_3)(S_2CS(1\text{-}C_3H_7))$, **6d**.

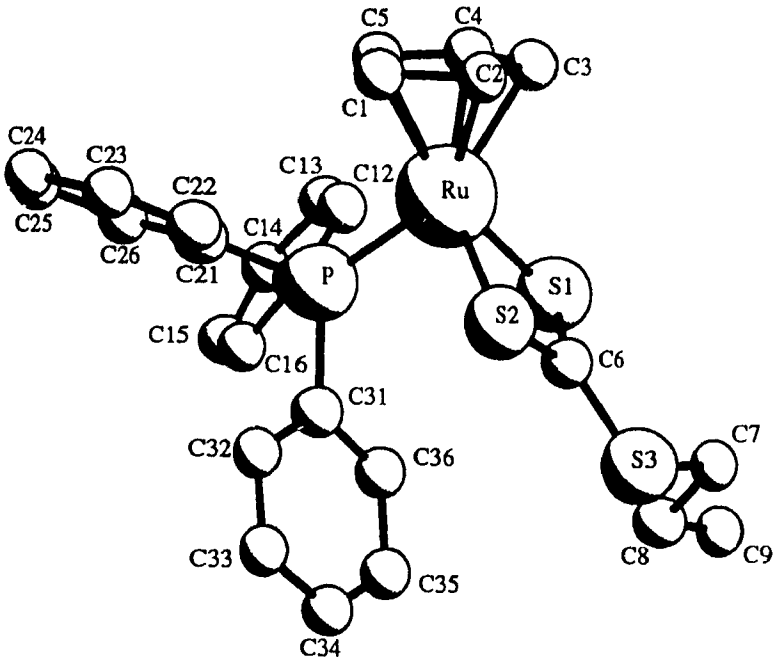

Table A2.1 Crystal data for $CpRu(PPh_3)(S_2CS(1\text{-}C_3H_7))$.

Space Group: Triclinic, $P\bar{1}$

Cell Dimensions:

a = 10.88(1)	b = 10.06(1)	c = 12.82(2)
α = 105.05(12)	β = 95.00(11)	γ = 101.17(9)

Volume = 1314.9 $Å^3$

Empirical formula : $C_{27}H_{27}PRuS_3$

Cell dimensions were obtained from 24.

Crystal dimensions: 0 .52 × 0.30 × 0.30 mm

FW = 579.65 Z = 2 F(000) = 592

D_{calc} = 1.446 Mg m^{-3}, μ = 8.86 mm^{-1}, λ = 0.70930 Å, (Mo Kα) $2\Theta_{(max)}$= 45°

The intensity data were collected on a Picker FACS-1 defractometer, using the Ω scan mode.

The h,k,l ranges are: 0 11, 0 11, 0 13

No. of reflections measured	3433
No. of unique reflection	3433
No. of reflections with Inet > 3.0 σ (Inet)	2715

No correction was made for absorption

Data set was solved by Patterson method

The last least squares cycle was calculated with 33 atoms, 307 parameters and 2715 out of 3433 reflections.

Weights based on counting-statistics were used.

For significant reflections, R = 0.065, Rw = 0.104, GoF = 1.75

where $R = \Sigma|Fo\text{-}Fc|/\Sigma|Fo|$,

$Rw = \sqrt{[\Sigma(w(Fo\text{-}Fc)^2)/\Sigma(wFo^2)]}$ and

$GoF = \sqrt{[\Sigma(w(Fo\text{-}Fc)^2)/(\text{No. of reflns - No. of params.})]}$

The last D-map, showed random noise.

Table A2.2 Atom coordinates, x,y,z and B_{iso} for $CpRu(PPh_3)(S_2CS(1\text{-}C_3H_7))$. E.S.Ds. refer to the last digit printed.

	x	y	z	B_{iso}
Ru	0.37437(6)	0.07406(7)	0.21193(6)	4.07(3)
P	0.22463(20)	0.03157(22)	0.31961(18)	3.77(10)
S1	0.28571(22)	-0.14735(24)	0.08165(20)	4.78(12)
S2	0.48064(22)	-0.0950(3)	0.25083(24)	5.66(14)
S3	0.4051(4)	-0.3907(4)	0.10910(4)	9.5(3)
C1	0.4726(11)	0.2937(10)	0.2897(9)	6.5(6)
C2	0.5435(10)	0.2279(11)	0.2058(11)	7.0(6)
C3	0.4699(11)	0.1867(11)	0.1062(10)	6.9(6)
C4	0.3543(11)	0.2236(11)	0.1200(10)	6.7(6)
C5	0.3557(10)	0.2877(10)	0.2280(9)	6.0(5)
C6	0.3882(9)	-0.2171(10)	0.1438(9)	5.5(9)
C7	0.3078(14)	-0.4704(14)	-0.0258(14)	10.7(16)
C8	0.1808(19)	-0.5256(18)	-0.0029(22)	17.7(23)
C9	0.118(3)	-0.597(4)	-0.099(3)	17.1(15)
C9′	0.101(2)	-0.655(3)	-0.0117(24)	7.1(15)
C11	0.0596(7)	0.0091(8)	0.2611(7)	4.0(4)
C12	0.0349(9)	0.0603(11)	0.1721(8)	5.4(5)
C13	-0.0892(11)	0.0515(14)	0.1286(9)	7.3(7)
C14	-0.1859(9)	-0.0056(12)	0.1745(9)	6.5(6)
C15	-0.1651(9)	-0.0568(11)	0.2615(9)	6.2(6)
C16	-0.0412(8)	-0.0495(10)	0.3046(8)	5.4(5)
C21	0.2434(8)	0.1775(9)	0.4465(7)	4.3(4)
C22	0.3643(10)	0.2261(10)	0.5086(9)	5.9(5)
C23	0.3848(12)	0.3352(11)	0.6042(10)	7.4(6)
C24	0.2862(13)	0.3942(11)	0.6397(9)	7.6(7)
C25	0.1701(12)	0.3487(10)	0.5778(10)	7.2(6)
C26	0.1475(9)	0.2373(9)	0.4814(8)	5.2(5)
C31	0.2139(8)	-0.1254(9)	0.3682(7)	4.4(4)
C32	0.2607(12)	-0.1175(12)	0.4756(10)	7.3(7)
C33	0.2603(15)	-0.2385(15)	0.5053(11)	9.0(9)
C34	0.2119(13)	-0.3686(13)	0.4331(12)	8.2(8)
C35	0.1639(12)	-0.3801(11)	0.3280(10)	6.9(6)
C36	0.1640(9)	-0.2563(10)	0.2950(8)	5.5(5)

B_{iso} is the Mean of the Principal Axes of the Thermal Ellipsoid

Table A2.3 Anisotropic thermal factors for $CpRu(PPh_3)(S_2CS(1\text{-}C_3H_7))$. U(i,j) values ×100. E.S.Ds. refer to the last digit printed.

	U11	U22	U33	U12	U13	U23
Ru	3.99(4)	5.21(4)	7.05(5)	1.06(3)	2.13(3)	2.64(4)
P	4.06(11)	5.15(12)	5.76(13)	1.29(10)	1.84(10)	2.10(10)
S1	5.56(14)	6.00(14)	7.12(15)	1.60(11)	2.21(11)	2.11(12)
S2	4.29(13)	8.40(17)	10.59(21)	2.60(12)	2.13(13)	4.58(15)
S3	15.40(4)	8.19(21)	16.30(4)	7.41(24)	7.40(3)	4.94(22)
C1	11.0(9)	5.6(6)	7.7(7)	-0.4(6)	3.6(6)	1.9(5)
C2	5.8(6)	7.0(7)	14.1(10)	0.0(5)	3.2(6)	4.3(7)
C3	8.9(8)	7.7(7)	11.0(9)	0.7(6)	5.5(7)	4.9(7)
C4	9.0(8)	7.3(7)	10.6(9)	0.9(6)	2.0(6)	5.8(6)
C5	9.2(8)	5.4(5)	10.4(8)	3.2(5)	4.7(6)	3.7(5)
C6	6.7(6)	6.8(6)	9.9(7)	3.1(5)	5.1(6)	4.3(5)
C7	11.2(11)	8.9(9)	19.0(16)	2.8(8)	8.3(11)	-1.3(10)
C8	15.8(15)	11.0(12)	36.2(29)	2.8(12)	11.2(18)	-2.7(16)
C9	10.9(20)	26.4(38)	16.1(26)	1.4(23)	0.1(18)	-11.6(25)
C9	6.9(18)	6.4(17)	11.3(23)	0.0(14)	2.6(16)	-0.6(15)
C11	4.2(5)	5.7(5)	5.9(5)	1.6(4)	2.1(4)	1.9(4)
C12	5.1(5)	9.0(7)	7.7(7)	2.6(5)	2.1(5)	3.5(5)
C13	7.4(8)	13.1(10)	8.4(8)	3.4(7)	-0.2(6)	4.8(7)
C14	4.5(6)	10.3(8)	9.6(8)	2.2(6)	1.6(5)	1.9(6)
C15	4.3(5)	9.1(7)	10.4(8)	1.5(5)	2.3(5)	2.7(6)
C16	4.4(5)	7.8(7)	8.4(7)	1.0(5)	2.2(5)	2.6(5)
C21	6.2(6)	5.1(5)	5.6(5)	1.1(4)	2.0(4)	2.0(4)
C22	6.7(7)	6.8(6)	8.7(7)	0.5(5)	1.8(5)	2.1(5)
C23	10.6(9)	6.6(7)	8.2(8)	-2.3(6)	-1.6(7)	1.7(6)
C24	13.8(11)	6.2(6)	8.0(8)	0.5(7)	4.3(7)	1.0(6)
C25	12.0(10)	6.0(6)	9.8(9)	1.5(6)	5.7(7)	2.3(6)
C26	7.3(6)	5.7(5)	7.2(6)	1.5(5)	3.0(5)	1.8(5)
C31	5.1(5)	6.3(5)	6.3(6)	1.8(4)	2.4(4)	2.8(4)
C32	9.9(9)	8.1(8)	10.0(9)	0.9(7)	0.7(7)	3.9(7)
C33	15.8(14)	11.4(10)	9.5(9)	4.7(10)	0.9(9)	6.5(8)
C34	11.3(10)	9.5(8)	14.5(12)	4.0(8)	4.9(9)	8.1(8)
C35	11.7(9)	5.9(6)	11.3(9)	3.2(6)	6.4(8)	4.5(6)
C36	6.6(6)	6.9(6)	7.8(7)	1.5(5)	2.7(5)	2.5(5)

Anisotropic Temperature Factors are of the form:

$$Temp = -2\pi^2(h^2a^{*2}U_{11} + k^2b^{*2}U_{22} + l^2c^{*2}U_{33} + 2hka^*b^*U_{12} + 2hla^*c^*U_{13} + 2klb^*c^*U_{23})$$

Table A2.4 Selected bond lenghts and angles for $CpRu(PPh_3)(S_2CS(1\text{-}C_3H_7))$.

Ru-P	2.2740(29)	C(8)-C(9)	1.3086(26)
Ru-S(1)	2.374(4)	C(8)-C(9')	1.3838(18)
Ru-S(2)	2.3617(24)	C(9)-C(9')	1.3999(21)
Ru-C(1)	2.184(4)	C(11)-C(12)	1.3941(21)
Ru-C(2)	2.1847(25)	C(11)-C(16)	1.3740(16)
Ru-C(3)	2.188(3)	C(12)-C(13)	1.3926(15)
Ru-C(4)	2.1682(27)	C(13)-C(14)	1.3538(16)
Ru-C(5)	2.1558(26)	C(14)-C(15)	1.3635(21)
P-C(11)	1.8328(21)	C(15)-C(16)	1.3919(15)
P-C(21)	1.851(3)	C(21)-C(22)	1.4037(20)
P-C(31)	1.8294(22)	C(21)-C(26)	1.3546(14)
S(1)-C(6)	1.6760(18)	C(22)-C(23)	1.3830(26)
S(2)-C(6)	1.676(3)	C(23)-C(24)	1.3794(14)
S(3)-C(6)	1.7370(22)	C(24)-C(25)	1.3597(20)
S(3)-C(7)	1.840(4)	C(25)-C(26)	1.4015(26)
C(1)-C(2)	1.4708(21)	C(31)-C(32)	1.4015(25)
C(1)-C(5)	1.4204(18)	C(31)-C(36)	1.3789(25)
C(2)-C(3)	1.3649(25)	C(32)-C(33)	1.3656(16)
C(3)-C(4)	1.3917(12)	C(33)-C(34)	1.3655(24)
C(4)-C(5)	1.3634(26)	C(34)-C(35)	1.3684(25)
C(7)-C(8)	1.4697(15)	C(35)-C(36)	1.4156(17)

P-Ru-S(1)	90.76(12)	Ru-C(3)-C(2)	71.68(12)
P-Ru-S(2)	93.35(9)	Ru-C(3)-C(4)	70.60(8)
P-Ru-C(1)	103.88(11)	C(2)-C(3)-C(4)	108.37(11)
P-Ru-C(2)	142.16(8)	Ru-C(4)-C(3)	72.14(9)
P-Ru-C(3)	154.17(4)	Ru-C(4)-C(5)	71.13(12)
P-Ru-C(4)	117.38(8)	C(3)-C(4)-C(5)	108.76(11)
P-Ru-C(5)	93.92(10)	Ru-C(5)-C(1)	71.99(11)
S(1)-Ru-S(2)	71.47(11)	Ru-C(5)-C(4)	72.11(12)
S(1)-Ru-C(1)	163.36(4)	C(1)-C(5)-C(4)	110.72(12)
S(1)-Ru-C(2)	127.01(10)	S(1)-C(6)-S(2)	111.21(11)
S(1)-Ru-C(3)	99.52(13)	S(1)-C(6)-S(3)	127.92(10)
S(1)-Ru-C(4)	102.88(12)	S(2)-C(6)-S(3)	120.87(10)
S(1)-Ru-C(5)	134.41(8)	S(3)-C(7)-C(8)	105.07(12)
S(2)-Ru-C(1)	114.74(10)	C(7)-C(8)-C(9)	103.78(13)
S(2)-Ru-C(2)	96.55(9)	C(7)-C(8)-C(9')	138.92(6)
S(2)-Ru-C(3)	112.35(8)	C(9)-C(8)-C(9')	62.58(12)
S(2)-Ru-C(4)	149.08(5)	C(8)-C(9)-C(9')	61.34(11)
S(2)-Ru-C(5)	152.92(5)	C(8)-C(9')-C(9)	55.08(11)
C(1)-Ru-C(2)	39.34(7)	P-C(11)-C(12)	118.67(9)
C(1)-Ru-C(3)	63.90(11)	P-C(11)-C(16)	122.82(9)
C(1)-Ru-C(4)	63.50(11)	C(12)-C(11)-C(16)	118.41(9)
C(1)-Ru-C(5)	38.20(6)	C(11)-C(12)-C(13)	120.44(9)
C(2)-Ru-C(3)	36.38(7)	C(12)-C(13)-C(14)	119.36(9)
C(2)-Ru-C(4)	61.80(9)	C(13)-C(14)-C(15)	121.66(9)
C(2)-Ru-C(5)	62.76(8)	C(14)-C(15)-C(16)	119.19(9)
C(3)-Ru-C(4)	37.26(6)	C(11)-C(16)-C(15)	120.92(9)
C(3)-Ru-C(5)	62.07(9)	P-C(21)-C(22)	116.94(11)
C(4)-Ru-C(5)	36.76(8)	P-C(21)-C(26)	123.58(10)
Ru-P-C(11)	116.73(10)	C(22)-C(21)-C(26)	119.47(10)
Ru-P-C(21)	112.71(12)	C(21)-C(22)-C(23)	119.89(11)

Ru-P-C(31)	118.00(8)	C(22)-C(23)-C(24)	120.16(10)
C(11)-P-C(21)	102.75(12)	C(23)-C(24)-C(25)	119.59(10)
C(11)-P-C(31)	100.96(9)	C(24)-C(25)-C(26)	120.80(11)
C(21)-P-C(31)	103.65(13)	C(21)-C(26)-C(25)	120.00(10)
Ru-S(1)-C(6)	88.45(12)	P-C(31)-C(32)	122.24(11)
Ru-S(2)-C(6)	88.86(11)	P-C(31)-C(36)	118.67(11)
C(6)-S(3)-C(7)	103.65(12)	C(32)-C(31)-C(36)	119.01(12)
Ru-C(1)-C(2)	70.34(11)	C(31)-C(32)-C(33)	119.97(11)
Ru-C(1)-C(5)	69.81(11)	C(32)-C(33)-C(34)	121.38(11)
C(2)-C(1)-C(5)	102.84(12)	C(33)-C(34)-C(35)	120.18(12)
Ru-C(2)-C(1)	70.32(11)	C(34)-C(35)-C(36)	119.52(11)
Ru-C(2)-C(3)	71.94(12)	C(31)-C(36)-C(35)	119.91(11)
C(1)-C(2)-C(3)	109.29(11)		

Appendix III

Structural Analysis of $CpRu(SO_2)(PPh_3)S(SO_2)(4\text{-}C_6H_4Me)$, **8b**.

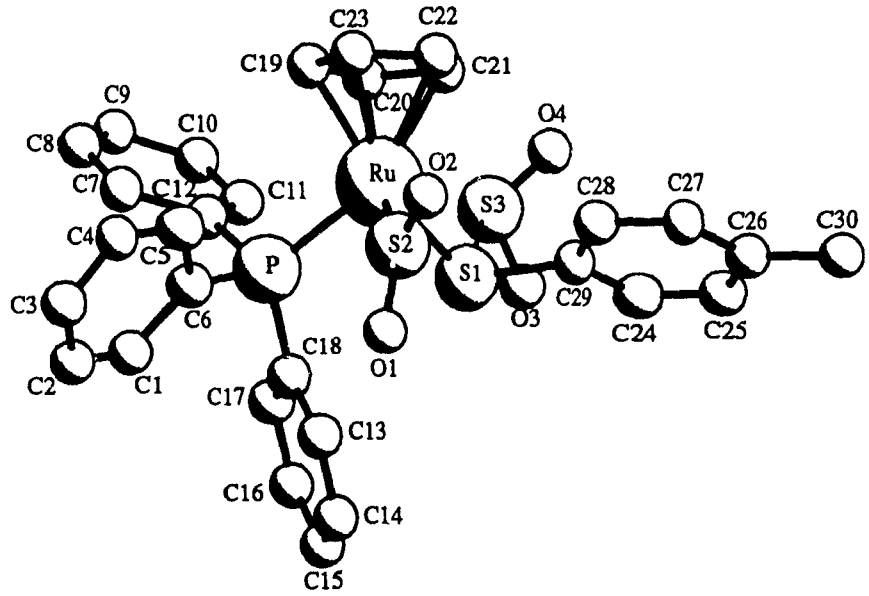

Table A3.1 Crystal data for $CpRu(PPh_3)(SO_2)S(SO_2)(4\text{-}C_6H_4Me)$.

Space Group: Monoclinic, P $2_1/c$
Cell Dimensions:
a = 9.9540(20) b = 18.423(5) c = 16.111(4)
β = 95.130(20)
Volume = 2942.6(12) $Å^3$

Empirical formula: $C_{30}H_{27}O_4PRuS_3$

Cell dimensions were obtained from 15 reflections with 2Θ angle in the range 45.00 - 65.00°.

Crystal dimensions: 0.07 × 0.28 × 0.36 mm

FW = 676.73 Z = 4 F(000) = 1383.87

D_{calc} = 1.528 Mg m^{-3}, μ = 7.18 mm^{-1}, λ = 1.54056 Å, $2\Theta_{(max)}$= 120.0

The intensity data were collected on a Nicolet Auto diffractometer, using the $\Theta/2\Theta$ scan mode.
The h,k,l ranges are: -11 11, 0 20, 0 18

No. of reflections measured	4387
No. of unique reflections	4387
No. of reflections with Inet > 3.0 σ (Inet)	3615

A psi correction was made for absorption.

Data set was solved by Patterson method
The last least squares cycle was calculated with 63 atoms, 348 parameters and 3615 out of 4387 reflections.
Weights based on counting-statistics were used.

For significant reflections, R = 0.062, Rw = 0.057
GoF = 7.01
For all reflections, R = 0.071, Rw = 0.058
where $R = \Sigma|Fo-Fc|/\Sigma|Fo|$
$Rw = \sqrt{[\Sigma(w(Fo-Fc)^2)/\Sigma(wFo^2)]}$
$GoF = \sqrt{[\Sigma(w(Fo-Fc)^2)/(\text{No. of reflns - No. of params.})]}$

The maximum shift/σ ratio was 0.481.

In the last D-map, the deepest hole was -1.110 $e^-/Å^3$, and the highest peak 1.870 $e^-/Å^3$ and is lacated near the metal.

Secondary ext. coeff. = 0.89(6)

Table A3.2 Atom coordinates x,y,z and B_{iso} for $CpRu(PPh_3)(SO_2)S(SO_2)(4\text{-}C_6H_4Me)$. E.S.Ds. refer to the last digit printed.

	x	y	z	B_{iso}
Ru	0.06569(7)	0.35464(4)	0.63700(5)	2.57(3)
S1	0.11166(25)	0.22874(14)	0.62128(17)	3.32(12)
S2	0.0982(3)	0.38191(15)	0.51244(17)	3.34(12)
S3	0.0482(5)	0.15372(23)	0.76701(24)	7.15(23)
P	0.29254(24)	0.37175(14)	0.68744(16)	2.72(11)
O1	0.2128(7)	0.3705(5)	0.4692(4)	6.7(5)
O2	-0.0077(8)	0.4202(4)	0.4603(5)	5.5(4)
O3	0.1218(15)	0.0903(7)	0.7496(8)	14.4(11)
O4	-0.0832(12)	0.1437(10)	0.7543(9)	19.7(13)
C1	0.5067(10)	0.4628(6)	0.6529(7)	4.4(6)
C2	0.5616(12)	0.5262(7)	0.6286(9)	5.8(7)
C3	0.4816(12)	0.5843(6)	0.6044(7)	4.7(6)
C4	0.3461(12)	0.5770(6)	0.6023(7)	5.0(6)
C5	0.2885(10)	0.5134(6)	0.6247(7)	3.9(5)
C6	0.3673(9)	0.4551(5)	0.6502(6)	2.9(4)
C7	0.3470(10)	0.4489(6)	0.8371(7)	3.9(5)
C8	0.3490(12)	0.4568(8)	0.9235(8)	5.8(8)
C9	0.3157(14)	0.4011(10)	0.9730(8)	6.2(9)
C10	0.2771(12)	0.3365(8)	0.9367(8)	5.7(8)
C11	0.2717(10)	0.3270(6)	0.8508(7)	4.1(6)
C12	0.3049(9)	0.3839(6)	0.7998(6)	3.2(5)
C13	0.4461(10)	0.2914(7)	0.5855(7)	4.5(6)
C14	0.5378(13)	0.2412(8)	0.5655(8)	6.2(7)
C15	0.6041(12)	0.1958(7)	0.6290(10)	5.4(7)
C16	0.5736(13)	0.2067(7)	0.7088(9)	6.7(8)
C17	0.4835(13)	0.2600(7)	0.7304(7)	5.4(6)
C18	0.4147(9)	0.3008(5)	0.6670(7)	3.2(5)
C19	-0.0052(10)	0.4257(7)	0.7326(7)	4.5(6)
C20	-0.0277(10)	0.3548(7)	0.7543(7)	3.9(6)
C21	-0.1217(11)	0.3255(7)	0.6952(7)	4.5(6)
C22	-0.1546(10)	0.3824(8)	0.6315(8)	5.5(7)
C23	-0.0803(11)	0.4425(6)	0.6572(8)	4.5(6)
C24	-0.0207(11)	0.1137(6)	0.5488(8)	4.2(6)
C25	-0.1098(13)	0.0773(6)	0.4928(8)	5.0(7)
C26	-0.1979(12)	0.1161(7)	0.4343(8)	4.5(6)
C27	-0.1913(10)	0.1908(7)	0.4375(7)	4.2(6)
C28	-0.1041(11)	0.2282(6)	0.4941(7)	3.8(5)
C29	-0.0147(10)	0.1872(6)	0.5509(6)	3.2(5)
C30	-0.2966(12)	0.0767(7)	0.3663(7)	5.3(3)

B_{iso} is the Mean of the Principal Axes of the Thermal Ellipsoid.

Table A3.3 Anisotropic thermal factors for $CpRu(PPh_3)(SO_2)S(SO_2)(4\text{-}C_6H_4Me)$. U(i,j) values ×100. E.S.Ds. refer to the last digit printed.

	U11	U22	U33	U12	U13	U23
Ru	2.56(4)	3.42(4)	3.70(5)	0.09(4)	-0.08(3)	0.15(5)
S1	3.49(15)	3.59(16)	5.34(18)	0.22(12)	-0.59(12)	-0.16(13)
S2	3.49(15)	4.86(18)	4.22(17)	-0.58(13)	-0.20(12)	0.89(14)
S3	13.0(4)	6.2(3)	7.6(3)	0.1 (3)	-1.07(25)	-2.03(22)
P	2.79(13)	4.14(18)	3.35(15)	0.10(12)	-0.13(11)	0.34(13)
O1	6.0(5)	15.8(10)	3.8(5)	1.2 (6)	1.2(4)	2.8(6)
O2	6.8(5)	7.1(6)	6.5(6)	2.3 (5)	-1.0(4)	2.9(5)
O3	26.7(18)	9.7(10)	17.7(14)	-6.2 (11)	-1.5(11)	-3.9(9)
O4	8.8(9)	39.8(25)	26.7(17)	-1.7 (13)	2.7(10)	-24.5(18)
C1	3.6(6)	4.6(8)	8.4(10)	0.4 (6)	-0.2(6)	1.4(7)
C2	3.9(7)	7.4(10)	10.6(12)	-2.2 (7)	0.4(7)	1.3(9)
C3	6.4(8)	4.2(8)	7.3(9)	-1.4 (7)	0.7(7)	1.1(7)
C4	6.0(8)	4.9(8)	7.7(10)	-0.4 (7)	-1.3(7)	2.2(7)
C5	4.3(7)	3.8(7)	6.3(8)	0.2 (5)	-1.3(6)	1.2(6)
C6	3.0(6)	3.9(6)	4.1(6)	-0.6 (5)	0.7(5)	0.5(5)
C7	4.5(7)	5.2(8)	4.8(7)	0.3 (6)	0.0(6)	-0.6(6)
C8	6.5(9)	10.1(12)	5.4(9)	1.3(8)	0.0(7)	-2.1(9)
C9	7.1(10)	12.0(14)	4.4 (9)	1.4(10)	-0.1(7)	-0.9(9)
C10	5.6(8)	11.2(13)	5.2 (9)	2.1(8)	1.6(7)	2.6(9)
C11	4.5(7)	6.3(8)	4.9 (7)	0.0(6)	0.2(6)	1.7(6)
C12	2.5(5)	6.5(8)	2.9 (6)	0.7(5)	-0.6(4)	0.1(6)
C13	4.2(7)	7.9(9)	5.0(8)	2.3(6)	0.0(6)	-1.1(7)
C14	5.0(8)	11.7(13)	6.7(10)	1.8(8)	-0.3(7)	-4.0(9)
C15	4.3(8)	4.9(8)	11.4(13)	0.2(6)	1.2(8)	-2.0(9)
C16	6.6(9)	7.4(10)	11.4(13)	3.5(8)	1.4(9)	4.1(10)
C17	6.3(8)	7.8(10)	6.7(9)	2.9(7)	1.8(7)	3.4(7)
C18	2.2(5)	2.9(6)	7.1(8)	0.0(4)	-0.5(5)	-0.2(6)
C19	3.1(6)	8.2(10)	5.7(9)	1.5(7)	-0.5(6)	-2.7(8)
C20	3.6(6)	4.4(7)	7.0(8)	0.1(6)	0.4(5)	0.8(7)
C21	5.0(7)	6.3(9)	6.2(9)	-0.4(6)	2.7(6)	0.5(7)
C22	1.7(6)	9.1(11)	9.9(11)	1.7(6)	-0.2(6)	-1.6(9)
C23	3.8(7)	3.9(7)	9.5(11)	1.4(6)	1.1(6)	-0.7(7)
C24	4.9(8)	4.1(7)	6.7(9)	-0.1(6)	-1.4(6)	-0.6(7)
C25	6.3(9)	4.2(8)	8.5(11)	-1.1(7)	0.7(7)	-0.2(7)
C26	5.2(8)	6.4(9)	5.8(9)	-1.8(7)	2.0(6)	-1.3(7)
C27	3.5(7)	7.4(10)	5.0(8)	-0.6(6)	-0.4(5)	0.2(7)
C28	4.3(7)	4.6(7)	5.7(8)	-0.8(6)	0.6(6)	-0.6(6)
C29	3.0(6)	5.4(8)	3.8(7)	-0.7(5)	0.4(5)	-0.6(6)
C30	6.8(4)					

Anisotropic Temperature Factors are of the form:

$$Temp = -2\pi^2(h^2a^{*2}U_{11} + k^2b^{*2}U_{22} + l^2c^{*2}U_{33} + 2hka^*b^*U_{12} + 2hla^*c^*U_{13} + 2klb^*c^*U_{23})$$

Table A3.4 Selected bond lengths and angles for $CpRu(PPh_3)(SO_2)S(SO_2)(4\text{-}C_6H_4Me)$.

Ru-S(1)	2.382(3)	C(7)-C(12)	1.389(16)
Ru-S(2)	2.121(3)	C(8)-C(9)	1.358(23)
Ru-P	2.3517(25)	C(9)-C(10)	1.366(23)
Ru-C(19)	2.186(11)	C(10)-C(11)	1.391(17)
Ru-C(20)	2.180(11)	C(11)-C(12)	1.389(15)
Ru-C(21)	2.227(10)	C(13)-C(14)	1.360(17)
Ru-C(22)	2.245(10)	C(13)-C(18)	1.387(16)
Ru-C(23)	2.219(10)	C(14)-C(15)	1.434(21)
S(1)-S(3)	2.844(5)	C(15)-C(16)	1.362(22)
S(1)-C(29)	1.788(10)	C(16)-C(17)	1.394(18)
S(2)-O(1)	1.405(8)	C(17)-C(18)	1.396(15)
S(2)-O(2)	1.469(7)	C(19)-C(20)	1.375(19)
S(3)-O(3)	1.420(14)	C(19)-C(23)	1.404(17)
S(3)-O(4)	1.319(13)	C(20)-C(21)	1.384(17)
P-C(6)	1.830(10)	C(21)-C(22)	1.483(19)
P-C(12)	1.817(10)	C(22)-C(23)	1.374(18)
P-C(18)	1.835(10)	C(24)-C(25)	1.380(17)
C(1)-C(2)	1.362(17)	C(24)-C(29)	1.355(16)
C(1)-C(6)	1.392(14)	C(25)-C(26)	1.422(19)
C(2)-C(3)	1.369(18)	C(26)-C(27)	1.379(18)
C(3)-C(4)	1.353(17)	C(26)-C(30)	1.581(17)
C(4)-C(5)	1.367(16)	C(27)-C(28)	1.384(16)
C(5)-C(6)	1.372(14)	C(28)-C(29)	1.434(16)
C(7)-C(8)	1.397(17)		

S(1)-Ru-S(2)	94.76(11)	C(3)-C(4)-C(5)	121.3(10)
S(1)-Ru-P	88.83(9)	C(4)-C(5)-C(6)	120.5(10)
S(1)-Ru-C(19)	137.3(4)	P-C(6)-C(1)	120.5(8)
S(1)-Ru-C(20)	101.2(3)	P-C(6)-C(5)	121.1(7)
S(1)-Ru-C(21)	89.2(3)	C(1)-C(6)-C(5)	118.2(9)
S(1)-Ru-C(22)	114.4(4)	C(8)-C(7)-C(12)	119.8(11)
S(1)-Ru-C(23)	149.4(3)	C(7)-C(8)-C(9)	121.7(13)
S(2)-Ru-P	94.14(10)	C(8)-C(9)-C(10)	118.6(12)
S(2)-Ru-C(19)	127.7(4)	C(9)-C(10)-C(11)	121.4(12)
S(2)-Ru-C(20)	158.9(3)	C(10)-C(11)-C(12)	120.2(11)
S(2)-Ru-C(21)	131.3(3)	P-C(12)-C(7)	121.9(8)
S(2)-Ru-C(22)	98.1(4)	P-C(12)-C(11)	119.9(8)
S(2)-Ru-C(23)	97.1(3)	C(7)-C(12)-C(11)	118.2(9)
P-Ru-C(19)	92.1(3)	C(14)-C(13)-C(18)	121.4(11)
P-Ru-C(20)	99.8(3)	C(13)-C(14)-C(15)	120.2(11)
P-Ru-C(21)	134.5(3)	C(14)-C(15)-C(16)	117.4(11)
P-Ru-C(22)	152.5(3)	C(15)-C(16)-C(17)	122.7(11)
P-Ru-C(23)	118.2(3)	C(16)-C(17)-C(18)	118.8(11)
C(19)-Ru-C(20)	36.7(5)	P-C(18)-C(13)	117.8(8)
C(19)-Ru-C(21)	60.8(5)	P-C(18)-C(17)	122.8(9)
C(19)-Ru-C(22)	61.0(4)	C(13)-C(18)-C(17)	119.2(10)
C(19)-Ru-C(23)	37.2(5)	Ru-C(19)-C(20)	71.4(7)
C(20)-Ru-C(21)	36.6(4)	Ru-C(19)-C(23)	72.7(6)
C(20)-Ru-C(22)	62.8(4)	C(20)-C(19)-C(23)	110.1(10)
C(20)-Ru-C(23)	62.4(4)	Ru-C(20)-C(19)	71.9(6)
C(21)-Ru-C(22)	38.7(5)	Ru-C(20)-C(21)	73.6(6)
C(21)-Ru-C(23)	62.0(4)	C(19)-C(20)-C(21)	108.1(10)

C(22)-Ru-C(23)	35.8(5)	Ru-C(21)-C(20)	69.9(6)
Ru-S(1)-S(3)	109.05(13)	Ru-C(21)-C(22)	71.3(6)
Ru-S(1)-C(29)	110.7(4)	C(20)-C(21)-C(22)	107.1(10)
S(3)-S(1)-C(29)	96.9(4)	Ru-C(22)-C(21)	70.0(6)
Ru-S(2)-O(1)	129.3(3)	Ru-C(22)-C(23)	71.0(6)
Ru-S(2)-O(2)	119.5(3)	C(21)-C(22)-C(23)	106.4(10)
O(1)-S(2)-O(2)	111.2(5)	Ru-C(23)-C(19)	70.2(6)
S(1)-S(3)-O(3)	94.6(6)	Ru-C(23)-C(22)	73.1(6)
S(1)-S(3)-O(4)	103.3(9)	C(19)-C(23)-C(22)	108 2(11)
O(3)-S(3)-O(4)	112.1(9)	C(25)-C(24)-C(29)	121.8(11)
Ru-P-C(6)	113.9(3)	C(24)-C(25)-C(26)	120.7(11)
Ru-P-C(12)	109.8(3)	C(25)-C(26)-C(27)	116.9(10)
Ru-P-C(18)	118.3(3)	C(25)-C(26)-C(30)	122.5(11)
C(6)-P-C(12)	103.3(5)	C(27)-C(26)-C(30)	120.6(11)
C(6)-P-C(18)	104.1(4)	C(26)-C(27)-C(28)	123.1(11)
C(12)-P-C(18)	106.2(5)	C(27)-C(28)-C(29)	118.4(10)
C(2)-C(1)-C(6)	120.1(10)	S(1)-C(29)-C(24)	118.1(8)
C(1)-C(2)-C(3)	121.0(11)	S(1)-C(29)-C(28)	122.7(8)
C(2)-C(3)-C(4)	118.9(10)	C(24)-C(29)-C(28)	119.1(9)

Appendix IV

Structural Analysis of $CpRu(PPh_3)(CO)SS(CHMe_2)$, **10d**.

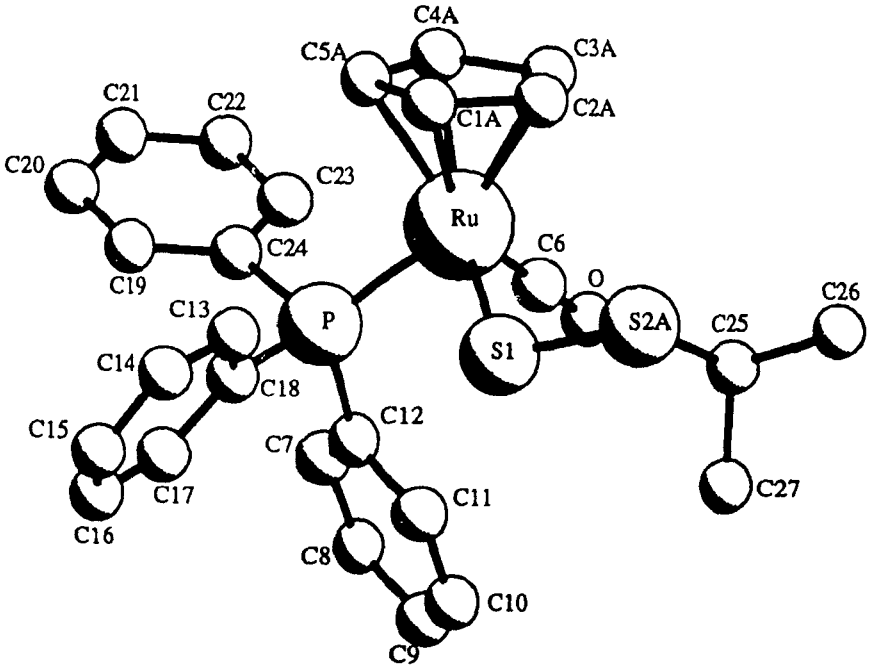

Table A4.1 Crystal data for $CpRu(PPh_3)(CO)SS(CHMe_2)$.

Space Group: Monoclinic, $P\ 2_1/n$
Cell Dimensions:
a = 9.2740(20) b = 11.345(3) c = 25.303(6)
β = 97.370(20)
Volume = 2640.2(11) $Å^3$

Empirical formula : $C_{27}H_{27}PORuS_2$

Cell dimensions were obtained from 15 reflections with 2Θ angle in the range 25.00 - 40.00 degrees.

Crystal dimensions: 0 .45 × 0.55 × 0.70 mm

FW = 556.61 Z = 4 F(000) = 1151.88

D_{calc} = 1.400 $Mg.m^{-3}$, μ = 0.81 mm-1, λ = 0.70930 Å, $2\Theta_{(max)}$= 50.6

The intensity data were collected on a Nicolet Auto defractometer, using the Ω scan mode.
The h,k,l ranges are: -11 11, 0 13, 0 30

No. of reflections measured	5336
No. of unique reflections	4839
No. of reflections with Inet > 3.0 σ (Inet)	2890

A psi-scan correction was made for absorption

Data set was solved by Patterson method
The last least squares cycle was calculated with 63 atoms, 314 parameters and 2890 out of 4839 reflections.
Weights based on counting-statistics were used.
The weight modifier K in KFo^2 is 0.0001

For significant reflections, R = 0.055, Rw = 0.058, GoF = 2.54
For all reflections, R = 0.095, Rw = 0.062
where $R = \Sigma|Fo-Fc|/\Sigma|Fo|$,
$Rw = \sqrt{[\Sigma(w(Fo-Fc)^2)/\Sigma(wFo^2)]}$
$GoF = \sqrt{[\Sigma(w(Fo-Fc)^2)/(\text{No. of reflns - No. of params.})]}$

The maximum shift/σ ratio was 6.721.

In the last D-map, the deepest hole was -0.750 $e^-/Å^3$, and the highest peak 0.850 $e^-/Å^3$.

Secondary ext. coeff. = 0.06(3)

Table A4.2 Atom coordinates, x,y,z and B_{iso} for $CpRu(PPh_3)(CO)SS(CHMe_2)$. E.S.Ds. refer to the last digit printed.

	x	y	z	B_{iso}
Ru	0.69081(9)	0.59551(7)	0.63562(3)	3.96(3)
S1	0.9443(3)	0.6049(3)	0.62645(10)	5.25(13)
S2A	1.0588(4)	0.4974(3)	0.68115(14)	7.28(19)
P	0.65251(24)	0.75434(20)	0.57945(9)	3.15(10)
O	0.7096(9)	0.7580(7)	0.7284(3)	7.8(5)
C1A	0.530(4)	0.4751(23)	0.5882(11)	4.8(5)
C2A	0.676(4)	0.412(3)	0.5980(14)	8.2(7)
C3A	0.707(3)	0.4034(25)	0.6587(12)	6.5(6)
C4A	0.597(4)	0.452(3)	0.6834(13)	7.0(7)
C5A	0.476(3)	0.4985(21)	0.6401(15)	4.8(5)
C6	0.7070(11)	0.6954(8)	0.6925(4)	4.6(5)
C7	0.6240(11)	0.9899(9)	0.6134(4)	5.0(5)
C8	0.6782(14)	1.0926(9)	0.6396(5)	6.5(6)
C9	0.8260(13)	1.1020(10)	0.6592(4)	7.9(6)
C10	0.9118(12)	1.0107(10)	0.6526(4)	7.1(6)
C11	0.8604(10)	0.9081(9)	0.6287(4)	5.3(5)
C12	0.7135(8)	0.8963(8)	0.6080(3)	3.1(4)
C13	0.7818(10)	0.6472(9)	0.4982(4)	4.5(5)
C14	0.8416(12)	0.6446(11)	0.4495(5)	6.1(6)
C15	0.8490(12)	0.7459(14)	0.4208(4)	6.6(7)
C16	0.8020(12)	0.8508(12)	0.4391(4)	6.2(6)
C17	0.7429(10)	0.8538(9)	0.4873(4)	4.7(5)
C18	0.7325(8)	0.7527(8)	0.5167(3)	3.4(4)
C19	0.3970(10)	0.7962(9)	0.5062(4)	4.7(5)
C20	0.2444(11)	0.8123(11)	0.4941(5)	5.9(6)
C21	0.1570(11)	0.8133(11)	0.5352(5)	6.5(7)
C22	0.2190(11)	0.7977(12)	0.5867(4)	6.8(7)
C23	0.3690(10)	0.7801(9)	0.5998(4)	5.2(5)
C24	0.4590(9)	0.7794(8)	0.5588(3)	3.8(4)
C25	1.0684(14)	0.5749(14)	0.7447(4)	8.7(9)
C26	1.1515(16)	0.4931(18)	0.7864(5)	13.2(12)
C27	1.1479(24)	0.6959(18)	0.7443(7)	15.3(15)
S2B	1.077(4)	0.667(4)	0.7026(17)	8.7(10)
C1B	0.482(3)	0.4985(22)	0.6102(15)	5.2(6)
C2B	0.523(4)	0.4752(24)	0.6654(14)	6.2(6)
C3B	0.641(4)	0.423(3)	0.6664(11)	5.2(6)
C4B	0.692(3)	0.412(3)	0.6211(15)	5.6(8)
C5B	0.595(4)	0.4492(23)	0.5832(10)	5.0(6)

B_{iso} is the Mean of the Principal Axes of the Thermal Ellipsoid

Table A4.3 Anisotropic thermal factors for $CpRu(PPh_3)(CO)SS(CHMe_2)$. U(i,j) values ×100. E.S.Ds. refer to the last digit printed.

	U11	U22	U33	U12	U13	U23
Ru	5.51(5)	4.51(4)	4.84(4)	-0.54(5)	-0.07(3)	0.31(5)
S	15.66(16)	8.05(18)	6.14(16)	1.54(15)	0.33(12)	0.70(16)
S2A	8.3(3)	11.2(3)	7.8(3)	3.89(22)	-0.40(19)	1.32(22)
P	3.53(13)	4.54(13)	3.84(13)	-0.07(11)	0.28(10)	-0.24(11)
O	14.9(8)	9.3(6)	5.4(5)	-0.1(5)	1.2(5)	-1.4(4)
C1A	6.1(6)					
C2A	10.4(8)					
C3A	8.3(8)					
C4A	8.9(9)					
C5A	6.1(6)					
C6	6.8(7)	5.1(6)	5.9(7)	0.8(5)	1.3(6)	0.9(5)
C7	5.8(7)	5.4(6)	7.9(8)	0.1(5)	1.5(6)	-0.2(6)
C8	10.9(10)	4.6(5)	10.0(9)	1.7(8)	4.5(7)	-0.9(8)
C9	9.0(8)	7.2(7)	6.3(7)	-2.2(8)	1.1(6)	-2.1(7)
C10	6.9(8)	5.9(7)	9.5(9)	-1.1(6)	-2.0(6)	-1.2(6)
C11	5.1(6)	5.2(5)	9.3(8)	0.6(6)	-0.9(5)	-0.1(7)
C12	4.2(5)	4.6(5)	3.2(4)	0.6(5)	0.9(4)	0.3(4)
C13	4.8(6)	7.0(7)	5.0(6)	0.3(5)	-0.3(5)	-1.3(5)
C14	5.9(7)	11.2(10)	6.0(8)	1.4(7)	0.3(6)	-3.2(7)
C15	6.5(7)	13.4(12)	5.3(7)	0.2(8)	1.1(6)	-0.2(8)
C16	6.9(8)	11.5(10)	5.3(7)	0.0(7)	1.3(6)	1.1(7)
C17	4.8(6)	7.8(7)	5.4(7)	0.3(5)	0.4(5)	0.1(6)
C18	2.8(4)	6.4(6)	3.7(5)	-0.3(4)	-0.2(4)	-0.6(5)
C19	4.6(6)	8.0(7)	5.2(6)	-0.2(5)	0.6(5)	-0.8(5)
C20	4.7(6)	10.7(9)	6.4(8)	-0.2(6)	-1.0(6)	-0.6(7)
C21	3.9(7)	12.8(10)	7.8(9)	0.3(7)	-0.5(6)	-0.6(8)
C22	3.8(6)	15.1(12)	7.4(8)	0.1(7)	2.1(6)	0.5(8)
C23	4.6(6)	10.3(9)	5.2(7)	-0.6(6)	1.0(5)	0.7(6)
C24	4.2(5)	5.9(6)	4.3(5)	0.0(4)	0.0(4)	0.6(5)
C25	9.9(10)	17.4(15)	5.3(8)	3.1(10)	-0.7(7)	0.3(9)
C26	12.2(13)	28.2(21)	9.2(11)	4.1(13)	-1.6(9)	8.1(13)
C27	26.8(25)	18.2(19)	11.8(14)	-6.8(18)	-2.4(15)	-3.6(14)
S2B	11.0(12)					
C1B	6.5(7)					
C2B	7.8(8)					
C3B	6.5(7)					
C4B	7.1(10)					
C5B	6.3(8)					

Anisotropic Temperature Factors are of the form:

$$Temp = -2\pi^2(h^2a^{*2}U_{11} + k^2b^{*2}U_{22} + l^2c^{*2}U_{33} + 2hka^*b^*U_{12} + 2hla^*c^*U_{13} + 2klb^*c^*U_{23})$$

Table A4.4 Selected bond lengths and angles for $CpRu(PPh_3)(CO)SS(CHMe_2)$.

Ru-S(1)	2.395(3)	C(9)-C(10)	1.330(18)
Ru-P	2.2942(24)	C(10)-C(11)	1.369(15)
Ru-C(1A)	2.249(23)	C(11)-C(12)	1.402(12)
Ru-C(6)	1.824(11)	C(13)-C(14)	1.414(15)
S(1)-S(2A)	2.038(4)	C(13)-C(18)	1.384(13)
S(1)-S(2B)	2.26(4)	C(14)-C(15)	1.365(20)
S(2A)-C(25)	1.825(13)	C(15)-C(16)	1.369(20)
S(2A)-S(2B)	2.00(4)	C(16)-C(17)	1.400(14)
P-C(12)	1.825(9)	C(17)-C(18)	1.378(14)
P-C(18)	1.836(8)	C(19)-C(20)	1.420(14)
P-C(24)	1.826(8)	C(19)-C(24)	1.395(13)
O-C(6)	1.150(13)	C(20)-C(21)	1.400(17)
C(1A)-C(2A)	1.52(5)	C(21)-C(22)	1.365(17)
C(1A)-C(5A)	1.49(5)	C(22)-C(23)	1.403(14)
C(2A)-C(3A)	1.53(5)	C(23)-C(24)	1.412(13)
C(3A)-C(4A)	1.38(5)	C(25)-C(26)	1.537(19)
C(4A)-C(5A)	1.56(5)	C(25)-C(27)	1.56(3)
C(7)-C(8)	1.403(16)	C(25)-S(2B)	1.50(4)
C(7)-C(12)	1.366(13)	C(27)-S(2B)	1.21(5)
C(8)-C(9)	1.401(18)		

S(1)-Ru-P	88.91(9)	P-C(12)-C(11)	118.0(7)
S(1)-Ru-C(1A)	124.4(10)	C(7)-C(12)-C(11)	117.5(8)
S(1)-Ru-C(6)	93.8(3)	C(14)-C(13)-C(18)	119.8(10)
P-Ru-C(1A)	96.2(6)	C(13)-C(14)-C(15)	119.9(10)
P-Ru-C(6)	89.5(3)	C(14)-C(15)-C(16)	120.7(10)
C(1A)-Ru-C(6)	141.3(10)	C(15)-C(16)-C(17)	119.6(11)
Ru-S(1)-S(2A)	109.88(15)	C(16)-C(17)-C(18)	120.8(10)
Ru-S(1)-S(2B)	111.5(10)	P-C(18)-C(13)	119.4(7)
S(2A)-S(1)-S(2B)	55.1(11)	P-C(18)-C(17)	121.5(7)
S(1)-S(2A)-C(25)	105.8(5)	C(13)-C(18)-C(17)	119.2(8)
S(1)-S(2A)-S(2B)	68.1(12)	C(20)-C(19)-C(24)	120.0(9)
C(25)-S(2A)-S(2B)	46.0(13)	C(19)-C(20)-C(21)	119.8(10)
Ru-P-C(12)	115.6(3)	C(20)-C(21)-C(22)	119.7(9)
Ru-P-C(18)	118.7(3)	C(21)-C(22)-C(23)	121.9(9)
Ru-P-C(24)	111.6(3)	C(22)-C(23)-C(24)	119.2(9)
C(12)-P-C(18)	102.2(4)	P-C(24)-C(19)	124.3(7)
C(12)-P-C(24)	102.7(4)	P-C(24)-C(23)	116.3(7)
C(18)-P-C(24)	104.2(4)	C(19)-C(24)-C(23)	119.4(8)
Ru-C(1A)-C(2A)	71.9(14)	S(2A)-C(25)-C(26)	106.1(11)
Ru-C(1A)-C(5A)	72.5(14)	S(2A)-C(25)-C(27)	112.9(10)
C(2A)-C(1A)-C(5A)	109.7(23)	S(2A)-C(25)-S(2B)	73.2(17)
C(1A)-C(2A)-C(3A)	104.2(23)	C(26)-C(25)-C(27)	109.9(13)
C(2A)-C(3A)-C(4A)	111(3)	C(26)-C(25)-S(2B)	147.0(19)
C(3A)-C(4A)-C(5A)	109(3)	C(27)-C(25)-S(2B)	46.7(19)
C(1A)-C(5A)-C(4A)	105.1(23)	C(25)-C(27)-S(2B)	64.2(22)
Ru-C(6)-O	176.5(9)	S(1)-S(2B)-S(2A)	56.7(12)

C(8)-C(7)-C(12)	120.5(10)	S(1)-S(2B)-C(25)	108.3(24)
C(7)-C(8)-C(9)	120.4(9)	S(1)-S(2B)-C(27)	177(3)
C(8)-C(9)-C(10)	118.1(10)	S(2A)-S(2B)-C(25)	60.9(16)
C(9)-C(10)-C(11)	122.5(10)	S(2A)-S(2B)-C(27)	120(3)
C(10)-C(11)-C(12)	120.9(9)	C(25)-S(2B)-C(27)	69.1(24)
P-C(12)-C(7)	124.3(7)		

Appendix V

Structural Analysis of $CpRu(PPh_3)(CO)SSS(1\text{-}C_3H_7)$, **11c**.

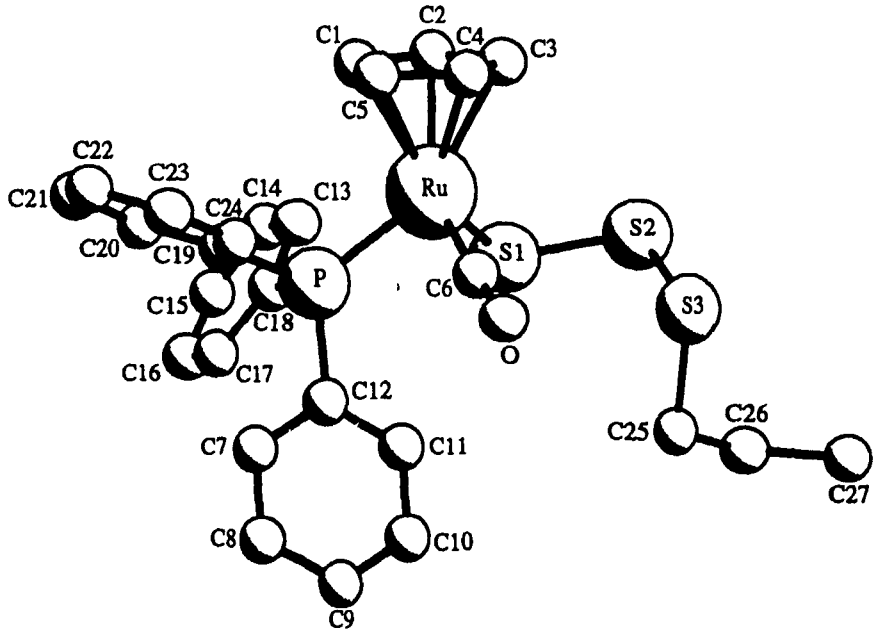

Table A5.1 Crystal data for $CpRu(PPh_3)(CO)SSS(1\text{-}C_3H_7)$.

Space Group: Triclinic, $P\bar{1}$

Cell Dimensions:

a = 10.6430(20)	b = 14.040(3)	c = 9.205(3)
α = 98.110(20)	β = 97.260(20)	γ = 96.460(20)

Volume 1338.9(6) $Å^3$

Empirical formula: $C_{27}H_{27}OPRuS_3$

Cell dimensions were obtained from 25 reflections with 2Θ angle in the range 40.63 - 44.07°.

Crystal dimensions: 0.10 × 0.10 × 0.35 mm

FW = 590.69 Z = 2 F(000) = 607.94

D_{calc}= 1.465 $Mg.m^{-3}$, μ = 0.87 mm-1, λ = 0.70930 Å, $2\Theta_{(max)}$= 49.9

The intensity data were collected on a Rigaku AFC6R diffractometer, using the Θ/2Θ scan mode. T = 23°C

The h,k,l ranges are : -11 11, 0 16, -10 10

No. of reflections measured	3767
No. of unique reflections	3540
No. of reflections with Inet > 3.0 σ(Inet)	2777

A psi correction was made for absorption

Data set was solved by Patterson method

The last least squares cycle was calculated with 55 atoms, 321 parameters and 2777 out of 3540 reflections.

Weights based on counting-statistics were used.

The weight modifier K in KFo^2 is 0.001

The residuals are as follows :--

For significant reflections, R = 0.048, Rw = 0.072, GoF = 1.56

For all reflections, R = 0.066, Rw = 0.076

where $R = \Sigma|Fo-Fc|/\Sigma(Fo)$

$Rw = \sqrt{[\Sigma(w(Fo-Fc)^2)/\Sigma(wFo^2)]}$

$GoF = \sqrt{[\Sigma(w(Fo-Fc)^2)/(\text{No. of reflns - No. of params.})]}$

The maximum shift/σ ratio was 0.167.

In the last D-map, the deepest hole was -0.620 $e^-/Å^3$, and the highest peak 0.810 $e^-/Å^3$.

Secondary ext. coeff. = 0.17(8)

Table A5.2 Atom coordinates, x,y,z and B_{iso} for $CpRu(PPh_3)(CO)SSS(1\text{-}C_3H_7)$. E.S.Ds. refer to the last digit printed.

	x	y	z	B_{iso}
Ru	0.17027(6)	0.33280(5)	0.27935(7)	3.05(3)
S1	0.19219(23)	0.33716(19)	0.02724(25)	4.69(11)
S2	0.0202(3)	0.34954(24)	-0.0901(3)	6.88(16)
S3	-0.0964(4)	0.2242(3)	-0.1130(4)	8.80(21)
P	0.35725(19)	0.26506(15)	0.30856(21)	2.92(9)
O	0.0147(7)	0.1376(6)	0.2268(9)	6.9(4)
C1	0.2403(10)	0.4636(7)	0.4556(11)	5.0(5)
C2	0.1800(11)	0.4966(7)	0.3336(12)	5.3(5)
C3	0.0510(10)	0.4536(8)	0.3076(12)	5.4(5)
C4	0.0312(10)	0.3954(8)	0.4155(12)	5.6(5)
C5	0.1487(12)	0.4006(7)	0.5098(10)	5.6(5)
C6	0.0763(8)	0.2097(7)	0.2392(10)	4.2(4)
C7	0.4237(9)	0.0756(7)	0.2990(10)	4.7(5)
C8	0.4273(12)	-0.0180(8)	0.2313(14)	6.5(6)
C9	0.3638(13)	-0.0493(8)	0.0909(15)	6.7(6)
C10	0.2938(12)	0.0117(8)	0.0174(12)	6.1(6)
C11	0.2891(9)	0.1057(7)	0.0855(10)	4.6(5)
C12	0.3554(8)	0.1388(6)	0.2264(9)	3.6(4)
C13	0.4953(8)	0.4193(6)	0.2113(9)	3.6(4)
C14	0.5985(9)	0.4646(7)	0.1578(10)	4.7(4)
C15	0.7036(8)	0.4189(8)	0.1371(10)	4.6(5)
C16	0.7052(8)	0.3269(7)	0.1707(10)	4.5(5)
C17	0.6031(8)	0.2809(6)	0.2241(9)	3.8(4)
C18	0.4966(7)	0.3250(6)	0.2436(7)	3.0(4)
C19	0.5286(8)	0.3064(6)	0.5781(9)	4.1(4)
C20	0.5574(10)	0.3047(7)	0.7289(10)	5.2(5)
C21	0.4693(11)	0.2606(7)	0.8061(10)	5.0(5)
C22	0.3536(10)	0.2163(8)	0.7315(10)	5.3(5)
C23	0.3227(9)	0.2181(7)	0.5824(9)	4.6(5)
C24	0.4103(7)	0.2632(6)	0.5046(8)	3.2(3)
C25	-0.0203(10)	0.1293(7)	-0.2377(12)	5.5(5)
C26	-0.0486(20)	0.1524(19)	-0.3986(20)	14.5(15)
C27	-0.1988(18)	0.1231(24)	-0.4860(22)	17.7(22)

B_{iso} is the Mean of the Pricipal Axes of the Thermal Ellipsoid

Table A5.3 Anisotropic thermal parameters for $CpRu(PPh_3)(CO)SSS(1\text{-}C_3H_7)$. U(i,j) values ×100. E.S.Ds. refer to the last digit printed.

	U11	U22	U33	U12	U13	U23
Ru	3.84(4)	4.13(4)	3.66(4)	0.80(3)	0.46(3)	0.64(3)
S1	5.99(15)	7.39(16)	4.73(13)	0.60(12)	0.81(11)	2.07(12)
S2	9.53(22)	9.50(22)	7.08(18)	2.51(18)	-1.68(16)	2.79(16)
S3	8.56(24)	14.1(3)	9.83(25)	-0.30(22)	0.90(19)	0.47(23)
P	4.05(12)	3.89(12)	3.29(11)	0.66(9)	0.69(9)	0.77(9)
O	8.3(5)	7.2(5)	9.8(6)	-1.6(5)	1.3(4)	0.6(4)
C1	6.1(6)	5.6(6)	6.3(6)	1.0(5)	0.2(5)	-1.9(5)
C2	8.6(8)	3.9(5)	7.5(7)	1.0(5)	1.3(6)	0.7(5)
C3	6.0(7)	6.8(7)	7.9(7)	3.1(6)	0.1(5)	0.9(6)
C4	6.3(7)	7.0(7)	8.5(8)	2.5(6)	3.7(6)	-0.9(6)
C5	11.1(9)	6.3(7)	4.4(5)	4.0(7)	1.5(6)	-0.3(5)
C6	4.4(5)	4.9(6)	6.4(6)	-0.1(5)	1.0(4)	0.6(5)
C7	6.8(6)	5.4(6)	6.0(6)	1.8(5)	1.3(5)	0.5(5)
C8	11.0(10)	4.9(6)	9.5(9)	2.7(6)	2.6(7)	1.5(6)
C9	11.1(10)	4.6(6)	9.9(9)	0.2(7)	3.9(8)	-0.5(6)
C10	10.4(9)	5.8(7)	6.1(7)	0.0(6)	1.5(6)	-0.9(5)
C11	7.4(7)	5.2(6)	5.0(6)	0.8(5)	1.7(5)	0.6(5)
C12	4.6(5)	4.1(5)	5.8(5)	0.9(4)	2.2(4)	1.2(4)
C13	4.7(5)	5.0(5)	3.9(4)	0.3(4)	0.1(4)	0.7(4)
C14	6.3(6)	6.2(6)	5.0(5)	-1.2(5)	-0.1(5)	2.3(5)
C15	4.4(6)	7.6(7)	5.1(5)	-0.2(5)	0.4(4)	1.2(5)
C16	3.6(5)	8.1(7)	5.6(5)	1.0(5)	1.0(4)	0.5(5)
C17	5.2(5)	4.8(5)	4.7(5)	1.2(4)	1.4(4)	0.9(4)
C18	4.6(5)	4.3(5)	2.7(4)	0.5(4)	0.4(3)	0.6(3)
C19	5.5(6)	5.4(5)	4.6(5)	0.7(4)	0.7(4)	1.0(4)
C20	8.5(7)	6.3(6)	4.2(5)	0.1(6)	-1.3(5)	0.6(5)
C21	9.7(8)	6.3(6)	3.7(5)	2.8(6)	0.5(5)	1.3(4)
C22	7.3(7)	8.6(7)	5.5(6)	2.3(6)	2.3(5)	3.3(5)
C23	5.1(6)	8.6(7)	4.1(5)	1.2(5)	0.4(4)	2.2(5)
C24	4.3(5)	4.5(5)	3.7(4)	1.5(4)	0.8(4)	1.0(4)
C25	5.6(6)	5.2(6)	8.9(8)	-1.3(5)	0.6(5)	-1.7(5)
C26	17.2(19)	25.3(26)	10.6(14)	-3.4(18)	2.7(13)	-0.2(14)
C27	10.8(15)	45.1(43)	13.7(17)	5.6(20)	2.8(12)	9.5(22)

Anisotropic Temperature Factors are of the form;

$$Temp = -2\pi^2(h^2a^{*2}U_{11} + k^2b^{*2}U_{22} + l^2c^{*2}U_{33} + 2hka^*b^*U_{12} + 2hla^*c^*U_{13} + 2klb^*c^*U_{23})$$

Table A5.4 Selected bond lengths and angles for $CpRu(PPh_3)(CO)SSS(1\text{-}C_3H_7)$.

Ru-S(1)	2.3701(24)	C(7)-C(12)	1.397(13)
Ru-P	2.3021(21)	C(8)-C(9)	1.369(19)
Ru-C(3)	2.236(9)	C(9)-C(10)	1.388(19)
Ru-C(4)	2.232(8)	C(10)-C(11)	1.388(14)
Ru-C(5)	2.250(9)	C(11)-C(12)	1.386(13)
Ru-C(6)	1.861(10)	C(13)-C(14)	1.386(12)
S(1)-S(2)	2.042(4)	C(13)-C(18)	1.397(11)
S(2)-S(3)	2.005(5)	C(14)-C(15)	1.371(14)
S(3)-C(25)	1.949(11)	C(15)-C(16)	1.371(15)
P-C(12)	1.824(8)	C(16)-C(17)	1.381(12)
P-C(18)	1.831(8)	C(17)-C(18)	1.371(11)
P-C(24)	1.827(8)	C(19)-C(20)	1.388(12)
O-C(6)	1.125(12)	C(19)-C(24)	1.382(12)
C(1)-C(2)	1.386(15)	C(20)-C(21)	1.389(15)
C(1)-C(5)	1.426(16)	C(21)-C(22)	1.367(16)
C(2)-C(3)	1.413(15)	C(22)-C(23)	1.374(12)
C(3)-C(4)	1.393(16)	C(23)-C(24)	1.395(12)
C(4)-C(5)	1.418(16)	C(25)-C(26)	1.560(23)
C(7)-C(8)	1.379(14)	C(26)-C(27)	1.67(3)

S(1)-Ru-P	89.42(8)	C(3)-C(4)-C(5)	108.1(9)
S(1)-Ru-C(3)	97.1(3)	Ru-C(5)-C(1)	71.9(5)
S(1)-Ru-C(4)	130.1(3)	Ru-C(5)-C(4)	70.9(5)
S(1)-Ru-C(5)	153.6(3)	C(1)-C(5)-C(4)	106.9(9)
S(1)-Ru-C(6)	93.6(3)	Ru-C(6)-O	173.5(8)
P-Ru-C(3)	154.3(3)	C(8)-C(7)-C(12)	120.9(9)
P-Ru-C(4)	139.9(3)	C(7)-C(8)-C(9)	119.6(10)
P-Ru-C(5)	104.6(3)	C(8)-C(9)-C(10)	120.5(10)
P-Ru-C(6)	90.3(3)	C(9)-C(10)-C(11)	120.0(10)
C(3)-Ru-C(4)	36.3(4)	C(10)-C(11)-C(12)	119.9(9)
C(3)-Ru-C(5)	60.9(4)	P-C(12)-C(7)	121.7(7)
C(3)-Ru-C(6)	113.9(4)	P-C(12)-C(11)	119.1(7)
C(4)-Ru-C(5)	36.9(4)	C(7)-C(12)-C(11)	119.1(8)
C(4)-Ru-C(6)	93.5(4)	C(14)-C(13)-C(18)	120.0(8)
C(5)-Ru-C(6)	108.3(4)	C(13)-C(14)-C(15)	121.1(9)
Ru-S(1)-S(2)	110.04(14)	C(14)-C(15)-C(16)	118.7(8)
S(1)-S(2)-S(3)	109.61(20)	C(15)-C(16)-C(17)	120.9(8)
S(2)-S(3)-C(25)	105.9(4)	C(16)-C(17)-C(18)	121.2(8)
Ru-P-C(12)	118.4(3)	P-C(18)-C(13)	119.3(6)
Ru-P-C(18)	117.5(3)	P-C(18)-C(17)	122.5(6)
Ru-P-C(24)	110.48(25)	C(13)-C(18)-C(17)	118.1(7)
C(12)-P-C(18)	102.0(3)	C(20)-C(19)-C(24)	119.0(8)
C(12)-P-C(24)	102.3(4)	C(19)-C(20)-C(21)	121.0(9)
C(18)-P-C(24)	104.3(3)	C(20)-C(21)-C(22)	119.4(8)
C(2)-C(1)-C(5)	108.5(9)	C(21)-C(22)-C(23)	120.4(9)
C(1)-C(2)-C(3)	108.0(9)	C(22)-C(23)-C(24)	120.4(9)
Ru-C(3)-C(2)	73.1(5)	P-C(24)-C(19)	123.5(6)
Ru-C(3)-C(4)	71.7(5)	P-C(24)-C(23)	116.7(6)
C(2)-C(3)-C(4)	108.5(9)	C(19)-C(24)-C(23)	119.7(7)
Ru-C(4)-C(3)	72.0(5)	S(3)-C(25)-C(26)	105.8(11)
Ru-C(4)-C(5)	72.3(5)	C(25)-C(26)-C(27)	117.5(14)

Appendix VI

Structural Analysis of $CpRu(PPh_3)(CO)SS(O)(CHMe_2)$, **12d**.

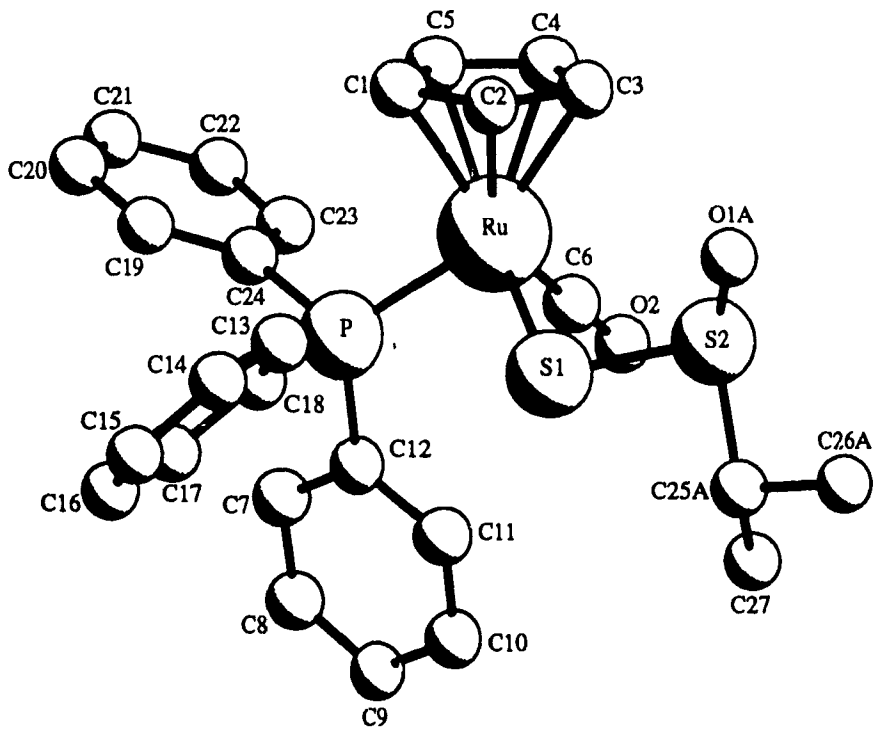

Table A6.1 Crystal data for $CpRu(PPh_3)(CO)SS(O)(CHMe_2)$.

Space Group: Triclinic, $P\bar{1}$

Cell Dimensions:

a = 10.4900(20)	b = 14.663(4)	c = 8.606(4)
α = 97.85(3)	β = 105.210(20)	γ = 82.940(20)

Volume = 1260.1(7) $Å^3$

Empirical formula: $C_{27}H_{27}O_2PS_2Ru$

Cell dimensions were obtained from 25 reflections with 2Θ angle in the range 75.74 - 79.67°.

Crystal dimensions: 0.30 × 0.10 × 0.06 mm

FW = 572.61 Z = 2 F(000) = 591.94

D_{calc}= 1.509 $Mg.m^{-3}$, μ = 7.47 mm^{-1}, λ = 1.54056 Å, $2\Theta_{(max)}$= 120.0

The intensity data were collected on a Rigaku AFC5R diffractometer, using the $\Theta/2\Theta$ scan mode. T = -120.0°C
The h,k,l ranges are : -11 11, 0 16, -9 9

No. of reflections measured	3988
No. of unique reflections	3750
No. of reflections with Inet > 3.0σ(Inet)	3092

A psi correction was made for absorption

Data set was solved by Patterson method
The last least squares cycle was calculated with 56 atoms, 310 parameters and 3092 out of 3750 reflections. Weights based on counting-statistics were used.
The weight modifier K in KFo^2 is 0.0004

The residuals are as follows :--

For significant reflections,	R = 0.053,	Rw = 0.073
	GoF = 1.97	
For all reflections,	R = 0.066,	Rw = 0.076.

where $R = \Sigma|Fo-Fc|/\Sigma|Fo|$
$Rw = \sqrt{[\Sigma(w(Fo-Fc)^2)/\Sigma(wFo^2)]}$
$GoF = \sqrt{[\Sigma(w(Fo-Fc)^2)/(\text{No. of reflns - No. of params.})]}$

The maximum shift/σ ratio was 0.038.

In the last D-map, the deepest hole was -1.160 $e^-/Å^3$, and the highest peak 1.550 $e^-/Å^3$, near the disordered R-group.

Table A6.2 Atom coordinates, x,y,z and B_{iso} for $CpRu(PPh_3)(CO)SS(O)(CHMe_2)$. E.S.Ds. refer to the last digit printed.

	x	y	z	B_{iso}
Ru	0.45496(6)	0.31550(4)	0.28668(7)	2.325(25)
S1	0.42643(19)	0.16528(14)	0.33999(24)	2.83(8)
S2	0.24764(23)	0.18582(19)	0.4063(3)	4.30(12)
P	0.67822(18)	0.27412(13)	0.31419(22)	2.05(7)
O1A	0.1380(10)	0.1787(7)	0.2635(12)	4.13(19)
O1B	0.2338(21)	0.2613(14)	0.513(3)	5.1(4)
O2	0.5012(7)	0.3824(5)	0.6404(8)	4.4(3)
C1	0.4134(9)	0.3412(7)	0.0240(10)	3.8(4)
C2	0.3077(10)	0.2988(7)	0.0434(12)	4.5(5)
C3	0.2468(9)	0.3597(8)	0.1554(14)	4.9(5)
C4	0.3182(10)	0.4361(7)	0.2011(12)	4.1(4)
C5	0.4224(9)	0.4270(6)	0.1252(11)	3.6(4)
C6	0.4871(8)	0.3564(6)	0.5076(12)	3.2(4)
C7	0.9149(8)	0.2795(5)	0.5632(9)	2.7(3)
C8	0.9949(8)	0.2589(6)	0.7156(10)	3.1(4)
C9	0.9490(9)	0.2118(6)	0.8133(10)	3.2(4)
C10	0.8210(9)	0.1874(6)	0.7662(10)	3.3(4)
C11	0.7386(8)	0.2081(5)	0.6164(9)	2.7(4)
C12	0.7850(7)	0.2546(5)	0.5156(8)	2.0(3)
C13	0.6246(8)	0.1231(5)	0.0779(9)	2.4(3)
C14	0.6569(9)	0.0395(6)	-0.0121(10)	3.1(4)
C15	0.7856(9)	0.0020(6)	0.0124(10)	3.2(4)
C16	0.8852(9)	0.0485(7)	0.1253(12)	4.1(4)
C17	0.8527(8)	0.1308(6)	0.2138(10)	3.1(4)
C18	0.7214(8)	0.1672(5)	0.1916(9)	2.4(3)
C19	0.8147(8)	0.3491(6)	0.1267(10)	3.2(4)
C20	0.8749(10)	0.4203(7)	0.0891(12)	4.0(4)
C21	0.8801(9)	0.5024(6)	0.1798(12)	3.8(4)
C22	0.8206(10)	0.5198(6)	0.3113(12)	4.2(5)
C23	0.7608(9)	0.4492(6)	0.3473(11)	3.3(4)
C24	0.7576(7)	0.3633(5)	0.2572(9)	2.4(3)
C25A	0.2829(13)	0.0675(11)	0.5005(17)	2.94(24)
C25B	0.2490(24)	0.1142(18)	0.539(3)	2.8(4)
C26A	0.1507(16)	0.0401(11)	0.5129(19)	4.5(3)
C26B	0.263(3)	0.0181(19)	0.461(3)	3.1(4)
C27	0.3752(17)	0.1019(12)	0.6807(21)	9.1(4)

B_{iso} is the Mean of the Principal Axes of the Thermal Ellipsoid

Table A6.3 Anisotropic temerature factors for $CpRu(PPh_3)(CO)SS(O)(CHMe_2)$. U(i,j) values ×100. E.S.Ds. refer to the last digit printed.

	U11	U22	U33	U12	U13	U23
Ru	2.14(3)	3.44(4)	3.01(4)	0.123(24)	0.148(24)	0.814(25)
S1	2.90(10)	4.00(11)	3.84(11)	-0.62(8)	0.60(9)	0.63(9)
S2	3.51(12)	7.94(18)	5.43(14)	-1.26(12)	1.41(11)	1.33(13)
P	2.19(10)	3.00(10)	2.45(9)	-0.16(8)	0.25(8)	0.54(8)
O1A	5.23(24)					
O1B	6.5(5)					
O2	5.4(4)	6.5(4)	4.1(4)	0.1(3)	1.0(3)	-1.5(3)
C1	4.4(5)	6.6(6)	2.7(4)	1.0(5)	-0.7(4)	2.0(4)
C2	4.3(6)	6.3(6)	4.8(6)	-0.9(5)	-3.2(5)	2.4(5)
C3	2.3(5)	8.4(8)	7.8(7)	0.9(5)	-0.3(5)	4.5(7)
C4	4.5(6)	5.3(6)	5.2(6)	1.8(5)	0.6(5)	2.2(5)
C5	4.9(6)	4.7(5)	3.9(5)	0.0(4)	-0.3(4)	2.3(4)
C6	2.7(4)	3.8(5)	5.3(6)	0.9(4)	0.7(4)	1.3(4)
C7	3.0(4)	3.8(4)	3.2(4)	-0.4(3)	0.6(3)	0.4(3)
C8	2.9(4)	5.2(5)	3.1(4)	-0.2(4)	-0.4(4)	0.3(4)
C9	4.1(5)	4.6(5)	2.9(4)	0.4(4)	-0.3(4)	1.1(4)
C10	4.5(5)	5.1(5)	3.1(4)	-0.4(4)	0.9(4)	1.8(4)
C11	3.3(4)	3.8(4)	3.0(4)	-0.3(4	0.6(3)	0.4(4)
C12	2.4(4)	2.1(4)	2.6(4)	0.2(3)	0.3(3)	-0.2(3)
C13	3.3(4)	3.1(4)	2.5(4)	-0.2(3)	0.3(3)	-0.1(3)
C14	4.6(5)	4.1(5)	3.1(4)	-1.0(4)	0.9(4)	0.2(4)
C15	5.0(5)	3.4(4)	3.8(5)	-0.1(4)	1.5(4)	0.2(4)
C16	4.1(5)	5.6(6)	5.5(6)	1.2(5)	1.2(5)	0.4(5)
C17	3.2(5)	4.0(5)	3.8(5)	0.2(4)	0.4(4)	-0.6(4)
C18	3.2(4)	3.2(4)	2.7(4)	-0.2(3)	0.8(3)	0.3(3)
C19	3.9(5)	4.7(5)	4.1(5)	-0.3(4)	1.1(4)	1.8(4)
C20	5.7(6)	4.9(6)	5.4(6)	0.0(5)	2.3(5)	1.7(5)
C21	3.7(5)	4.1(5)	6.7(6)	-0.6(4)	0.8(5)	2.2(5)
C22	6.1(6)	3.9(5)	5.5(6)	-0.8(5)	0.6(5)	1.1(4)
C23	4.5(5)	3.9(5)	4.6(5)	-1.2(4)	1.6(4)	0.3(4)
C24	2.8(4)	3.3(4)	2.8(4)	0.2(3)	0.1(3)	1.2(3)
C25A	3.7(3)					
C25B	3.5(5)					
C26A	5.7(4)					
C26B	3.9(6)					
C27	11.5(5)					

Anisotropic Temperature Factors are of the form;

$$Temp = -2\pi^2(h^2a^{*2}U_{11} + k^2b^{*2}U_{22} + l^2c^{*2}U_{33} + 2hka^*b^*U_{12} + 2hla^*c^*U_{13} + 2klb^*c^*U_{23})$$

Table A6.4 Selected bond lengths and angles for $CpRu(PPh_3)(CO)SS(O)(CHMe_2)$.

Ru-S(1)	2.3794(22)	C(9)-C(10)	1.374(13)
Ru-P	2.3040(20)	C(10)-C(11)	1.399(11)
Ru-C(3)	2.241(9)	C(11)-C(12)	1.385(11)
Ru-C(4)	2.215(9)	C(13)-C(14)	1.411(11)
Ru-C(5)	2.226(8)	C(13)-C(18)	1.369(11)
Ru-C(6)	1.868(10)	C(14)-C(15)	1.367(13)
S(1)-S(2)	2.076(3)	C(15)-C(16)	1.400(14)
S(2)-O(1A)	1.448(10)	C(16)-C(17)	1.392(12)
S(2)-O(1B)	1.358(21)	C(17)-C(18)	1.389(11)
S(2)-C(25A)	1.968(15)	C(19)-C(20)	1.399(12)
S(2)-C(25B)	1.653(23)	C(19)-C(24)	1.386(11)
P-C(12)	1.838(7)	C(20)-C(21)	1.340(14)
P-C(18)	1.844(8)	C(21)-C(22)	1.409(15)
P-C(24)	1.817(8)	C(22)-C(23)	1.383(13)
O(2)-C(6)	1.132(12)	C(23)-C(24)	1.385(12)
C(1)-C(2)	1.392(15)	C(25A)-C(25B)	0.81(3)
C(1)-C(5)	1.428(14)	C(25A)-C(26A)	1.524(21)
C(2)-C(3)	1.443(18)	C(25A)-C(26B)	0.79(3)
C(3)-C(4)	1.379(16)	C(25A)-C(27)	1.648(23)
C(4)-C(5)	1.398(14)	C(25B)-C(26A)	1.54(3)
C(7)-C(8)	1.409(11)	C(25B)-C(26B)	1.49(4)
C(7)-C(12)	1.396(11)	C(25B)-C(27)	1.56(3)
C(8)-C(9)	1.366(12)	C(26A)-C(26B)	1.35(3)

S(1)-Ru-P	90.23(7)	C(10)-C(11)-C(12)	120.2(7)
S(1)-Ru-C(3)	100.1(3)	P-C(12)-C(7)	121.1(6)
S(1)-Ru-C(4)	134.6(3)	P-C(12)-C(11)	119.1(6)
S(1)-Ru-C(5)	152.37(25)	C(7)-C(12)-C(11)	119.6(7)
S(1)-Ru-C(6)	90.3(3)	C(14)-C(13)-C(18)	120.6(7)
P-Ru-C(3)	155.8(3)	C(13)-C(14)-C(15)	120.3(8)
P-Ru-C(4)	134.4(3)	C(14)-C(15)-C(16)	119.3(8)
P-Ru-C(5)	100.3(3)	C(15)-C(16)-C(17)	120.2(8)
P-Ru-C(6)	90.35(25)	C(16)-C(17)-C(18)	120.3(8)
C(3)-Ru-C(4)	36.0(4)	P-C(18)-C(13)	120.5(6)
C(3)-Ru-C(5)	61.4(4)	P-C(18)-C(17)	120.2(6)
C(3)-Ru-C(6)	111.3(4)	C(13)-C(18)-C(17)	119.4(7)
C(4)-Ru-C(5)	36.7(4)	C(20)-C(19)-C(24)	120.1(8)
C(4)-Ru-C(6)	96.6(4)	C(19)-C(20)-C(21)	120.6(9)
C(5)-Ru-C(6)	114.9(4)	C(20)-C(21)-C(22)	120.7(8)
Ru-S(1)-S(2)	102.63(11)	C(21)-C(22)-C(23)	118.3(8)
S(1)-S(2)-O(1A)	110.1(4)	C(22)-C(23)-C(24)	121.6(8)
S(1)-S(2)-O(1B)	115.7(9)	P-C(24)-C(19)	122.7(6)
S(1)-S(2)-C(25A)	91.5(4)	P-C(24)-C(23)	118.7(6)
S(1)-S(2)-C(25B)	109.6(9)	C(19)-C(24)-C(23)	118.6(7)
O(1A)-S(2)-O(1B)	114.2(10)	S(2)-C(25A)-C(25B)	55.6(18)
O(1A)-S(2)-C(25A)	108.7(6)	S(2)-C(25A)-C(26A)	107.5(10)
O(1A)-S(2)-C(25B)	114.1(9)	S(2)-C(25A)-C(26B)	129.8(21)
O(1B)-S(2)-C(25A)	114.5(10)	S(2)-C(25A)-C(27)	99.0(10)
O(1B)-S(2)-C(25B)	92.3(13)	C(25B)-C(25A)-C(26A)	76.0(20)
C(25A)-S(2)-C(25B)	23.7(10)	C(25B)-C(25A)-C(26B)	137(3)
Ru-P-C(12)	119.08(24)	C(25B)-C(25A)-C(27)	69.2(20)
Ru-P-C(18)	116.0(3)	C(26A)-C(25A)-C(26B)	62.5(21)

Ru-P-C(24)	111.31(25)	C(26A)-C(25A)-C(27)	111.0(12)
C(12)-P-C(18)	101.4(3)	C(26B)-C(25A)-C(27)	131.1(23)
C(12)-P-C(24)	102.2(3)	S(2)-C(25B)-C(25A)	100.7(22)
C(18)-P-C(24)	105.1(4)	S(2)-C(25B)-C(26A)	124.5(16)
C(2)-C(1)-C(5)	108.3(9)	S(2)-C(25B)-C(26B)	108.2(17)
C(1)-C(2)-C(3)	107.8(9)	S(2)-C(25B)-C(27)	118.5(16)
Ru-C(3)-C(2)	71.8(5)	C(25A)-C(25B)-C(26A)	73.5(20)
Ru-C(3)-C(4)	71.0(5)	C(25A)-C(25B)-C(26B)	20.8(17)
C(2)-C(3)-C(4)	106.8(9)	C(25A)-C(25B)-C(27)	81.9(22)
Ru-C(4)-C(3)	73.0(5)	C(26A)-C(25B)-C(26B)	53.1(14)
Ru-C(4)-C(5)	72.0(5)	C(26A)-C(25B)-C(27)	115.1(17)
C(3)-C(4)-C(5)	110.4(9)	C(26B)-C(25B)-C(27)	95.1(18)
Ru-C(5)-C(1)	72.9(5)	C(25A)-C(26A)-C(25B)	30.4(12)
Ru-C(5)-C(4)	71.3(5)	C(25A)-C(26A)-C(26B)	31.0(14)
C(1)-C(5)-C(4)	106.7(9)	C(25B)-C(26A)-C(26B)	61.3(17)
Ru-C(6)-O(2)	177.1(7)	C(25A)-C(26B)-C(25B)	21.3(17)
C(8)-C(7)-C(12)	118.9(7)	C(25A)-C(26B)-C(26A)	86.5(24)
C(7)-C(8)-C(9)	121.1(8)	C(25B)-C(26B)-C(26A)	65.6(16)
C(8)-C(9)-C(10)	119.9(7)	C(25A)-C(27)-C(25B)	28.9(12)
C(9)-C(10)-C(11)	120.3(7)		

Table A7.1 Crystal data for $CpRu(PPh_3)(CO)SS(O)_2(4\text{-}C_6H_4Me)$.

Space Group: Monoclinic, $P\ 2_1$
Cell Dimensions:
a = 10.941(2) b = 9.569(2) c = 14.573(2)
β = 107.58(1)
Volume = 1454.5(4) $Å^3$

Empirical formula : $C_{31}H_{27}PO_3RuS_2$

Cell dimensions were obtained from 25 reflections with 2Θ angle in the range 28.00 - 33.33 degrees.

Crystal dimensions: 0 .10 × 0.15 × 0.32 mm

FW = 643.72 Z = 2 F(000) = 656

D_{calc} = 1.470 $Mg.m^{-3}$, μ = 7.49 cm-1, λ = 0.70930 Å, $2\Theta_{(max)}$= 55.0

The intensity data were collected on a Rigaku AFC6S defractometer, using the ω-2Ω scan mode.
The h,k,l ranges are: 0 14, -12 12, -18 18

No. of reflections measured	7016
No. of unique reflections	6679
No. of reflections with Inet > 3.0 σ (Inet)	4258

A Lorentz-polarization correction was made for absorption wich resulted in a transmission factor ranging from 0.93 to 1.00.

Data set was solved by direct method.
The last least squares cycle was calculated with 63 atoms, 342 parameters and 4258 out of 6679 reflections.
Weights based on counting-statistics were used.

For significant reflections, R = 0.044, Rw = 0.038, GoF = 1.55

where $R = \Sigma|Fo-Fc|/\Sigma|Fo|$
$Rw = \sqrt{[\Sigma(w(Fo-Fc)^2)/\Sigma(wFo^2)]}$
$GoF = \sqrt{[\Sigma(w(Fo-Fc)^2)/(\text{No. of reflns - No. of params.})]}$

The maximum shift/σ ratio was 0.03.

In the last D-map, the deepest hole was -0.75 $e^-/Å^3$, and the highest peak 0.66 $e^-/Å^3$.

Ru-P-C(24)	111.31(25)	C(26A)-C(25A)-C(27)	111.0(12)
C(12)-P-C(18)	101.4(3)	C(26B)-C(25A)-C(27)	131.1(23)
C(12)-P-C(24)	102.2(3)	S(2)-C(25B)-C(25A)	100.7(22)
C(18)-P-C(24)	105.1(4)	S(2)-C(25B)-C(26A)	124.5(16)
C(2)-C(1)-C(5)	108.3(9)	S(2)-C(25B)-C(26B)	108.2(17)
C(1)-C(2)-C(3)	107.8(9)	S(2)-C(25B)-C(27)	118.5(16)
Ru-C(3)-C(2)	71.8(5)	C(25A)-C(25B)-C(26A)	73.5(20)
Ru-C(3)-C(4)	71.0(5)	C(25A)-C(25B)-C(26B)	20.8(17)
C(2)-C(3)-C(4)	106.8(9)	C(25A)-C(25B)-C(27)	81.9(22)
Ru-C(4)-C(3)	73.0(5)	C(26A)-C(25B)-C(26B)	53.1(14)
Ru-C(4)-C(5)	72.0(5)	C(26A)-C(25B)-C(27)	115.1(17)
C(3)-C(4)-C(5)	110.4(9)	C(26B)-C(25B)-C(27)	95.1(18)
Ru-C(5)-C(1)	72.9(5)	C(25A)-C(26A)-C(25B)	30.4(12)
Ru-C(5)-C(4)	71.3(5)	C(25A)-C(26A)-C(26B)	31.0(14)
C(1)-C(5)-C(4)	106.7(9)	C(25B)-C(26A)-C(26B)	61.3(17)
Ru-C(6)-O(2)	177.1(7)	C(25A)-C(26B)-C(25B)	21.3(17)
C(8)-C(7)-C(12)	118.9(7)	C(25A)-C(26B)-C(26A)	86.5(24)
C(7)-C(8)-C(9)	121.1(8)	C(25B)-C(26B)-C(26A)	65.6(16)
C(8)-C(9)-C(10)	119.9(7)	C(25A)-C(27)-C(25B)	28.9(12)
C(9)-C(10)-C(11)	120.3(7)		

Appendix VII

Structural Analysis of $CpRu(PPh_3)(CO)SS(O)_2(4\text{-}C_6H_4Me)$, **13b**.

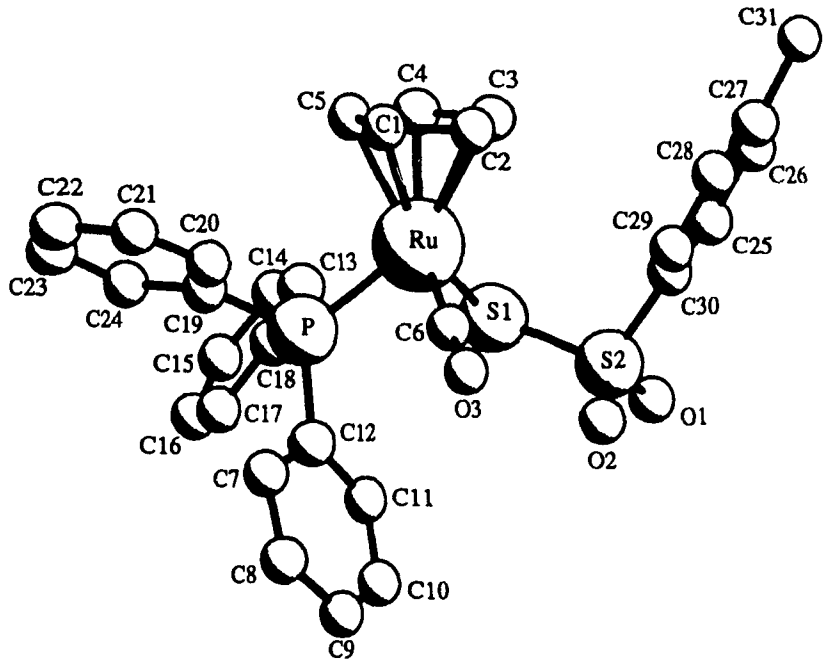

Table A7.1 Crystal data for $CpRu(PPh_3)(CO)SS(O)_2(4\text{-}C_6H_4Me)$.

Space Group: Monoclinic, $P\,2_1$
Cell Dimensions:
a = 10.941(2) b = 9.569(2) c = 14.573(2)
β = 107.58(1)
Volume = 1454.5(4) $Å^3$

Empirical formula : $C_{31}H_{27}PO_3RuS_2$

Cell dimensions were obtained from 25 reflections with 2Θ angle in the range 28.00 - 33.33 degrees.

Crystal dimensions: 0 .10 × 0.15 × 0.32 mm

FW = 643.72 Z = 2 F(000) = 656

D_{calc} = 1.470 $Mg.m^{-3}$, μ = 7.49 cm-1, λ = 0.70930 Å, $2\Theta_{(max)}$= 55.0

The intensity data were collected on a Rigaku AFC6S defractometer, using the ω-2Ω scan mode.
The h,k,l ranges are: 0 14, -12 12, -18 18

No. of reflections measured	7016
No. of unique reflections	6679
No. of reflections with Inet > 3.0 σ (Inet)	4258

A Lorentz-polarization correction was made for absorption wich resulted in a transmission factor ranging from 0.93 to 1.00.

Data set was solved by direct method.
The last least squares cycle was calculated with 63 atoms, 342 parameters and 4258 out of 6679 reflections.
Weights based on counting-statistics were used.

For significant reflections, R = 0.044, Rw = 0.038, GoF = 1.55

where $R = \Sigma|Fo-Fc|/\Sigma|Fo|$
$Rw = \sqrt{[\Sigma(w(Fo-Fc)^2)/\Sigma(wFo^2)]}$
$GoF = \sqrt{[\Sigma(w(Fo-Fc)^2)/(\text{No. of reflns - No. of params.})]}$

The maximum shift/σ ratio was 0.03.

In the last D-map, the deepest hole was -0.75 $e^-/Å^3$, and the highest peak 0.66 $e^-/Å^3$.

Table A7.2 Atom coordinates, x,y,z and B_{iso} for $CpRu(PPh_3)(CO)SS(O)_2(4\text{-}C_6H_4Me)$. E.S.Ds. refer to the last digit printed.

	x	y	z	B_{iso}
Ru	0.70189(5)	0.1839	0.65886(4)	2.77(2)
S1	0.6744(2)	-0.0624(2)	0.6668(1)	3.18(8)
S2	0.8368(2)	-0.1621(2)	0.6652(2)	3.64(8)
P	0.6281(2)	0.2050(2)	0.7913(1)	2.92(8
O1	0.8069(5)	-0.3093(8)	0.6615(4)	5.3(2)
O2	0.9477(5)	-0.1158(6)	0.7400(4)	4.6(3)
O3	0.9719(5)	0.201(1)	0.7905(4)	5.9(3)
C1	0.690(1)	0.3831(8)	0.5809(6)	5.3(4)
C2	0.750(1)	0.286(1)	0.5381(7)	5.1(5)
C3	0.6642(7)	0.187(1)	0.4984(5)	4.3(3)
C4	0.5482(8)	0.2112(8)	0.5173(6)	4.3(4)
C5	0.562(1)	0.336(1)	0.5684(6)	4.8(4)
C6	0.8688(6)	0.187(1)	0.7432(5)	3.7(3)
C7	0.807(1)	0.254(1)	0.9712(7)	5.7(5)
C8	0.906(1)	0.208(2)	1.0525(8)	7.9(8)
C9	0.940(1)	0.073(2)	1.0679(8)	8.6(8)
C10	0.874(1)	-0.020(1)	1.0029(8)	9.2(8)
C11	0.780(1)	0.020(1)	0.9227(7)	6.2(5)
C12	0.7449(7)	0.1551(8)	0.9043(5)	3.3(3)
C13	0.4069(7)	0.048(1)	0.7096(6)	4.2(4)
C14	0.2971(8)	-0.022(1)	0.7089(7)	5.0(4)
C15	0.265(1)	-0.041(1)	0.792(1)	6.7(6)
C16	0.347(1)	0.010(1)	0.8750(8)	7.0(6)
C17	0.4569(9)	0.081(1)	0.8763(6)	5.4(5)
C18	0.4886(7)	0.1041(7)	0.7916(6)	3.6(3)
C19	0.664(1)	0.491(1)	0.8046(8)	6.3(5)
C20	0.636(1)	0.628(1)	0.8195(9)	8.6(7)
C21	0.526(1)	0.661(1)	0.8423(8)	8.2(7)
C22	0.447(1)	0.557(1)	0.8493(8)	7.3(6)
C23	0.4740(9)	0.418(1)	0.8347(7)	5.2(4)
C24	0.5824(8)	0.3848(8)	0.8112(6)	3.8(4)
C25	0.7985(8)	-0.1899(8)	0.4718(7)	4.0(4)
C26	0.8157(8)	-0.150(1)	0.3872(7)	4.7(4)
C27	0.8962(8)	-0.044(1)	0.3812(6)	4.5(4)
C28	0.9623(8)	0.024(1)	0.4641(7)	4.5(4)
C29	0.9477(7)	-0.0113(8)	0.5508(6)	3.8(4)
C30	0.8643(7)	-0.1191(7)	0.5550(6)	3.2(3)
C31	0.908(1)	0.002(1)	0.2842(7)	6.5(6)

B_{iso} is the Mean of the Principal Axes of the Thermal Ellipsoid

Table A7.3 Anisotropic thermal factors for $CpRu(PPh_3)(CO)SS(O)_2(4\text{-}C_6H_4Me)$. U(i,j) values ×100. E.S.Ds. refer to the last digit printed.

	U11	U22	U33	U12	U13	U23
Ru	3.81(3)	2.73(2)	3.59(3)	-0.26(4)	0.53(2)	0.27(4)
S1	4.1(1)	3.0(1)	5.0(1)	-0.31(8)	1.4(1)	-0.06(9)
S2	4.6(1)	3.4(1)	5.8(1)	0.51(9)	1.4(1)	0.9(1)
P	3.9(1)	2.9(1)	4.0(1)	-0.25(9)	0.76(8)	-0.13(9)
O1	9.0(4)	2.6(3)	9.7(4)	0.2(4)	4.7(3)	0.7(5)
O2	5.2(4)	6.1(4)	4.9(4)	0.8(3)	-0.2(3)	1.5(3)
O3	4.4(3)	8.5(5)	7.7(4)	-1.9(4)	-0.7(3)	-0.1(5)
C1	9.9(8)	3.6(5)	4.9(6)	-1.7(5)	-0.6(5)	1.4(4)
C2	7.0(7)	6.8(6)	5.6(6)	-0.4(5)	2.1(5)	1.2(5)
C3	6.9(5)	4.8(4)	4.3(4)	-0.1(7)	1.4(4)	1.0(7)
C4	6.8(5)	3.2(6)	5.0(5)	-0.3(4)	0.1(4)	0.5(4)
C5	8.0(7)	5.0(5)	3.8(5)	1.9(5)	-0.4(5)	1.0(4)
C6	4.4(4)	3.6(3)	5.8(4)	-0.5(6)	1.4(3)	0.1(6)
C7	7.0(7)	8.1(7)	6.0(7)	-0.4(5)	1.2(6)	-1.5(5)
C8	6.2(7)	17(2)	5.5(7)	-2.(1)	0.1(5)	-1.(1)
C9	7.7(9)	20(2)	4.8(7)	5.(1)	1.9(6)	3.(1)
C10	15(1)	14(1)	5.1(8)	8.(1)	2.1(8)	3.0(8)
C11	10.4(8)	6.4(7)	5.1(6)	3.5(6)	0.0(6)	0.3(5)
C12	4.4(4)	4.1(6)	4.1(4)	0.5(3)	1.2(3)	0.2(3)
C13	3.5(5)	5.1(5)	7.0(6)	0.4(4)	1.1(4)	-0.3(5)
C14	3.4(5)	6.4(6)	8.3(7)	-0.0(4)	0.7(5)	-0.9(5)
C15	5.7(7)	8.0(8)	13(1)	-2.1(6)	4.0(7)	-0.2(7)
C16	9.4(9)	11(1)	7.5(8)	-2.5(7)	4.4(7)	0.5(7)
C17	6.6(7)	8.6(7)	5.8(6)	-2.6(6)	2.8(5)	-0.5(5)
C18	4.0(5)	4.2(5)	5.4(5)	-0.4(3)	1.2(4)	-0.2(4)
C19	12(1)	3.9(6)	9.8(9)	-1.3(6)	6.5(8)	-0.4(6)
C20	21(2)	3.2(5)	10(1)	-0.1(8)	8.(1)	-0.2(6)
C21	17(1)	3.9(8)	8.7(8)	3.6(8)	2.1(8)	-0.1(6)
C22	7.7(8)	9.0(8)	9.4(8)	3.4(7)	0.3(6)	-4.1(8)
C23	6.9(7)	5.1(6)	7.4(7)	0.4(5)	1.4(5)	-2.1(5)
C24	6.3(6)	4.0(5)	4.2(5)	0.9(4)	1.8(4)	-0.4(4)
C25	4.5(5)	4.2(5)	6.3(6)	-1.1(4)	1.2(5)	-0.4(4)
C26	4.7(5)	6.8(6)	5.8(6)	-0.7(5)	0.9(5)	-0.7(5)
C27	4.8(5)	6.4(6)	6.1(6)	-0.3(5)	2.0(5)	0.4(5)
C28	4.4(5)	5.9(6)	7.1(6)	-1.3(4)	2.2(5)	-0.2(5)
C29	4.0(5)	4.8(5)	5.8(6)	-1.1(4)	1.6(4)	-0.7(4)

Anisotropic Temperature Factors are of the form:

$$temp = -2\pi^2(h^2a^{*2}U_{11} + k^2b^{*2}U_{22} + l^2c^{*2}U_{33} + 2hka^*b^*U_{12} + 2hla^*c^*U_{13} + 2klb^*c^*U_{23})$$

Table A7.4 Selected bond lengths and angles for $CpRu(PPh_3)(CO)SS(O)_2(4\text{-}C_6H_4Me)$.

Ru-S1	2.383(2)	C8-C9	1.34(2)
Ru-P	2.315(2)	C9-C10	1.34(2)
Ru-C1	2.202(8)	C10-C11	1.36(1)
Ru-C2	2.214(9)	C11-C12	1.35(1)
Ru-C3	2.249(7)	C13-C14	1.37(1)
Ru-C4	2.249(8)	C13-C18	1.37(1)
Ru-C5	2.233(8)	C14-C15	1.36(1)
Ru-C6	1.868(7)	C15-C16	1.36(1)
S1-S2	2.023(3)	C16-C17	1.37(1)
S2-O1	1.444(8)	C17-C18	1.40(1)
S2-O2	1.435(6)	C19-C20	1.38(1)
S2-C30	1.770(8)	C19-C24	1.37(1)
P-C12	1.817(7)	C20-C21	1.38(2)
P-C18	1.808(7)	C21-C22	1.34(2)
P-C24	1.839(8)	C22-C23	1.39(1)
O3-C6	1.138(7)	C23-C24	1.37(1)
C1-C2	1.39(1)	C25-C26	1.36(1)
C1-C5	1.42(1)	C25-C30	1.39(1)
C2-C3	1.34(1)	C26-C27	1.36(1)
C3-C4	1.40(1)	C27-C28	1.37(1)
C4-C5	1.39(1)	C27-C31	1.52(1)
C7-C8	1.42(1)	C28-C29	1.36(1)
C7-C12	1.38(1)	C29- C30	1.391(9)

S1-Ru-P	87.98(7)	Ru-C2-C1	71.2(5)
S1-Ru-C1	153.2(2)	Ru-C2-C3	73.9(5)
S1-Ru-C2	122.7(3)	C1-C2-C3	107.4(9)
S1-Ru-C3	94.3(3)	Ru-C3-C2	71.1(5)
S1-Ru-C4	95.1(2)	Ru-C3-C4	71.9(4)
S1-Ru-C5	127.0(3)	C2-C3-C4	111(1)
S1-Ru-C6	95.6(4)	Ru-C4-C5	71.2(5)
P-Ru-C1	111.8(3)	Ru-C4-C3	71.9(4)
P-Ru-C2	148.3(3)	C3-C4-C5	106.8(9)
P-Ru-C3	149.9(2)	Ru-C5-C1	70.1(5)
P-Ru-C4	113.7(2)	Ru-C5-C4	72.5(5)
P-Ru-C5	95.0(2)	C1-C5-C4	106.6(8)
P-Ru-C6	88.1(2)	Ru-C6-O3	173(1)
C1-Ru-C2	36.7(3)	C8-C7-C12	118(1)
C1-Ru-C3	59.4(4)	C7-C8-C9	123(1)
C1-Ru-C4	60.9(3)	C8-C9-C10	118(1)
C1-Ru-C5	37.4(3)	C9-C10-C11	121(1)
C1-Ru-C6	102.7(4)	C10-C11-C12	122(1)
C2-Ru-C3	35.0(3)	P-C12-C7	121.4(7)
C2-Ru-C4	60.7(3)	P-C12-C11	120.7(7)
C2-Ru-C5	61.7(3)	C7-C12-C11	117.8(9)
C2-Ru-C6	95.4(3)	C14-C13-C18	122.6(9)
C3-Ru-C4	36.2(3)	C13-C14-C15	121.0(9)
C3-Ru-C5	60.0(4)	C14-C15-C16	117.7(9)
C3-Ru-C6	121.3(3)	C15-C16-C17	122(1)
C4-Ru-C5	36.3(3)	C16-C17-C18	121.1(9)
C4-Ru-C6	155.9(3)	P-C18-C13	122.5(7)
C5-Ru-C6	137.3(4)	P-C18-C17	121.6(7)

Ru-S1-S2	110.0(1)
S1-S2-O1	105.7(2)
S1-S2-O2	113.0(3)
S1-S2-C30	107.0(3)
O1-S2-O2	117.4(3)
O1-S2-C30	106.9(3)
O2-S2-C30	106.3(4)
Ru-P-C12	13.9(2)
Ru-P-C18	17.6(3)
Ru-P-C24	13.1(3)
C12-P-C18	102.8(4)
C12-P-C24	104.7(4)
C18-P-C24	103.2(4)
Ru-C1-C2	72.1(5)
Ru-C1-C5	72.5(5)
C2-C1-C5	108.3(8)

C13-C18-C17	115.9(8)
C20-C19-C24	121(1)
C19-C20-C21	120(1)
C20-C21-C22	119(1)
C21-C22-C23	121(1)
C22-C23-C24	120(1)
P-C24-C19	117.8(7)
P-C24-C23	123.8(7)
C19-C24-C23	118.3(8)
C26-C25-C30	118.7(8)
C25-C26-C27	122.4(9)
C26-C27-C28	118.5(9)
C26-C27-C31	120.8(9)
C28-C27-C31	120.7(8)
C27-C28-C29	121.4(8)
C28-C29-C30	119.1(8)
S2-C30-C25	119.7(6)
S2-C30-C29	120.4(6)
C25-C30-C29	119.9(7)